Fourth Edition

Building Scientific Apparatus

John H. Moore, Christopher C. Davis,
and Michael A. Coplan

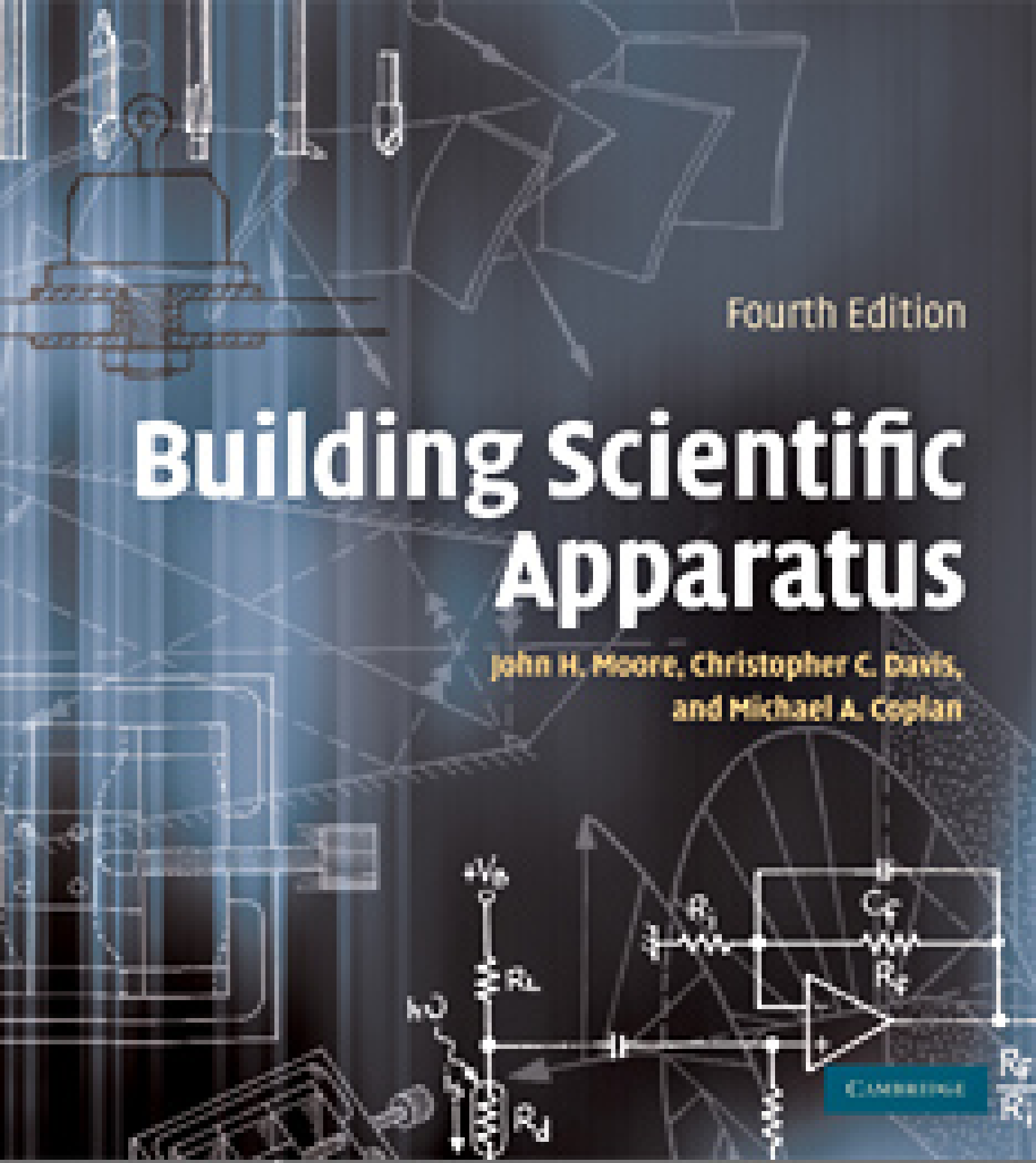

CAMBRIDGE www.cambridge.org/9780521878586

This page intentionally left blank

BUILDING SCIENTIFIC APPARATUS

Fourth Edition

Unrivalled in its coverage and unique in its hands-on approach, this guide to the design and construction of scientific apparatus is essential reading for all scientists and students in the physical, chemical, and biological sciences and engineering.

Covering the physical principles governing the operation of the mechanical, optical and electronic parts of an instrument, the fourth edition contains new sections on detectors, low-temperature measurements, high-pressure apparatus, and updated engineering specifications. There are over 400 figures and tables to permit specification of the components of apparatus, many new to this edition. Data on the properties of materials and components used by manufacturers are included. Mechanical, optical, and electronic construction techniques carried out in the laboratory, as well as those let out to specialized shops, are also described. Step-by-step instruction, supported by many detailed figures, is given for laboratory skills such as soldering electrical components, glassblowing, brazing, and polishing.

JOHN H. MOORE is Professor Emeritus at the University of Maryland. He is a Fellow of the American Physical Society and the American Association for the Advancement of Science. His research has included plasma chemistry, high-energy electron scattering, and the design and fabrication of instruments for use in the laboratory and on spacecraft.

CHRISTOPHER C. DAVIS is Professor of Electrical and Computer Engineering at the University of Maryland. He is a Fellow of the Institute of Physics, and a Fellow of the Institute of Electrical and Electronics Engineers. Currently his research deals with free space optical and directional RF communication systems, plasmonics, near-field scanning optical microscopy, chemical and biological sensors, interferometry, optical systems, bioelectromagnetics, and RF dosimetry.

MICHAEL A. COPLAN is Professor and Director of the Chemical Physics Program at the University of Maryland. He is a Fellow of the American Physical Society and has research programs in space science, electron scattering, and neutron detection.

SANDRA C. GREER is Professor Emerita of Chemistry and Biochemistry and Professor of Chemical and Biomolecular Engineering at the University of Maryland and is now Provost and Dean of the Faculty at Mills College in Oakland, California. She is a Fellow of the American Physical Society and the American Association for the Advancement of Science, and recipient of the American Chemical Society Francis P. Garvan–John M. Olin Medal.

Building Scientific Apparatus covers a wide range of topics critical to the construction, use, and understanding of scientific equipment. It serves as a reference to a wealth of technical information, but is also written in a familiar style that makes it accessible as an introductory text. This new edition includes updates throughout, and will continue to serve as a bookshelf standard in laboratories around the world. I never like to be too far from this book!
Jason Hafner, Rice University, Houston, Texas

For many years, *Building Scientific Apparatus* has been the first book I reach for to remind myself of an experimental technique, or to start learning a new one. And it has been one of the first references I've recommended to new students. With valuable additions (e.g. tolerances table for machining, formula for aspheric lenses, expanded information on detector signal-to-noise ratios, solid-state detectors...) and updated lists of suppliers, the newest addition will be a welcome replacement for our lab's well-thumbed previous editions of BSA.
Brian King, McMaster University, Canada

I like this book a lot. It is comprehensive in its coverage of a wide range of topics that an experimentalist in the physical sciences may encounter. It usefully extends the scope of previous editions and highlights new technical developments and ways to apply them. The authors share a rich pool of knowledge and practical expertise and they have produced a unique and authoritative guide to the building of scientific apparatus. The book provides lucid descriptions of underlying physical principles. It is also full of hands-on advice to enable the reader to put these principles into practice. The style of the book is very user-friendly and the text is skillfully illustrated and informed by numerous figures. The book is a mine of useful information ranging from tables of the properties of materials to lists of manufacturers and suppliers. This book would be an invaluable resource in any laboratory in the physical sciences and beyond.
George King, University of Manchester

The construction of novel equipment is often a prerequisite for cutting-edge scientific research. Jack Moore and his coauthors have made this task easier and more efficient by concentrating several careers' worth of equipment-building experience into a single volume – a thoroughly revised and updated edition of a 25-year-old classic. Covering areas ranging from glassblowing to electron optics and from temperature controllers to lasers, the invaluable information in this book is destined to save years of collective frustration for students and scientists. It is a ''must-have'' on the shelf of every research lab.
Nicholas Spencer, Eidgenössische Technische Hochschule, Zürich.

This book is a unique resource for the beginning experimenter, and remains valuable throughout a scientist's career. Professional engineers I know also own and enjoy using the book.
Eric Zimmerman, University of Colorado at Boulder, Colorado

BUILDING SCIENTIFIC APPARATUS

Fourth Edition

John H. Moore ✦ Christopher C. Davis ✦ Michael A. Coplan,
with a chapter by Sandra C. Greer

CAMBRIDGE
UNIVERSITY PRESS

CAMBRIDGE UNIVERSITY PRESS
Cambridge, New York, Melbourne, Madrid, Cape Town, Singapore,
São Paulo, Delhi, Dubai, Tokyo

Cambridge University Press
The Edinburgh Building, Cambridge CB2 8RU, UK

Published in the United States of America by Cambridge University Press, New York

www.cambridge.org
Information on this title: www.cambridge.org/9780521878586

First published in print format 2009

ISBN-13 978-0-511-58009-3 eBook (EBL)

ISBN-13 978-0-521-87858-6 Hardback

To our families

CONTENTS

Preface xiii

1 MECHANICAL DESIGN AND FABRICATION 1

1.1 Tools and Shop Processes 2
1.1.1 Hand Tools 2
1.1.2 Machines for Making Holes 2
1.1.3 The Lathe 4
1.1.4 Milling Machines 7
1.1.5 Electrical Discharge Machining (EDM) 9
1.1.6 Grinders 9
1.1.7 Tools for Working Sheet Metal 10
1.1.8 Casting 10
1.1.9 Tolerance and Surface Quality for Shop Processes 12
1.2 Properties of Materials 12
1.2.1 Parameters to Specify Properties of Materials 13
1.2.2 Heat Treating and Cold Working 14
1.2.3 Effect of Stress Concentration 16
1.3 Materials 18
1.3.1 Iron and Steel 18
1.3.2 Nickel Alloys 20
1.3.3 Copper and Copper Alloys 21
1.3.4 Aluminum Alloys 22
1.3.5 Other Metals 22
1.3.6 Plastics 23
1.3.7 Glasses and Ceramics 24
1.4 Joining Materials 25
1.4.1 Threaded Fasteners 25
1.4.2 Rivets 28
1.4.3 Pins 29
1.4.4 Retaining Rings 29
1.4.5 Soldering 30
1.4.6 Brazing 31
1.4.7 Welding 33
1.4.8 Adhesives 34
1.4.9 Design of Joints 34
1.4.10 Joints in Piping and Pressure Vessels 37
1.5 Mechanical Drawing 39
1.5.1 Drawing Tools 39
1.5.2 Basic Principles of Mechanical Drawing 40
1.5.3 Dimensions 44
1.5.4 Tolerances 46
1.5.5 From Design to Working Drawings 48
1.6 Physical Principles of Mechanical Design 49
1.6.1 Bending of a Beam or Shaft 50
1.6.2 Twisting of a Shaft 52
1.6.3 Internal Pressure 52
1.6.4 Vibration of Beams and Shafts 54
1.6.5 Shaft Whirl and Vibration 55
1.7 Constrained Motion 57
1.7.1 Kinematic Design 57
1.7.2 Plain Bearings 59
1.7.3 Ball Bearings 60
1.7.4 Linear-Motion Bearings 61
1.7.5 Springs 62
1.7.6 Flexures 63
Cited References 66
General References 66
Chapter 1 Appendix 68

2 WORKING WITH GLASS 76

2.1 Properties of Glasses 76
2.1.1 Chemical Composition and Chemical Properties of Some Laboratory Glasses 76
2.1.2 Thermal Properties of Laboratory Glasses 77
2.1.3 Optical Properties of Laboratory Glassware 78
2.1.4 Mechanical Properties of Glass 78
2.2 Laboratory Components Available in Glass 78
2.2.1 Tubing and Rod 78
2.2.2 Demountable Joints 79
2.2.3 Valves and Stopcocks 80
2.2.4 Graded Glass Seals and Glass-to-Metal Seals 81
2.3 Laboratory Glassblowing Skills 81
2.3.1 The Glassblower's Tools 81
2.3.2 Cutting Glass Tubing 82
2.3.3 Pulling Points 83
2.3.4 Sealing Off a Tube: The Test-Tube End 84
2.3.5 Making a T-Seal 85
2.3.6 Making a Straight Seal 87
2.3.7 Making a Ring Seal 87
2.3.8 Bending Glass Tubing 88
2.3.9 Annealing 88
2.3.10 Sealing Glass to Metal 89
2.3.11 Grinding and Drilling Glass 91
Cited References 92
General References 92

3 VACUUM TECHNOLOGY 93

3.1 Gases 93
3.1.1 The Nature of the Residual Gases in a Vacuum System 93
3.1.2 Gas Kinetic Theory 93
3.1.3 Surface Collisions 95
3.1.4 Bulk Behavior versus Molecular Behavior 95
3.2 Gas Flow 95
3.2.1 Parameters for Specifying Gas Flow 95
3.2.2 Network Equations 96
3.2.3 The Master Equation 96
3.2.4 Conductance Formulae 97
3.2.5 Pumpdown Time 98
3.2.6 Outgassing 98
3.3 Pressure and Flow Measurement 98
3.3.1 Mechanical Gauges 98
3.3.2 Thermal-Conductivity Gauges 100
3.3.3 Viscous-Drag Gauges 101
3.3.4 Ionization Gauges 101
3.3.5 Mass Spectrometers 103
3.3.6 Flowmeters 103
3.4 Vacuum Pumps 104
3.4.1 Mechanical Pumps 105
3.4.2 Vapor Diffusion Pumps 109
3.4.3 Entrainment Pumps 112
3.5 Vacuum Hardware 115
3.5.1 Materials 115
3.5.2 Demountable Vacuum Connections 118
3.5.3 Valves 120
3.5.4 Mechanical Motion in the Vacuum System 123
3.5.5 Traps and Baffles 124
3.5.6 Molecular Beams and Gas Jets 127
3.5.7 Electronics and Electricity *in Vacuo* 130
3.6 Vacuum-System Design and Construction 131
3.6.1 Some Typical Vacuum Systems 132
3.6.2 Differential Pumping 138
3.6.3 The Construction of Metal Vacuum Apparatus 139
3.6.4 Surface Preparation 142
3.6.5 Leak Detection 143
3.6.6 Ultrahigh Vacuum 144
Cited References 145
General References 145

4 OPTICAL SYSTEMS 147

4.1 Optical Terminology 147
4.2 Characterization and Analysis of Optical Systems 150
4.2.1 Simple Reflection and Refraction Analysis 150
4.2.2 Paraxial-Ray Analysis 151
4.2.3 Nonimaging Light Collectors 162
4.2.4 Imaging Systems 162
4.2.5 Exact Ray Tracing and Aberrations 166
4.2.6 The Use of Impedances in Optics 174
4.2.7 Gaussian Beams 179

4.3 Optical Components 182
4.3.1 Mirrors 182
4.3.2 Windows 187
4.3.3 Lenses and Lens Systems 187
4.3.4 Prisms 196
4.3.5 Diffraction Gratings 201
4.3.6 Polarizers 204
4.3.7 Optical Isolators 211
4.3.8 Filters 212
4.3.9 Fiber Optics 217
4.3.10 Precision Mechanical Movement Systems 219
4.3.11 Devices for Positional and Orientational Adjustment of Optical Components 222
4.3.12 Optical Tables and Vibration Isolation 229
4.3.13 Alignment of Optical Systems 229
4.3.14 Mounting Optical Components 230
4.3.15 Cleaning Optical Components 232
4.4 Optical Materials 236
4.4.1 Materials for Windows, Lenses, and Prisms 236
4.4.2 Materials for Mirrors and Diffraction Gratings 245
4.5 Optical Sources 247
4.5.1 Coherence 248
4.5.2 Radiometry: Units and Definitions 248
4.5.3 Photometry 249
4.5.4 Line Sources 250
4.5.5 Continuum Sources 252
4.6 Lasers 261
4.6.1 General Principles of Laser Operation 267
4.6.2 General Features of Laser Design 268
4.6.3 Specific Laser Systems 270
4.6.4 Laser Radiation 283
4.6.5 Coupling Light from a Source to an Aperture 284
4.6.6 Optical Modulators 287
4.6.7 How to Work Safely with Light Sources 289
4.7 Optical Dispersing Instruments 291
4.7.1 Comparison of Prism and Grating Spectrometers 293
4.7.2 Design of Spectrometers and Spectrographs 295
4.7.3 Calibration of Spectrometers and Spectrographs 299
4.7.4 Fabry–Perot Interferometers and Etalons 299
4.7.5 Design Considerations for Fabry–Perot Systems 308
4.7.6 Double-Beam Interferometers 309
Endnotes 314
Cited References 314
General References 318

5 CHARGED-PARTICLE OPTICS 324

5.1 Basic Concepts of Charged-Particle Optics 324
5.1.1 Brightness 324
5.1.2 Snell's Law 325
5.1.3 The Helmholtz–Lagrange Law 325
5.1.4 Vignetting 326
5.2 Electrostatic Lenses 327
5.2.1 Geometrical Optics of Thick Lenses 327
5.2.2 Cylinder Lenses 329
5.2.3 Aperture Lenses 331
5.2.4 Matrix Methods 332
5.2.5 Aberrations 333
5.2.6 Lens Design Example 336
5.2.7 Computer Simulations 338
5.3 Charged-Particle Sources 338
5.3.1 Electron Guns 338
5.3.2 Electron-Gun Design Example 341
5.3.3 Ion Sources 343
5.4 Energy Analyzers 345
5.4.1 Parallel-Plate Analyzers 346
5.4.2 Cylindrical Analyzers 347
5.4.3 Spherical Analyzers 348
5.4.4 Preretardation 350
5.4.5 The Energy-Add Lens 350
5.4.6 Fringing-Field Correction 352
5.4.7 Magnetic Energy Analyzers 353
5.5 Mass Analyzers 354
5.5.1 Magnetic Sector Mass Analyzers 354
5.5.2 Wien Filter 354
5.5.3 Dynamic Mass Spectrometers 355
5.6 Electron- and Ion-Beam Devices: Construction 355
5.6.1 Vacuum Requirements 355
5.6.2 Materials 356
5.6.3 Lens and Lens-Mount Design 357
5.6.4 Charged-Particle Detection 358
5.6.5 Magnetic-Field Control 358
Cited References 360

6 ELECTRONICS 362

6.1 Preliminaries 362
6.1.1 Circuit Theory 362
6.1.2 Circuit Analysis 365
6.1.3 High-Pass and Low-Pass Circuits 369
6.1.4 Resonant Circuits 372
6.1.5 The Laplace-Transform Method 374
6.1.6 *RLC* Circuits 377
6.1.7 Transient Response of Resonant Circuits 378
6.1.8 Transformers and Mutual Inductance 379
6.1.9 Compensation 380
6.1.10 Filters 380
6.1.11 Computer-Aided Circuit Analysis 381
6.2 Passive Components 382
6.2.1 Fixed Resistors and Capacitors 383
6.2.2 Variable Resistors 384
6.2.3 Transmission Lines 388
6.2.4 Coaxial Connectors 399
6.2.5 Relays 401
6.3 Active Components 402
6.3.1 Diodes 403
6.3.2 Transistors 406
6.3.3 Silicon-Controlled Rectifiers 419
6.3.4 Unijunction Transistors 420
6.3.5 Thyratrons 421
6.4 Amplifiers and Pulse Electronics 421
6.4.1 Definition of Terms 421
6.4.2 General Transistor-Amplifier Operating Principles 424
6.4.3 Operational-Amplifier Circuit Analysis 428
6.4.4 Instrumentation and Isolation Amplifiers 432
6.4.5 Stability and Oscillators 434
6.4.6 Detecting and Processing Pulses 435
6.5 Power Supplies 441
6.5.1 Power-Supply Specifications 442
6.5.2 Regulator Circuits and Programmable Power Supplies 443
6.5.3 Bridges 445
6.6 Digital Electronics 447
6.6.1 Binary Counting 447
6.6.2 Elementary Functions 447
6.6.3 Boolean Algebra 448
6.6.4 Arithmetic Units 448
6.6.5 Data Units 448
6.6.6 Dynamic Systems 450
6.6.7 Digital-to-Analog Conversion 453
6.6.8 Memories 458
6.6.9 Logic and Function 460
6.6.10 Implementing Logic Functions 464
6.7 Data Acquisition 467
6.7.1 Data Rates 467
6.7.2 Voltage Levels and Timing 469
6.7.3 Format 469
6.7.4 System Overhead 470
6.7.5 Analog Input Signals 472
6.7.6 Multiple Signal Sources: Data Loggers 474
6.7.7 Standardized Data-Acquisition Systems 474
6.7.8 Control Systems 479
6.7.9 Personal Computer (PC) Control of Experiments 482
6.8 Extraction of Signal from Noise 491
6.8.1 Signal-to-Noise Ratio 491
6.8.2 Optimizing the Signal-to-Noise Ratio 492
6.8.3 The Lock-In Amplifier and Gated Integrator or Boxcar 493
6.8.4 Signal Averaging 494
6.8.5 Waveform Recovery 495
6.8.6 Coincidence and Time-Correlation Techniques 496
6.9 Grounds and Grounding 500
6.9.1 Electrical Grounds and Safety 500
6.9.2 Electrical Pickup: Capacitive Effects 503
6.9.3 Electrical Pickup: Inductive Effects 504
6.9.4 Electromagnetic Interference and r.f.i 505
6.9.5 Power-Line-Coupled Noise 505
6.9.6 Ground Loops 506
6.10 Hardware and Construction 508
6.10.1 Circuit Diagrams 508
6.10.2 Component Selection and Construction Techniques 508
6.10.3 Printed Circuit Boards 513
6.10.4 Wire Wrap™ Boards 523
6.10.5 Wires and Cables 524
6.10.6 Connectors 528
6.11 Troubleshooting 533
6.11.1 General Procedures 533
6.11.2 Identifying Parts 535
Cited References 537
General References 538
Chapter 6 Appendix 541

7 DETECTORS 547

7.1 Optical Detectors 547
7.2 Noise in Optical Detection Process 548
7.2.1 Shot Noise 548
7.2.2 Johnson Noise 549
7.2.3 Generation-Recombination (gr) Noise 549
7.2.4 1/f Noise 549
7.3 Figures of Merit for Detectors 550
7.3.1 Noise-Equivalent Power 550
7.3.2 Detectivity 550
7.3.3 Responsivity 551
7.3.4 Quantum Efficiency 552
7.3.5 Frequency Response and Time Constant 553
7.3.6 Signal-to-Noise Ratio 553
7.4 Photoemissive Detectors 554
7.4.1 Vacuum Photodiodes 554
7.4.2 Photomultipliers 555
7.4.3 Photocathode and Dynode Materials 556
7.4.4 Practical Operating Considerations for Photomultiplier Tubes 561
7.5 Photoconductive Detectors 566
7.6 Photovoltaic Detectors (Photodiodes) 572
7.6.1 Avalanche Photodiodes 574
7.6.2 Geiger Mode Avalanche Photodetectors 577
7.7 Detector Arrays 578
7.7.1 Reticons 578
7.7.2 Quadrant Detectors 578
7.7.3 Lateral Effect Photodetectors 578
7.7.4 Imaging Arrays 580
7.7.5 Image Intensifiers 581
7.8 Signal-to-Noise Ratio Calculations 582
7.8.1 Photomultipliers 582
7.8.2 Direct Detection with *p–i–n* Photodiodes 582
7.8.3 Direct Detection with APDs 584
7.8.4 Photon Counting 585
7.9 Particle and Ionizing Radiation Detectors 585
7.9.1 Solid-State Detectors 589
7.9.2 Scintillation Counters 591
7.9.3 X-Ray Detectors 591
7.10 Thermal Detectors 591
7.10.1 Thermopiles 593
7.10.2 Pyroelectric Detectors 593
7.10.3 Bolometers 594
7.10.4 The Golay Cell 595
7.11 Electronics to be Used With Detectors 596
7.12 Detector Calibration 597
Endnotes 597
Cited References 597
General References 599

8 MEASUREMENT AND CONTROL OF TEMPERATURE 600

8.1 The Measurement of Temperature 600
8.1.1 Expansion Thermometers 601
8.1.2 Thermocouples 602
8.1.3 Resistance Thermometers 605
8.1.4 Semiconductor Thermometers 609
8.1.5 Temperatures Very Low: Cryogenic Thermometry 610
8.1.6 Temperatures Very High 611
8.1.7 New, Evolving, and Specialized Thermometry 612
8.1.8 Comparison of Main Categories of Thermometers 612
8.1.9 Thermometer Calibration 612
8.2 The Control of Temperature 613
8.2.1 Temperature Control at Fixed Temperatures 613
8.2.2 Temperature Control at Variable Temperatures 613
Cited References 621
General References 623

Index 625

PREFACE

Building Scientific Apparatus provides an overview of the physical principles that one must grasp to make useful and creative decisions in the design of scientific apparatus. We also describe skills, such as mechanical drawing, circuit analysis, and optical ray-tracing and matrix methods that are required to design an instrument. A large part of the text is devoted to components. For each class of components – electrical, optical, thermal and so on – the parameters used by manufacturers to specify their products are defined. Useful materials and components such as infrared detectors, metal alloys, optical materials, and operational amplifiers are discussed, and examples and performance specifications are given. Of course, having designed an apparatus and chosen the necessary components, one must *build* it. We deal in considerable detail with basic laboratory skills: soldering electrical components, glassblowing, brazing, polishing, and so on. Described in lesser detail are operations such as lathe turning, milling, casting, laser cutting, and printed-circuit production, which one might let out to an outside shop. Understanding the capabilities and limitations of shop processes is necessary to fully exploit them in designing and building an instrument. Overall, we recognize that there are many engineering and technical texts that cover every aspect of instrument design; our goal in *Building Scientific Apparatus* has been to winnow the available information down to the essentials required for practical work by the designer and builder of scientific instruments.

In the 25 years since *Building Scientific Apparatus* first appeared, there have been profound changes in the way in which unique apparatus is assembled, as well as in the scientists who require unique apparatus. Twenty-five years ago the technology discussed in the first edition – optics, electronics, charged-particle beams, and vacuum systems – was generally the purview of engineers. Today sophisticated apparatus is conceived of and built by chemists, physicists, and biologists, as well as medical and social scientists. In the past, microprocessors were a component that needed to be programmed and wired into an apparatus. Now computer controls are an integral part of devices such as power supplies, pressure gauges, and machine tools. Similarly, lasers were once assembled in the lab from individual optical components; today a complete laser is itself a component, less expensive than the elements from which it is assembled. The fourth edition of *Building Scientific Apparatus* recognizes this evolution in the complexity of available components and the concomitant implications for the instrument designer.

We acknowledge the importance that the World Wide Web has acquired as a resource for research. Throughout the text we mention particular suppliers of materials and components. There are certainly many that have escaped our attention. The suppliers of equipment, devices, components, and materials along with specifications, availability, and cost can be readily located using a suitable search engine.

This book was written with the goal of contributing to the quality and functionality of apparatus designed and built for research in disciplines from the engineering and physical sciences to the life sciences. We welcome comments; many suggestions from the past have been incorporated in the current text.

CHAPTER
4

OPTICAL SYSTEMS

Physical, chemical, and biological phenomena are regularly studied or induced optically. Such experiments can involve light absorption, light emission, or light scattering. We can characterize any experimental arrangement where light is used, produced, measured, modified, or detected as an *overall optical system*. Any such optical system will always be reducible to three parts: a source of light, a detector of that light, and everything in between. We will frequently refer to this important and varied intermediary arrangement as the *optical system*. Consequently, our discussion of overall optical system design and construction will involve three key topics: sources, optical systems, and detectors (to be discussed in detail in Chapter 7). The light source may be a laser, lamp, light-emitting diode, or the Sun. The detector may be a vacuum tube, solid-state device, or even the eye. Light intensity may vary from continuous wave (CW) to pulsed, and these pulses may have durations as short as a few femtoseconds. Passive elements in the system may transmit, reflect, combine, polarize, or separate light according to its spectral content. Nonlinear optical elements change the spectral content of light.

It is our aim in this chapter to explain the basic concepts that need to be understood by the experimentalist who uses optical techniques. In addition, we will provide examples of useful techniques for producing, controlling, analyzing, and modulating light.

4.1 OPTICAL TERMINOLOGY

Light is one form of electromagnetic radiation, the many categories of which make up the electromagnetic spectrum. Electromagnetic radiation, which transports energy from point to point at the velocity of light, can be described in terms of both *wave* and *particle* ''pictures'' or ''models''. This is the famous ''wave-particle'' duality of all fields or particles in our model of the Universe. In the electromagnetic-wave picture, waves are characterized by their frequency v, wavelength λ, and the velocity of light c, which are related by $c = v\lambda$. A propagating electromagnetic wave is characterized by a number of field vectors, which vary in time and space. These include the electric field **E** (measured in Volt/m), the magnetic field **H** (measured in Amp/m), the displacement vector **D** (measured in Coulomb/m^2, and the magnetic flux density **B** (measured in Webers/m^2 or Tesla). For a complete description the *polarization* state of the wave must also be specified. *Linearly polarized* waves have fixed directions for their field vectors, which do not re-orient themselves as the wave propagates. *Circular* or *elliptically* polarized waves have field vectors that trace out circular or elliptic helical paths as the wave travels along. In the particle picture, electromagnetic energy is carried from point to point as quantized packets of energy called *photons*. The energy of a photon of frequency v is hv, where h is Planck's constant – 6.626×10^{-34} J s. Photons have zero mass, travel at the velocity of light, and also carry both linear and angular momentum. The linear momentum of a photon of wavelength is $p = h/\lambda$, the angular momentum depends on the equivalent polarization state of the corresponding wave. Circularly polarized photons have angular momentum $h/2\pi = \hbar$.

Our everyday experience of ''light'' generally only encompasses the small part of the electromagnetic spectrum to which the human eye is sensitive, a wavelength range running roughly from 400–700 nm. The full electromagnetic

Table 4.1 Fundamental parameters of electromagnetic radiation and optical media

Parameter	Symbol	Value	Units
Velocity of light *in vacuo*	$c_0 = (\mu_0 \epsilon_0)^{1/2}$	2.99792458×10^8	m/sec
Permeability of free space	μ_0	$4\pi \times 10^{-7}$	henry/m
Permittivity of free space	ϵ_0	8.85416×10^{-12}	farad/m
Velocity of light in a medium	$c = (\mu_r \mu_0 \epsilon_r \epsilon_0)^{-1/2} = c_0/n$		m/sec
Refractive index	$n = (\mu_r \epsilon_r)^{1/2}$		(dimensionless)
Relative permeability of a medium	μ_r	Usually 1	(dimensionless)
Dielectric constant of a medium	ϵ_r		(dimensionless)
Frequency	$v = c/\lambda$		Hz 10^9 Hz = 1 GHz (gigahertz) 10^{12} Hz = 1 THz (terahertz)
Wavelength *in vacuo*	$\lambda_0 = c_0/v$		
Wavelength in a medium	$\lambda = c/v = \lambda_0/n$		m 10^{-3} m = 1 mm (millimeter) 10^{-6} m = 1 μm (micrometer) = 1 μ (micron) 10^{-9} m = 1 nm (nanometer) = 1 mμ (millimicron) 10^{-12} m = 1 pm (picometer) 10^{-10} m = 1 A (Angstrom)
Wavenumber	$\bar{v} = 1/\lambda$		cm^{-1} (kayser)
Wavevector	$\mathbf{k}$, $\lvert\mathbf{k}\rvert = 2\pi/\lambda$		m^{-1}
Photon energy	$E = hv$		J 1.60202×10^{19} J = 1 eV (electron volt)
Electric field of wave	$\mathbf{E}$		V/m
Magnetic field of wave	$\mathbf{H}$		A/m
Poynting vector	$\mathbf{P} = \mathbf{E} \times \mathbf{H}$		W/m^2
Intensity	$I = <\lvert\mathbf{P}\rvert>_{av} = \lvert\mathbf{E}\rvert^2/2Z$		W/m^2
Impedance of medium	$Z = \frac{E_x}{H_y} = -\frac{E_y}{H_x} = \left(\frac{\mu_r \mu_0}{\epsilon_r \epsilon_0}\right)^{1/2}$		Ω
Impedance of free space	$\mathbf{Z}_0 = (\mu_0/\epsilon_0)^{1/2}$	376.7	Ω

spectrum, going from low to high frequencies, is divided into radiowaves (0–1 GHz), microwaves (1–300 GHz), infrared waves (λ 0.7–1000 μm) (300 GHz–430 THz)[a] visible light (λ 400–700 nm), ultraviolet light (λ 10–400 nm), X-rays (λ 0.1–10 nm), and γ waves ($\lambda < 0.1$ nm).

The wavelength region between 10 nm and 200 nm is often called the vacuum-ultraviolet region because these wavelengths are absorbed by air and most gases. Optical systems can somewhat arbitrarily be classified as systems that handle light in the spectral region between 10 nm and 100 μm. Beyond the far-infrared, between 100 and 1000 μm (the submillimeter wave region of the spectrum), lies a spectral region where conventional optical methods can still be used, but become difficult, as does the extension of microwave techniques for the centimeter- and millimeter-wave regions. The use of optical techniques in this region, and even in the millimeter region, is often called *quasi-optics*.[1–4] Only a few experimental techniques and devices that are noteworthy in this region will be mentioned.

Table 4.1 summarizes the important parameters that are used to characterize light and the media through which it passes. A few comments on the table are appropriate.

Although the velocity of light in a medium depends both on the relative magnetic permeability μ_r, and dielectric constant ϵ_r of the medium, for all practical optical materials $\mu_r = 1$, so the refractive index and dielectric constant are related by:

$$n = \sqrt{\epsilon_r} \tag{4.1}$$

When light propagates in an anisotropic medium, such as a crystal of lower than cubic symmetry, n and ϵ_r will, in general, depend on the direction of propagation of the wave and its polarization state. The velocity of light *in vacuo* is currently the most precisely known of all the physical constants – its value is known[5] within 40 cm/s. A redefinition of the meter has been adopted[6] based on the cesium-atomic-clock frequency standard[7] and a velocity of light in a vacuum of exactly 2.99792458×10^8 m/s. Consequently, the meter is now a derived SI unit, defined as the distance traveled *in vacuo* by light in $1/2.99792458 \times 10^8$ seconds. The velocity, wavelength, and wavenumber of light traveling in the air have slightly different values than they have *in vacuo*. Tables that give corresponding values of $\bar{\nu}$ *in vacuo* and in standard air are available.[8]

A plane electromagnetic wave traveling in the z-direction can, in general, be decomposed into two independent, linearly polarized components. The electric and magnetic fields associated with each of these components are themselves mutually orthogonal and transverse to the direction of propagation. They can be written as (E_x, H_y) and (E_y, H_x). The ratio of the mutually orthogonal **E** and **H** components is called the *impedance* Z of the medium:

$$\frac{E_x}{H_y} = -\frac{E_y}{H_x} = Z = \sqrt{\frac{\mu_r \mu_0}{\epsilon_r \epsilon_0}} \tag{4.2}$$

Most optical materials have $\mu_r = 1$. The negative sign in Equation (4.2) arises because (y, x, z) is not a right-handed coordinate system. The Poynting vector:

$$\mathbf{P} = \mathbf{E} \times \mathbf{H} \tag{4.3}$$

is a vector that points in the direction of energy propagation of the wave, as shown in Figure 4.1. The local direction of the Poynting vector at a point in a medium is called the *ray* direction. The average magnitude of the Poynting vector is called the *intensity* and is given by:

$$I = <|\mathbf{P}|>_{av} = \frac{|\mathbf{E}|^2}{2Z} \tag{4.4}$$

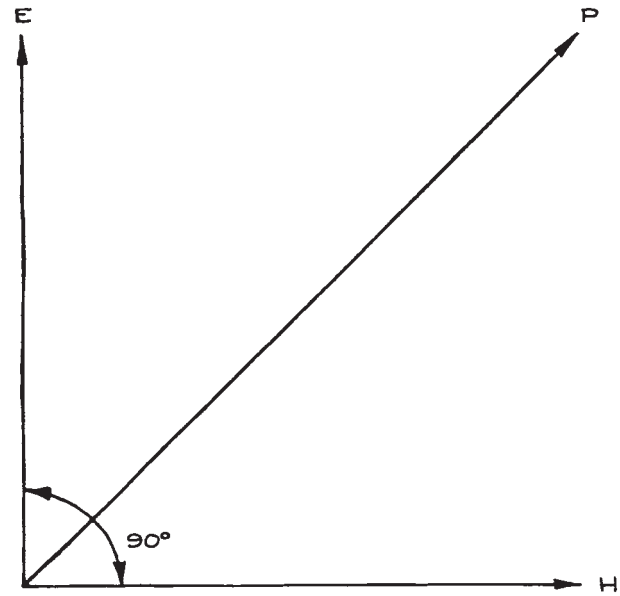

Figure 4.1 Orientation of the mutually orthogonal electric-field vector **E**, magnetic-field vector **H**, and Poynting vector **P**.

The factor of two comes from time-averaging the square of the sinusoidally varying electric field.

The wavevector **k** points in the direction perpendicular to the phase front of the wave (the surface of constant phase). In an isotropic medium **k** and **P** are always parallel.

The photon flux corresponding to an electromagnetic wave of average intensity I and frequency ν is:

$$N = \frac{I}{h\nu} = \frac{I\lambda}{hc} \tag{4.5}$$

where h is Planck's constant, 6.6×10^{-34} J s. For a wave of intensity 1 Wm^2 and wavelength 1 μm *in vacuo*, $N = 5.04 \times 10^{18}$ photons sec^{-1} m^{-2}. Photon energy is sometimes measured in electron volts (eV): 1 eV = 1.60202×10^{-19} J. A photon of wavelength 1 μm has an energy of 1.24 eV. It is often important, particularly in the infrared, to know the correspondence between photon and thermal energies. The characteristic thermal energy at absolute temperature T is kT. At 300 K, $kT = 4.14 \times 10^{-21}$J = 208.6 cm^{-1} = 0.026 eV.

4.2 CHARACTERIZATION AND ANALYSIS OF OPTICAL SYSTEMS

Before embarking on a detailed discussion of the properties and uses of passive optical components and systems containing them, it is worthwhile reviewing some of the parameters that are important in characterizing passive optical systems and some of the methods that are useful in analyzing the way in which light passes through an optical system.

Optical materials have refractive indices that vary with wavelength. This phenomenon is called *dispersion*. It causes a wavelength dependence of the properties of an optical system containing transmissive components. The change of index with wavelength is very gradual, and often negligible, unless the wavelength approaches a region where the material is not transparent. Most materials exhibit *normal dispersion*, where the refractive index decreases with wavelength. In specific spectral regions they may exhibit *anomalous dispersion*, where the refractive index increases with wavelength over a limited range of wavelengths. A description of the performance of an optical system is often simplified by assuming that the light is *monochromatic* (light that contains only a small spread of wavelength components).

4.2.1 Simple Reflection and Refraction Analysis

The phenomena of reflection and refraction are most easily understood in terms of plane electromagnetic waves – those in which the direction of energy flow (the ray direction) is unique. Other types of wave, such as spherical waves and Gaussian beams, are also important in optical science; however, the part of their wavefront that strikes an optical component can frequently be approximated as a plane wave, so plane-wave considerations of reflection and refraction still hold true.

When light is reflected from a plane mirror, or the planar boundary between two media of different refractive index, the *angle of incidence* is always equal to the *angle of reflection*, as shown in Figure 4.2. This is the fundamental *law of reflection*.

When a light ray crosses the boundary between two media of different refractive index, the *angle of refraction*

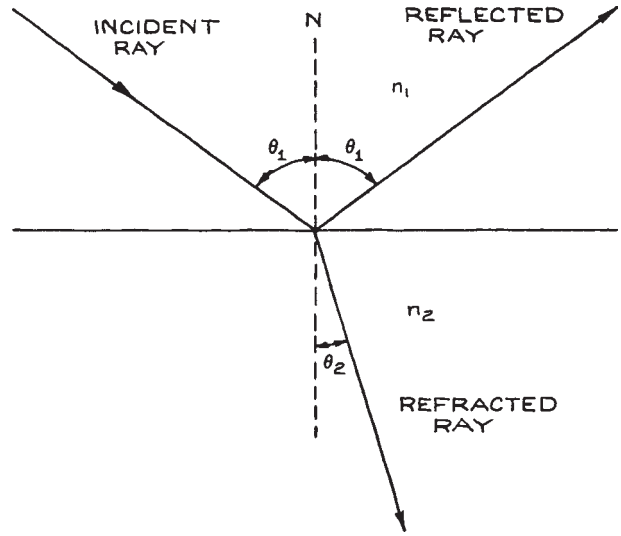

Figure 4.2 Reflection and refraction of a light ray at the boundary between two different isotropic media of refractive indices n_1 and n_2, respectively. The case shown is for $n_2 > n_1$. The incident, reflected, and transmitted rays and the surface normal N are coplanar.

θ_2, shown in Figure 4.2, is related to the angle of incidence θ_1 by *Snell's* law:

$$\frac{\sin\theta_1}{\sin\theta_2} = \frac{n_2}{n_1} \tag{4.6}$$

This result is modified if one or both of the media is anisotropic.

If $n_2 < n_1$ there is a maximum angle of incidence for which there can be a refracted wave, since $\sin\theta_2$ cannot be greater than unity for a real angle. This is called the *critical angle* θ_c and is given by:

$$\sin\theta_c = n_2/n_1 \tag{4.7}$$

as illustrated in Figure 4.3(a)

If θ_1 exceeds θ_c, the boundary acts as a very good mirror, as illustrated in Figure 4.3(b). This phenomenon is called *total internal reflection*. Several types of reflecting prisms discussed in Section 4.3.4 operate this way. When total internal reflection occurs, there is no transmission of energy through the boundary. The fields of the wave do not, however, go abruptly to zero at the boundary. There is an *evanescent wave* on the other side of the boundary, the field

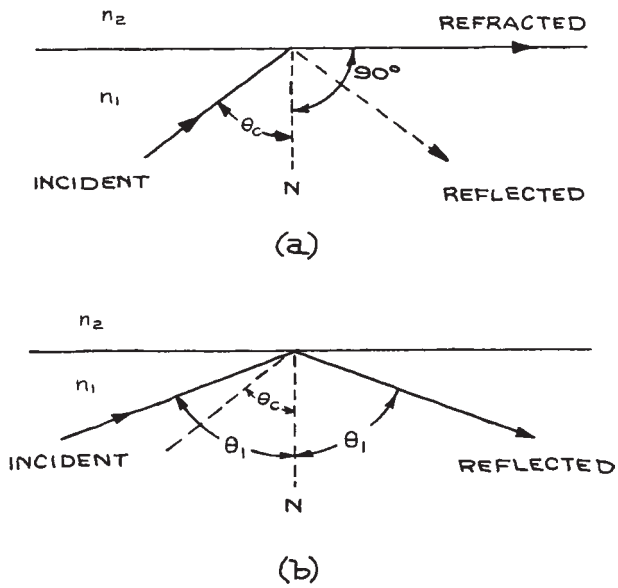

Figure 4.3 (a) Critical angle ($n_1 > n_2$); (b) total internal reflection ($n_1 > n_2$). *N* is the surface normal.

amplitudes of which decay exponentially with distance. For this reason, other optical components should not be brought too close to a totally reflecting surface, or energy will be coupled to them via the evanescent wave and the efficiency of total internal reflection will be reduced. With extreme care this effect can be used to produce a variable-reflectivity, totally internally reflecting surface, as can be seen in Figure 4.4. Studies of total internal reflection at interfaces are important in a number of optical measurement techniques, such as attenuated total (internal) reflection[9] and photon scanning tunneling microscopy.[10]

One or both of the media in Figure 4.2 may be anisotropic, like calcite, crystalline quartz, ammonium dihydrogen phosphate (ADP), potassium dihydrogen phosphate (KDP), or tellurium. Then the incident wave in general will split into two components, one of which obeys Snell's law directly (the ordinary wave) and one for which Snell's law is modified (the extraordinary wave). This phenomenon is called *double refraction*.[11–13]

If an optical system contains only planar interfaces, the path of a ray of light through the system can be easily calculated using only the law of reflection and Snell's law. This simple approach neglects diffraction effects,

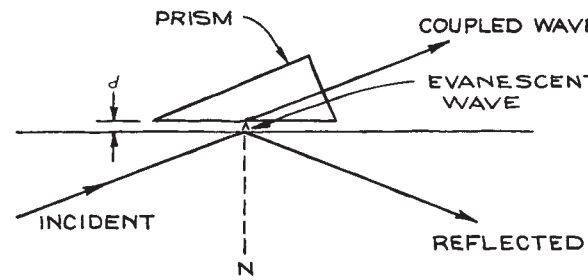

Figure 4.4 Schema of an evanescent-wave coupler. The amount of intensity reflected or coupled is varied by adjusting the spacing *d*; shown greatly exaggerated in the figure. This spacing is typically on the order of the wavelength. The surface boundary and adjacent prism face must be accurately flat and parallel.

which become significant unless the lateral dimensions (*apertures*) of the system are all much larger than the wavelength (say 10 times larger). The simple behavior of light rays in more complex systems containing nonplanar components, but where diffraction effects are negligible, can be described with the aid of *paraxial-ray* analysis.[14,15] Transmitted and reflected intensities and polarization states cannot be determined by the above methods and are most easily determined by the *method of impedances*.

4.2.2 Paraxial-Ray Analysis

A plane wave is characterized by a unique propagation direction given by the wave vector **k**. All fields associated with the wave are, at a given time, equal at all points in infinite planes orthogonal to the propagation direction. In real optical systems, ideal plane waves do not exist, as the finite size of the elements of the system restricts the lateral extent of the waves. Nonplanar optical components will cause further deviations of the wave from planarity. Consequently, the wave acquires a ray direction that varies from point to point on the phase front. The behavior of the optical system must be characterized in terms of the deviations its elements cause to the bundle of rays that constitute the propagating, laterally restricted wave. This is most easily done in terms of paraxial rays. In a cylindrically symmetric optical system (for example, a coaxial system of spherical lenses or mirrors), *paraxial rays* are those rays whose directions of propagation occur at sufficiently small angles θ to the symmetry axis of the system that it is possible to replace

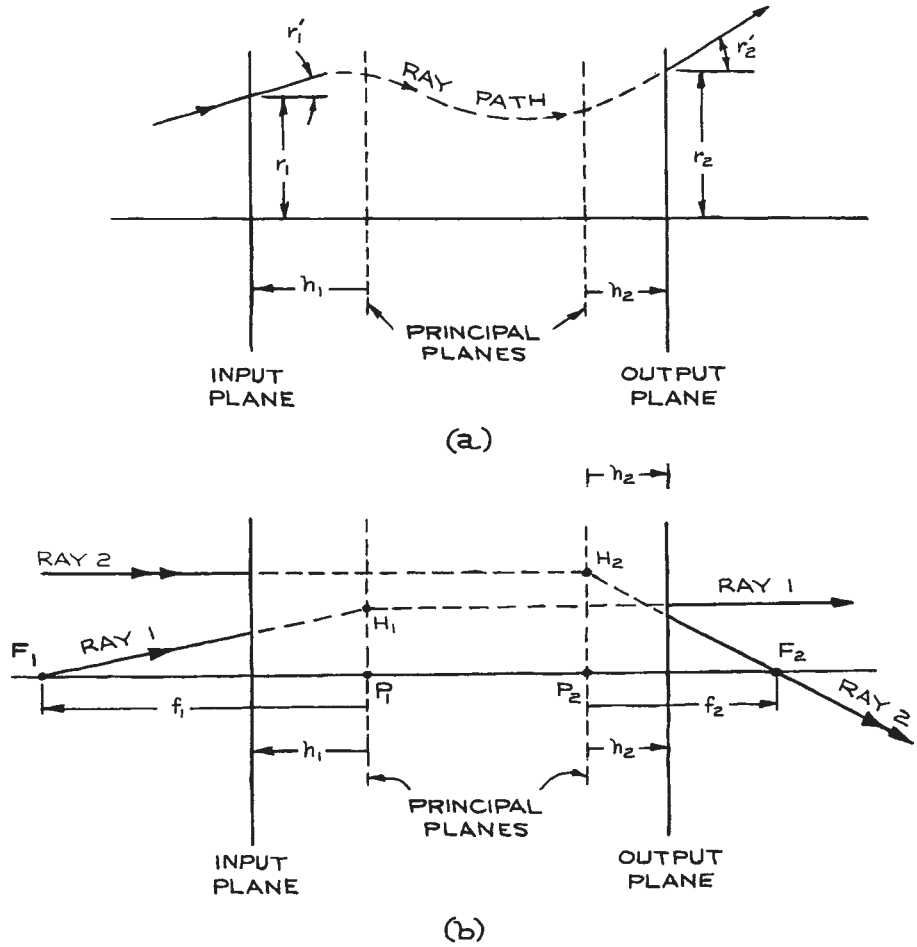

Figure 4.5 (a) Generalized schematic diagram of an optical system, showing a typical ray and its paraxial-ray parameters at the input and output planes; (b) focal points F_1 and F_2 and principal rays of a generalized optical system.

sin θ or tan θ by θ – in other words, paraxial rays obey the small-angle approximation:

$$\sin\theta \simeq \tan\theta \simeq \theta \tag{4.8}$$

Matrix Formulation. In an optical system whose symmetry axis is in the z-direction, a paraxial ray in a given cross-section (z = constant) is characterized by its distance r from the z-axis and the angle r' it makes with that axis. Suppose the values of these parameters at two planes of the system (an *input* and an *output* plane) are r_1, r'_1 and r_2, r'_2, respectively, as shown in Figure 4.5(a). Then in the paraxial-ray approximation, there is a linear relation between them of the form:

$$\begin{aligned} r_2 &= Ar_1 + Br'_1 \\ r'_2 &= Cr_1 + Dr'_1 \end{aligned} \tag{4.9}$$

or, in matrix notation:

$$\begin{pmatrix} r_2 \\ r'_2 \end{pmatrix} = \begin{pmatrix} A & B \\ C & D \end{pmatrix} \begin{pmatrix} r_1 \\ r'_1 \end{pmatrix} \tag{4.10}$$

Here:

$$\mathbf{M} = \begin{pmatrix} A & B \\ C & D \end{pmatrix} \tag{4.11}$$

is called the *ray transfer matrix*. If the media where the input and output ray parameters are measured have the same refractive index, then the determinant of the ray transfer matrix is unity, i.e., AD − BC = 1.

Optical systems made of isotropic material are generally reversible – a ray that travels from right to left with input parameters r_2, r'_2 will leave the system with parameters r_1, r'_1. Thus:

$$\begin{pmatrix} r_1 \\ r'_1 \end{pmatrix} = \begin{pmatrix} A' & B' \\ C' & D' \end{pmatrix} \begin{pmatrix} r_2 \\ r'_2 \end{pmatrix} \tag{4.12}$$

where the reverse ray transfer matrix is:

$$\begin{pmatrix} A' & B' \\ C' & D' \end{pmatrix} = \begin{pmatrix} A & B \\ C & D \end{pmatrix}^{-1} \tag{4.13}$$

The ray transfer matrix allows the properties of an optical system to be escribed in general terms by the location of its *focal points* and *principal planes*, whose location are determined from the elements of the matrix. The significance of these features of the system can be illustrated with the aid of Figure 4.5(b). An input ray that passes through the *first focal point* F_1 (or would pass through this point if it did not first enter the system) emerges traveling parallel to the axis. The intersection point of the extended input and output rays, point H_1 in Figure 4.5(b), defines the location of the *first principal plane*. Conversely, an input ray traveling parallel to the axis will emerge at the output plane and pass through the second focal point F_2 (or appear to have come from this point). The intersection of the extension of these rays, point H_2, defines the location of the *second principal plane*. Rays 1 and 2 in Figure 4.5(b) are called the *principal rays* of the system. The location of the principal planes allows the corresponding emergent ray paths to be determined, as shown in Figure 4.5(b). The dashed lines in this figure, which permit the geometric construction of the location of output rays 1 and 2, are called *virtual ray paths*. Both F_1 and F_2 lie on the axis of the system. The axis of the system intersects the principal planes at the *principal points*, P_1 and P_2, in Figure 4.5(b). The distance, f_1, from the first principal plane to the first focal point is called the *first focal length*; f_2 is called the *second focal length*.

In many practical situations, the refractive indices of the media to the left of the input plane (the *object space*) and to the right of the output plane (the *image space*) are equal. In this case, several simplifications arise:

$$\begin{aligned} f_1 = f_2 &= f = -\frac{1}{C} \\ h_1 &= \frac{D-1}{C} \\ h_2 &= \frac{A-1}{C} \end{aligned} \tag{4.14}$$

h_1 and h_2 are the distances of the input and output planes from the principal planes, measured in the sense shown in Figure 4.5(b).

Thus, if the elements of the transfer matrix are known, the location of the focal points and principal planes is determined. Graphical construction of ray paths through the system using the methods of paraxial *ray tracing* is then straightforward (see below).

In using the matrix method for optical analysis, a consistent sign convention must be employed. In the present discussion, a ray is assumed to travel in the positive z-direction from left to right through the system. The distance from the first principal plane to an object is measured positive from right to left – in the negative z-direction. The distance from the second principal plane to an image is measured positive from left to right – in the positive z-direction. The lateral distance of the ray from the axis is positive in the upward direction, negative in the downward direction. The acute angle between the system-axis direction and the ray, say r_1 in Figure 4.5(a), is positive if a counterclockwise motion is necessary to go from the positive z-direction to the ray direction. When the ray crosses a spherical interface, the radius of curvature is positive if the interface is convex to the input ray. The use of ray transfer matrices in optical-system analysis can be illustrated with some specific examples.

(i) Uniform optical medium. In a uniform optical medium of length d, no change in ray angle occurs, as illustrated in Figure 4.6(a); so:

$$\begin{aligned} r'_2 &= r'_1 \\ r_2 &= r_1 + dr'_1 \end{aligned} \tag{4.15}$$

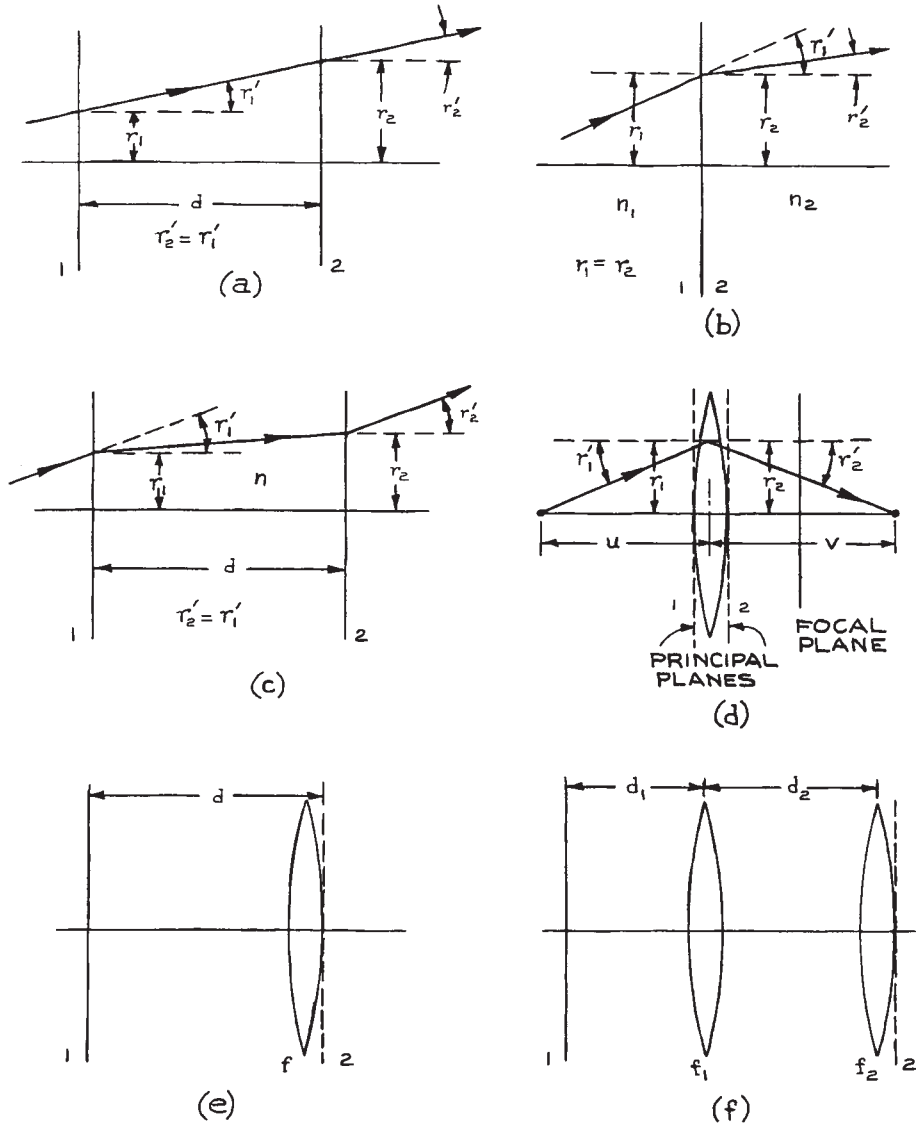

Figure 4.6 Simple optical systems for illustrating the application of ray transfer matrices, with input and output planes marked 1 and 2: (a) uniform optical medium; (b) planar interface between two different media; (c) a parallel-sided slab of refractive index n bounded on both sides with media of refractive index 1; (d) thins lens (r'_2 is a negative angle; for a thin lens, $r_2 = r_1$); (e) a length of uniform medium plus a thin lens; (f) two thin lenses.

Therefore:

$$\mathbf{M} = \begin{pmatrix} 1 & d \\ 0 & 1 \end{pmatrix} \tag{4.16}$$

The focal length of this system is infinite and it has no specific principal planes.

(ii) Planar interface between two different media. At the interface, as shown in Figure 4.6(b), we have $r_1 = r_2$, and from Snell's law, using the approximation $\sin\theta \simeq \theta$:

$$r'_2 = \frac{n_1}{n_2} r'_1 \tag{4.17}$$

Therefore:

$$\mathbf{M} = \begin{pmatrix} 1 & 0 \\ 0 & n_1/n_2 \end{pmatrix} \tag{4.18}$$

(iii) A parallel-sided slab of refractive index *n* bounded on both sides with media of refractive index I [Figure 4.6(c)]. In this case:

$$\mathbf{M} = \begin{pmatrix} 1 & d/n \\ 0 & 1 \end{pmatrix} \tag{4.19}$$

The principal planes of this system are the boundary faces of the optically dense slab.

(iv) Thick lens. The ray transfer matrix of the thick lens shown in Figure 4.7(a) is the product of the three transfer matrices:

$$\begin{aligned} \mathbf{M}_3\mathbf{M}_2\mathbf{M}_1 = {} & (\text{matrix for second spherical interface}) \\ & \times (\text{matrix for medium of length } d) \\ & \times (\text{matrix for first spherical interface}) \end{aligned} \tag{4.20}$$

Note the order of these three matrices; $\mathbf{M}_1$ comes on the right because it operates first on the column vector that describes the input ray.

At the first spherical surface:

$$n'(r'_1 + \phi_1) = nr = n(r''_2 + \phi_1) \tag{4.21}$$

and, since $\theta_1 = r_1/R_1$, this equation can be rewritten as:

$$r''_2 = \frac{nr'_1}{n} + \frac{(n' - n)r_1}{nR_1} \tag{4.22}$$

The transfer matrix at the first spherical surface is:

$$\mathbf{M}_1 = \begin{pmatrix} 1 & 0 \\ \dfrac{n' - n}{nR_1} & \dfrac{n'}{n} \end{pmatrix} = \begin{pmatrix} 1 & 0 \\ -\dfrac{D_1}{n} & \dfrac{n'}{n} \end{pmatrix} \tag{4.23}$$

where $D_1 = (n - n')/R_1$ is called the *power* of the surface. If R_1 is measured in meters, the units of D_1 are *diopters*.

In the paraxial approximation, all the rays passing through the lens travel the same distance d in the lens.

Thus:

$$\mathbf{M}_2 = \begin{pmatrix} 1 & d \\ 0 & 1 \end{pmatrix} \tag{4.24}$$

The ray transfer matrix at the second interface is:

$$\mathbf{M}_3 = \begin{pmatrix} 1 & 0 \\ \dfrac{n - n'}{n'R_2} & \dfrac{n}{n'} \end{pmatrix} = \begin{pmatrix} 1 & 0 \\ -\dfrac{D_2}{n'} & \dfrac{n}{n'} \end{pmatrix} \tag{4.25}$$

which is identical in form to $\mathbf{M}_1$. Note that in this case both r'_2 and R_2 are negative. The overall transfer matrix of the thick lens is:

$$\mathbf{M} = \mathbf{M}_3\mathbf{M}_2\mathbf{M}_1 = \begin{pmatrix} 1 - \dfrac{dD_1}{n} & \dfrac{dn'}{n} \\ \dfrac{dD_1D_2}{nn'} - \dfrac{D_1}{n'} & 1 - \dfrac{D_2}{n'} \end{pmatrix} \tag{4.26}$$

If Equations (4.26) and (4.14) are compared, it is clear that the locations of the principal planes of the thick lens are:

$$h_1 = \frac{d}{\dfrac{n}{n'}\left(1 + \dfrac{D_1}{D_2} - \dfrac{dD_1}{n}\right)} \tag{4.27}$$

$$h_2 = \frac{d}{\dfrac{n}{n'}\left(1 + \dfrac{D_2}{D_1} - \dfrac{dD_2}{n}\right)} \tag{4.28}$$

A numerical example will best illustrate the location of the principal planes for a biconvex thick lens. Suppose that:

$$\begin{aligned} n' &= 1(\text{air}),\ n = 1.5(\text{glass}) \\ R_1 &= -R_2 = 50\ \text{mm}, \\ d &= 10\ \text{mm} \end{aligned} \tag{4.29}$$

In this case, $D_1 = D_2 = 0.01$ mn and, from Equations (4.27) and (4.28), $h_1 = h_2 = 3.448$ mm. These principal

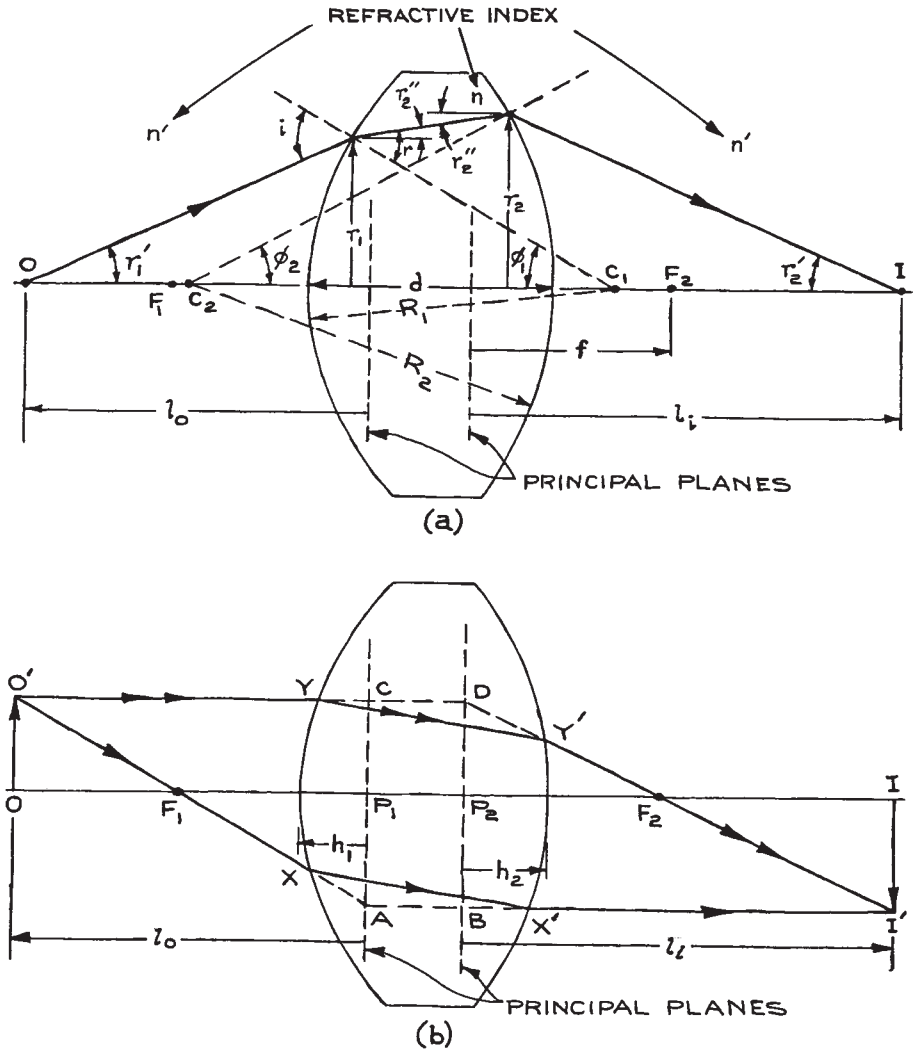

Figure 4.7 (a) Diagram illustrating ray propagation through a thick lens; (b) diagram showing the use of the principal planes to determine the principal-ray paths through the lens. The dashed paths *XABX′* and *YCDY′* are the virtual-ray paths; the solid lines *XX′* and *YY′* are the real-ray paths.

planes are symmetrically placed inside the lens. Figure 4.7(b) shows how the principal planes can be used to trace the principal-ray paths through a thick lens.

From Equation (4.26):

$$r'_2 = -\frac{r_1}{f} + \left(1 - \frac{dD_2}{n'}\right) r'_1 \qquad (4.30)$$

where the focal length is:

$$f = \left(\frac{D_1 + D_2}{n'} - \frac{dD_1D_2}{nn'}\right)^{-1} \qquad (4.31)$$

If l_0 is the distance from the object O to the first principal plane, and l_i the distance from the second principal plane to

the image I in Figure 4.7(b), then from the similar triangles $OO'F_1$, P_1AF_1, and P_2DF_2, $II'F_2$,

$$\frac{OO'}{II'} = \frac{OF_1}{F_1P_1} = \frac{l_0 - f_1}{f_1}$$
$$\frac{OO'}{II'} = \frac{P_2F_2}{F_2I} = \frac{f_2}{l_1 - f_2} \tag{4.32}$$

If the media on both sides of the lens are the same, then $f_1 = f_2 = f$ and it immediately follows that:

$$\frac{1}{l_0} + \frac{1}{l_i} = \frac{1}{f} \tag{4.33}$$

This is the fundamental imaging equation.

(v) Thin lens. If a lens is sufficiently thin that to a good approximation $d = 0$, the transfer matrix is:

$$\mathbf{M} = \begin{pmatrix} 1 & 0 \\ -\dfrac{D_1 + D_2}{n'} & 1 \end{pmatrix} \tag{4.34}$$

As shown in Figure 4.6(d), the principal planes of such a thin lens are at the lens. The focal length of the thin lens is f, where:

$$\frac{1}{f} = \frac{D_1 + D_2}{n'} = \left(\frac{n}{n'} - 1\right)\left(\frac{1}{R_1} - \frac{1}{R_2}\right) \tag{4.35}$$

so the transfer matrix can be written very simply as:

$$\mathbf{M} = \begin{pmatrix} 1 & 0 \\ -1/f & 1 \end{pmatrix}. \tag{4.36}$$

The focal length of the lens depends on the refractive indices of the lens material and of the medium within which it is immersed. In air:

$$\frac{1}{f} = (n-1)\left(\frac{1}{R_1} - \frac{1}{R_2}\right) \tag{4.37}$$

For a biconvex lens, R_2 is negative and:

$$\frac{1}{f} = (n-1)\left(\frac{1}{|R_1|} + \frac{1}{|R_2|}\right) \tag{4.38}$$

For a biconcave lens:

$$\frac{1}{f} = -(n-1)\left(\frac{1}{|R_1|} + \frac{1}{|R_2|}\right) \tag{4.39}$$

The focal length of any diverging lens is negative. For a thin lens the object and image distances are measured to a common point. It is common practice to rename the distances l_0 and l_i in this case, so that the imaging Equation (4.33) reduces to its familiar form:

$$\frac{1}{v} + \frac{1}{u} = \frac{1}{f} \tag{4.40}$$

Then u is called the object distance (or object *conjugate*) and v the image distance (or image conjugate).

(vi) A length of uniform medium plus a thin lens [Figure 4.6(e)]. This is a combination of the systems in (i) and (v); its overall transfer matrix is found from Equations (4.16) and (4.36) as:

$$\mathbf{M} = \begin{pmatrix} 1 & 0 \\ -1/f & 1 \end{pmatrix}\begin{pmatrix} 1 & d \\ 0 & 1 \end{pmatrix} = \begin{pmatrix} 1 & d \\ -1/f & 1 - d/f \end{pmatrix} \tag{4.41}$$

(vii) Two thin lenses. As a final example of the use of ray transfer matrices, consider the combination of two thin lenses shown in Figure 4.6(f). The transfer matrix of this combination is:

$$\begin{aligned} \mathbf{M} = {} & (\text{matrix of second lens}) \\ & \times (\text{matrix of uniform medium of length } d_2) \\ & \times (\text{matrix of first lens}), \\ & \times (\text{matrix of uniform medium of length } d_1) \end{aligned} \tag{4.42}$$

which can be shown to be:

$$\mathbf{M} = \begin{pmatrix} 1 - \dfrac{d_2}{f_1} & d_1 + d_2 - \dfrac{d_1 d_2}{f_1} \\ -\dfrac{1}{f_1} - \dfrac{1}{f_2} + \dfrac{d_2}{f_1 f_2} & 1 - \dfrac{d_1}{f_1} - \dfrac{d_2}{f_2} - \dfrac{d_1}{f_2} + \dfrac{d_1 d_2}{f_1 f_2} \end{pmatrix} \tag{4.43}$$

The focal length of the combination is:

$$f = \frac{f_1 f_2}{(f_1 + f_2) - d_2} \tag{4.44}$$

The optical system consisting of two thin lenses is the standard system used in analyses of the stability of lens waveguides and optical resonators.[14–16]

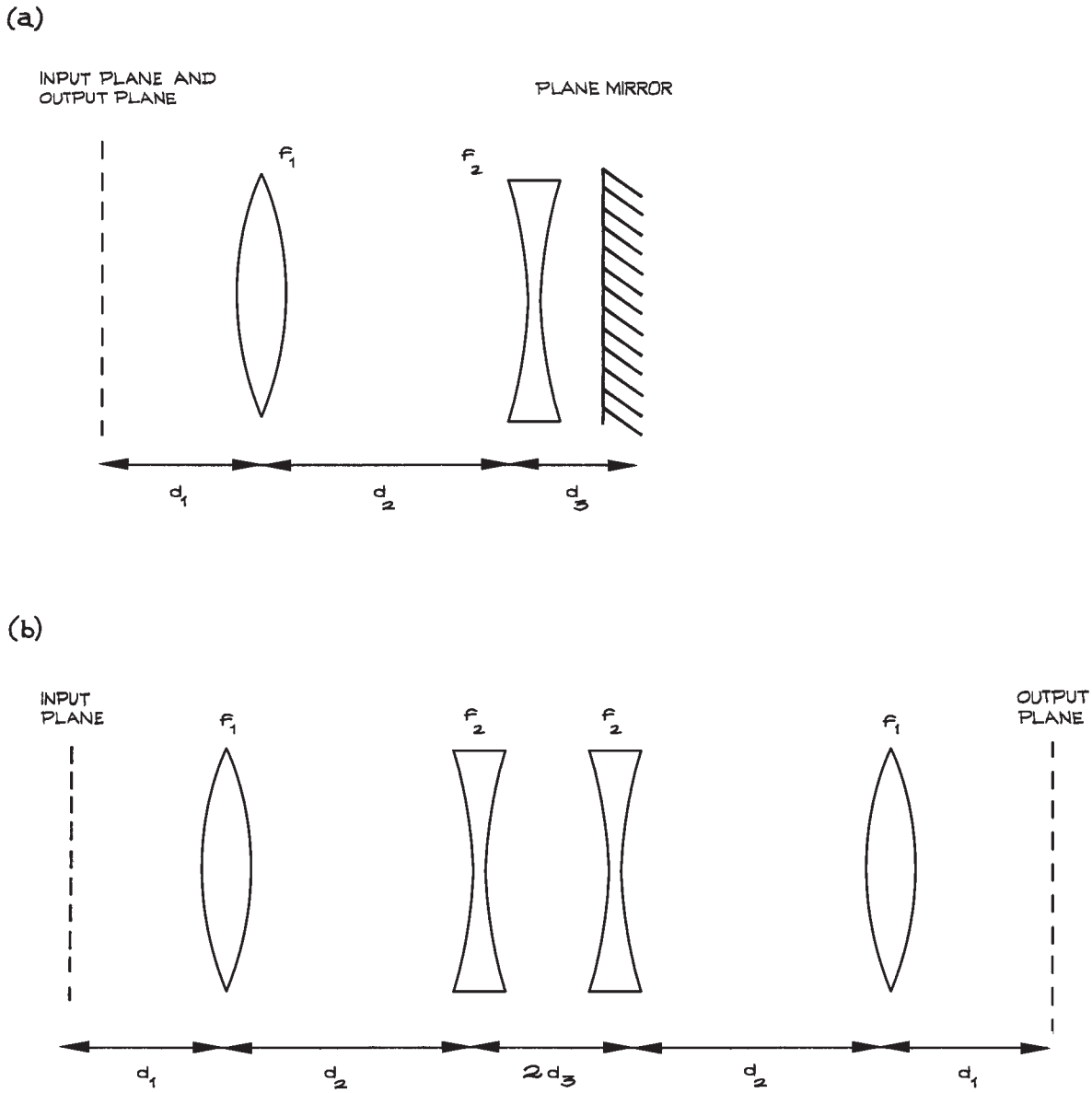

Figure 4.8 (a) A simple optical system with two lenses and a plane mirror; (b) the equivalent "unfolded" system that can be used for ray transfer matrix analysis.

(viii) Optical systems with plane mirrors. Optical systems in which a plane mirror is arranged perpendicular to the system axis are most easily analyzed by an *unfolding* technique. For, example if an optical system with ray transfer matrix **M** is terminated by a plane mirror, as shown in Figure 4.8(a), the "unfolded" system is as shown in Figure 4.8(b). The ray parameters at the original input plane, after a ray has

passed back through the systems can be found as follows:

$$\begin{pmatrix} r_2 \\ r'_2 \end{pmatrix} = \mathbf{M}_{\text{rev}}\mathbf{M}\begin{pmatrix} r_1 \\ r'_1 \end{pmatrix} \tag{4.45}$$

where $\mathbf{M}_{\text{rev}}$ is the ray transfer matrix for the optical system in the reverse direction. Equation (4.45) can be also written as

$$\begin{pmatrix} r_2 \\ r'_2 \end{pmatrix} = \mathbf{M}^{-1}\begin{pmatrix} 1 & 0 \\ 0 & -1 \end{pmatrix}\mathbf{M}\begin{pmatrix} r_1 \\ r'_1 \end{pmatrix} \tag{4.46}$$

(ix) Spherical mirrors. The object and image distances from a spherical mirror also obey Equation (4.40), where the focal length of the mirror is $R/2$; f is positive for a concave mirror, negative for a convex mirror. Positive object and image distances for a mirror are measured positive in the normal direction away from its surface. If a negative image distance results from Equation (4.40), this implies a *virtual image* (behind the mirror).

Ray Tracing. In designing an optical system, ray tracing is a powerful technique for analyzing the design and assessing its performance. Ray tracing follows the trajectories of light rays through the system. These light rays represent, at each point within the system, the local direction of energy flow, represented mathematically by the Poynting vector:

The trajectory of a light ray is governed by the laws of reflection and refraction. At a mirror surface the angle of reflection is equal to the angle of incidence. At the boundary between two media of different refractive index n_1, n_2, respectively, the angle of incidence, θ_1, and refraction, θ_2, are related by Snell's law[b]:

$$n_1 \sin\theta_1 = n_2 \sin\theta_2 \tag{4.47}$$

In a medium where the refractive index varies from point to point, Equation (4.47) still holds true, but it is better in this case to use the equation of light rays:

$$\frac{\mathrm{d}}{\mathrm{d}s}\left(n\frac{\mathrm{d}\mathbf{r}}{\mathrm{d}s}\right) = \text{grad } n \tag{4.48}$$

where s is the distance measured along the path of the light ray, and $n(\mathbf{r})$ is the index of refraction at point $\mathbf{r}$, measured with respect to the origin.[15]

Ray tracing provides an accurate description of the way light passes through an optical system unless diffraction effects become important. This happens when any apertures in the system become comparable in size to the wavelength, or when two adjacent apertures in the system subtend angles that are comparable to the diffraction angle.

At a surface of diameter $2a$, the diffraction angle for light of wavelength λ is:

$$\theta_{\text{diff}} = \frac{1.22\lambda}{2a_1} \tag{4.49}$$

This is the angular position of the first intensity minimum in the ring-shaped diffraction pattern that results when a plane-wave passes through a circular aperture. If a second aperture of diameter $2a_2$ is placed a distance d from the first, the angle subtended is:

$$\theta = \frac{2a_2}{d} \tag{4.50}$$

For diffraction to be negligible requires $\theta_{\text{diff}} << \theta$, which gives:

$$\frac{\lambda d}{4a_1a_2} << 1 \tag{4.51}$$

often called the Fresnel criterion.

Paraxial Ray Tracing. Practical implementation of paraxial-ray analysis in optical-system design can be very conveniently carried out graphically by *paraxial ray tracing*. In ray tracing a few simple rules allow geometrical construction of the principal-ray paths from an object point. (These constructions do not take into account the nonideal behavior, or *aberrations*, of real lenses, which will be discussed later.) The first principal ray from a point on the object passes through (or its projection passes through) the first focal point. From the point where this ray, or its projection, intersects the first principal plane, the output ray is drawn parallel to the axis. The actual ray path between input and output planes can be found in simple cases – for example, the path XX′ in the thick lens shown in Figure 4.7(b). The second principal ray is directed parallel to the axis; from the intersection of this ray, or its projection, with the second principal plane, the output ray passes through (or appears to have come from) the second focal point. The actual ray path between input and output planes can again be found in simple cases – for example, the path YY′ in the thick lens shown in Figure 4.7(b). The intersection of the two principal

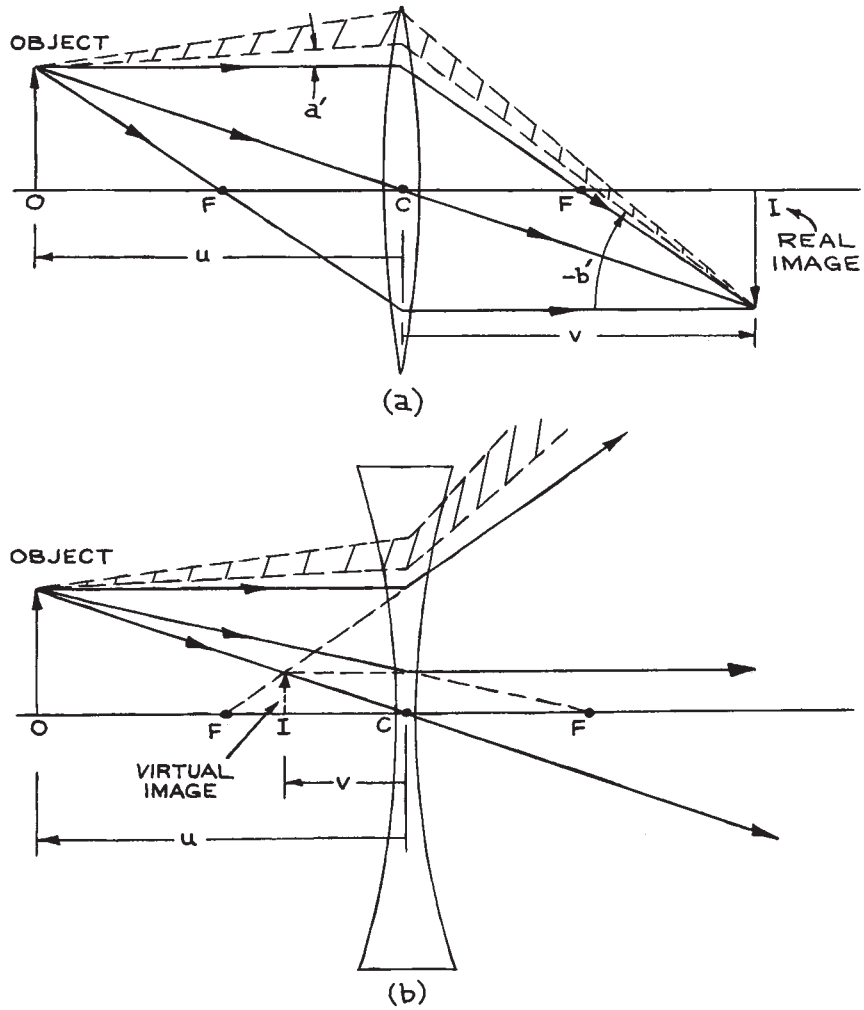

Figure 4.9 Ray-tracing techniques for locating image and ray paths for: (a) a converging thin lens; (b) a diverging thin lens. F = focal point; C = center of lens. The principal rays and a general ray pencil are shown in each case.

rays in the image space produces the image point that corresponds to the original point on the object. If only the back projections of the output principal rays appear to intersect, this intersection point lies on a *virtual* image.

In the majority of applications of paraxial ray tracing, a quick analysis of the system is desired. In this case, if all lenses in the system are treated as thin lenses, the position of the principal planes need not be calculated beforehand and ray tracing becomes particularly easy. For each lens, the position of the image of an object is obtained, and this image then becomes the "object" for the next lens, and so on. For a thin lens, a third principal ray is useful for determining the image location. The ray from a point on the object that passes through the center of the lens is not deviated by the lens.

The use of paraxial ray tracing to determine the size and position of the real image produced by a convex lens, and the virtual image produced by a concave lens are shown in Figure 4.9. Figure 4.9(a) shows a converging lens; the input

principal ray parallel to the axis actually passes through the focal point. Figure 4.9(b) shows a diverging lens; the above ray now emerges from the lens so as to appear to have come from the focal point. More complex systems of lenses can be analyzed the same way. Once the image location has been determined by the use of the principal rays, the path of any group of rays, a ray *pencil*, can be found. See, for example, the cross-hatched ray pencils shown in Figure 4.9.

The use of paraxial ray-tracing rules to analyze spherical-mirror systems is similar to those described above, except that the ray striking the center of the mirror in this case reflects so that the angle of reflection equals the angle of incidence. In all applications of ray tracing, a check on whether this is being done correctly involves examining the way in which a ray is bending at each surface. The refraction (or reflection) relative to the local surface normal should be in the correct direction.

Imaging and Magnification. Imaging systems include microscopes, telescopes, periscopes, endoscopes, and cameras. They aim to reproduce at a particular plane in the image space – the *image plane* – an exact replica in terms of relative spatial luminous intensity distribution and spectral content of an object located in the *object plane*. Each point on the object is imaged to a unique point in the image. The relative position and luminous intensity of points in the image plane preserve these qualities from their positions in the object plane. If the image is not a faithful, scaled replica of the object, then the imaging system suffers from *aberrations*.

In paraxial descriptions of an imaging system, often called the *Gaussian* description of the system, the ray transfer matrix from a point on the object to a point on the image can be written as:

$$\begin{pmatrix} r_2 \\ r'_2 \end{pmatrix} = \begin{pmatrix} A & B \\ C & D \end{pmatrix} \begin{pmatrix} r_1 \\ r'_1 \end{pmatrix} \tag{4.52}$$

For any ray angle of r'_1 leaving a point distant r_1 from the axis on the object, the ray in the image plane must pass through a point that is distant r_2 from the axis.

It is clear from Equation (4.52) that for this to be so, the element B of the ray transfer matrix must be zero. So:

$$r_2 = Ar_1 \tag{4.53}$$

The ratio of image height to object height is the *linear magnification* m so:

$$m = A = r_2/r_1 \tag{4.54}$$

Note that if the image is inverted, m is negative. The *angular magnification* of the system is defined as:

$$m' = \left(\frac{r'_2}{r'_1}\right)_{r_1 \to 0} \tag{4.55}$$

so $D = m'$.

If we use the focal length of the imaging system $f = -1/C$, then the ray transfer matrix is:

$$\begin{pmatrix} A & B \\ C & D \end{pmatrix} = \begin{pmatrix} m & 0 \\ -1/f & m' \end{pmatrix} \tag{4.56}$$

If the media in the space where the object is located (the object space) and the image space are the same then:

$$\det\begin{pmatrix} A & B \\ C & D \end{pmatrix} = 1 \tag{4.57}$$

which gives $mm' = 1$.

This is also a consequence of the conservation of brightness in an optical system, which will be discussed later.

In Figure 4.9(a) the ratio of the height of the image, b to the height of the object a is called the *magnification* m. In the case of a thin lens:

$$m = \frac{b}{a} = -\frac{v}{u} \tag{4.58}$$

Note that in Figure 4.9(a), b is negative. In Figure 4.9(b), v is negative, but b is positive. The ray transfer matrix M for a complete description of the imaging systems in Figure 4.9 includes the entire system from object O to image I. So, in Figure 4.9(a):

$$\begin{aligned} \mathbf{M} = &(\text{matrix for uniform medium of length } v) \\ &\times(\text{matrix for lens}) \\ &\times(\text{matrix for uniform medium of length } u) \end{aligned} \tag{4.59}$$

Imaging and Nonimaging Optical Systems. The techniques of optical-system analysis that we have discussed so far will provide an approximate description of simple systems. In many situations, however, a more detailed analysis is needed. Additional parameters are also introduced to characterize the system. More sophisticated

methods of analysis can be illustrated through a discussion of *imaging* and *nonimaging* optical systems.

In any experimental setup that involves the collection of light from a source and its delivery to a light detection system, the properties of the optical system between source and detector should be optimized. This optimization will take different forms depending on the application. For example, in an experiment in which a weak fluorescent signal from a liquid in a curvette is to be detected, it is generally the aim to maximize the amount of collected fluorescence and deliver this light to the active surface of the detector. This application does not require an *imaging* optical system, although an imaging system is often quite satisfactory. On the other hand, if an image of some object is being delivered to a CCD camera, then an imaging optical system is required.

4.2.3 Nonimaging Light Collectors

The properties of a *nonimaging* optical system can be described schematically with the aid of Figure 4.10. Light that enters the front aperture of the system within some angular range, will leave the system through the exit aperture. In such an arrangement, the *brightness* of the light leaving the exit aperture cannot exceed the brightness of the light entering the entrance aperture. The brightness of an emitting object is measured in units of $W\,m^{-2}$ *per steradian*. In Figure 4.10, if the brightness of the radiation entering the apertive is B_1(W $m^{-2}\,sr^{-1}$) then the power entering S_1 from the source is:

$$P_1 = \pi B_1 S_1 \theta_1^2 \tag{4.60}$$

where the angular range of the enetering rays is θ_1. Assuming that $R_1{}^2 >> S_1$, this angular range is $\theta_1 \simeq 1/R\sqrt{S_1/\pi}$, or $\theta_1^2 \simeq S_1/\pi R_1^2$. If all the power entering S_1 leaves through S_2, then the brightness of the emerging radiation is:

$$B_2 \simeq \frac{P_1}{\pi S_2 \theta_2^2} = \frac{\pi B_1 S_1 \theta_1^2}{\pi S_2 \theta_2^2} \tag{4.61}$$

where θ_2 is the angular spread of emerging rays. So:

$$B_2 = \frac{B_1 S_1 \theta_1^2}{S_2 \theta_2^2} \tag{4.62}$$

and if $B_2 \leq B_1$,

$$\theta_2 \geq \sqrt{\frac{S_2}{S_1}}\theta_1 \tag{4.63}$$

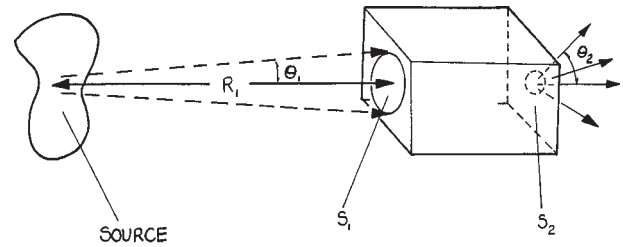

Figure 4.10 Generalized diagram of a nonimaging system. Light from the source enters the system though the aperture S_1 over an angular range defined by θ_1 and leaves through aperture S_2 over a range of angles defined by θ_2.

Practical examples of these devices are given in Section 4.3.3.

4.2.4 Imaging Systems

Generalized Imaging Systems. In a generalized imaging system, light from an object, located in the *object plane,* passes through the system until it reaches the *image plane*. In an ideal imaging system all the light rays that leave a point on the object arrive at a single point in the imaging plane. Furthermore, the locations of points in the image plane are such as to preserve the scaling of the image relative to the object. The image may be magnified or demagnified, but it should not be distorted.

A type of imaging called *aplanatic imaging* occurs when rays parallel to the axis produce a sharp image, independent of their distance from the axis. More specifically, if the angle of an input ray with the axis is θ_1 and the output angle with the axis θ_2, then an aplanatic system satisfies the *sine condition*, namely:

$$\frac{\sin\theta_1}{\sin\theta_2} = \text{constant} \tag{4.64}$$

for rays at all distances from the axis that can pass through the system. *Stigmatic imaging* is sharp imaging of a point object to a point image. An object point that is imaged to an image point are together called *conjugate points*.

The Numerical Aperture. If an optical system is illuminated by a point source on its axis, then the amount of light collected by the system depends on the angle that an effective aperture, called the *entrance pupil*, subtends at

the source. This concept will be discussed further in the next section. In Figure 4.11 this angle is defined by:

$$\sin\theta = \frac{D}{2u} \tag{4.65}$$

the *numerical* aperture of the system is:

$$NA = n\sin\theta \tag{4.66}$$

where n is the refractive index of the object space (which is generally 1, but could be higher – for example in microscopy, when an oil-immersion objective lens is used). Now, a good imaging system obeys the sine condition, which relates the angles subtended by the exit and entrance pupils and the magnification m by:

$$m = \frac{n\sin\theta}{n'\sin\theta'} \tag{4.67}$$

where the primed quantities refer to the image space. The numerical aperture in the image space is:

$$(NA)' = n'sin\theta' \tag{4.68}$$

The entrance pupil plays an important geometrical role in determining the amount of light from an object (or light source) that can enter and pass through an optical system. For example, for an entrance pupil diameter (EPD) of D_1 located a distance d_1 from a point source of light, the fraction of the light emitted by the source that will pass through the system is:

$$\mathcal{F} = \frac{1}{2}(1-\cos\theta) = \frac{1}{2}\left[1-\left(1+\frac{D^2}{4d^2}\right)^{-1/2}\right], \tag{4.69}$$

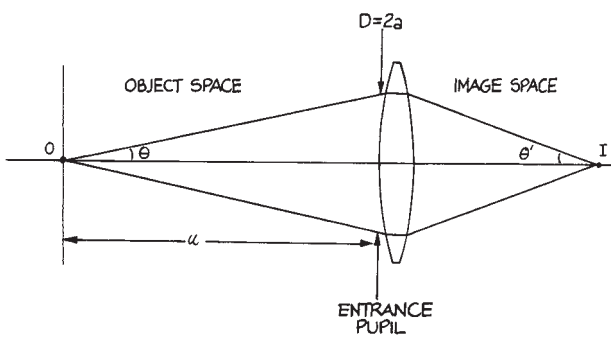

Figure 4.11 Single lens optical system to illustrate the concepts of numerical aperture and entrance pupil.

where θ is the angle shown in Figure 4.11. For $D << d$ Equation (4.69) reduces to:

$$\mathcal{F} = \frac{D^2}{16d^2} \tag{4.70}$$

For a lens, the ratio of focal length to EPD is called the *f*/number (*f*/#) of the lens. An *f*/1 lens has a ratio of its focal length to aperture (the open lens diameter) equal to unity. For a point source at the focal point of such a lens, $\mathcal{F} = 0.067$.

Apertures, Stops, and Pupils. Apertures control the ray trajectories that can pass through an optical system. The *aperture stop* is the aperture within the system that limits the angular spread, or diameter, of a cone of rays from an axial point on the object, which can pass through the system. Another aperture in the system may restrict the size or angular extent of an object that the system can image. Awareness of the position and size of these stops in an optical design is crucial in determining the light-gathering power of the system, and its ability to deliver light to an image or detector. The role of the aperture and field stop can be illustrated with Figure 4.12, which shows a single lens being used to image light from a distant object. The circular aperture behind the lens clearly limits the diameter of a bundle of rays from an axial point on the object and is clearly the aperture stop. The second stop, placed in the image plane, clearly controls the maximum angle at which rays from off-axis points on the object can pass through the system. This is the *field stop* in this case.

Whether a given aperture in an optical system is an aperture stop or a field stop is not always so easy to determine as was the case in Figure 4.12. Figure 4.13 shows a three-element optical system, which actually constitutes what is called a Gullstrand opthalmoscope[c]. The first lens closest to the object, called the *objective* lens, produces a real inverted image, which is then re-inverted by the *erector* lens, to form an image at the focal point of the *eyepiece* lens. Aperture *A* is the aperture stop, and clearly restricts the angular range of rays from an axial point on the object that can pass through the system. Aperture *B* restricts from what height on the object rays can originate, and still pass through the system. This aperture is acting as a field stop.

The *entrance pupil* is the image of the aperture stop produced by all the elements of the system between the aperture stop and the object. In Figure 4.13 the two

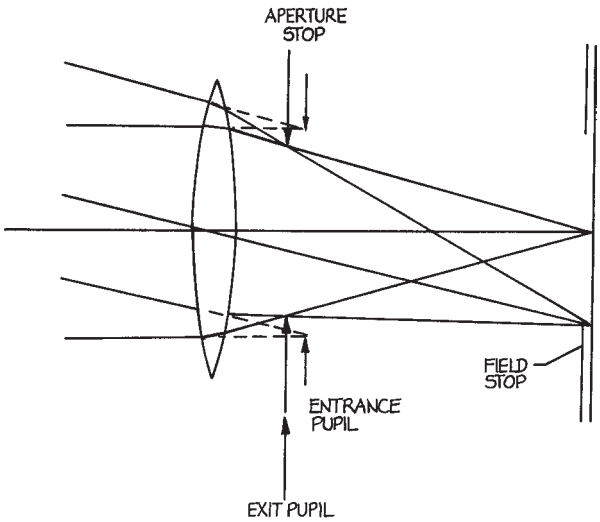

Figure 4.12 Single lens imaging system to illustrate the concepts of aperture stop, field stop, and entrance and exit pupils.

elements producing the image are the erector lens and objective lens. The *exit* pupil is the image of the aperture stop produced by all the elements between the aperture stop and the image, which in Figure 4.13 is just the eye lens. The size and location of the entrance and exit pupils determines the light-gathering and light-delivery properties of the system. For example, if the entrance pupil has diameter D, and lies a distance L from a point source of radiant power P (watts) then the power entering the entrance pupil is:

$$P_1 = \frac{P}{2}(1 - \cos\theta), \tag{4.71}$$

where $\tan\theta = D/2L$.

For a point source that is far from the entrance pupil this result becomes:

$$P_1 = \frac{PD_1^2}{16L^2}. \tag{4.72}$$

The solid angle subtended by the entrance pupil in this case is $\Delta\omega = D_1^2/4L^2$.

The light that leaves the system can be characterized by the total power that leaves the exit pupil, and the angular range of the rays that leave the exit pupil.

Somewhere in an imaging system there is always an *aperture stop*. This may be an actual aperture in an opaque thin screen placed on the system axis, or it may be the clear aperture of a lens or mirror in the system. In either case the aperture stop limits the range of rays that can pass through the system. This concept is illustrated in Figure 4.14. A ray of light such as A, that enters the system and just passes the edge of the aperture stop, is called a *marginal ray*. A ray such as B, that enters the system and passes through the center of the aperture stop, is called a *chief ray*. An aperture stop will always allow some light from every point on an object to reach the corresponding point on the image. If the amount of light from the edge of the object (say) that reaches the corresponding point or the object is severely reduced this is referred to as *vignetting*.

In Figure 4.13, a ray from an off-axis point on the object that passes through the center of the aperture stop is called the *principal ray* of the cone of light from the off-axis point.

The ray that enters the system half-way between the highest and lowest rays of an oblique beam is called the *chief*

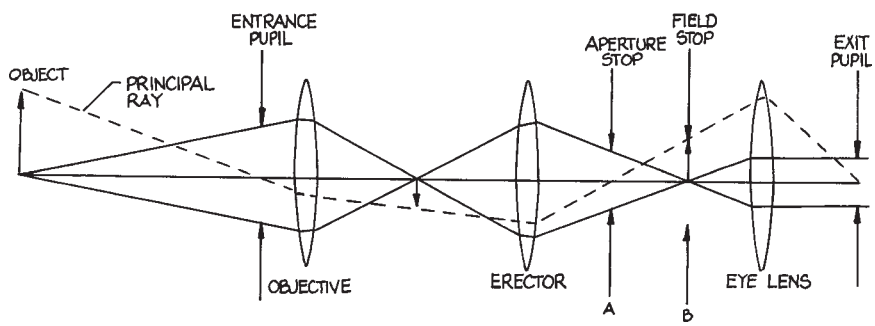

Figure 4.13 Three-lens imaging system showing an aperture stop, a field stop, and the location of the entrance and exit pupils.

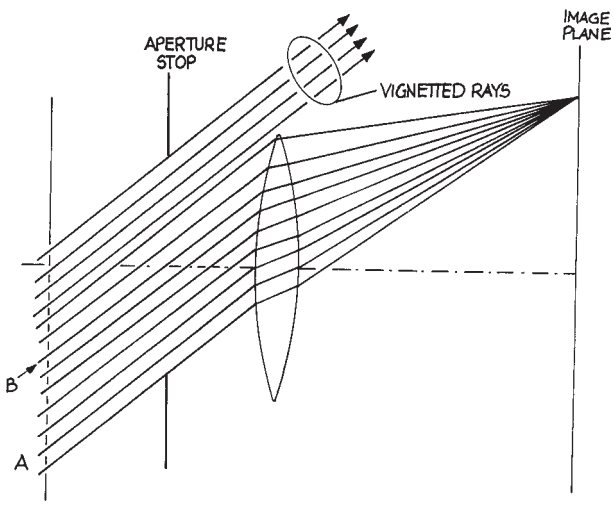

Figure 4.14 Aperture stop in front of a single lens showing vignetting of a family of rays from a distant off-axis point passing through the lens.

ray of the beam. In the absence of aberrations, the principal ray and chief ray are the same, and both pass through the center of the entrance pupil and aperture stop.

Vignetting. In our previous discussion we have simplified the actual performance of a real optical system, because for oblique rays passing through the system the roles of aperture and field stops become intertwined.

This can be illustrated with Figure 4.15, which shows a simple compound lens in which the apertures of the lenses themselves restrict the rays that can pass through the system. A family of oblique rays no longer fills the aperture stop, because the following lens is acting as a stop. This is called *vignetting*. In imaging systems it does not actually remove points of the object from the image but parts of the image that depend for their illumination on oblique rays (especially at large angles) become less bright. Vignetting is often deliberately allowed to occur in an imaging system so as to remove certain rays from the system that would otherwise suffer severe aberration.

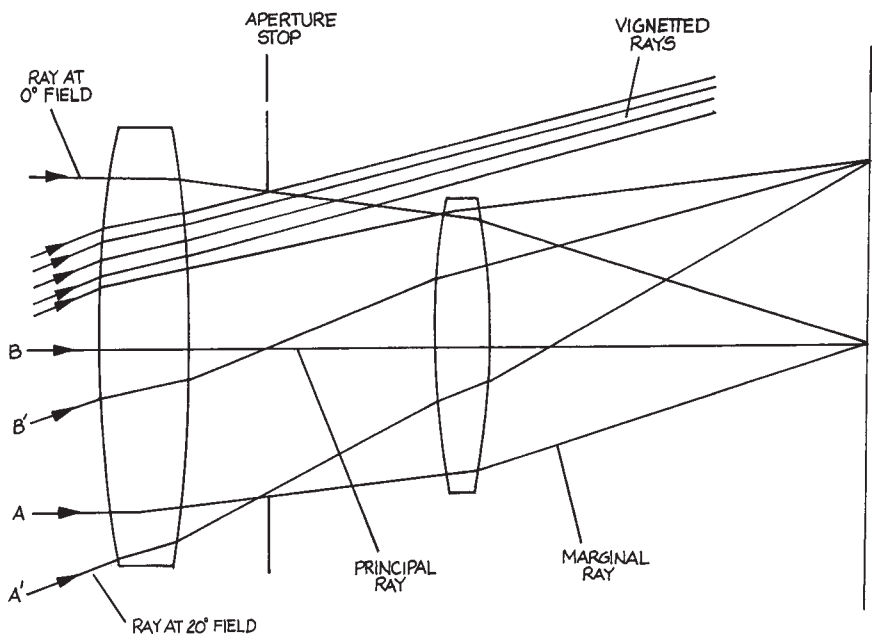

Figure 4.15 Two-lens imaging system showing aperture stop, principal and marginal rays, and vignetted rays.

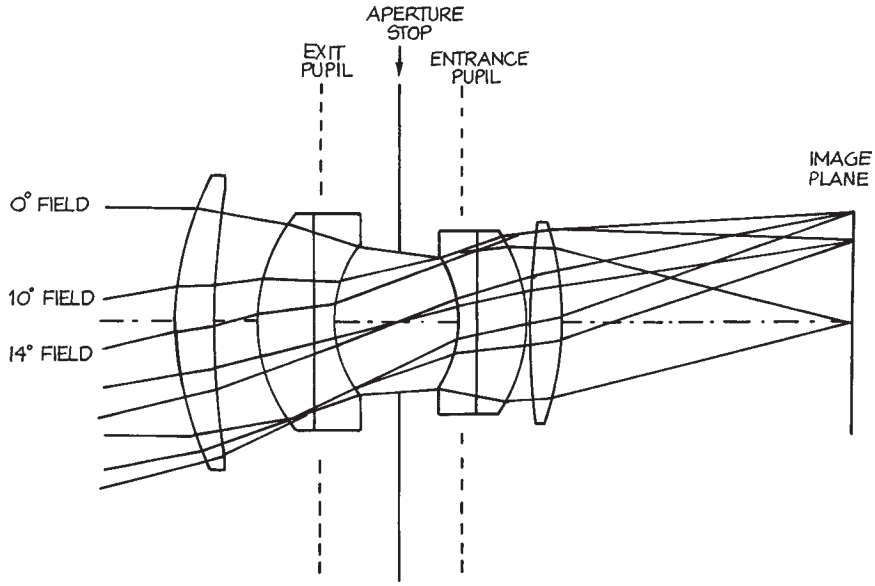

Figure 4.16 Double Gauss lens.

4.2.5 Exact Ray Tracing and Aberrations

If an imaging system is built with a series of lenses and/or mirrors, then there are inevitably various aberrations. For refraction at a spherical surface this results because, for angles of incidence and refraction θ_1, θ_2, respectively, when light travels from a medium with refractive index n_1 to one of refractive index n_2:

$$n_1 \sin\theta_1 = n_2 \sin\theta_2 \tag{4.73}$$

The paraxial approximation, which lacks aberrations, fails because $\theta_1 \neq \sin\theta_1$, whereas, in reality, $\sin\theta = \theta - \theta^3/3! + \theta^5/5! - \theta^7/7!$. The overall effect of aberrations can be greatly reduced, and some types of aberrations can be eliminated, by using several spherical surfaces, or in some situations by using an appropriate *aspheric* surface, a surface that is not part of a sphere but which is generally describable in terms of some other conic function or power series of the coordinates.

Analysis of imaging systems is most conveniently carried out using exact ray tracing techniques. In exact ray tracing the small-angle approximation, Equation (4.8), is not made and Snell's Law is solved exactly for each ray, at each interface.

By injecting many light rays into the system over some defining aperture or range of angles the performance of the system in imaging, focusing, light collection, or light delivery can be evaluated precisely. These days this procedure is carried out with optical design software. The most notable software packages in this regard are Code V[18], Zemax[19], Oslo[20], Solstis[21] and Optikwerk[22]. The wide availability of these software tools, and the essentially generic way in which they are used, makes a brief description of how they work and are used worthwhile. Just as an electronic circuit designer would be likely to evaluate a circuit with an analog design tool such as PSpice, or a digital design tool such as Cadence, Magic, or Xilinx, an optical designer can ultimately save time, and avoid mistakes, by numerical simulation of a design.

We will illustrate the use of numerical ray tracing using the set up procedures appropriate to Code V and with a specific example: a double Gauss lens used for imaging.

The various optical elements that make up a double Gauss lens are shown in Figure 4.16. For Code V analysis, the axial position, curvature, material, and aperture size (radius of each surface perpendicular to the axis) must be specified in an *optical table* shown in this case as Table 4.2. Note the entries that are specified in each column.

Table 4.2 Optical table for Code V analysis

Double Gauss – U.S. Patent 2, 532, 751

	RDY	THI	RMD	GLA	CCY	THC	GLC
> OBJ:	INFINITY	INFINITY			100	100	
1:	65.81739	8.746658		BSM24_OHARA	0	100	
2:	179.17158	9.100796			0	0	
3:	36.96542	12.424230		SK1_SCHOTT	0	100	
4:	INFINITY	3.776966		F15_SCHOTT	100	100	
5:	24.34641	15.135377			0	0	
STO:	INFINITY	12.869768			100	0	
7:	−27.68891	3.776966		F15_SCHOTT	0	100	
8:	INFINITY	10.833928		SK16_SCHOTT	100	100	
9:	−37.46023	0.822290			0	0	
10:	156.92645	6.858175		SK16_SCHOTT	0	100	
11:	−73.91040	63.268743			0	PIM	
IMG:	INFINITY	−0.279291			100	0	
SPECIFICATION DATA							
EPD	50.00000						
DIM	MM						
WL	656.30	587.60	486.10				
REF	2						
WTW	1	1	1				
XAN	0.00000	0.00000	0.00000				
YAN	0.00000	10.00000	14.00000				
VUY	0.00000	0.20000	0.40000				
VLY	0.00000	0.30000	0.40000				
REFRACTIVE INDICES							
GLASS CODE		656.30		587.60	486.10		
BSM24_OHARA		1.614254		1.617644	1.625478		
SK1_SCHOTT		1.606991		1.610248	1.617756		
F15_SCHOTT		1.600935		1.605648	1.616951		
SK16_SCHOTT		1.617271		1.620408	1.627559		
SOLVES							
PIM							
NO Pickups defined in system							
INFINITE CONJUGATES							
EFL	99.9866						
EFL	63.2687						
FFL	−17.7398						
FNO	1.9997						
IMG DIS	62.9895						
OAL	84.3452						
PARAXIAL IMAGE							
HT	24.9295						
ANG	14.0000						
ENTRANCE PUPIL							
DIA	50.0000						
THI	68.3242						
EXIT PUPIL							
DIA	58.0886						
THI	−52.8928						

With ray tracing software the various parameters of this lens system can be simultaneously optimized so as to produce the sharpest possible image of an object.

For the double Gauss lens, for example, the curvatures of the various surfaces, their spacings, and the type of glass used for each element can be simultaneously varied. In practice, various constraints must be included in this process: lens elements should not be too thick or too thin, and the glasses chosen must be available. The variable parameters for a glass are its refractive index n and its *dispersion* $dn/d\lambda$, both of which vary with wavelength.

The dispersion is frequently characterized by the Abbe V number, which provides a relative measure of dispersion:

$$V = \frac{n_d - 1}{n_F - n_C} \tag{4.74}$$

where the refractive index n is specified at the three wavelengths d (the helium d line at 587.6 nm), F (the hydrogen F line at 486.1 nm), and C (the hydrogen C line at 656.3 nm). Some of the standard wavelengths that are used in optical design are listed in Table 4.3. The different glasses that are available from a manufacturer are generally plotted on a glass chart, which plots $(n_d - 1)$ against V. Figure 4.17 shows such a chart for glasses available from Schott. Other major suppliers of optical glass are Corning, Hoya, and Ohara.

Two old classifications of glass into *crown* and *flint* glasses can be related to the glass chart. Crown glasses are glasses with a V value greater than 55 if $n_d < 1.6$ and $V > 50$ if $n_d > 1.6$. The flint glasses have V values below these limits. The rare-earth glasses contain rare-earths instead of SiO_2, which is the primary constituent of crown and flint glasses.

Table 4.3 Standard wavelengths used in optical design

Wavelength (nm)	Designation	Source
312.59		mercury
334.15		mercury
365.01	ℓ	mercury
404.66	h	mercury
435.83	g	mercury
479.99	F′	mercury
486.13	F	hydrogen
546.07	e	mercury
587.56	d	helium
589.29	D	sodium (doublet)
632.80		He-Ne laser
643.85	c′	cadmium
656.27	c	hydrogen
706.52	r	helium
852.11	s	cesium
1013.98	t	mercury
1060.00		neodymium laser
1529.58		mercury
1970.09		mercury
2325.42		mercury

Spot Diagram. If very many rays are launched from a point on the object so as to cover the entrance pupil of the system, the resulting pattern of ray intersections with the image plane is called the *spot diagram*. A tight spot diagram indicates that the effects of several aberrations, notably spherical, astigmatism, coma, and curvature of field have been markedly reduced. It must be remembered that this does not imply that the aberrations themselves have necessarily been eliminated, but that their effects have been reduced in the situation examined. A tighter spot diagram can always be produced by reducing the size of the entrance pupil.[d] Figure 4.18 shows such a spot diagram for a double Gauss lens being operated with a relatively large entrance pupil.

Chromatic Aberrations. Because, in general, the index of refraction increases with decreasing wavelength, the focal length of a singlet lens[e] will, for example, be shorter for blue light than it is for red light. This effect leads to imperfect imaging, so that in white light illumination both axial and off-axis object points will be imaged, not as bright points, but as regions that show blurring from red to blue. For axial object points this blurring is spherically symmetric and results from the image being closer to the lens for blue light than for red light. This is simple *chromatic aberration*. For off-axis object points, the magnification of the system varies with wavelength, leading to what is called *lateral color* or *transverse chromatic aberration*.

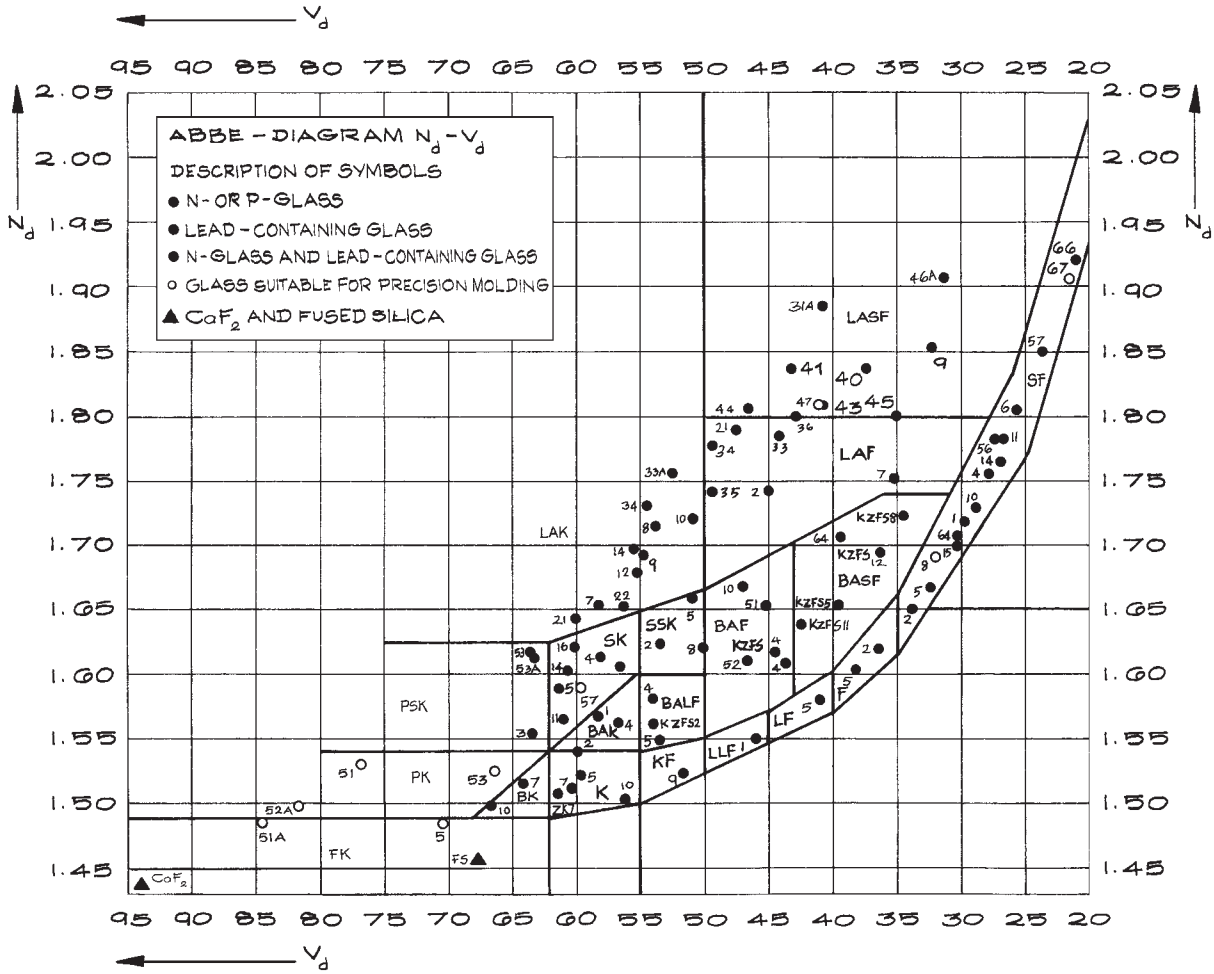

Figure 4.17 The glass chart for glasses available from Schott.

Chromatic aberration can be corrected for two colors (generally red and blue) and the imaging of axial points. Such lenses take the form of an achromatic doublet where a doublet lens is generally fabricated from a positive (converging) crown glass element and a negative (diverging) flint glass element.

If a compound lens is designed to remove chromatic aberration at three wavelengths it is called an *apochromat* and if correcting for four wavelengths a *superachromat*.

Achromatic doublets, because they have at least three spherical surfaces (or four in an air-spaced achromat), can also better correct for other aberrations than a singlet lens. Such lenses are available in a range of apertures and focal lengths from many manufacturers.

Geometrical Aberrations. In a perfect imaging system, all rays from a point on the object would pass through an identical point on the image and there

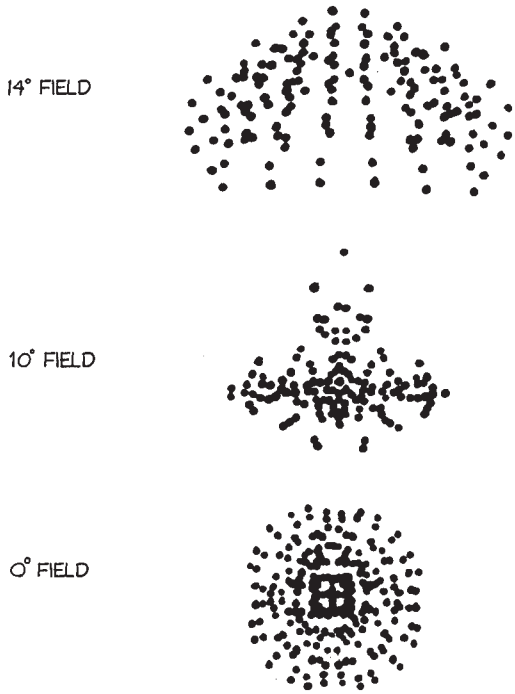

Figure 4.18 Spot diagrams for a double Gauss lens showing the spot diagrams for families of rays entering the lens at angles of 0°, 10°, and 14° – the *field angles*.

would be a linear relation between the coordinates of points on the image and corresponding points on the object.

For an axially symmetric system we can arbitrarily choose the object point in Figure 4.19 to be at the (x, y) point $(0, h)$ in the object. We take the polar coordinates of a ray from this point to a point P in the entrance pupil as (ρ, θ). In the general case this ray will intersect the image plane at point I' with coordinates in the image plane (x', y'). The aberrations $\Delta x'$, $\Delta y'$ are the displacements of (x', y') from the paraxial image point $I(x'_0, y'_0)$ for which there is a linear transformation from the coordinates of the point on the object. The lowest-order aberration terms contain terms in either h^3, $h^2\rho$, or $h\rho^2$ and are referred to as *third-order aberrations*. Although there are differences in terminology concerning these terms in the literature we can write (following Born and Wolf[11])

$$\Delta y' = B\rho^3 \cos\theta - Fh\rho^2(2 + \cos Z\theta) + (2C + D)h^2\rho\cos\theta - Eh^3 \quad (4.75)$$

$$\Delta x' = B\rho^3 \sin\theta - Fh\rho^2 \sin 2\theta + Dh^2\rho\sin\theta \quad (4.76)$$

The coefficients B, C, D, E, and F characterize the five *primary* or *Seidel* aberrations. Their magnitude in any given optical design can be calculated and visualized with ray tracing optical software.

Spherical Aberration $B \neq 0$. When all the coefficients in Equations (4.75) and (4.76) are zero except for B, the remaining effect is spherical aberration. This aberration is strikingly observed in the imaging of an axial point source, which will be imaged to a circular bright region whose radius reveals the extent of the aberration. For an axial point $h = 0$ and from Equations (4.75) and (4.76), $\Delta y' = B\rho^3 \cos\theta$, $\Delta x' = B\rho^3 \sin\theta$, which can be written as:

$$\Delta r = B\rho^3 \quad (4.77)$$

For focusing of parallel light the "best-form" singlet lens for minimum spherical aberration is close to convex-plane (with the convex surface towards the incoming parallel light).

Coma $F \neq 0$. Coma is the aberration in which the image of an off-axis point varies for rays passing through different regions of the entrance pupil. It is difficult to produce a lens where coma alone can be observed. The spot diagram in Figure 4.18 shows the characteristic "flaring" of the spot pattern, like a comet tail, which gives the aberration its name. Coma can be controlled by varying the curvatures of surfaces in the system.

Astigmatism $C \neq 0$. All the aberrations discussed so far are defects in the imaging of *meridional rays*, that is, rays in the plane containing the axis of the lens and the line from the object point through the center of the lens. The imaging is different for *sagittal rays*, that is, rays in the sagittal plane, which is perpendicular to the meridional plane, as illustrated in Figure 4.20. The

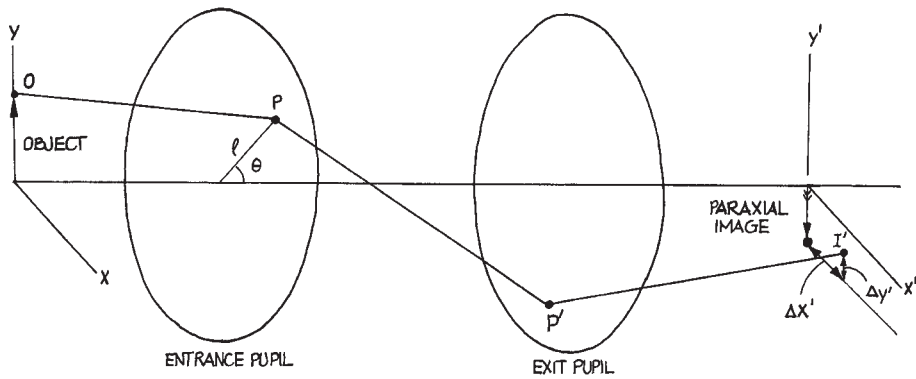

Figure 4.19 Diagram of a generalized imaging system used to discuss aberrations.

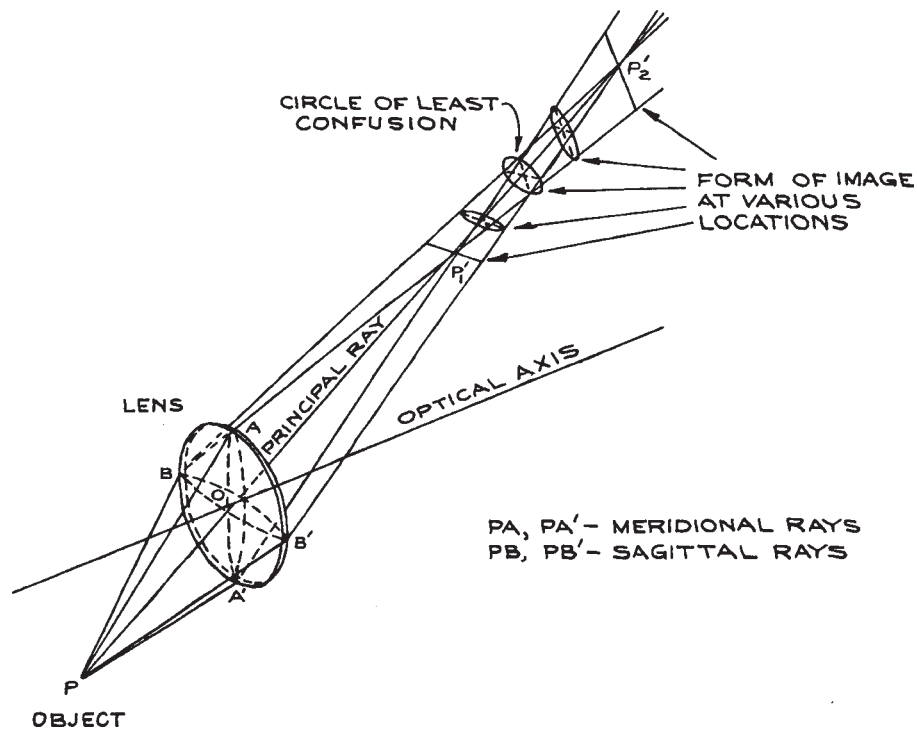

Figure 4.20 Illustrating astigmatism. Meridional rays *PA* and *PA'* are imaged at P'_1, sagittal rays *PB* and *PB'* are imaged at P'_2. (After A. C. Hardy and F. H. Perrin, *Principles of Optics*, McGraw-Hill, New York, 1932; by permission of McGraw-Hill Book Company, Inc.).

resulting aberration is called *astigmatism*. It can be controlled by lens curvature and refractive-index variations and by the use of apertures to restrict the range of angles and off-axis distances at which rays can traverse the lens.

Distortion, E $\neq$ 0. In distortion, the magnification varies across the image plane. The height of the image above the axis relative to the height of the object varies across the image.

Each object point appears as a point in the image, and the images of object points on a plane orthogonal to the axis are also on such a plane. The magnification of an object line segment may, however, vary with its distance from the axis. This is called *distortion*. It takes two common forms: *pincushion* and *barrel* distortion, as illustrated in Figure 4.21. Distortion is sensitive to the lens shape and spacing, and to the size and position of apertures in the system – called *stops*.

For further details of aberrations and how to deal with them, we refer the reader to specialized texts on optics (especially lens design), such as those by Born and Wolf,[11] Ditchburn,[23] Levi,[24] Smith,[25,26] Shannon,[27] and Laikin.[28]

Curvature of Field, D $\neq$ 0. In this aberration, the image of a plane object perpendicular to the axis is sharp over a curved surface in the image space.

Modulation Transfer Function. A common way of characterizing the performance of an imaging system is through its *modulation transfer function* or MTF. This refers to the ability of the system to replicate in the image, periodic features in the object. An optical test pattern used to show this consists of a series of white and black bands. These bands will be smeared out in the image to a greater or lesser extent because of aberrations, and ultimately, if geometrical aberrations are absent, by diffraction.

The relative brightness of the object and image will appear schematically as shown in Figure 4.22. We can

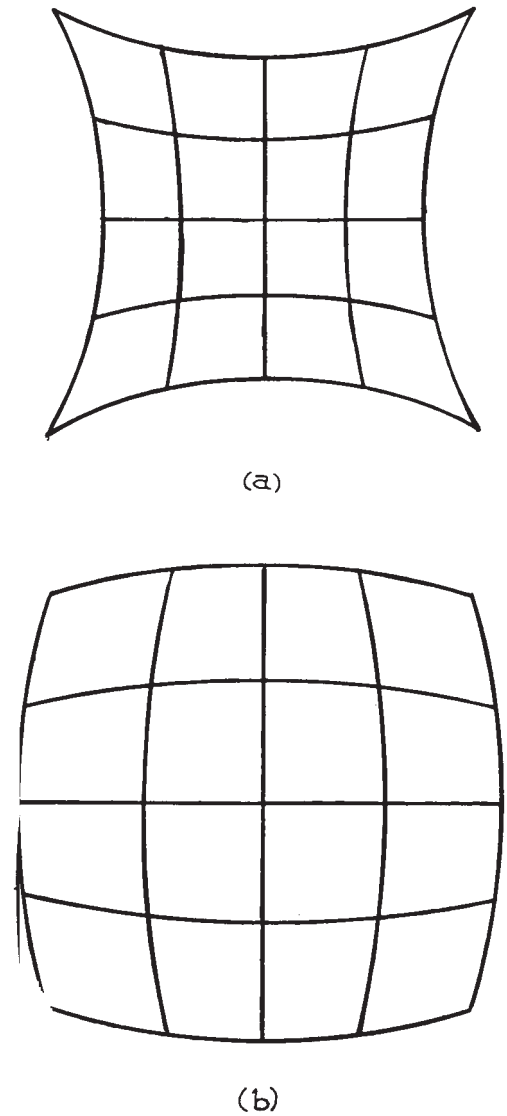

Figure 4.21 (a) "Pincushion" distortion; (b) "barrel" distortion.

characterize the *visibility*, *contrast* or *modulation* of the image as:

$$\text{visibility} = \frac{\max - \min}{\max + \min} \tag{4.78}$$

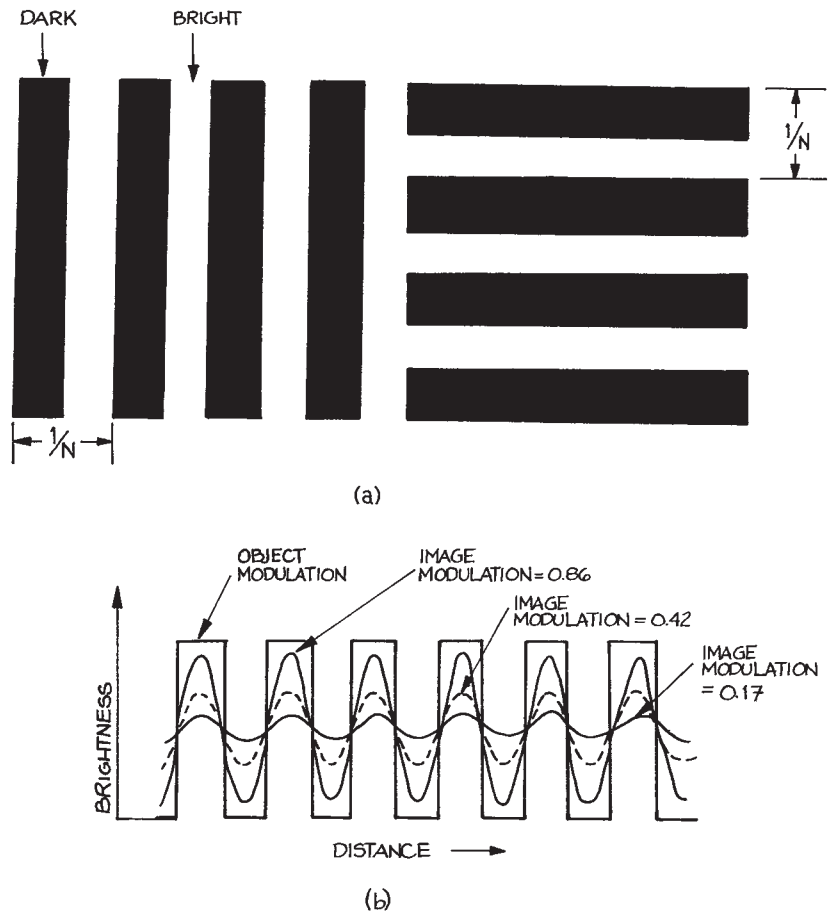

Figure 4.22 (a) An object with sharp contrast between bright and dark bands; (b) the corresponding image brightness variation for differing degrees of modulation.

If the visibility is plotted versus the number of lines per millimeter in the object in this case, this shows the modulation transfer function. Figure 4.23 shows an example for the double Gauss lens system shown in Figure 4.16. The MTF is ultimately limited by diffraction. In this case, for a pattern with v lines per millimeter:

$$\mathrm{MTF}(v) = \frac{1}{\pi}(2\phi - \sin 2\phi) \tag{4.79}$$

where

$$\phi = \cos^{-1}\left(\frac{\lambda_0 v}{2\mathrm{NA}}\right) \tag{4.80}$$

In Equation (4.80) λ_0 is measured in mm and NA is the numerical aperture of the system.

A quantity, closely related to the MTF, for charactering MTF, and also the focusing of a light beam, or laser beam, is the *Strehl ratio*. The Strehl ratio is the ratio of the

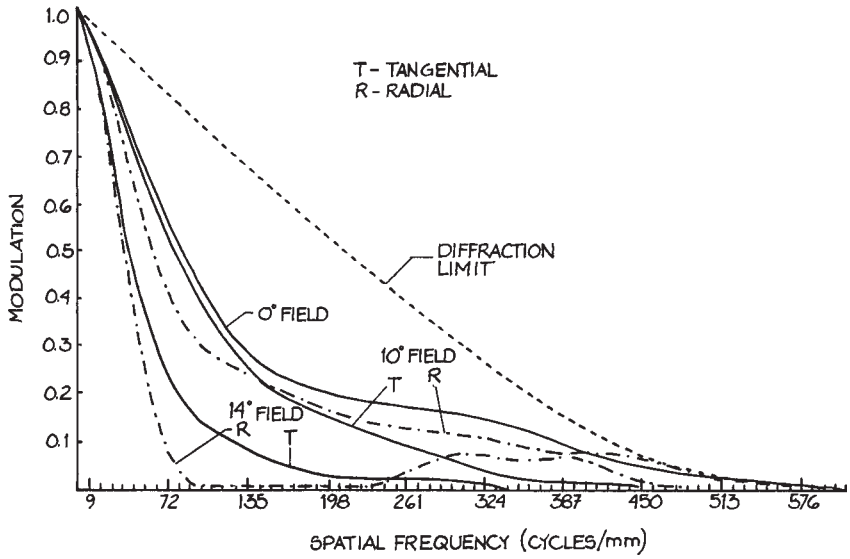

Figure 4.23 Modulation transfer function (MTF) for a double Gauss lens. The MTF for 0°, 10°, and 14° fields in both the tangential and radial directions are shown, and also the diffraction limit of an aberration-free system.

illumination at the center of a focused or circular image to the illumination of an equivalent unaberrated image. The interested reader can see a more detailed discussion in Smith.[25]

4.2.6 The Use of Impedances in Optics

The method of impedances is the easiest way to calculate the fraction of incident intensity transmitted and reflected in an optical system. It is also the easiest way to follow the changes in polarization state that result when light passes through an optical system.

As we have seen in Section 4.1, the impedance of a plane wave traveling in a medium of relative permeability μ_r, and dielectric constant ϵ_r is:

$$Z = \sqrt{\frac{\mu_r \mu_0}{\epsilon_r \epsilon_0}} = Z_0 \sqrt{\frac{\mu_r}{\epsilon_r}} \tag{4.81}$$

If $\mu_r = 1$, as is usually the case for optical media, the impedance can be written as:

$$Z = Z_0/n \tag{4.82}$$

This impedance relates the transverse **E** and **H** fields of the wave:

$$Z = \frac{E_{tr}}{H_{tr}} \tag{4.83}$$

When a plane wave crosses a planar boundary between two different media, the components of both **E** and **H** parallel to the boundary have to be continuous across that boundary. Figure 4.24(a) illustrates a plane wave polarized in the plane of incidence striking a planar boundary between two media of refractive indices n_1 and n_2. In terms of the magnitudes of the vectors involved:

$$E_i \cos\theta_1 + E_r \cos\theta_1 = E_t \cos\theta_2 \tag{4.84}$$

$$H_i - H_r = H_t \tag{4.85}$$

Equation (4.82) can be written as:

$$\frac{E_i}{Z_1} - \frac{E_r}{Z_1} = \frac{E_t}{Z_2} \tag{4.86}$$

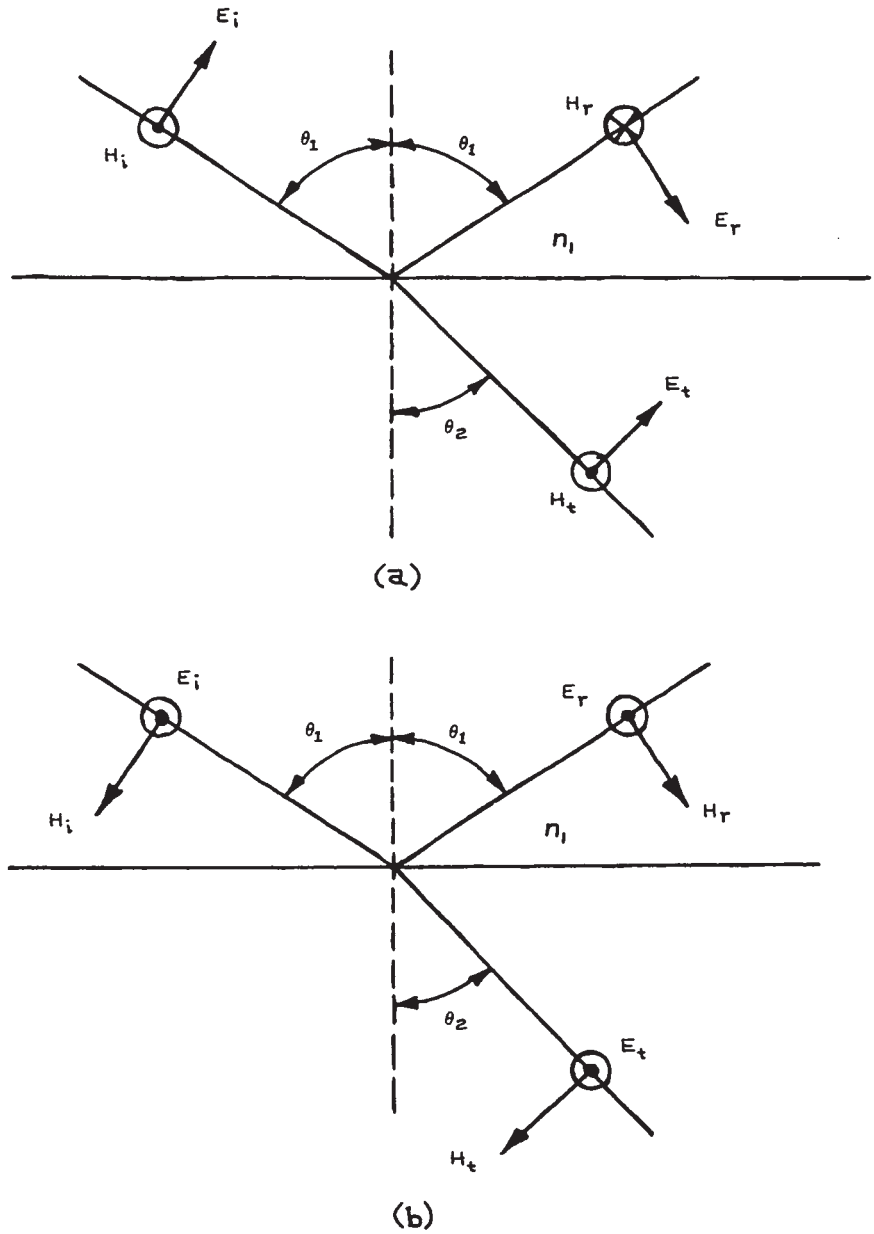

Figure 4.24 Reflection and refraction at a planar boundary between two different dielectric media: (a) wave polarized in the plane of incidence (*P*-polarization); (b) wave polarized perpendicular to the plane of incidence (*S*-polarization).

It is easy to eliminate E_t between Equations (4.84) and (4.86) to give:

$$\rho = \frac{E_r}{E_i} = \frac{Z_2 \cos\theta_2 - Z_1 \cos\theta_1}{Z_2 \cos\theta_2 + Z_1 \cos\theta_1} \tag{4.87}$$

where ρ is the *reflection coefficient* of the surface. The fraction of the incident energy reflected from the surface is called the reflectance, $R = \rho^2$. Similarly, the *transmission coefficient* of the boundary is:

$$\tau = \frac{E_t \cos\theta_2}{E_i \cos\theta_1} = \frac{2Z_2 \cos\theta_2}{Z_2 \cos\theta_2 + Z_1 \cos\theta_1} \tag{4.88}$$

By a similar treatment applied to the geometry shown in Figure 4.24(b), it can be shown that for a plane wave polarized perpendicular to the plane of incidence:

$$\rho = \frac{E_r}{E_i} = \frac{Z_2 \sec\theta_2 - Z_1 \sec\theta_1}{Z_2 \sec\theta_2 + Z_1 \cos\theta_1} \tag{4.89}$$

$$\tau = \frac{2Z \sec\theta_2}{Z_2 \sec\theta_2^2 + Z_1 \sec\theta_1} \tag{4.90}$$

If the effective impedance for a plane wave polarized in the plane of incidence (*P-polarization*)[f] and incident on a boundary at angle θ is defined as:

$$Z' = Z \sec\theta \tag{4.91}$$

and for a wave polarized perpendicular to the plane of incidence (*S-polarization*)[g] as:

$$Z' = Z \sec\theta \tag{4.92}$$

then a universal pair of formulae for ρ and τ results:

$$\rho = \frac{Z'_2 - Z'_1}{Z'_1 + Z'_2} \tag{4.93}$$

$$\tau = \frac{2Z'_2}{Z'_1 + Z'_2} \tag{4.94}$$

It will be apparent from an inspection of Figure 4.24 that Z' is just the ratio of the electric-field component parallel to the boundary and the magnetic-field component parallel to the boundary. For reflection from an ideal mirror, $Z'_2 = 0$.

In normal incidence, Equations (4.87) and (4.89) become identical and can be written as:

$$\rho = \frac{Z_2 - Z_1}{Z_2 + Z_1} = \frac{n_1 - n_2}{n_1 + n_2} \tag{4.95}$$

Note that there is a change of phase of π in the reflected field relative to the incident field when $n_2 > n_1$.

Since intensity $\propto$ (electric field)^2, the fraction of the incident energy that is reflected is:

$$R = \rho^2 = \left(\frac{n_1 - n_2}{n_1 - n_2}\right)^2 \tag{4.96}$$

R increases with the index mismatch between the two media, as shown in Figure 4.25. If there is no absorption of energy at the boundary, the fraction of energy transmitted, called the *transmittance*, is

$$T = 1 - R = \frac{4n_1 n_2}{(n_1 + n_2)^2} \tag{4.97}$$

Note that because the media on the two sides of the boundary are different, $T \neq |\tau|^2$.

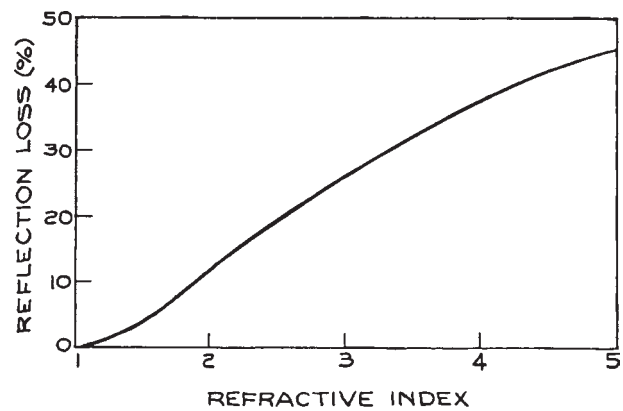

Figure 4.25 Reflection loss per surface for normal incidence as a function of refractive index.

Reflectance for Waves Incident on an Interface at Oblique Angles. If the wave is not incident normally, it must be decomposed into two linearly polarized components, one polarized in the plane of incidence, and the other polarized perpendicular to the plane of incidence.

For example, consider a plane-polarized wave incident on an air glass ($n = 1.5$) interface at an angle of incidence of 30°, with a polarization state exactly intermediate between the *S*-polarization and the *P*-polarization. The angle of refraction at the boundary is found from Snell's law:

$$\sin\theta_2 = \frac{\sin 30^\circ}{1.5} \tag{4.98}$$

and so $\theta_2 = 19.47^\circ$.

The effective impedance of the *P*-component in the air is:

$$Z'_{P1} = 376.7\cos\theta_1 = 326.23\,\Omega \tag{4.99}$$

and in the glass:

$$Z'_{P2} = \frac{376.7}{1.5}\cos\theta_2 = 236.77\Omega \tag{4.100}$$

Thus, from Equation (4.87), the reflection coefficient for the *P*-component is:

$$\rho_P = \frac{236.77 - 326.33}{236.77 + 326.23} = -0.159 \tag{4.101}$$

The fraction of the intensity associated with the *P*-component that is reflected is ${\rho_P}^2 = 0.0253$.

For the *S*-component of the input wave:

$$Z'_{S1} = \frac{376.7}{\cos\theta_1} = 434.98\Omega \tag{4.102}$$

$$\begin{aligned} Z'_{S2} &= \frac{376.7}{1.5\cos\theta_2} = 266.37\Omega \\ \rho_S &= \frac{266.37 - 434.98}{266.37 + 434.98} = -0.240 \end{aligned} \tag{4.103}$$

The fraction of the intensity associated with the *S*-polarization component that is reflected is ${\rho_S}^2 = 0.0578$. Since the input wave contains equal amounts of *S*- and *P*-polarization, the overall reflectance in this case is:

$$R = <\rho^2>_{\text{av}} = 0.0416 \simeq 4\% \tag{4.104}$$

Note that the reflected wave now contains more *S*-polarization than *P*, so the polarization state of the reflected wave has been changed – a phenomenon that will be discussed further in Section 4.3.6.

Brewster's Angle. Returning to Equation (4.87), it might be asked whether the reflectance is ever zero. It is clear that ρ will be zero if:

$$n_1\cos\theta_2 = n_2\cos\theta_1 \tag{4.105}$$

which, from Snell's law [Equation (4.6)], gives:

$$\cos\theta_1 = \frac{n_1}{n_2}\sqrt{1 - \left(\frac{n_1}{n_2}\right)^2\sin^2\theta_1} \tag{4.106}$$

giving the solution:

$$\theta_1 = \theta_B = \arcsin\sqrt{\frac{n_2^2}{n_1^2 + n_2^2}} = \arctan\frac{n_2}{n_1} \tag{4.107}$$

The angle θ_B is called *Brewster's angle*. A wave polarized in the plane of incidence and incident on a boundary at this angle is totally transmitted. This allows the design of low-reflection-loss windows in laser systems, as will be seen in Section 4.6.2. If Equation (4.89) is inspected carefully, it will be seen that there is no angle of incidence that yields zero reflection for a wave polarized perpendicular to the plane of incidence.

Transformation of Impedance through Multilayer Optical Systems. The impedance concept allows the reflection and transmission characteristics of multilayer optical systems to be evaluated very simply. If the incident light is incoherent (a concept discussed in more detail later in Section 4.5.1), then the overall transmission of a multilayer structure is just the product of the transmittances of its various interfaces. For example, an air–glass interface transmits

about 96% of the light in normal incidence. The transmittance of a parallel-sided slab is $0.96 \times 0.96 = 92\%$. This simple result ignores the possibility of interference effects between reflected and transmitted waves at the two faces of the slab. If the faces of the slab are very flat and parallel, and if the light is coherent, such effects cannot be ignored. In this case, the method of transformed impedances is useful.

Consider the three-layer structure shown in Figure 4.26(a). The path of a ray of light through the structure is shown. The angles θ_1, θ_2, and θ_3 can be calculated from Snell's law. As an example, consider a wave polarized in the plane of incidence. The effective impedances of media 1, 2, and 3 are

$$\begin{aligned} Z'_1 &= Z_1 \cos\theta_1 = \frac{Z_0 \cos\theta_1}{n_1} \\ Z'_2 &= Z_2 \cos\theta_2 = \frac{Z_0 \cos\theta_2}{n_2} \\ Z'_3 &= Z_3 \cos\theta_3 = \frac{Z_0 \cos\theta_3}{n_3} \end{aligned} \tag{4.108}$$

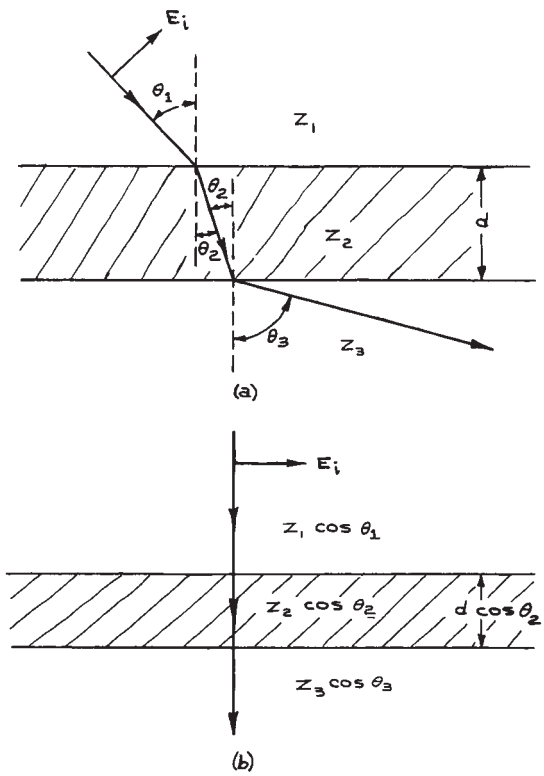

Figure 4.26 (a) Wave polarized in the plane of incidence passing through a dielectric slab of thickness d and impedance Z_2 separating two semi-infinite media of impedances Z_1 and Z_3, respectively; (b) equivalent structure for normal incidence.

It can be shown that the reflection coefficient of the structure is exactly the same as for the equivalent structure in Figure 4.26(b) in normal incidence, where the effective thickness of layer 2 is now:

$$d' = d \cos\theta_2 \tag{4.109}$$

The reflection coefficient of the structure can be calculated from its equivalent structure using the transformed impedance concept.[15,29]

The transformed impedance of medium 3 at the boundary between media 1 and 2 is:

$$Z''_3 = Z'_2 \left(\frac{Z'_3 \cos k_2 d' + iZ'_2 \sin k_2 d'}{Z'_2 \cos k_2 d' + iZ'_3 \sin k_2 d'} \right) \tag{4.110}$$

where $k_2 = 2\pi/\lambda_2 = 2\pi n_2/\lambda_0$. The reflection coefficient of the whole structure is now just:

$$\rho = \frac{Z''_3 - Z'_1}{Z''_3 + Z'_1} \tag{4.111}$$

the reflectance of the whole structure is $R = |\rho|^2$, and its transmittance is:

$$T = 1 - R \tag{4.112}$$

In a structure with more layers, the transformed impedance formula [Equation (4.108)] can be used sequentially, starting at the last optical surface and working back to the first. More examples of the use of the technique of transformation of impedance will be given in Sections 4.3.1 and 4.3.7.

Optical System Design Software. As well as the ray tracing optical design programs mentioned earlier, such as Code V, there is a broad range of other software available

commercially for optical system design including: laser system design (GLAD, PARAXIA, ASC, and LASFIT); atmospheric optical properties and sensors (ONTAR); optical system solid modeling (LightTools, TracePro); projection systems, fiber optics, and complex sources (ASAP); beam propagation for integrated and fiber optics (BeamProp); vector diffraction grating analysis software and simulation (GSOLVER); optical thin-film and coating design, material analysis, ellipsometry, spectrophotometry and thin-film metrology; [Film Wizard, FilmSpectrum, TFCalc, Thin Film Design Package (Thin Film Center)]; and analysis of laser beam propagation (FRESNEL).

4.2.7 Gaussian Beams

Gaussian beams are propagating-wave solutions of Maxwell's equations that are restricted in lateral extent even in free space. They do not need any beam-confining reflective planes, as do the confined electromagnetic-field modes of waveguides.[29] Lasers frequently emit narrow beams of light that are very close in character to ideal Gaussian beams.

The field components of a plane transverse electromagnetic wave of angular frequency ω propagating in the z-direction are of the form:

$$V = V_0 e^{i(\omega t - kz)} \tag{4.113}$$

where V_0 is a constant. A Gaussian beam is of the form:

$$V = \Psi(x, y, z) e^{i(\omega t - kz)} = U(x, y, z) e^{i\omega t} \tag{4.114}$$

where, for example, for a particular value of z, $\Psi(x, y, z)$ gives the spatial variation of the fields in the xy plane. $\Psi^*\Psi$ gives the relative intensity distribution in the plane; for a Gaussian beam this gives a localized intensity pattern. The various Gaussian-beam solutions of Maxwell's equations are denoted as TEM_{mn} modes; a detailed discussion of their properties is given by Kogelnik and Li.[16] The output beam from an ideal laser is generally a TEM mode or a combination of TEM modes. Many laser systems operate in the fundamental Gaussian mode, denoted TEM_{00}. This is the only mode that will be considered in detail here.

For the TEM_{00} mode, $\Psi(x, y, z)$ has the form:

$$\Psi(x,y,z) = \exp\left\{-i\left[P(z) + \frac{kr^2}{2q(z)}\right]\right\} \tag{4.115}$$

where $P(z)$ is a *phase factor*, $q(z)$ is called the *beam parameter*, k equals $2\pi/\lambda$, and r^2 equals $x^2 + y^2$. The beam parameter, $q(z)$, is usually written in terms of the phase-front *curvature* of the beam $R(z)$, and its *spot size*, $w(z)$, as:

$$\frac{1}{q} = \frac{1}{R} - \frac{i\lambda}{\pi w^2} \tag{4.116}$$

q and P obey the following relations:

$$\frac{dq}{dz} = 1 \tag{4.117}$$

$$\frac{dP}{dz} = -\frac{i}{q} \tag{4.118}$$

For a particular value of z, the intensity variation in the xy plane (the mode pattern) is, from Equation (4.115):

$$\Psi^*\Psi = \exp\left[\frac{-ikr^2}{2}\left(\frac{1}{q(z)} - \frac{1}{q^*(z)}\right)\right] \tag{4.119}$$

which, from Equation (4.116) gives:

$$\Psi^*\Psi = e^{-2r^2/\omega^2} \tag{4.120}$$

Thus, $w(z)$ is the distance from the axis of the beam ($x = y = 0$) where the intensity has fallen to $1/e^2$ of its axial value and the fields to $1/e$ of their axial magnitude. The radial distribution of both intensity and field strength of the TEM_{00} mode is Gaussian, as shown in Figure 4.27. Clearly, from Equation (4.117):

$$q = q_0 + z \tag{4.121}$$

where q_0 is the value of the beam parameter at $z = 0$. From Equation (4.118):

$$\begin{aligned} P(z) &= -i \ln q + \text{constant} \\ &= -i \ln(q_0 + z) + \text{constant} \end{aligned} \tag{4.122}$$

Writing the constant in Equation (4.122) as $\theta + i \ln q_0$, the full spatial variation of the Gaussian beam is:

$$U = \exp\left\{-i\left[kz - i \ln\left(1 + \frac{z}{q_0}\right) + \theta + \frac{kr^2}{2}\left(\frac{1}{R(z)} - \frac{i\lambda}{\pi w^2}\right)\right]\right\} \tag{4.123}$$

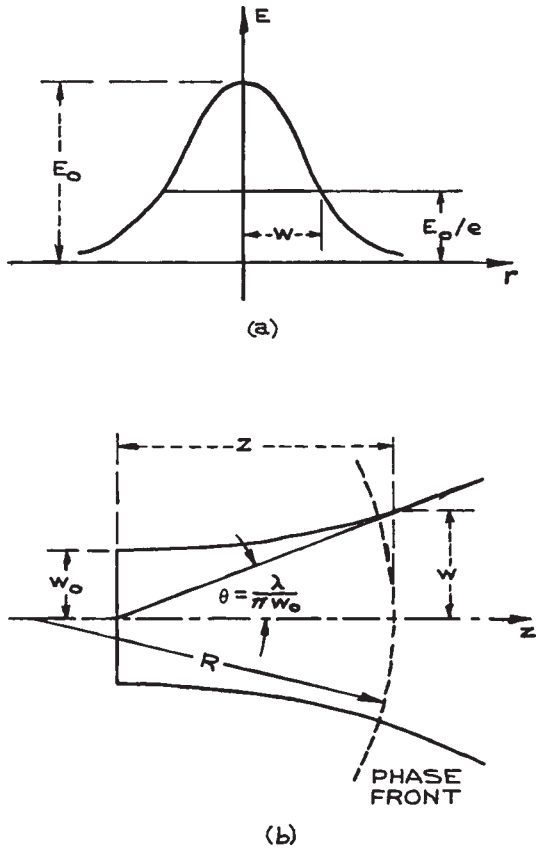

Figure 4.27 (a) Radial amplitude variation of the TEM_{00} Gaussian beam; (b) contour of a Gaussian beam.

The phase angle θ is usually set equal to zero. In the plane $z = 0$:

$$U = \exp\left\{-i\frac{kr^2}{2}\left(\frac{1}{R(0)} - \frac{i\lambda}{\pi w(0)^2}\right)\right\} \tag{4.124}$$

The surface of constant phase at this point is defined by the equation:

$$\frac{kr^2}{2R(0)} = \text{constant} \tag{4.125}$$

If the constant is taken to be zero and $R(0)$ infinite, then r becomes indeterminate and the surface of constant phase is the plane $z = 0$. In this case, $w(0)$ can have its minimum value anywhere. This minimum value is called the *minimum spot size* w_0, and the plane $z = 0$ is called the *beam waist*. At the beam waist:

$$\frac{1}{q_0} = \frac{-i\lambda}{\pi w_0^2} \tag{4.126}$$

Using Equations (4.116) and (4.121), for any arbitrary value of z:

$$w^2(z) = w_0^2\left[1 + \left(\frac{\lambda z}{\pi w_0^2}\right)^2\right] \tag{4.127}$$

The radius of curvature of the phase front at this point is:

$$R(z) = z\left[1 + \left(\frac{\pi w_0^2}{\lambda z}\right)^2\right] \tag{4.128}$$

From Equation (4.127) it can be seen that the Gaussian beam expands in both the positive and negative z-directions from its beam waist along a hyperbola that has asymptotes inclined to the axis at an angle:

$$\theta_{\text{beam}} = \arctan\frac{\lambda}{\pi w_0} \tag{4.129}$$

as illustrated in Figure 4.27(b). The surfaces of constant phase of the Gaussian beam are, in reality, parabolic. For $r_2 << z_2$ (which is generally true, except close to the beam waist), they are spherical surfaces with the radius of curvature $R(z)$. Although they will not be discussed further here, the higher-order Gaussian beams, denoted TEM_{mn}, are also characterized by spot sizes and radii of curvature that are identical to those of the TEM_{00} mode and obey Equations (4.127) and (4.128).

Focusing a Laser beam with a Lens. A lens can be used to focus a laser beam to a small spot, or systems of lenses may be used to expand the beam and recollimate it (i.e., minimize the beam divergence). In such an application a thin lens will not alter the transverse intensity pattern of the beam at the lens, but it will alter its radius of curvature. Far enough from the beam waist, the radius of curvature of a Gaussian beam behaves exactly

as a true spherical wave, since, for $z >> \pi\omega_0^2/\lambda$, Equation (4.128) becomes:

$$R(z) = z \tag{4.130}$$

Now, when a spherical wave of radius R_1 strikes a thin lens, the object distance is clearly also R_1 – the distance to the point of origin of the wave. Therefore, the radius of curvature R_2 immediately after passage through the lens must obey:

$$\frac{1}{R_2} = \frac{1}{R_1} - \frac{1}{f} \tag{4.131}$$

as shown in Figure 4.28. Thus, if w is unchanged at the lens, the beam parameter after passage through the lens obeys

$$\frac{1}{q_2} = \frac{1}{q_1} - \frac{1}{f} \tag{4.132}$$

It is straightforward to use this result in conjunction with Equations (4.116) and (4.121) to give the minimum spot size w_f of a TEM_{00} Gaussian beam focused by a lens as:

$$w_f = \frac{f\lambda}{\pi w_1}\left[\left(1 - \frac{f}{R_1}\right)^2 + \left(\frac{\lambda f}{\pi w_1^2}\right)^2\right]^{1/2} \tag{4.133}$$

where w_1 and R_1 are the laser-beam spot size and radius of curvature at the input face of the lens. If the lens is placed very close to the waist of the beam being focused, Equation (4.133) reduces to:

$$\omega_f = f\theta_B \tag{4.134}$$

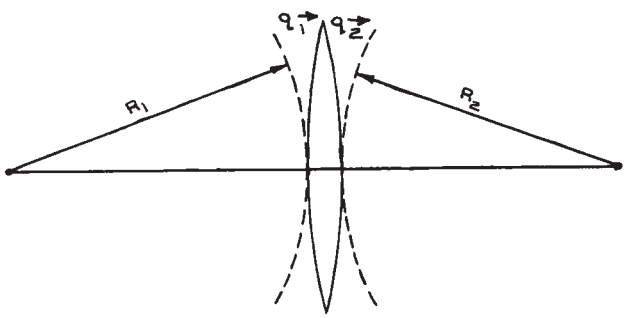

Figure 4.28 Transformation of a Gaussian beam by a thin lens.

where θ_B is the beam divergence at the input face of the lens. If θ_B is a small angle, then w_f is located almost at the focal point of the lens – in reality very slightly closer to the lens. It is worthwhile comparing the result given by Equation (4.134) with the result obtained for a plane wave being focused by a lens. In the latter case, the lens diameter D is the factor that limits the lateral extent of the wave being focused. Diffraction theory[11,23] shows that, in this case, 84% of the energy is focused into a region of diameter:

$$S = 2.44\lambda f/D \tag{4.135}$$

This is the diameter of the focused Airy disk diffraction pattern of the lens aperture.

It should be noted that the spot size to which a laser beam can be focused cannot be reduced without limit merely by reducing the focal length of the focusing lens. In the limit the lens becomes a sphere and, of course, is then no longer a thin lens. In practice, to focus a laser beam to a small spot, the value of θ_B should be first reduced by expanding the beam and then recollimating it – generally with a Galilean telescope, as will be seen in Section 4.3.3. To prevent diffraction effects, the lens aperture should be larger than the spot size at the lens: $D = 2.8w$ is a common size used. In this case, if the focusing lens is placed at the beam waist of the collimated beam, the focal-spot diameter is:

$$2w_f = \frac{5.6\lambda f}{\pi D} = \frac{1.78\lambda f}{D} \tag{4.136}$$

In practice, it is difficult to manufacture spherical lenses with very small values of f / D (called the f/# or *f/number*) and at the same time achieve the diffraction-limited performance predicted by this equation. Commercially available spherical lenses[30] achieve values of $2w_f$ of about 10λ. Smaller spot sizes are possible with aspheric lenses.

The Beam Parameter M^2. Real laser beams are often characterized by their M^2 parameter or *focusability parameter*. Because of deviations from perfect Gaussian behavior, whan a real laser beam is focused by an ideal

lens placed at the beam waist the focused spotsize is not $w_f = f\theta_B$, as predicted by Equation (4.134), but is instead:

$$\omega_{fr} = M^2 f\theta_B \tag{4.137}$$

For asymmetrical laser beams there will be two beam parameters M_x^2 amd M_y^2 for the two lateral coordinates of the laser beam. The M^2 parameter cannot be measured from a single measurement of the laser beam. A series of measurements on a focused beam are made, such as the position of the focus relative to the focal length of the lens, the new beam divergence angle after the focus, the spotsize(s) at the focal point of the lens, and the new minimum spotsize(s). Commercial instruments that measure M^2 are available from Coherent, Photon, Inc., and Spiricon. Here, and wherever suppliers are mentioned in the text, the list is intended to be representative, but not necessarily exhaustive.

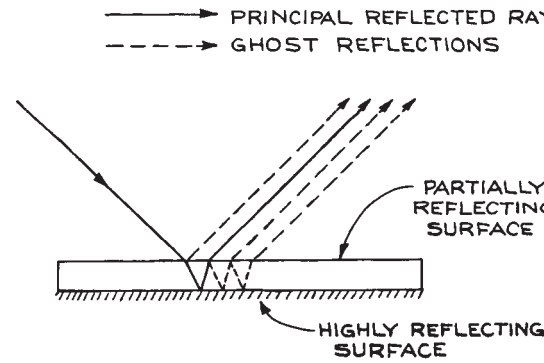

Figure 4.29 Production of ghost reflections by a rear-surface mirror whose front surface is not antireflection coated.

4.3 OPTICAL COMPONENTS

4.3.1 Mirrors

When light passes from one medium to another of different refractive index, there is some reflection, so the interface acts as a partially reflecting mirror. By applying an appropriate single-layer or multilayer coating to the interface between the two media, the reflection can be controlled so that the reflectance has any desired value between 0 and 1. Both flat and spherical mirrors made in this way are available – there are numerous suppliers.[31] If no transmitted light is required, high-reflectance mirrors can be made from metal-coated substrates or from metals themselves. Mirrors that reflect and transmit roughly equal amounts of incident light are often referred to as *beamsplitters*.

Flat Mirrors. Flat mirrors are used to deviate the path of light rays without any focusing. These mirrors can have their reflective surface on the front face of any suitable substrate, or on the rear face of a transparent substrate. Front-surface, totally reflecting mirrors have the advantage of producing no unwanted additional or *ghost* reflections; however, their reflective surface is exposed. Rear-surface mirrors produce ghost reflections, as illustrated in Figure 4.29, unless their front surface is antireflection coated; but the reflective surface is protected. Most household mirrors are made this way. The cost of flat mirrors depends on their size and on the degree of flatness required.

Mirrors for high-precision applications – for example, in visible lasers – are normally specified to be flat between $\lambda/10$ and $\lambda/20$ for visible light. This degree of flatness is not required when the mirror is merely for light collection and redirection, for example to reflect light onto the surface of a detector. Mirrors for this sort of application are routinely flat to within a few wavelengths of visible light. Excellent mirrors for this purpose can be made from "float" plate glass,[32] which is flat to 1 or 2 wavelengths per inch.

New superpolishing techniques have allowed the production of *super mirrors*, which have surface roughness down to 0.1nm or below and loss (absorption plus scattering) below 10^{-6} per reflection. Super mirrors allow the construction of optical resonators with very high Q values, up to 1 million, for applications such as cavity ring down spectroscopy and high finesse interferometry (see Section 4.7.4). Such mirrors are available from Los Gatos Research, Newport Corporation, and the Optical Corporation. More discussion of the issues involved in fabricating such mirrors is available in references 34–37.

Spherical Mirrors. Spherical mirrors are widely used in laser construction, where the radii of curvature are typically rather long – frequently 20 m radius or more. They can be used whenever light must be collected and focused; however, spherical mirrors are only good for focusing nearly parallel beams of light that strike the mirror close to normal. In common with spherical lenses, spherical mirrors suffer from various imaging defects called aberrations, which have been discussed in Section 4.2.5. A parallel beam of light that strikes a spherical mirror far from normal is not focused to a small spot. When used this way the mirror is *astigmatic*, that is, off-axis rays are focused at different distances in the horizontal and vertical planes. This leads to blurring of the image, or at best the focusing of a point source into a line image.

A useful practical way to distinguish between a flat mirror and one with a large radius of curvature is to use the mirror to view a sharp object in grazing incidence. A curved mirror surface will reveal itself through the blurring of the image, while a flat mirror will give a sharp image.

Paraboloidal and Ellipsoidal Mirrors. *Paraboloidal mirrors* will produce a parallel beam of light when a point source is placed at the focus of the paraboloidal surface. Thus, these mirrors are very useful in projection systems. They are usually made of polished metal, although versions using Pyrex substrates are also available. An important application of parabolic mirrors is in the off-axis focusing of laser beams, using off-axis mirrors in which the axis of the paraboloid does not pass through the mirror. When they are used in this way there is complete access to the focal region without any shadowing, as shown in Figure 4.30. Spherical mirrors, on the other hand, do not focus well if they are used in this way. Off-axis paraboloidal mirrors, as well as metal axial paraboloidal mirrors, are available from Edmund Optics, II-VI Infrared, Kugler, Lightwave Enterprises, Melles Griot, Newport, Opti-Forms, OptoSigma, Space Optics Research Lab, and Thorlabs.

Ellipsoidal mirrors are also used for light collecting. Light that passes through one focus of the ellipsoid will, after reflection, also pass through the other. These mirrors, like all-metal paraboloidal mirrors, are generally made by electroforming. The surface finish obtained in this way is quite good, although not so good as can be obtained by optical polishing. Rhodium-plated electroformed ellipsoidal mirrors are available from Edmund Optics, Melles Griot, Opti-Forms, and Spectrum Scientific.

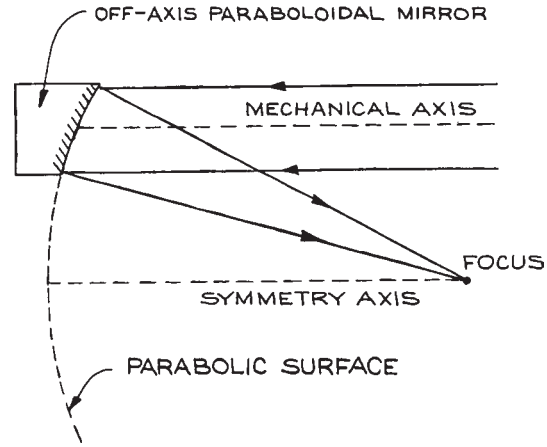

Figure 4.30 Off-axis paraboloidal mirror.

Dielectric Coatings. Several different kinds of single-layer and multilayer dielectric coatings are available commercially on the surface of optical components. These coatings can either reduce the reflectance or enhance it in some spectral region.

(i) Single-layer antireflection coatings. The mode of operation of a single-layer antireflection (AR) coating can be conveniently illustrated by the method of transformed impedances. Suppose medium 3 in Figure 4.31(a) is the surface to be AR coated. Apply to the surface a coating with an effective thickness:

$$d' = \lambda_2/4 \tag{4.138}$$

where $\lambda_2 = c_0/vn_2$. The actual thickness of layer 2 is:

$$d = d'/\cos\theta_2 \tag{4.139}$$

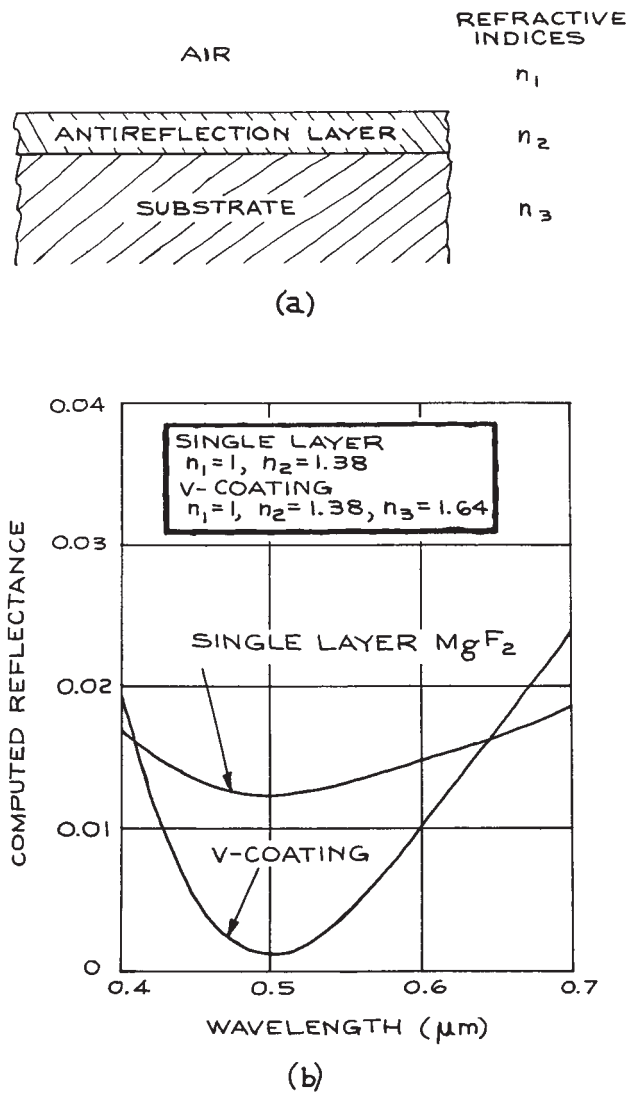

Figure 4.31 (a) Geometry of single-layer antireflection coating; (b) reflectances of single- and double-layer antireflection coatings on a substrate of refractive index 1.64. (From *Handbook of Lasers*, R.J. Pressley (Ed.), CRC Press, Cleveland, 1971; by permission of CRC Press, Inc.)

The transformed impedance of medium 3 at the first interface is found by substitution in Equation (4.110):

$$Z''_3 = Z'^2_2/Z'_3 \tag{4.140}$$

To reduce the reflection coefficient to zero, we need $Z''_3 = Z'_1$; so the effective impedance of the antireflection layer must be:

$$Z'_2 = \sqrt{Z'_1 Z'_3} \tag{4.141}$$

Thus, to eliminate reflection of waves linearly polarized in the plane of incidence and incident at angle θ_1, n_2 must be chosen to satisfy:

$$\frac{\cos\theta_2}{n_2} = \sqrt{\frac{\cos\theta_1 \cos\theta_3}{n_1 n_3}} \tag{4.142}$$

For use in normal incidence, $n_2 = \sqrt{n_1 n_3}$ and $d = \lambda_2/4$. In normal incidence, an AR coating works for any incident polarization. To minimize reflection at an air–flint-glass ($n = 1.7$) interface, we would need:

$$n_2 = \sqrt{1.7} = 1.3 \tag{4.143}$$

Magnesium fluoride with a refractive index of 1.38 and cryolite (sodium aluminum fluoride) with a refractive index of 1.36 come closest to meeting this requirement in the visible region of the spectrum. Optical components such as camera lenses are usually coated with one of these materials to minimize reflection at 550 nm. The slightly greater Fresnel reflection that results in the blue and red gives rise to the characteristic purple color of these components in reflected light often called ''blooming''.

(ii) Multilayer antireflection coatings. The minimum reflectance of a single-layer antireflection-coated substrate is $(n_2^2 - n_1 n_3)/(n_2^2 + n_1 n_3)^2$. Available robust optical coating materials such as MgF_2, however, do not have a sufficiently low refractive index to reduce the reflectance to zero with a single layer. Two-layer coatings, often called V-coatings because of the shape of their transmission characteristic, reduce reflection better than a single layer, as shown in Figure 4.31(b). Multilayer coatings can be used to reduce reflectance over a broader wavelength region than a V-coating, as shown in Figure 4.32. Such broad-band coatings are usually of proprietary design: they are available

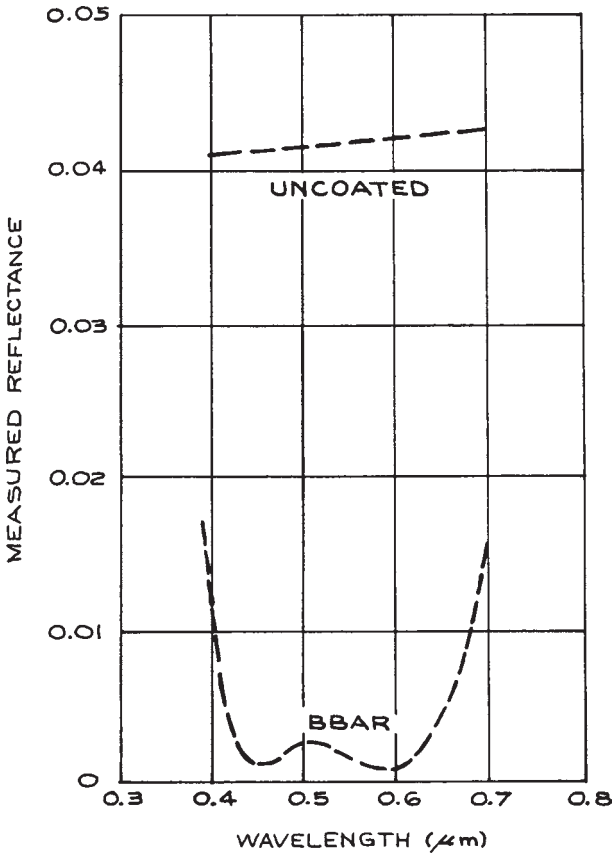

Figure 4.32 Reflectance of a typical broad-band antireflection coating (BBAR) showing considerable reduction in reflectance below the uncoated substrate. (From *Handbook of Lasers*, R.J. Pressley (Ed.), CRC Press, Cleveland, 1971; by permission of CRC Press, Inc.

commercially from many sources, as are coatings of other types.[31] Some companies offer both optical components and coatings, while others specialize in coatings and will coat customers' own materials. Melles Griot offer a HEBBAR (high efficiency broad-band antireflection) coating that provides very low reflectance over a broad bandwidth, and is relatively insensitive to angle of incidence, as shown in Figure 4.33.

(iii) High-reflectance coatings. The usually high reflectance of a metal surface can be further enhanced, as shown

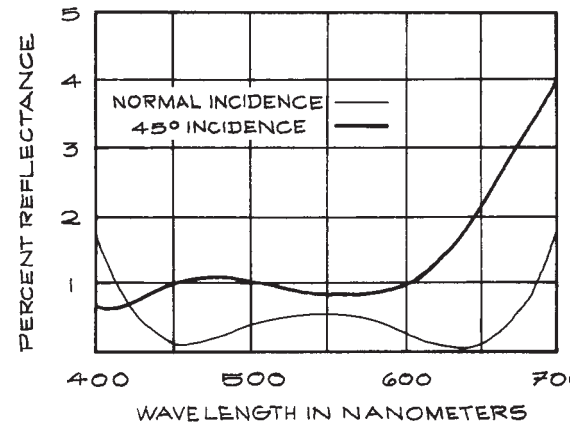

Figure 4.33 The reflectance spectrum of an HEBBAR high reflectance broad-band coating.

in Figure 4.34(a), by a multiple dielectric coating consisting of an even number of layers, each a quarter wavelength thick, and of alternately high and low refractive index, with a low-refractive-index material next to the metal. A very high reflectance over a narrow wavelength range can be achieved, as shown in Figure 4.34(b), by using a dielectric substrate, such as fused quartz, and an odd number of quarter-wavelength layers of alternately high and low refractive index with a high-index layer on the substrate. Broad-band high-reflectance coatings are also available where the thickness of the layers varies around an average value of a quarter wavelength.

Beamsplitters. Beamsplitters are semitransparent mirrors that both reflect and transmit light over a range of wavelengths. A good beamsplitter has a multilayer dielectric coating on a substrate that is slightly wedge-shaped to eliminate interference effects, and antireflection-coated on its back surface to minimize ghost images. The ratio of reflectance to transmittance of a beamsplitter depends on the polarization state of the light. The performance is usually specified for light linearly polarized in the plane of incidence (*P*-polarization) or orthogonal to the plane of incidence (*S*-polarization). Cube beamsplitters are pairs of identical right-angle prisms cemented together on their hypotenuse faces. Before cementing, a metal or dielectric semireflecting layer is placed on one of the hypotenuse

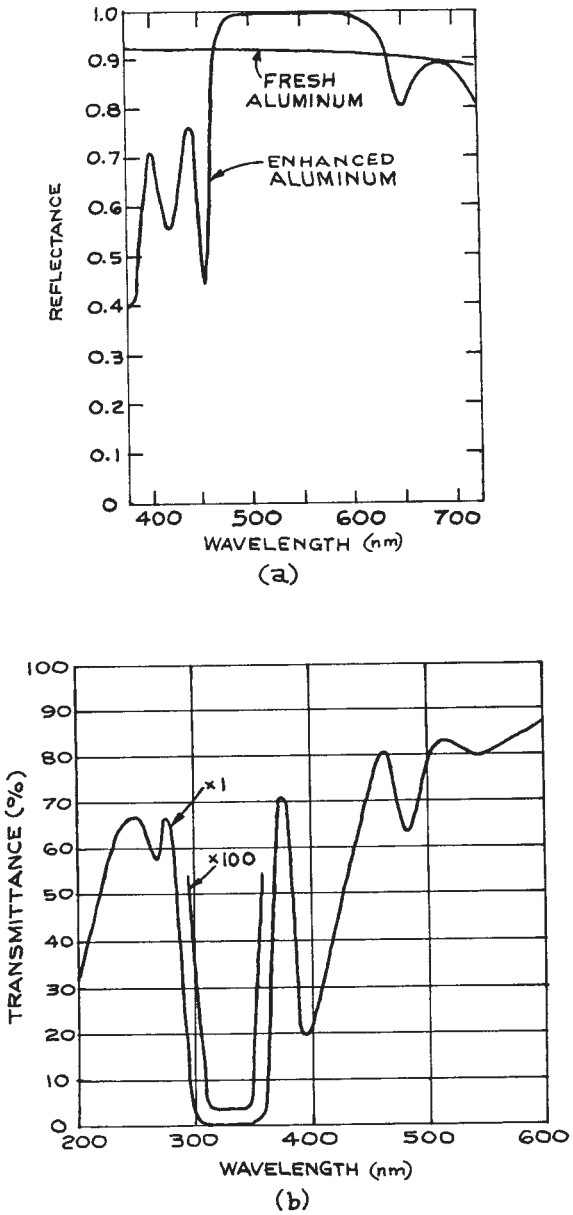

Figure 4.34 (a) Reflectance of a plain aluminum mirror and an aluminum mirror with four dielectric overlayers. (From *Handbook of Lasers*, R.J. Pressley (Ed.), CRC Press, Cleveland, 1971; by permission of CRC Press); (b) typical transmittance characteristic of a narrow-band, maximum-reflectance, multilayer dielectric coating on a dielectric substrate.

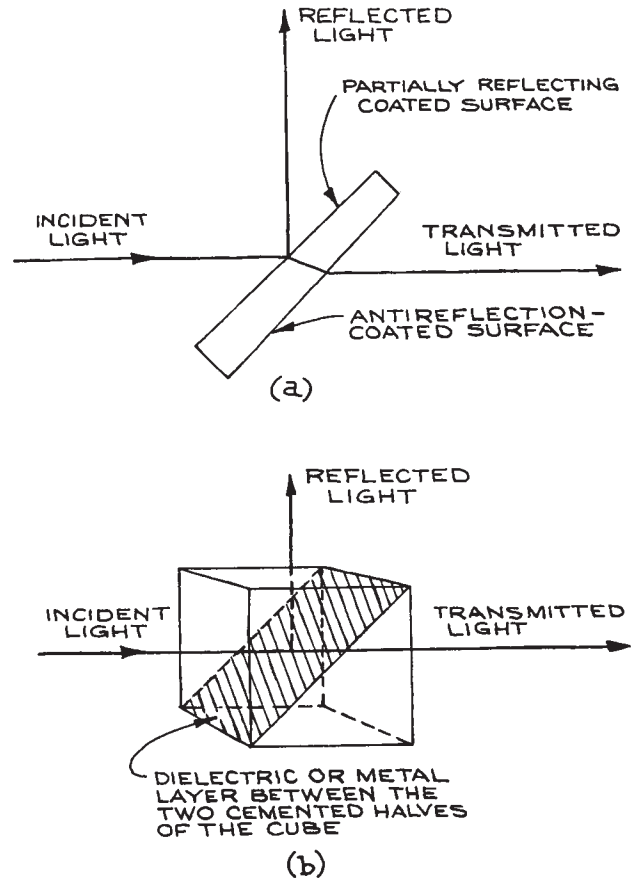

Figure 4.35 (a) Conventional planar beamsplitter (wedge angle greatly exaggerated); (b) cube beamsplitter.

faces. Antireflection-coated cube prisms have virtually no ghost image problems and are more rigid than plate type beamsplitters. The operation of both types of beamsplitter is illustrated in Figure 4.35.

Pellicles. Pellicles are beam-splitting mirrors made of a high-tensile-strength polymer stretched over a flat metal frame. The polymer film can be coated to modify the reflection–transmission characteristics of the film. The polymer generally used, nitrocellulose, transmits in the visible and near infrared to about 2μm. These devices have some advantages over conventional coated-glass or quartz beamsplitters; the thinness of the polymer

film virtually eliminates spherical and chromatic aberrations (see Section 4.3.3) when diverging or converging light passes through them, and ghost-image problems are virtually eliminated. They will, however, produce some wavefront distortion, typically about two waves per inch, and are not suitable for precision applications. Pellicles are available from several suppliers[31], such as Edmund Optics, Melles Griot, National Photocolor, and Newport.

4.3.2 Windows

An optical window serves as a barrier between two media, for example, as an observation window on a vacuum system or on a liquid or gas cell, or as a Brewster window on a laser. When light passes through a window that separates two media, there is, in general, some reflection from the window and a change in the state of polarization of both the reflected and the transmitted light. If the window material is not perfectly transparent at the wavelength of interest, there is also absorption of light in the window, which at high light intensities will cause the window to heat. This will cause optical distortion of the transmitted wave, and at worst – in high-power laser applications – damage the window on its surface, internally, or both. Additionally, if the two surfaces of a window are both very flat (roughly speaking, one wave per centimeter or better) and close to parallel, the window will act as an *etalon* (see Sections 4.3.8 and 4.7.4) and exhibit distinct variations in transmission with wavelength. To circumvent this difficulty, which is a particular nuisance in experiments using lasers, most precision flat optical windows are constructed as a slight wedge, with an angle usually about 30′.

The details of the reflection, refraction, and change of polarization state that occur when light strikes a window surface are dealt with in detail in Sections 4.2.6 and 4.3.6. These considerations also apply when light strikes a lens or prism. The reflection at such surfaces can be reduced by a single-layer or multilayer dielectric antireflection coating. In optical systems such as multielement camera lenses, where light crosses many such surfaces, antireflection coatings are very desirable. Otherwise a severe reduction in transmitted light intensity will result, as illustrated in Figure 4.36.

Optical cells, or cuvettes, are transparent containers, generally made of glass or fused quartz, which are used

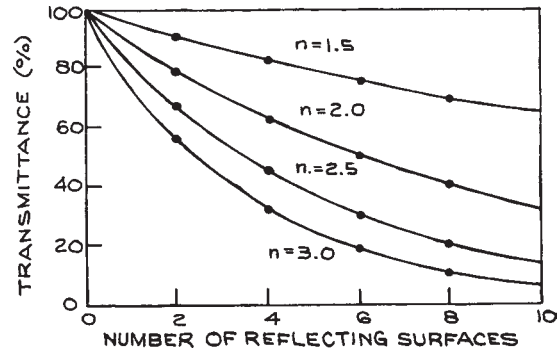

Figure 4.36 Transmittance of a multielement optical system as a function of the refractive index of the elements.

in absorption and fluorescence spectrophotometers, in light-scattering and turbidity measurements, and in many other specialized experiments. These cells are usually rectangular or cylindrical in shape and are available in many sizes and configurations, including provision for liquid circulation. Suppliers include Harrick Scientific, Hellma, International Crystal Laboratories, Newport/Oriel, NSG Precision Cells, Optiglas, Spectrocell, and Starna.

4.3.3 Lenses and Lens Systems

Singlet Lenses. *Singlet lenses* are the simplest and most readily available lenses for nonexacting applications. They come in six basic formats, shown in Figure 4.37. The lens is specified by the material of which it is made, the curvatures R_1 and R_2 of its two faces, the thickness d of the lens at its mid point, and its aperture diameter D, which also indirectly specifies its thickness at the edge. The lens has an effective focal length (EFL), f measured from its principal planes, and front and back focal lengths, which specify the distances of the focal points from the front and back surfaces of the lens, as shown in Figure 4.38. A *biconvex lens* has two generally spherical surfaces. In the standard sign convention the first of these has a positive radius and the second a negative radius. A symmetrical biconvex lens has $R_1 = -R_2$. A *plano-convex* lens has one flat face, while a *convex meniscus* lens has a first surface of positive radius and a second surface of a larger positive radius. Biconvex, plano-convex, and convex meniscus

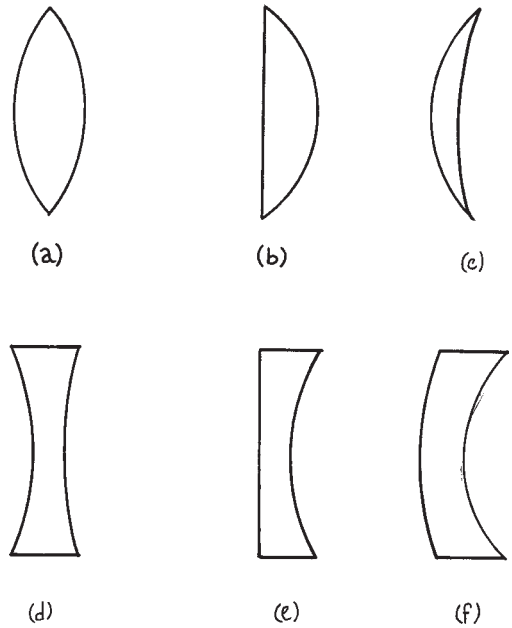

Figure 4.37 The six basic singlet lens types: (a) biconvex; (b) plano-convex; (c) convex meniscus; (d) biconcave; (e) plano-concave; (f) concave meniscus.

lenses all have a positive EFL. *Biconcave*, *plano-concave*, and *concave meniscus lenses* have surface curvatures, opposite in sign to their convex counterparts, and all have a negative EFL.

All singlet lenses suffer from spherical and chromatic aberration. They are inexpensive, but suffer from significant amounts of aberration, so are not a good choice in imaging situations. For focusing parallel light (infinite object conjugate), or for producing a parallel beam of light, plano-convex lenses or convex meniscus lenses that are close to plano-convex exhibit the least spherical aberration for a specified EFL. For best performance in these applications the parallel light should pass through the more strongly curved of the two surfaces. For imaging at different conjugate ratios the shape of singlet that produces the least spherical aberration is called the *best form* lens for that application. For example, for equal object and image distances (conjugate ratio = 1) the best form singlet is a symmetrical biconvex lens. Singlet lenses can provide satisfactory performance provided they are used with relatively large *f*/numbers. If singlet lenses are used with lasers then there is no chromatic aberration.

Doublets. If a positive focal length lens of one type of glass is combined with a weaker negative lens made from a different type of glass, then the lens combination can exhibit reduced spherical and chromatic aberration.

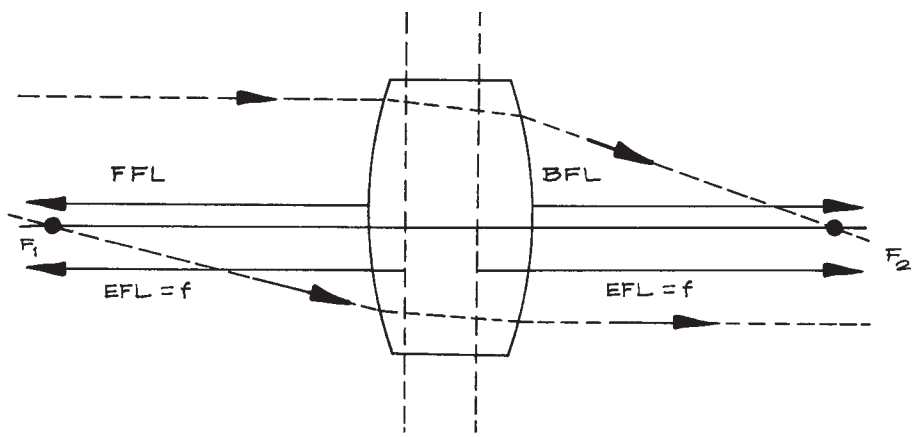

Figure 4.38 Diagram showing the effective focal length (EFL), the front focal length (FFL), and the back focal length (BFL) of a thick lens.

Doublets can be either air-spaced or cemented. They are widely available from many suppliers, such as CVI/Melles Griot, Newport Corporation, OptoSigma, Rolyn, and Thorlabs. For laser applications, even without the concern for chromatic aberration, doublets will provide superior focusing performance to singlets.

Camera lenses. *Compound lenses* involve more than two spherical surfaces and can be designed to have reduced aberrations. Camera lenses are multi element compound lenses especially designed for imaging applications. A wide variety of high-performance camera lenses is available commercially from companies such as Canon, Fujinon, Kodak, Leitz, Minolta, Nikon, Olympus, Sigma, and Zeiss. The choice of camera lenses for a specific application is generally guided by two parameters: (i) the *field of view* (FOV), which can be specified by the apex angle of the cone of light that can be collected by the lens and (ii) the aperture of the lens. Both these parameters influence the light-gathering power of the lens.

Telecentric lenses are special compound lenses used in applications such as machine vision and lithography where object or image movement does not produce a change in magnification.[33,38] For a lens with object space telecentricity, a change in the object distance will not result in the image changing size. For such a lens the aperture stop is located in the back focal plane and the entrance pupil is at infinity. All the principal rays in object space are parallel to the axis. For a lens with image space telecentricity, moving the image plane to focus or defocus the system will not change the size of the image. In this case the aperture stop is located in the front focal plane and the exit pupil is at infinity. In the image space all the principal rays are parallel to the axis. If a lens is telecentric for both the object and image spaces it is called *doubly telecentric*. The primary disadvantage of telecentric lenses is that they have a very limited field of view: object and image have to lie within a cylindrical region whose radius in object and image space is limited by the size of the lens elements. Telecentric lenses are available from Computer Optics, Edmund Optics, Mekoptik, Navitar, Opto-Engineering, and Sill Optics.

Simple and Galilean Telescopes. The operation of a *simple telescope* is illustrated in Figure 4.39(a). The objective is usually an *achromat* (a lens in which chromatic aberration – the variation of focal length with wavelength – has been minimized). It has a long focal length f_1 and produces a real image of a distant object, which can then be examined by the eyepiece lens of focal length f_2. This design, which produces an inverted image, is often called an *astronomical telescope*. If desired, the final image can be erected with a third lens, in which case the device is called a *terrestrial telescope*. The eyepiece of the telescope can be a singlet lens, but composite eyepiece designs such as the Ramsden and the Kellner[11] are also common. Most large astronomical telescopes use spherical mirrors as objectives, and various configurations are used, such as the Newtonian, Cassegrain, and Schmidt.[11,23–25] Since most telescope development has been for astronomical applications, it is outside the scope of this book to give a detailed discussion; for further details the reader should consult Born and Wolf,[11] Levi,[24] Meinel,[38] or Brouwer and Walther.[39]

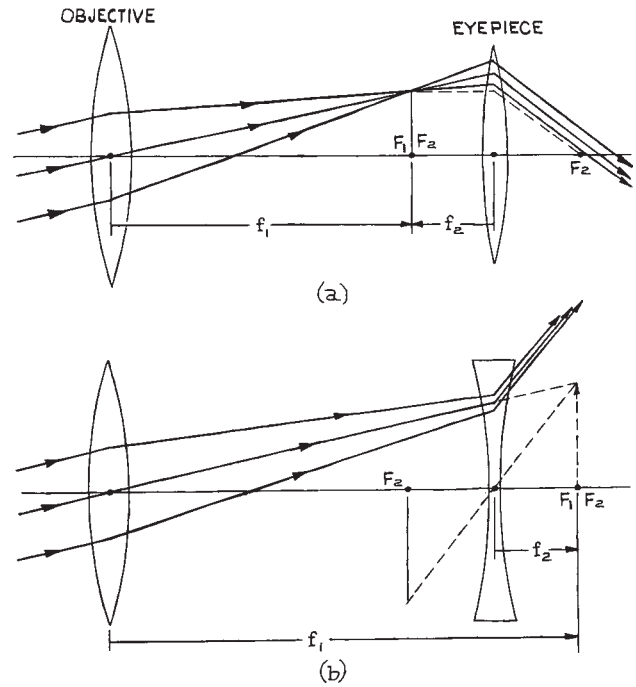

Figure 4.39 Ray paths through telescopes in *normal* adjustment (object and final image at infinity): (a) astronomical telescope; (b) Galilean telescope.

Small astronomical and terrestrial telescopes are widely available at relatively low cost. Two principal manufacturers are Celestron[40] and Meade.[41]

The *Galilean telescope* illustrated in Figure 4.39(b), first constructed by Galileo in 1609, is the earliest telescope of which there exists definite knowledge. It produces no real intermediate image, but the final image is erect. In *normal adjustment*, the focal point of the diverging eyepiece is outside the telescope and coincident with that of the objective. In the simple telescope the two focal points also coincide, but are between the two. The magnification M produced by either type of telescope can be written as:

$$M = -f_1/f_2 \tag{4.144}$$

Since the simple telescope has two positive (converging) lenses, its overall magnification is negative, which indicates that the final image is inverted.

Simple and Galilean telescopes have practical uses in the laboratory that are distinct from their traditional use for observing distant objects.

Laser-Beam Expanders and Spatial Filters. Laser beams can be expanded and recollimated (or focused and recollimated) with simple or Galilean telescope arrangements, as illustrated in Figure 4.40. For optimum recollimation the spacing of the two lenses should be adjustable, as fine adjustment about the spacing $f_2 + f_1$ will be necessary for recollimating a Gaussian beam. In this application the Galilean telescope has the advantage that the laser beam is not brought to an intermediate focus inside the beam expander. Gas breakdown at such an internal focus can occur with high-power laser beams, although this problem can be solved in simple-telescope beam expanders by evacuating the telescope. Since laser beams are highly monochromatic, beam expanders need not be constructed from achromatic lenses. Attempts should, however, be made to minimize spherical aberration and beam distortion. It is best to use precision antireflection-coated lenses if possible. Laser-beam-expanding telescopes that are very well corrected for spherical aberration are available from Janos, Melles Griot, Newport/Oriel, Rolyn, Sigma Koki, Space Optics Research Labs, and

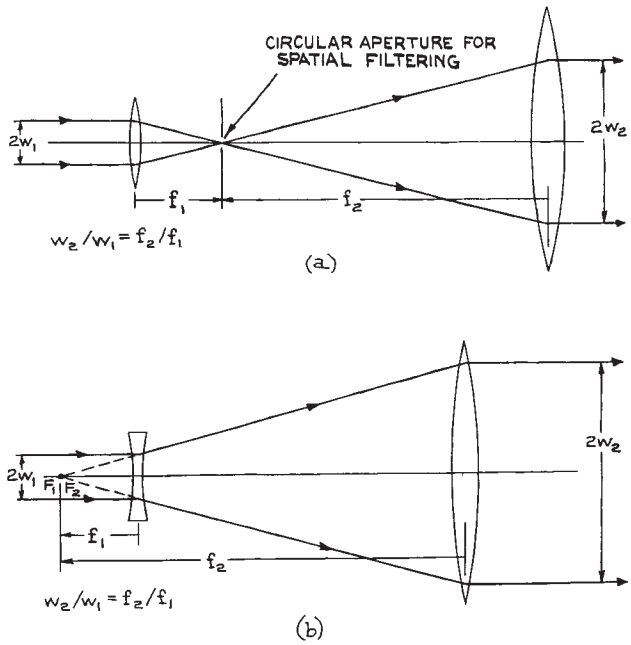

Figure 4.40 Laser-beam expanders: (a) focusing type with spatial filter; (b) Galilean type.

Special Optics, among others.[31] Infrared laser-beam expanders usually have ZnSe or germanium lenses. The use of biconvex and biconcave lenses distributes the focusing power of the lenses over their surfaces and minimizes spherical aberration. Better cancellation of spherical aberration is possible in Galilean beam expanders than with simple telescopes.

If a small circular aperture is placed at the common intermediate focus of a simple-telescope beam expander, the device becomes a spatial filter as well. Although ideally the output beam from a laser emitting a TEM_{00} mode has a Gaussian radial intensity profile, in practice the radial profile may have some irregular structure. Such beam irregularities may be produced in the laser or by passage of the beam through some medium. If such a beam is focused through a small enough aperture and then recollimated, the irregular structure on the radial intensity profile can be removed and a smooth

profile restored, as illustrated in Figure 4.41. This is called *spatial filtering*. The minimum aperture diameter that should be used is

$$D_{\min} = \frac{2f_1\lambda}{\pi w_1} \tag{4.145}$$

where f_1 is the focal length of the focusing lens and w_1 is the spot size at that lens. Typical aperture sizes used in commercial spatial filters for visible lasers are on the order of 10 μm. This aperture must be accurately and symmetrically positioned at the focal point, so it is usually mounted on an adjustable XY translation stage.

Lens Aberrations. As discussed in Section 4.2.5, real lenses suffer from various forms of aberration, which lead the image of an object to be an imperfect reconstruction of it. If a particular aberration is judged to be detrimental in a particular experimental situation, then a special lens combination can often be obtained that minimizes that aberration – occasionally at the expense of worsening others.

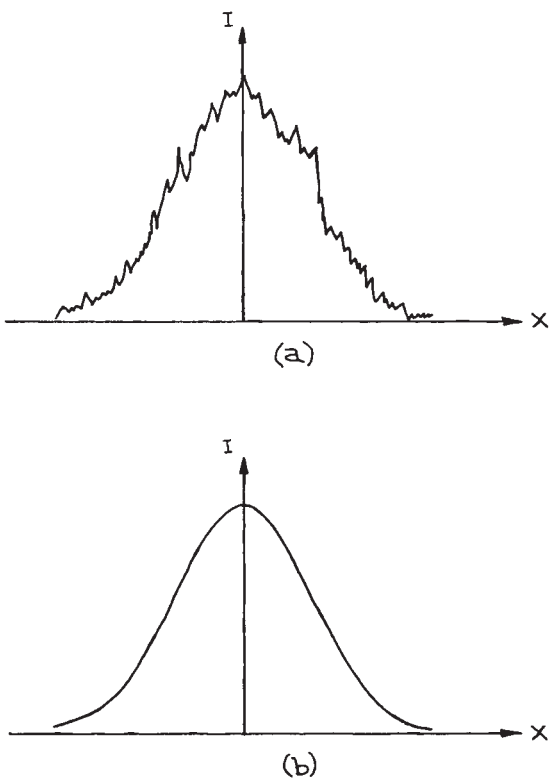

Figure 4.41 Intensity variation $I(x)$ along a diameter of a TEM_{00} laser beam possessing spatial noise structure: (a) before and (b) after spatial filtering.

(i) Chromatic aberrations. Because the refractive index of the material of a lens varies with wavelength, so does its focal length. Therefore rays of different wavelengths from an object form images in different locations. Chromatic aberration is almost eliminated with the use of an *achromatic doublet*. This is a pair of lenses, usually consisting of a positive crown-glass lens and a negative flint-glass lens, cemented together. These two lenses cancel each other's chromatic aberrations exactly, at specific wavelengths in the blue and red, and almost exactly in the region in between. Good camera lenses are well corrected for chromatic aberrations.

Achromatic doublets are available from numerous suppliers, including Edmund Optics.

(ii) Spherical aberration. This aberration can be minimized in a single lens by distributing the curvature between its two surfaces without altering the focal length. So, for example, a biconvex lens will produce less spherical aberration than a plano-convex one of the same focal length. Spherical aberration can be minimized in an achromatic doublet with appropriate choice of curvatures for the constituent lens elements.

(iii) Coma. When an object point is off the axis of a lens, its image is produced in different lateral positions by different zones of the lens. Coma can be controlled by an appropriate choice of lens curvatures.

Other forms of aberration also occur, such as *field curvature*, in which an object plane orthogonal to the lens axis is imaged as a curved surface.

(iv) Astigmatism. This aberration can be controlled by lens curvature and index variations, and by the use of apertures to restrict the range of angles and off-axis distances at which rays can traverse the lens.

Aspheric Lenses. If one face of a singlet lens is manufactured as a nonspherical (or *aspherical*), surface then at

a specified design wavelength all spherical aberration can be eliminated. With such a lens it is possible to obtain a much smaller focal length than with a conventional spherical lens of the same diameter, without increasing the spherical aberration of the lens. An ideal aspheric lens exactly cancels the spherical aberration that would otherwise be present in the optical system. Such lenses can produce the smallest focal spots when used with collimated laser light. The collimated beam should enter the aspherical surface and the focus will be on the opposite side, as shown in Figure 4.42. The second face of an aspherical lens is often plane, or weakly spherical as shown in Figure 4.43.

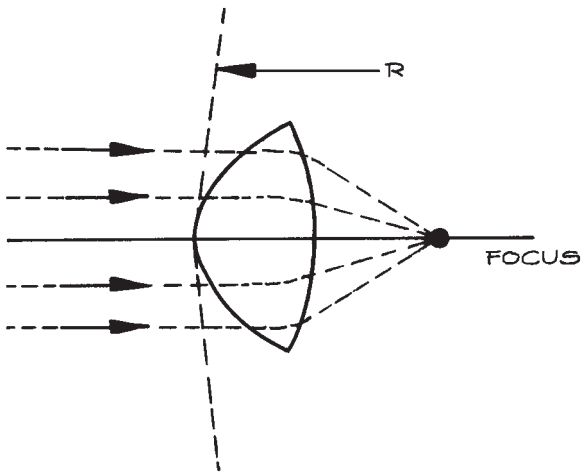

Figure 4.42 Focusing light with an aspherical lens.

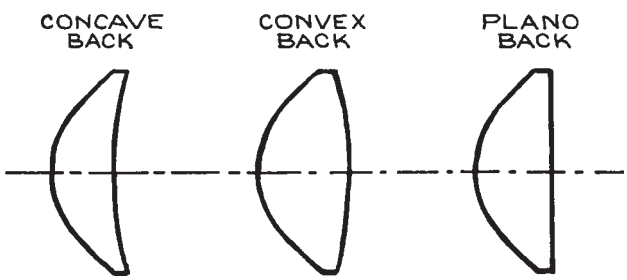

Figure 4.43 Cross-sections of three common types of aspheric lens.

If optimum performance at a particular wavelength and focal length is required, then a custom asphere can be manufactured, but this can be expensive, unless a large number of such lenses are required. Aspheres are often made by molding, so once the mold has been manufactured additional lenses are less expensive.

The standard formula that describes an aspheric surface is:

$$z = \left(\frac{1}{R}\right)\frac{r^2}{1 + \sqrt{1 - (1 + K)\frac{r^2}{R^2}}} + A_4 r^4 + A_6 r^6 + A_8 r^8 + A_{10} r^{10} + \cdots \quad (4.146)$$

where z is the depth (or sag) of the surface, r is the lateral position, K is the conic constant of the surface, and R is the effective curvature at the vertex of the surface, as shown in Figure 4.42. The conic constant K has the following values for different surface profiles: $K > 0$ ellipse, $K = 0$ sphere, $-1 < K < 0$ ellipse, $K = -1$ parabola, and $K < -1$ hyperbola. Most aspherical designs use only the even order terms, as shown in Equation (4.146), but the odd terms could also be included.

Aspheric lenses can collect and focus light rays over a much larger solid angle than conventional lenses and can be used at *f*/numbers as low as 0.6. Aspheric lenses save space and energy. They can be used as collection lenses very close to small optical sources, such as high-pressure mercury or xenon arc lamps, and for collecting radiation over a large solid angle and focusing it onto a detector element. Such lenses are often referred to as *condensers*. Condensers are widely used in microscopes, where they focus light from the microscope light source onto a specimen. In such applications the aspherical surface should be on the light source side. Because aspheric lenses are generally designed only to minimize spherical aberrations, they will contribute to chromatic aberration, coma, distortion, astigmatism, and curvature of field. Consequently, an aspheric lens should not be used under circumstances where these aberrations will be compounded by transmission through additional components of the optical system. Glass aspheric lenses are available in a range of diameters and focal lengths from several suppliers,[31] such as Fresnel Technologies, Melles Griot, Moritex, OptoSigma, and

Thorlabs. Aspheric lenses in exotic materials can be obtained as custom items.

Graded Index Lenses. Small lenses with a convenient cylindrical shape can be made from *graded index* material, which has a refractive index that varies from point to point inside the material. A commonly encountered axi-symmetric index variation is Gaussian, or approximately so. The refractive index as a function of distance r from the axis of symmetry is:

$$n = n_0 e^{-r^2/2\sigma^2} \tag{4.147}$$

For distances from the axis that satisfy $r \ll \sigma$, Equation (4.147) can be written as

$$n = n_0\left(1 - \frac{r^2}{2\sigma^2}\right) = n_0 - \frac{1}{2}n_2 r^2 \tag{4.148}$$

where $n_2 = n_0/\sigma^2$. This is a quadratic index profile. A cylindrical piece of such transparent material with flat ends has an overall ray transfer matrix from air, through a length d of the graded medium and back into air:

$$\begin{pmatrix} A & B \\ C & D \end{pmatrix} = \begin{pmatrix} 1 & 0 \\ 0 & n_0 \end{pmatrix}\begin{pmatrix} \cos\left(\frac{d}{\sigma}\right) & \sigma\sin\left(\frac{d}{\sigma}\right) \\ -\frac{1}{\sigma}\sin\left(\frac{d}{\sigma}\right) & \cos\left(\frac{d}{\sigma}\right) \end{pmatrix}\begin{pmatrix} 1 & 0 \\ 0 & 1/n_0 \end{pmatrix}$$
$$= \begin{pmatrix} \cos\left(\frac{d}{\sigma}\right) & \frac{\sigma}{n_0}\sin\left(\frac{d}{n\sigma}\right) \\ -\frac{n_0}{\sigma}\sin\left(\frac{d}{\sigma}\right) & \cos\left(\frac{d}{\sigma}\right) \end{pmatrix} \tag{4.149}$$

The focal length of this GRIN lens is:

$$f = \frac{\sigma}{n_0 \sin\left(\frac{d}{\sigma}\right)} \tag{4.150}$$

which can also be written as:

$$f = \frac{1}{\sqrt{n_0 n_2}\sin(d\sqrt{n_2/n_0})} \tag{4.151}$$

Rays that enter a graded index lens follow sinusoidal paths until they reach the back surface of the lens. The oscillation pattern inside the lens describes its *pitch*. Figure 4.44 shows schematically how the pitch is defined. A 1/4 pitch graded index lens, for example, will take input parallel light and bring it to a focus at the exit face of the lens. Graded index lenses are very convenient to use in small optical arrangements because their flat ends make them easy to couple to other structures, such as semiconductor lasers or optical fibers. They are available commercially as *GRIN* or *SELFOC* lenses from suppliers such as LINOS Photonics, Melles Griot, NSG, Red Optronics, Schott, and Thorlabs. These lenses should not be used in precision imaging applications because they generally suffer from relatively severe aberrations, especially chromatic aberration.

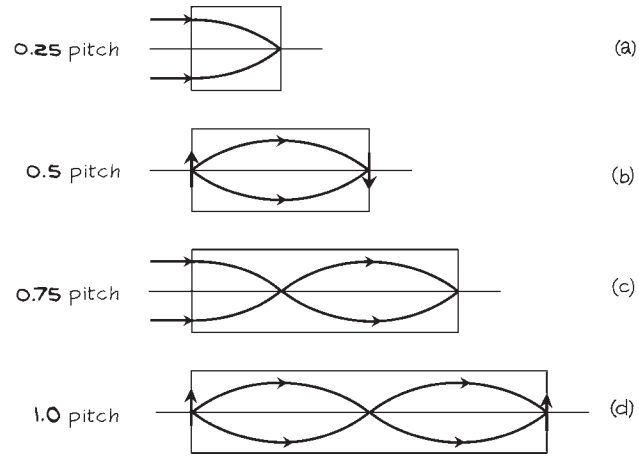

Figure 4.44 Schematic operation of graded index lenses: (a) a quarter pitch lens, which can be used to either focus parallel light or collimate light from a point source on one face of the lens; (b) a half pitch lens, which inverts an image at its front face; (c) a three quarter pitch lens; (d) a whole pitch lens.

Fresnel Lenses. A *Fresnel lens* is an aspheric lens whose surface is broken up into many concentric annular rings. Each ring refracts incident rays to a common focus, so that a very large-aperture, small *f*/number, thin aspheric lens results. Figure 4.45 illustrates the construction and focusing characteristics of such a lens. These lenses are generally manufactured from precision-molded acrylic. Because the refractive index of acrylic varies little with wavelength, from 1.51 at 410 nm to 1.488 at 700 nm, these lenses can be very free of chromatic and spherical aberration throughout the visible spectrum. Fresnel lenses should

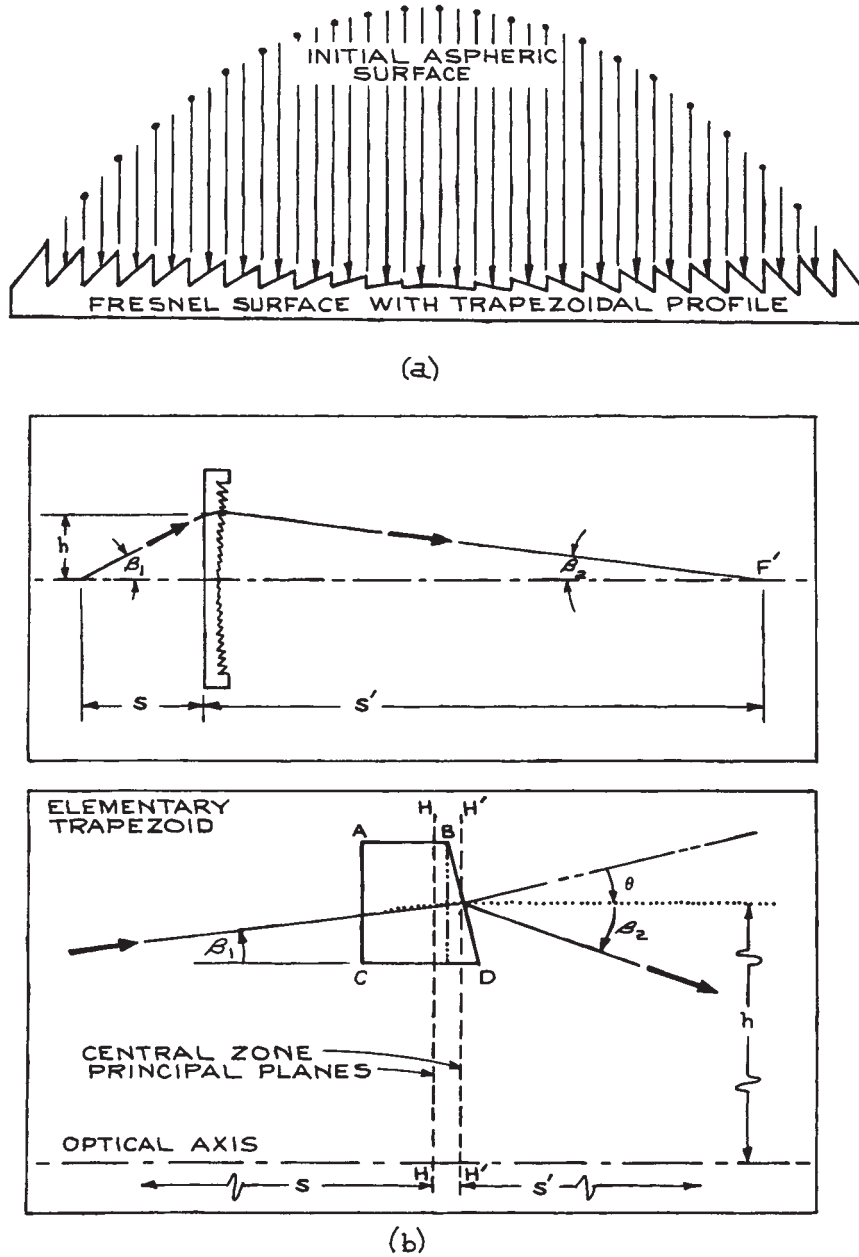

Figure 4.45 (a) A Fresnel lens, made up of trapezoidal concentric sections (it replaces a bulky aspheric lens); (b) illustration of how the focusing characteristics of a Fresnel lens result from refraction at the individual surface grooves. (Courtesy of Melles Griot, Inc.)

be used so that they focus to the plane side of the lens, and their surfaces should not be handled. They are inexpensive and available from very many suppliers, including Edmund Scientific, Fresnel Technologies, Lexitek, Newport/Oriel, and Wavelength Optics. They should not be considered for use in applications where a precision image or diffraction-limited operation is required. Fresnel lenses also scatter much more light than conventional lenses.

Fresnel lenses are an example of a more general class of optics called diffractive optics. These are structured optical elements that use diffraction to redirect light, split a light beam into many separate beams, focus light, produce diffuse light, or correct distorted wavefronts. They are available from Holographix, MEMS Optical, Optocraft, RPC Photonics, Silios Technologies, and Stocker Yale.

Cylindrical Lenses. *Cylindrical lenses* are planar on one side and cylindrical on the other. In planes perpendicular to the cylinder axis they have focusing properties identical to a spherical lens, but they do not focus at all in planes containing the cylinder axis. Cylindrical lenses focus an extended source into a line, and so are very useful for imaging sources onto monochromator slits, although perfect matching of *f*/numbers is not possible in this way. These lenses are also widely used for focusing the output of solid-state and nitrogen lasers into a line image in the dye cell of dye lasers (see Section 4.6.3). Cylindrical lenses are available from Bond Optics, Esco, Infrared Optical Products, Melles Griot, Newport/Oriel, OFR (now Thorlabs), Optimax, and Rolyn.

Optical Concentrators. *Optical concentrators* are nonimaging light collectors that are useful in delivering light to a detector. They effectively increase the collection area of the detector, although they affect the angles of light rays.

If light enters an optical system of entrance aperture diameter $2a$ over a range of angles 2θ and leaves through an aperture of diameter $2a'$ over a range of angles $2\theta'$ then in the paraxial approximation:

$$a\theta = a'\theta' \tag{4.152}$$

which follows from the brightness theorem. If the refractive indices of the input and output media are n, n', respectively, then this relation becomes:

$$na\theta = n'a'\theta' \tag{4.153}$$

The quantity $n^2a^2\theta^2$, which is unchanged in going through the system, is called the *étendue* of the system. Figure 4.46 shows two simple concentrator designs, a linear conical concentrator, and a compound parabolic concentrator (CPC), often called a "Winston" Cone. These devices are hollow or solid cones, which reflect entering rays one or more times before they leave the exit aperture. The range of light angles leaving such a device is greater than the range of light angle entering, by the linear ratio between the entrance and exit apertures. Such a nonimaging light collector could be used to collect light from a diffusely emitting source and direct it onto a small area

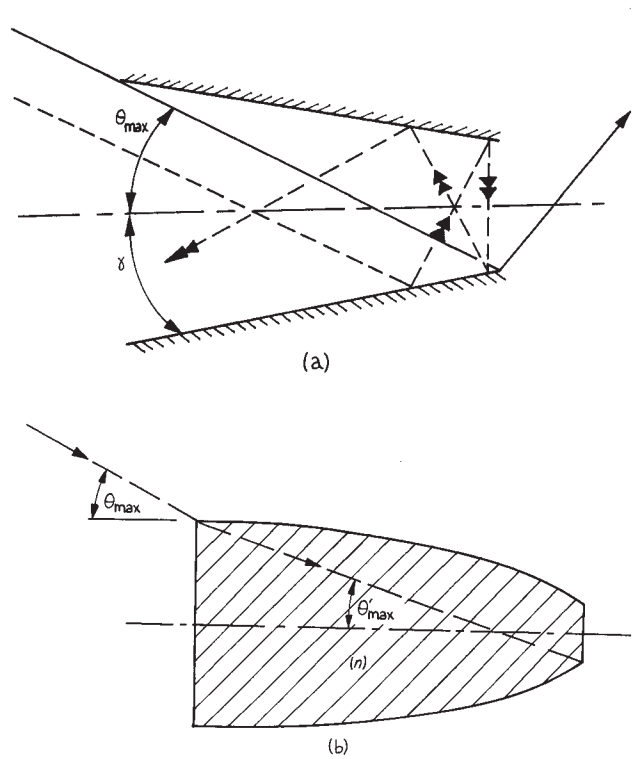

Figure 4.46 Simple optical concentrator designs: (a) linear cone; (b) compound parabolic concentrator.

photoelector; however, the detector's active surface must be placed close to the exit aperture because of the larger range of angles of the emerging light rays.

Nonimaging light collectors are useful for collecting light whose spatial distribution may be fluctuating, yet whose overall power may remain relatively constant, for example, in the case of a laser beam that has passed through a fluctuating medium.

The *concentration ratio* is:[42,43]

$$C = a/a' = \frac{n' \sin \theta'}{n \sin \theta} \tag{4.154}$$

In 2-D the maximum concentration ratio is:

$$C_{\max} = \left(\frac{n'}{n \sin \theta}\right) \tag{4.155}$$

and in 3-D for an axisymmetric concentrator:

$$C_{\max} = \left(\frac{n'}{n \sin \theta}\right)^2 \tag{4.156}$$

The CPC can be fabricated from a solid transparent material with refractive index n. For total internal reflection to occur for all internal rays that enter within a range of angles θ:

$$\sin \theta' \leq 1 - \left(\frac{2}{n^2}\right) \tag{4.157}$$

or

$$\sin \theta \leqslant n - \frac{2}{n} \tag{4.158}$$

To be useful as a material for a CPC it is clear that $n > \sqrt{2}$.

Since the rays leaving a concentrator can cover a solid angle up to 2π sr, when the maximum concentration ratio is used, a detector used in conjunction with the concentrator would need to have its photosensitive surface directly at the exit aperture.

Simple concentrators can be made by direct machining of plastic material such as lexan (refractive index ~ 1.585) using a numerically controlled lathe, followed by polishing. Alternatively, a stainless-steel mandrel could be machined to the required shape, and then a mold made by electroplating over the stainless steel. After the hollow mold is made, then plastic concentrators can be fabricated using transparent epoxy resin placed into the mold and allowed to harden.

4.3.4 Prisms

Prisms are used for the dispersion of light into its various wavelength components and for altering the direction of beams of light. Prisms are generally available in most materials that transmit ultraviolet, visible, and infrared light. High-refractive-index semiconductor materials, such as silicon, germanium, and gallium arsenide, however, are rarely used for prisms. Consult Section 4.4 for a list of suppliers of optical materials.

The deviation and dispersion of a ray of light passing through a simple prism can be described with the aid of Figure 4.47. The various angles α, β, γ, δ satisfy Snell's law irrespective of the polarization state of the input beam, provided the prism is made of an isotropic material. It is easy to show that:

$$\sin \delta = \sin A(n^2 - \sin^2 \alpha)^{1/2} - \cos A \sin \alpha \tag{4.159}$$

and:

$$D = \alpha + \delta - A \tag{4.160}$$

where A is the apex angle shown in Figure 4.47. The exit ray will not take the path shown if γ is greater than the critical angle.

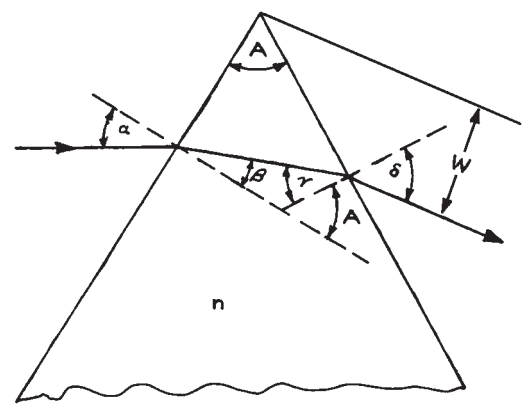

Figure 4.47 Passage of a ray of light through a prism.

The dispersion of the prism is defined as:

$$\frac{d\delta}{d\lambda} = \frac{d\delta}{dn}\frac{dn}{d\lambda} \tag{4.161}$$

Substituting from Equation (4.159), this becomes:

$$d\delta = \frac{\sin A}{\cos\beta\cos\delta}\frac{dn}{d\lambda} \tag{4.162}$$

When the prism is used in the position of minimum deviation:

$$\beta = \gamma = \frac{1}{2}A \tag{4.163}$$

and:

$$\alpha = \delta = \frac{1}{2}(D_{\min} + A) \tag{4.164}$$

By the sine rule, Equation (4.162) can be written in the form:

$$\frac{d\delta}{d\lambda} = \frac{t}{W}\frac{dn}{d\lambda} \tag{4.165}$$

where t is the distance traveled by the ray through the prism and W is the dimension shown in Figure 4.47.

A simple, yet important, application of a prism as a dispersing element is in the separation of a laser beam containing several well-spaced wavelengths into its constituent parts. Situations where this might be necessary include isolation of the 488.8 nm line in the output of an argon ion laser oscillating simultaneously at 476.5, 488.8, and 514.5 nm and other lines, or in nonlinear generation where a fundamental and second harmonic must be separated. If the spatial width of the laser beam is known, then an equation such as (4.165) will determine at what distance from the prism the different wavelengths are spatially separated from each other. The advantages of prisms in this application are that they can introduce very little scattered light, produce no troublesome ghost images, and can be cut so that they operate with $\alpha = \delta = \theta_B$, thereby eliminating reflection losses at their surfaces. Brewster-angle prisms are used in this way inside the cavity of a laser to select oscillation at a particular frequency. A modified prism called a reflecting *Littrow prism* is frequently used in this way, as shown in Figure 4.48. A Littrow prism is designed so that for a particular wavelength the refracted ray on entering the prism travels normal to the exit face. Thus, if the exit face is reflectively coated, for the specified wavelength the incident light is returned along its original path. Generally, a dispersing optical element used *in Littrow* has this retroreflective characteristic at a particular wavelength.

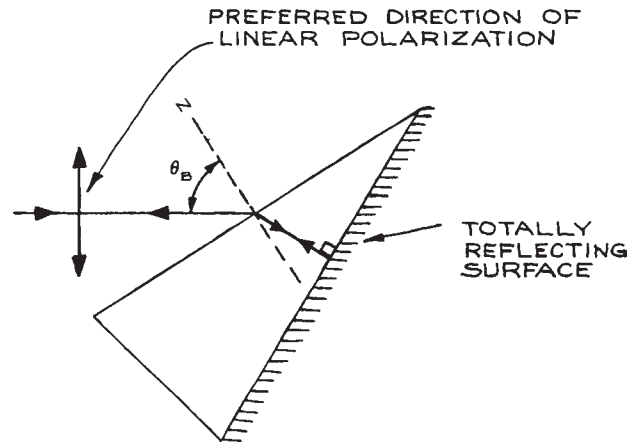

Figure 4.48 Reflecting prism used in Littrow at Brewster's angle. Only light of a specific wavelength will be refracted at the entrance face of the prism and then reflected back on itself at the coated reflecting face.

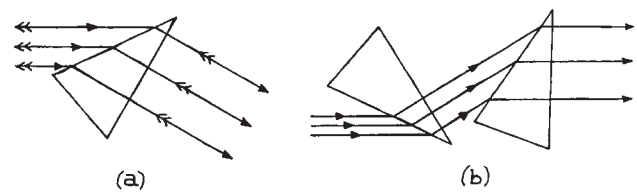

Figure 4.49 (a) One-dimensional beam expansion (or compression) with a prism; (b) one-dimensional beam expansion without beam deflection using two oppositely oriented, similar prisms.

If a beam of parallel monochromatic light passes through a prism, unless the prism is used in the symmetrical minimum-deviation position, the width of the beam will be increased or decreased in one dimension. This effect is illustrated in Figure 4.49. By the use of two identical prisms in an inverted configuration, the compression or expansion can be accomplished without an angular

change in beam direction. Prism beam expanders employing this principle are used in some commercial dye lasers for expanding a small-diameter, intracavity laser beam onto a diffraction grating to achieve greater laser line narrowing. Such prism pairs can be used, in conjunction with lenses, to produce *anamorphic* laser beam expanders. These devices are important for the circularization and collimation of the beams from semiconductor lasers. These lasers generally emit an elliptical-shaped laser beam whose beam divergence angle is different in two orthogonal planes containing the beam axis.

Triangular prisms with a wide range of shapes and vertex angles are available. The most common types are the equilateral prism, the right-angle prism, and isosceles and Littrow prisms designed for Brewster-angle operation. Such prisms are readily available in glass and fused silica from many suppliers.[31] Triangular and other prisms also find wide use as reflectors, utilizing total internal reflection inside the prism or a reflective coating on appropriate faces. Some specific reflective applications of prisms are worthy of special note.

Right-Angle Prisms. Right-angle prisms can be used to deviate a beam of light through 90°, as shown in Figure 4.50(a). Antireflection coatings on the faces shown are desirable in exacting applications. A right-angle prism can also be used to reflect a beam back parallel to its original path, as shown in Figure 4.50(b). The retroreflected beam is shifted laterally. The prism will operate in this way provided the incident beam is in the plane of the prism cross-section. The retroreflection effect is thus independent of rotation about the axis A in Figure 4.50(b). If the angle of incidence differs significantly from zero, the roof faces of the prism need to be coated; otherwise total internal reflection at these surfaces may not result. If such a prism is rotated about the axis B, only in a single orientation does retroreflection result. Roof prisms are available from numerous suppliers, including Ealing, Edmund Scientific, Melles Griot, Newport/Oriel, Opto-Sigma, and Rolyn.

Porro prisms are roof prisms with rounded corners on the hypotenuse face and beveled edges. They are widely

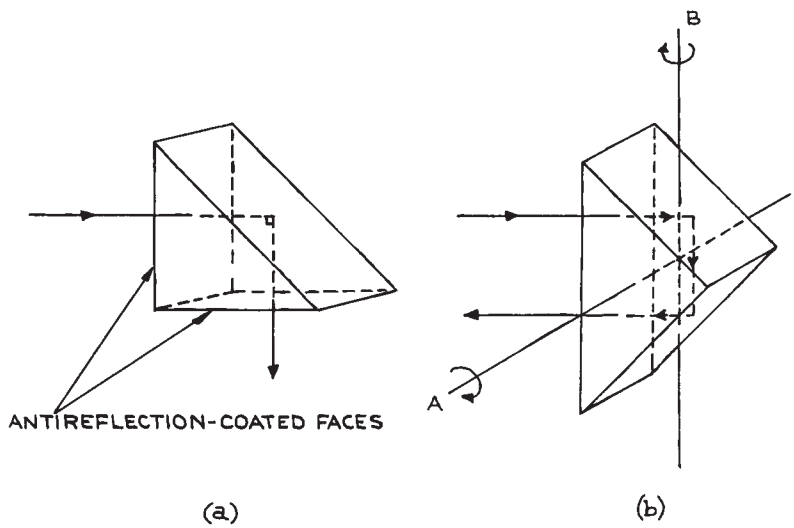

Figure 4.50 (a) Right-angle prism used for 90° beam deflection; (b) right-angle prism used for retroreflection. Incident and reflected ray are parallel only if the incident beam is in the plane of the prism cross-section; however, in this orientation, retroreflection is independent of orientation about the axis A within a large angular range.

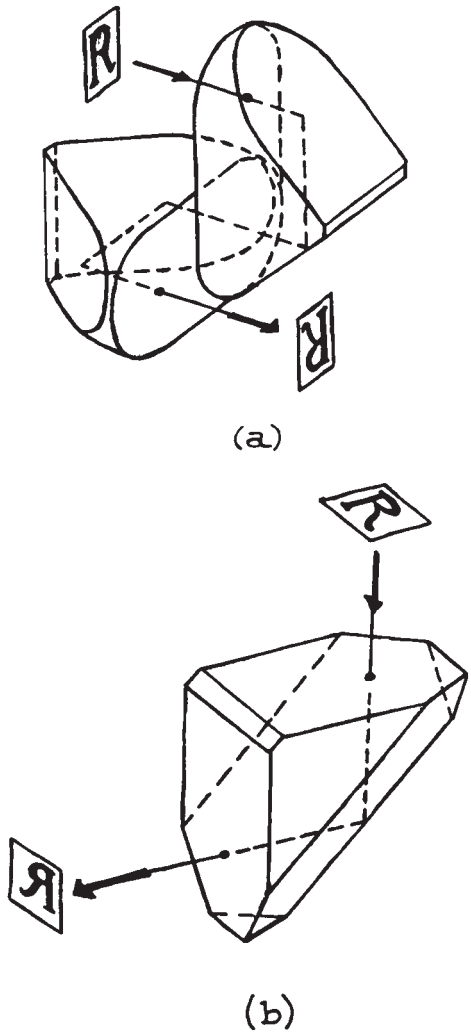

Figure 4.51 (a) Two Porro prisms used as an image-erecting element; (b) Amici prism. (Courtesy of Melles Griot, Inc.)

used in pairs for image erection in telescopes and binoculars, as shown in Figure 4.51(a). They are available from Anchor Optics, Edmund Optics, and Sunny Precision Optics. *Amici prisms* are right-angle prisms where the hypotenuse face has been replaced by a 90° roof. They are available from Anchor Optics, Edmund Optics, Red Optronics, Starna, and TrustOptics. An image viewed through an Amici prism is left-to-right reversed (reverted) and top-to-bottom inverted, as shown in Figure 4.51(b).

Dove, Penta, Polygon, Rhomboid, and Wedge Prisms. These prisms are illustrated in Figure 4.52.

Dove prisms are used to rotate the image in optical systems; rotation of the prism at a given angular rate causes the image to rotate at twice this rate. Dove prisms have a length-to-aperture ratio of about five, so they must be used with reasonably well-collimated light. They are available from Anchor Optics, Edmund Optics, Esco Optics, Melles Griot, Newport, Red Optronics, Rolyn, TrustOptics, and Sunny Precision Optics.

Penta prisms deviate a ray of light by 90° without inversion (turning upside down) or reversion (right-left reversal) of the image. This 90° deviation applies to all rays incident on the useful aperture of the prism, irrespective of their angle of incidence. Penta prisms do not operate by total internal reflection, so their reflective surfaces are coated. These prisms are useful for 90° deviation when vibrations or other effects prevent their alignment being well controlled. They are available from Anchor Optics, Edmund Optics, Melles Griot, Opto-Sigma, Red Optronics, Rolyn, Sunny Precision Optics, and TrustOptics.

Polygon prisms, usually octagonal, are available from Rolyn and are used for high-speed light-ray deviation, for example, in high-speed rotary prism cameras.

Rhomboid prisms are used for lateral deviation of a light ray. When used in imaging applications, there is no change of orientation of the image. Rhomboid prisms are available from Edmund Optics, JML Optical, Precision Glass and Optics, and Rolyn.

Wedge prisms are used in beam steering. The minimum angular deviation D of a ray passing through a thin wedge prism of apex angle A is:

$$D = \arcsin(n \sin A) - A \simeq (n-1)A \qquad (4.166)$$

where n is the refractive index of the prism material. A combination of two identical wedge prisms can be used to steer a light ray in any direction lying within a cone of semivertical angle $2D$ about the original ray direction. Wedge prisms are available from Anchor Optics, Edmund

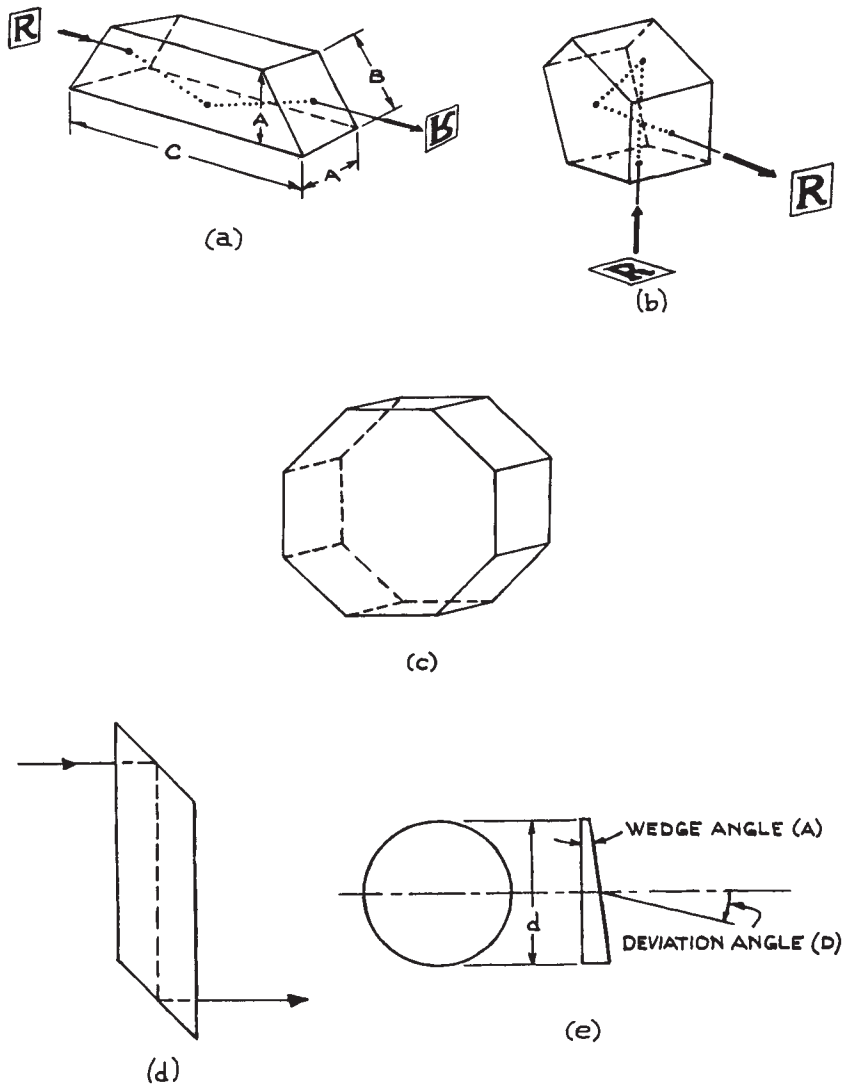

Figure 4.52 (a) Dove prism; (b) penta prism; (c) octagonal prism; (d) rhomboid prism; (e) wedge prism, [(a), (b), and (e) courtesy of Melles Griot, Inc.]

Optics, EKSPLA, Melles Griot, Precision Glass and Optics, Red Optronics, Rolyn, and Sunny Precision Optics.

Corner-Cube Prisms (Retroreflectors). *Corner-cube prisms* are exactly what their name implies, prisms with the shape of a corner of a cube, cut off orthogonal to one of its triad (body-diagonal) axes. The front face of the resultant prism is usually polished into a circle as shown in Figure 4.53. As a result of three total internal reflections, these prisms reflect an incident light ray back parallel to its original direction, no matter what the angle of incidence is. The reflected ray is shifted laterally by an amount that depends on the angle of incidence and the point of entry of the incident ray on the front surface of the prism. These prisms are

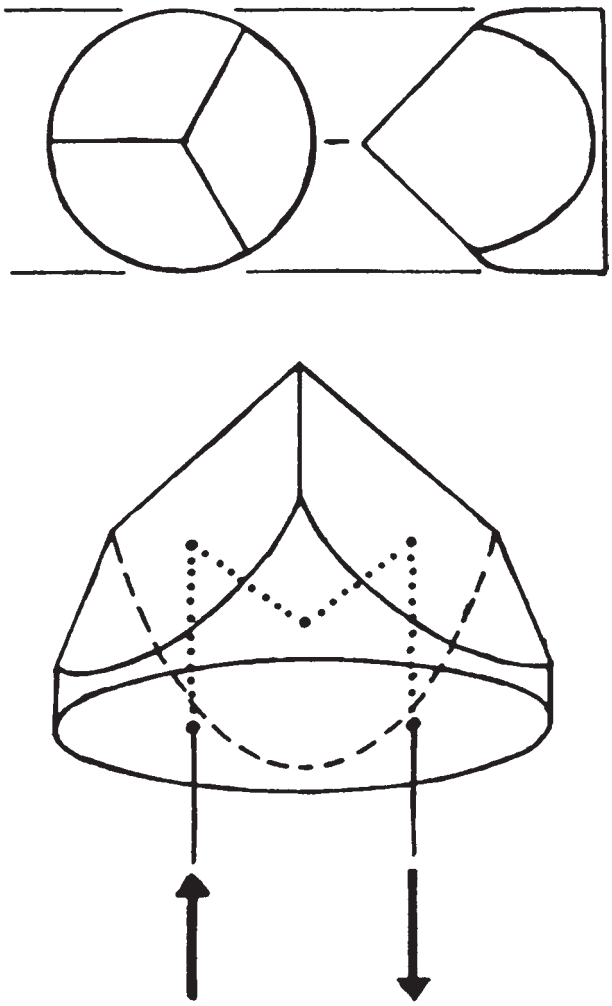

Figure 4.53 Corner-cube prism. (Courtesy of Melles Griot, Inc.)

invaluable in experiments where a light beam must be reflected back to its point of origin from some (usually distant) point – for example, in long-path absorption measurements through the atmosphere with a laser beam. They are available commercially from Edmund Optics, Knight Optical, Melles Griot, Newport, Precision Glass and Optics, Precision Optical, Red Optronics, Rolyn, and Sunny Precision Optics. The angular deviation of the reflected ray from its original direction can be held to less than a half second of arc in the best prisms. For infrared applications beyond the transmission of fused silica, corner-cube prisms are not readily available, but retroreflectors can be made by using three square mirrors butted together to form a hollow cube corner. Precision hollow corner cubes of this type are available from PLX.

4.3.5 Diffraction Gratings

A *diffraction grating* is a planar or curved optical surface covered with straight, parallel, equally spaced grooves. They are manufactured in three principal ways: by direct ruling on a substrate (called a *master* grating), by replication from a master grating, and holographically. Such gratings can be made for use in transmission, but are more commonly used in reflection. Light incident on the grooved face of a reflection grating is diffracted by the grooves; the angular intensity distribution of the diffracted light depends on the wavelength and angle of incidence of the incident light and on the spacing of the grooves. This can be illustrated with reference to the plane grating shown in Figure 4.54. The grooves are usually produced in an aluminum or gold

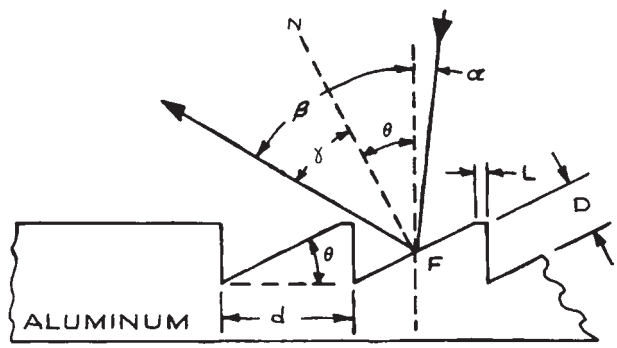

Figure 4.54 Blazed groove profile. The thickness of the aluminum is generally equal to the blaze wavelength, and the depth of the groove is about half the thickness. The dimensions shown are approximately those for a grating ruled with 1200 grooves per millimeter, blazed at 750 nm. D = depth of ruling; d = groove spacing; L = unruled land; α = angle of incidence; β = angle of diffraction; γ = angle of reflection; θ = blaze angle. The line N is normal to the groove face F. (From D. Richardson, "Diffraction Gratings," in *Applied Optics and Optical Engineering*, Vol. 5, R. Kingslake (Ed.), Academic Press, New York, 1969; by permission of Academic Press).

layer that has been evaporated onto a flat optical substrate. For high-intensity laser applications the substrate should have high thermal conductivity. Master gratings ruled on metal are available for this purpose from Diffraction Products, Jobin-Yvon, and Richardson Grating Laboratory (through Newport). If the light diffracted at angle β from a given groove differs in phase from light diffracted from the adjacent groove by an integral multiple m of 2π, a maximum in diffracted intensity will be observed. This condition can be expressed as:

$$m\lambda = d(\sin\alpha \pm \sin\beta) \tag{4.167}$$

The plus sign applies if the incident and the diffracted ray lie on the same side of the normal to the grating surface; m is called the order of the diffraction. For $m = 0$, $\alpha = \beta$ and the grating acts like a mirror. In any other order, the diffraction maxima of different wavelengths lie at different angles. The actual distribution of diffracted intensity among the various orders depends on the profile of the grating grooves. If the grooves are planar, cut at an angle θ to the plane of the grating, maximum diffracted intensity into a particular order results if the angle of diffraction and the angle of reflection are the same. In this case:

$$\beta - \theta = \gamma \tag{4.168}$$

θ is called the *blaze angle*. The wavelength for which the angle of reflection from the groove face and the diffraction angle are the same is called the *blaze wavelength*, λ_B. It is common to use a grating in a Littrow configuration so that the diffracted ray lies in the same direction as the incident ray. In this case:

$$m\lambda = 2d\sin\beta \tag{4.169}$$

The wavelength at which the light reflects normally from the grating groove satisfies:

$$m\lambda_B = 2d\sin\theta \tag{4.170}$$

Thus, for example, a grating could be specified to be blazed at 600 nm in the first order; it would, of course, be simultaneously blazed in the second order for 300 nm, the third order for 200 nm, and so on. Gratings are also available with rectangular shaped (laminar profile) or sinusoidal groove profiles. Laminar profile grooves have low second-order efficiency, which can be advantageous in vacuum ultraviolet applications: second-order rejection filters are not available at such short wavelengths. Sinusoidal gratings will operate over a broad spectral range, but their diffraction efficiency into a particular order is at best 33%. There are many suppliers of both plane and concave gratings, particularly Diffraction Products, Digital Optics, Gentec, Jobin-Yvon, Newport, Optometrics, Spectrogon, Spectrum Scientific, and TVC Jarrell-Ash.

Resolving Power. The *resolving power* of a grating is a measure of its ability to separate two closely spaced wavelengths. The resolving power depends both on the dispersion and the size of the grating. For a fixed angle of incidence, the *dispersion* is defined as:

$$\left(\frac{d\beta}{d\lambda}\right)_\alpha = \frac{m}{d\cos\beta} \tag{4.171}$$

Thus, the dispersion can be increased by increasing the number of lines per millimeter ($1/d$), by operating in a high order, and by using a large angle of incidence (grazing incidence). The incidence, however, must not be so flat as to make the projection of the groove width perpendicular to the incoming light smaller than the wavelength of the light.

The resolving power of a grating is $\Delta\lambda/\lambda$, where λ and $\lambda + \Delta\lambda$ are two closely spaced wavelengths that are just resolved by the grating. The limiting resolution depends on the projected width of the grating perpendicular to the diffracted beam. This width is $Nd\cos\beta$, where N is the total number of lines in the grating. Diffraction theory predicts that the angular resolution of an aperture of this size is $\Delta\phi \simeq \lambda/(Nd\cos\beta)$. The angle between the two closely spaced wavelengths, from the dispersion relation, is:

$$\Delta\beta = \frac{m\Delta\lambda}{d\cos\beta} \tag{4.172}$$

In the limit of resolution, $\Delta\phi = \Delta\beta$, which gives:

$$\lambda/\Delta\lambda = mN \tag{4.173}$$

Thus, from Equation (4.167):

$$\frac{\lambda}{\Delta\lambda} = \frac{Nd(\sin\alpha \pm \sin\beta)}{\lambda} \tag{4.174}$$

and so it is clear that large gratings used at high angles give the highest resolving power. The resolving powers available from 1 cm wide gratings range up to about 5×10^5.

Concave gratings. These have long been used in short wavelength applications because they provide diffractive and focusing functions simultaneously. The development of holographic concave gratings has made these devices widely available. They can be used to correct for aberrations which occur when they are used in spectrometers (see Section 4.7), and to allow compact versions of such instruments to be produced.

Efficiency. The efficiency of a grating is a measure of its ability to diffract a given wavelength into a particular order of the diffraction pattern. Blazing of the grating is the main means for obtaining efficiency in a particular order; without it, the diffracted energy is distributed over many orders. Gratings are available with efficiencies of 95% or more at their blaze wavelength, so they are virtually as efficient as a mirror, yet retain wavelength selectivity.

Defects in Diffraction Gratings. In principle, if an ideal grating is illuminated with a plane monochromatic beam of light, diffracted maxima occur only at angles that satisfy the diffraction equation (4.167). In practice, however, this is not so. Gratings manufactured by ruling a metal-coated substrate with a ruling engine exhibit undesirable additional maxima.

Periodic errors in the spacing of the ruled grooves produce *Rowland ghosts*. These are spurious intensity maxima, usually symmetrically placed with respect to an expected maximum and usually lying close to it. The strongest Rowland ghosts from a modern ruled grating will be less than 0.1% of the expected diffraction peaks. *Lyman ghosts* occur at large angular separations from their parent maximum, usually at positions corresponding to a simple fraction of the wavelength of the parent maximum – 4/9 or 5/9, for example. They are also associated with slow periodic errors in the ruling process. Lyman-ghost intensities from modern gratings are exceedingly weak (0.001% of the parent or less). Ghosts can be a problem when used for the detection of weak emissions in the presence of a strong laser signal, the ghosts of which can (and have been) mistakenly identified as other real spectral lines. If there is any suspicion of this, the weak signal should be checked for its degree of correlation with the laser signal – a linear correlation would be strong evidence for a ghost. The development of unruled holographic gratings, which are essentially perfect, plus the improvement of ruled gratings made by interferometrically controlled ruling engines, has considerably reduced the problem of ghosts.

There are other diffraction-grating defects. *Satellites* are misplaced spectral lines, which can be numerous, occurring very close to the parent, usually so close that they can only be discerned under conditions of high resolution: they arise from small local variations in groove spacing. *Scattering* gives rise to an apparent weak continuum over all diffraction angles when a grating is illuminated with an intense monochromatic source such as a laser. Scattering can arise from microscopic dust particles or nongroove-like, random defects on the diffraction-grating surface. In practice it does not follow that a diffraction grating that shows apparent blemishes, such as broad, shaded bands, will perform defectively. One should never attempt to remove such apparent visual blemishes by cleaning or polishing the grating.

Specialized Diffraction Gratings. Concave gratings are frequently used in vacuum-ultraviolet spectrometers and spectrographs, as they combine the functions of both dispersing element and focusing optics. Thus, fewer reflective surfaces are required – a highly desirable feature of an instrument used at short wavelengths, where reflectances of all materials decrease markedly.

Gratings for use at long wavelengths, above 50 μm, use relatively few grooves per millimeter. Such gratings are generally ruled directly on metal and are frequently called *echelettes* (little ladders) because of the shape of their grooves.

Echelle gratings are special gratings designed to give very high dispersion, up to 10^6 for ultraviolet wavelengths, when operated in a very high order. They have the surface profile illustrated in Figure 4.55, where the dimension D is much larger than in a conventional grating, and can range up to several micrometers. Echelles are widely used as the wavelength-tuning element in pulsed dye lasers because of their high dispersion and efficient operation. Other uses of diffraction gratings, such as in the production of Moiré fringes and in interferometers, will not be discussed here. These subjects have been dealt with by Girard and Jacquinot.[44]

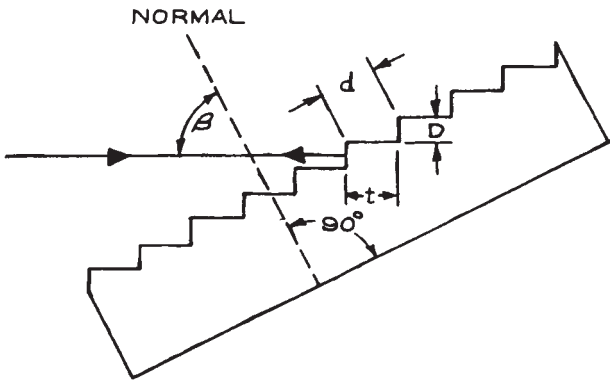

Figure 4.55 Echelle grating used in Littrow.

Practical Considerations in Using Diffraction Gratings. The main considerations in specifying a diffraction grating are the wavelength region where maximum efficiency is required (which will specify the blaze angle), and the number of grooves per millimeter and the size of the grating (which will determine the resolving power). Most gratings are rectangular or circular, the latter being primarily for laser-cavity wavelength selection. Diffraction gratings should be mounted with the care due all precision components. Their surfaces should *never* be touched and should be protected from dust. It is important to note that if a grating is illuminated with a given wavelength, say 300 nm, then diffraction maxima will occur in the same positions as would be found for 600 and 900 nm. This difficulty can be avoided by using appropriate filters to prevent unwanted wavelengths from passing through the system.

4.3.6 Polarizers

Polarized Light. If the electric vector of an electromagnetic wave always points in the same direction as the wave propagates through a medium, then the wave is said to be *linearly polarized*. The *direction of linear polarization* is defined as the direction of the electric displacement vector **D,** where:

$$\mathbf{D} = \epsilon_r \epsilon_0 \mathbf{E} \tag{4.175}$$

Except in anisotropic media, where ϵ_r is a tensor, **D** and **E** are parallel and the direction of linear polarization can be taken as the direction of **E**. If a combination of two linearly polarized plane waves of the same frequency, but having different phases, magnitudes, and polarization directions, is propagating in the z-direction, the resultant light is said to be *elliptically polarized*. Such a pair of waves, in general, have resultant electric fields in the x-and y-directions that can be written as:

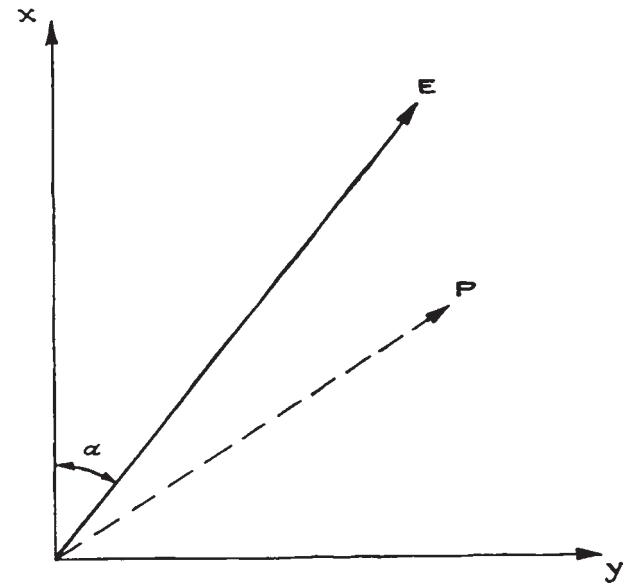

Figure 4.56 Instantaneous direction of the electric vector of an electromagnetic wave.

$$E_x = E_1 \cos \omega t \tag{4.176}$$

$$E_y = E_2 \cos(\omega t + \phi) \tag{4.177}$$

where ϕ is the phase difference between these two resultant field components. These are the parametric equations of an ellipse. If $\phi = \pm\pi/2$ and $E_1 = E_2 = E_0$, then:

$$E_x^2 + E_y^2 = E_0^2 \tag{4.178}$$

which is the equation of a circle. This represents *circularly polarized* light. Then the instantaneous angle that the total electric field vector makes with the x-axis, as illustrated in Figure 4.56, is:

$$\alpha = \arctan \frac{E_y}{E_x} = \arctan \mp \tan \omega t = \mp \omega t \tag{4.179}$$

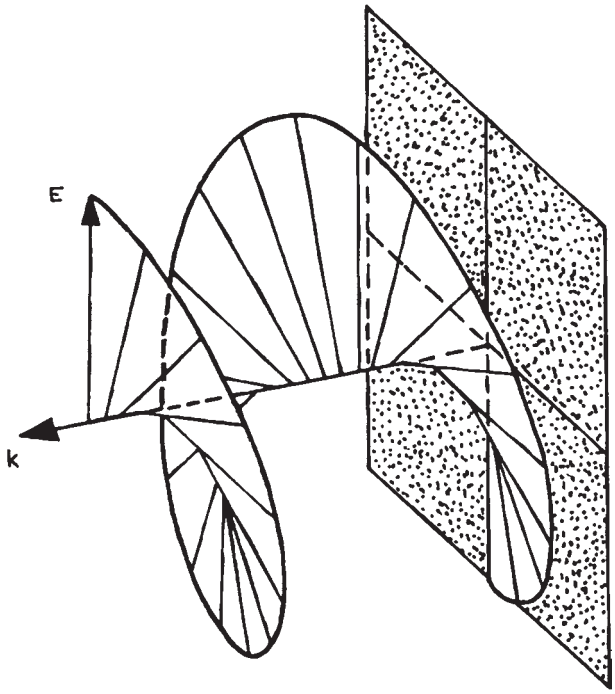

Figure 4.57 Left-hand circularly polarized light. (From E. Wahlstrom, *Optical Crystallography*, 3rd edn., John Wiley & Sons, Inc., New York, 1960; by permission of John Wiley & Sons, Inc.)

For $\phi = \pi/2$, the resultant electric vector rotates counterclockwise viewed in the direction of propagation – this is *right-hand circularly polarized light*. If $\phi = -\pi/2$ the rotation is clockwise – this is *left-hand circularly polarized light*. The motion of the total electric vector as it propagates is illustrated in Figure 4.57. If $\phi = 0$ or π we have *linearly polarized light*. Just as circularly polarized light can be viewed as a superposition of two linearly polarized waves with orthogonal polarizations, a linearly polarized wave can be regarded as a superposition of left- and right-hand circularly polarized waves. If an electromagnetic wave consists of a superposition of many independent linearly polarized waves of independent phase, amplitude, and polarization direction, it is said to be *unpolarized*.

In anisotropic media – media with lower than cubic symmetry – there is at least one direction, and at most two directions, along which light can propagate with no change in its state of polarization, independent of its state of polarization. This direction is called the *optic axis*. *Uniaxial crystals* have one such axis; *biaxial crystals* have two. When a wave does not propagate along the optic axis in such crystals, it is split into two polarized components with orthogonal linear polarizations. In uniaxial crystals these two components are called the *ordinary* and *extraordinary* waves. They travel with different phase velocities, characterized by two different refractive indices, n_o and $n_e(\theta)$, respectively, where θ is the angle between the **k** vector of the wave and the optic axis. This phenomenon is referred to as *birefringence*.

D and **E** are not necessarily parallel in an anisotropic medium; however, **D** and **H** are orthogonal to the wave vector of any propagating wave. Consequently the Poynting vector of the wave does not, in general, lie in the same direction as the wave vector. The direction of the Poynting vector is the direction of energy flow – the ray direction. When a plane wave crosses the boundary between an isotropic and an anisotropic medium, the path of the ray will not, in general, satisfy Snell's law. The angles of refraction of the ordinary and extraordinary rays will be different. This phenomenon is called *double refraction*. In uniaxial crystals, however, the ordinary ray direction at a boundary does satisfy Snell's law. For further details of these and other optical characteristics of anisotropic media, the reader should consult Born and Wolf,[11] Wahlstrom,[12] and Davis.[15]

If linearly polarized light propagates into a birefringent material, unless its polarization direction matches the allowed direction of the ordinary or extraordinary wave, it will be split into two components polarized in these two allowed directions. These two components propagate at different velocities and experience different phase changes on passing through the crystal. For light of free-space wavelength λ_0 passing through a uniaxial crystal of length L, the birefringent phase shift is:

$$\Delta\phi = \frac{2\pi L}{\lambda_0}[n_e(\theta) - n_o] \tag{4.180}$$

In uniaxial crystals the allowed polarization directions are perpendicular to the optic axis (for the ordinary wave) and in the plane containing the propagation direction and the optic axis (for the extraordinary wave), as shown in

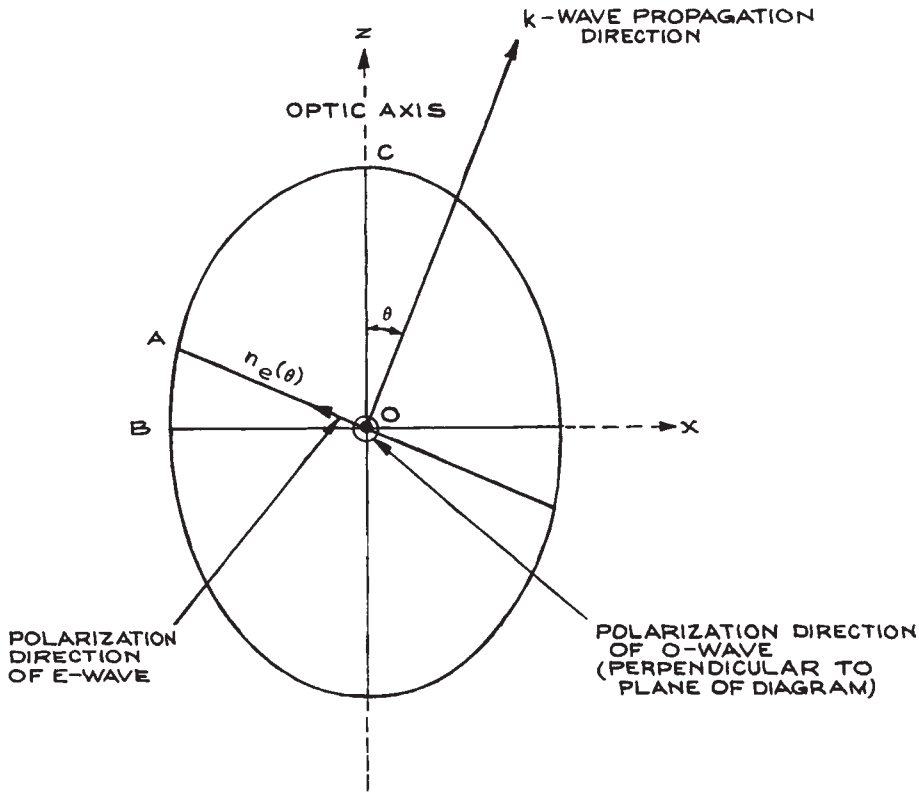

Figure 4.58 Cross-section of an ellipsoidal figure called the indicatrix, which allows determination of the refractive indices and permitted polarization directions of a wave traveling in a uniaxial crystal. The equation of the ellipse shown is $(x^2/n_o^2) + (z^2/n_e^2) = 1$, where $OB = n_o$ and $OC = n_e$, $OA = n(\theta)$ is the effective extraordinary refractive index for a wave traveling at angle θ to the optic axis. The ordinary refractive index for this wave is still n_o and is independent of θ.

Figure 4.58. If the input wave is polarized at an angle β to the ordinary polarization direction and $\Delta\phi = (2n + 1)\pi$, the output wave will remain linearly polarized, but its direction of polarization will have been rotated by an angle of 2β. This rotation is always toward the ordinary polarization direction, so a round-trip pass through the material does not affect the polarization state. It is usual to make $\beta = 45°$, in which case the crystal rotates the plane of polarization by 90°. Such a device is called a $(2n + 1)$th-order *half-wave plate*. On the other hand, if $\beta = 45°$ and $\Delta\phi = (2n + 1)\pi/2$, the ordinary and extraordinary waves recombine to form circularly polarized light. Such a device is called a $(2n + 1)$th-order *quarter-wave plate*. If β is not 45°, a quarter-wave plate will convert linearly polarized light into elliptically polarized light.

Polarization Changes on Reflection. As shown in Section 4.2.6, if a linearly polarized wave reflects from a dielectric surface (or mirror), its state of linear polarization may be changed. For example, if a vertically polarized wave traveling horizontally striking a mirror at 45° is polarized in the plane of incidence, then after reflection it will be traveling vertically and will be horizontally polarized. A reflection off a second mirror at 45°, so

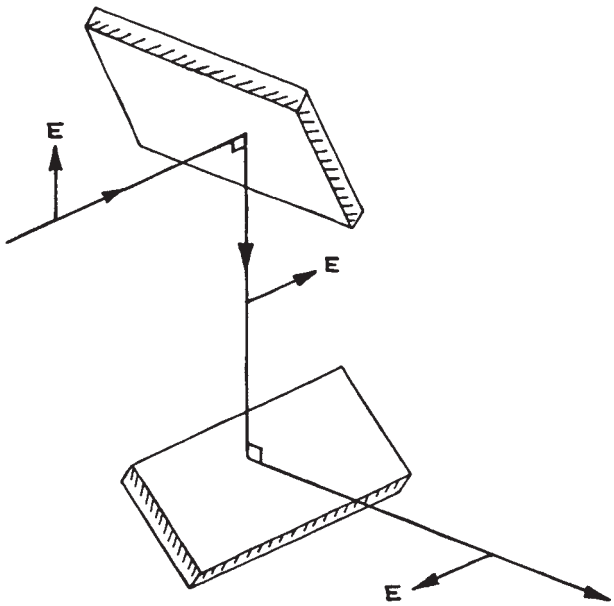

Figure 4.59 Rotation of the plane of polarization of a linearly polarized beam by successive reflection at two mirrors.

oriented that the plane of incidence is perpendicular to the polarization, will produce a horizontally traveling, horizontally polarized wave. This exemplifies how successive reflections can be used to rotate the plane of polarization of a linearly polarized wave, and is illustrated in Figure 4.59.

If circular or elliptically polarized light reflects from a dielectric surface or mirror, its polarization state will, in general, be changed. As an example, consider reflection at a metal mirror. From Equations (4.87) and (4.89), for the in-plane and perpendicular polarized components of the incident wave, respectively, we have:

$$\begin{aligned} \rho_{\parallel} &= -1 \\ \rho_{\perp} &= -1 \end{aligned} \tag{4.181}$$

These reflection coefficients ensure that the tangential component of the electric field goes to zero at the conducting surface of the mirror. As illustrated in Figure 4.60(a) and (b), this leads to a conversion of left- to right-hand circularly polarized light on reflection. The change of polarization state on reflection from a dielectric interface depends on the angle of incidence and whether $n_2 > n_1$.

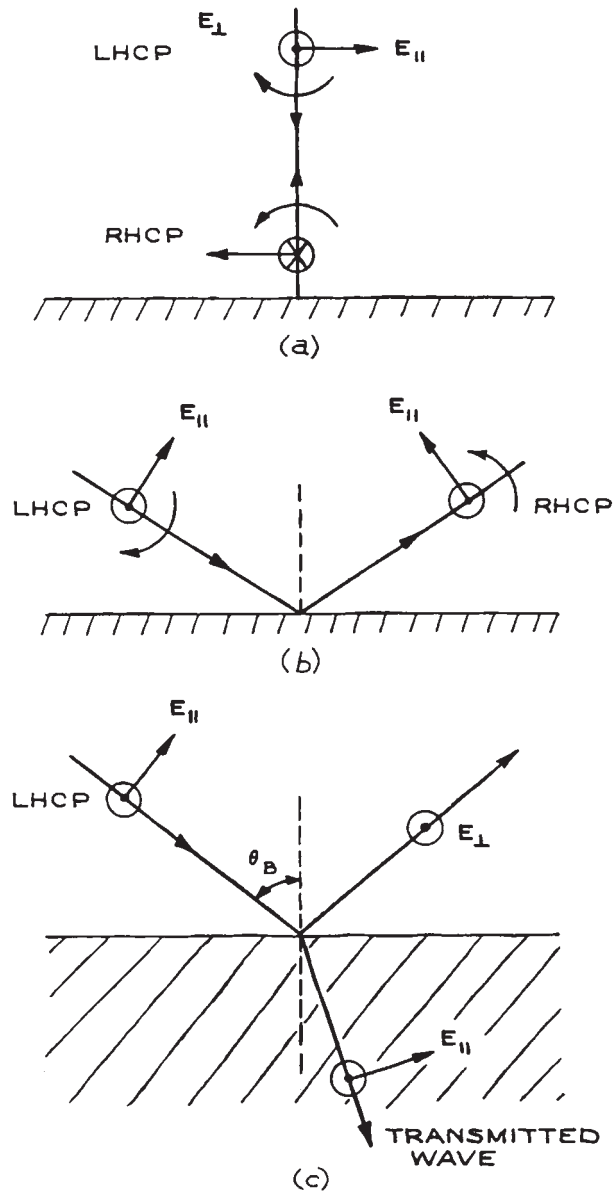

Figure 4.60 Changes of polarization state on reflection: (a) and (b) conversion of left-hand circularly polarized light (LHCP) to right-hand circularly polarized light (RHCP) on reflection at a perfect metal mirror; (c) conversion of LHCP to linear polariation on reflection at Brewster's angle.

A special case, illustrated in Figure 4.60(c), shows left-hand circularly polarized light being converted to linearly polarized light on reflection from an interface placed at Brewster's angle. Such changes of polarization state must be taken into account when designing an optical system to work with polarized light. The change in polarization of a beam of light as it passes through a series of optical components can be calculated very conveniently by the use of Jones or Mueller calculus, which use matrix methods to describe the state of polarization of the beam and its interaction with each component. Details of these techniques are given by Shurcliff.[13]

Linear Polarizers. A *linear polarizer* changes unpolarized light to linearly polarized light or changes polarized light to a desired linear polarization.

The simplest linear polarizers are made from dichroic materials – materials that transmit one polarization, either ordinary or extraordinary, and strongly absorb the other. Modern dichroic linear polarizers, the commonest of which is Polaroid, are made of polymer films in which long-chain molecules with appropriate absorbing side groups are oriented by stretching. The stretched film is then sandwiched between glass or plastic sheets. These polarizers are inexpensive, but cannot be used to transmit high intensities because they absorb all polarizations to some degree. They cannot be fabricated to very high optical quality, and generally only transmit about 50% of light already linearly polarized for maximum transmission. They do, however, work when the incident light strikes them at any angle up to grazing incidence. The extinction coefficient K that can be achieved with crossed polarizers is defined as:

$$K = \log_{10} \frac{T_0}{T_{90}} \tag{4.182}$$

where T_0 and T_{90} are the transmittances of parallel and crossed polarizers, respectively. K is a useful quantity for specifying a linear polarizer – the larger its value, the better the polarizer. For dichroic polarizers, values of K up to about 4 can be obtained. Polarizing beamsplitting cubes provide linearly polarized light of relatively high purity (98% or better) and can handle higher light intensities. Corning manufacture a sheet polarizer called Polacor made from glass containing billions of tiny silver crystals. This material provides high throughput in the red to near-infrared region, and extinction up to 4.

Higher quality, but more expensive, linear polarizers can be made by using the phenomenon of double refraction in transparent birefringent materials such as calcite, crystalline quartz, or magnesium fluoride. Figure 4.61 shows schematically the way in which various polarizing prisms of this type operate. Some of these polarizers generate two orthogonally polarized output beams separated by an angle, while others, for example the Glan–Taylor, reject one polarization state by total internal reflection at a boundary. Extinction coefficients as high as 6 and good optical quality can be obtained from such polarizers. The acceptance angle of these polarizers is generally quite small, although it can range up to about 38° with an Ahrens polarizer. Suppliers of polarizing prisms include Argyle International, Gooch and Housego, Karl Lambrecht Corporation, II-VI Infrared, Inrad, Lambda Research Optics, Meadowlark Optics, Melles Griot, Newport/Oriel, Opto-Sigmna, and Precision Optical.

Infrared polarizers (beyond about 7 μm) are often made in the form of very many fine, parallel, closely spaced metal wires. Waves with their electric vector perpendicular to the wires are transmitted; the parallel polarization is reflected. Such polarizers are available from Coherent/Molectron, Specac, and Thorlabs.

Linear polarizers for any wavelength where a transparent window material is available can be made using a stack of plates placed at Brewster's angle. Unpolarized light passing through one such plate becomes slightly polarized, since the component of incident light polarized in the plane of incidence is completely transmitted, whereas only about 90% of the energy associated with the orthogonal polarization is transmitted. A pile of 25 plates gives a high degree of polarization. Stacked-plate polarizers are rather cumbersome, but they are most useful for polarizing high-energy laser beams where prism polarizers would suffer optical damage. They are available commercially from Inrad and II-VI Infrared (using ZnSe). For visible and near-infrared light they can be easily made using a stack of microscope slides.

Retardation Plates. *Quarter-wave plates* are generally used for converting linear to circularly polarized light.

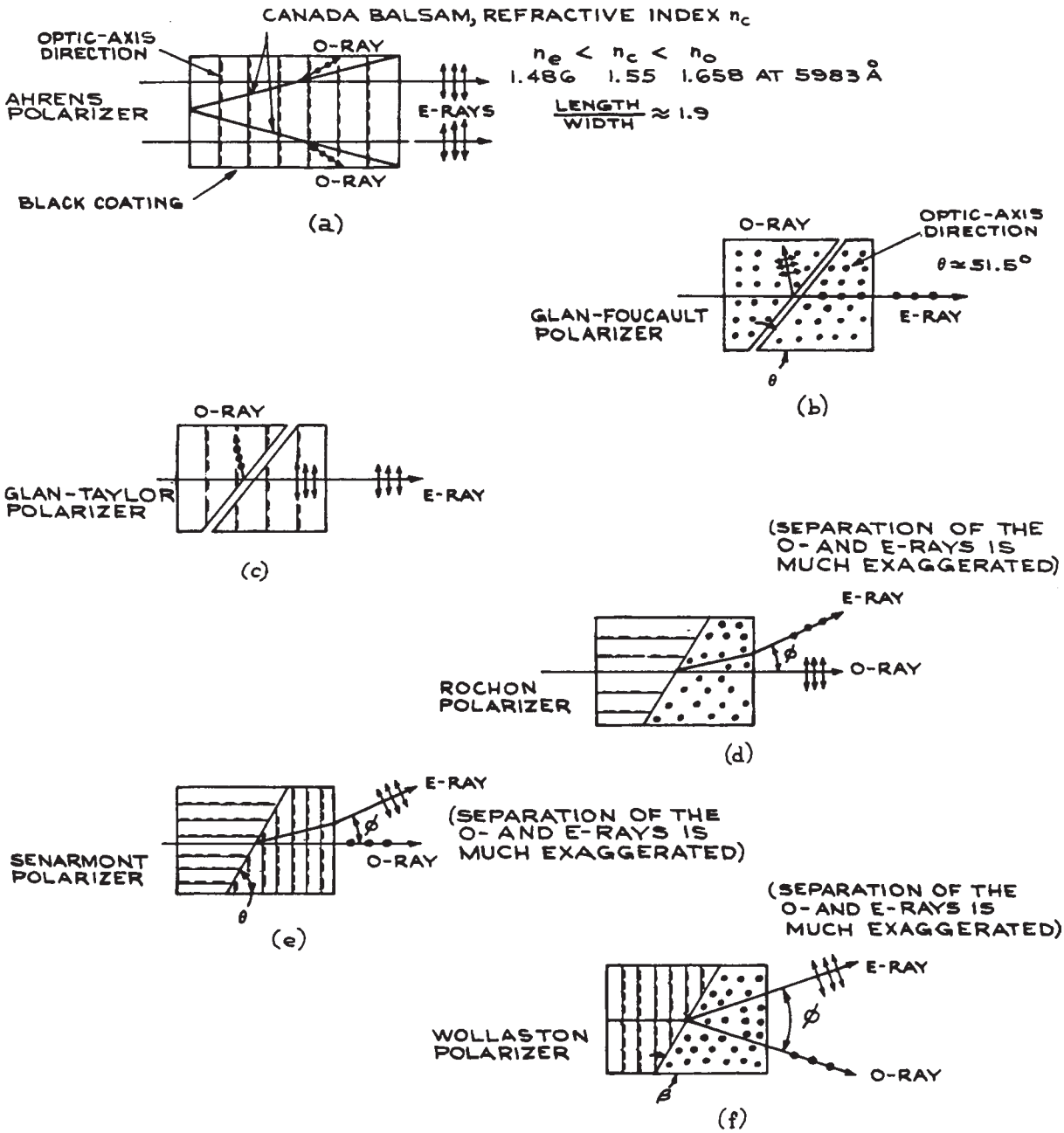

Figure 4.61 Construction of various polarizers using birefringent crystals: (a) Ahrens polarizer – three calcite prisms cemented together with Canada balsam, whose refractive index is intermediate between n_o and n_e for calcite. The O-ray suffers total internal reflection at the cement and is absorbed in the black coating on the sides; (b) Glan–Foucault polarizer – two calcite prisms separated with an air gap. The O-ray is totally internally reflected and either absorbed in the sides or transmitted

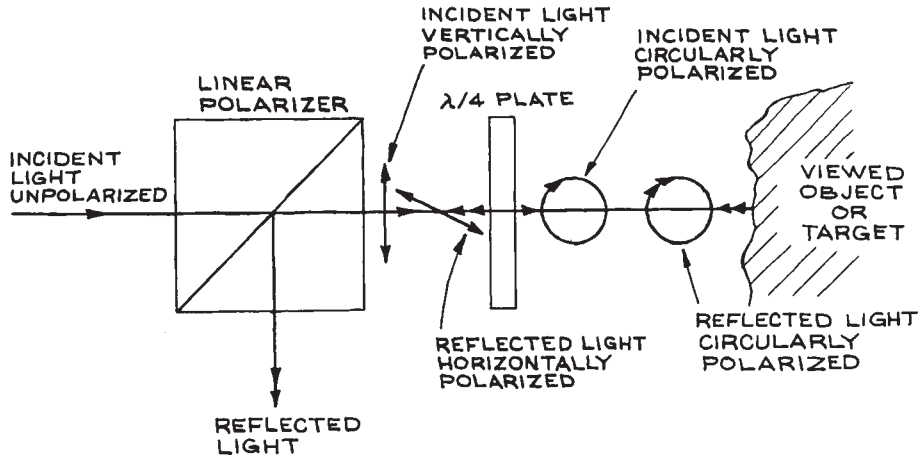

Figure 4.62 An optical isolator constructed from a linear polarizer and a quarter-wave plate.

They should be used with the optic-axis direction at 45° to the incident linear polarization direction. They are available commercially in two forms: multiple- and single-order. Multiple-order plates produce a phase change (retardation) between the ordinary and extraordinary waves of $(2n + 1)\pi/2$. This phase difference is very temperature-sensitive – a thickness change of one wavelength will produce a substantial change in retardation. Single-order plates are very thin, their thickness being:

$$L = \frac{\lambda_0}{4(n_e - n_o)} \tag{4.183}$$

For example, with calcite, which has $n_o = 1.658$, $n_e = 1.486$, and with $\lambda_0 = 500$ nm this thickness is only 726.7 nm. Consequently, most single-order plates are made by stacking a $(2n + 1)$th-order quarter-wave plate on top of a $2n$th-order plate whose optic axis is orthogonal to that of the first plate. The net retardation is just $\pi/2$ and is very much less temperature-sensitive.

Direct single-order quarter-wave plates for low-intensity applications can be made from mica, which cleaves naturally in thin slices. The production of a plate for a particular wavelength is a trial-and-error procedure.[12,45] Quarter-wave plates are invaluable, in combination with a linear polarizer, for reducing reflected glare and for reducing back reflections into an optical system, as shown in Figure 4.62.

Half-wave plates are generally used for rotating the plane of polarization of linearly polarized radiation.

Caption for Figure 4.61 *(cont.)* if the sides are polished. A Glan–Thompson polarizer is similar; (c) Glan–Taylor polarizer – similar to a Glan–Foucault polarizer except for the optic-axis orientation, which ensures that the transmitted E-ray passes through the air gap nearly at Brewster's angle; consequently, transmission losses are much reduced from those of a Glan–Foucault. For high-power laser applications, the side faces can be polished at Brewster's angle; (d) Rochon polarizer – two calcite prisms with orthogonal optic axes cemented together with Canada balsam. ϕ depends on the interface angle. The intensities of the transmitted O- and E-rays are different. Other birefringent materials can be used; in the case of quartz, for example, the E-ray would exit below the O-ray in the diagram shown here; (e) Senarmont polarizer – two calcite prisms cemented together with Canada balsam. The angle ϕ depends on θ. This type of polarizer is less commonly used than the Rochon polarizer; (f) Wollaston polarizer – two calcite prisms cemented together with Canada balsam. The O- and E-ray transmitted intensities are different. The beam separation angle ϕ depends on the interface angle θ.

Multiple- and zero-order plates are available; as in the case of quarter-wave plates, the operating wavelength must be specified in buying one. This operating wavelength can be tuned to some extent by tilting the retardation plate. Half-wave plates cannot be used to make an optical isolator, as the polarization change that occurs on one pass through the plate is reversed on the return path.

Retardation plates only produce their specified retardation at a particular wavelength, and are usually specified for normal, or almost normal incidence. Retardation plates are available from several suppliers, including Karl Lambrecht Corporation, Optics for Research, Inrad, II-VI Infrared, Esco, Melles Griot, Newport, OptoSigma and Thorlabs. Continuously adjustable retardation plates, called Babinet-Soleil compensators, are available from Karl Lambrecht Corporation, Melles Griot, II-VI Infrared, New Focus, Continental Optical, and OFR (now Thorlabs), among others.[31]

Retardation Rhombs. Because, in general, there is a different phase shift on total internal reflection for waves polarized in and perpendicular to the plane of incidence, a retarder that is virtually achromatic can be made by the use of two internal reflections in a rhomboidal prism of appropriate apex angle and refractive index. Two examples are shown in Figure 4.63. The Fresnel rhomb, for example, uses glass of index 1.51, and with an apex angle of approximately 54.6° produces a retardation of exactly 90°. The optimum angle must, however, be determined by trial and error, and the desired retardation will only be obtained for a specific angle of incidence. Fresnel rhombs are available from II-VI Infrared, Karl Lambrecht (KLC), and Newport/Oriel.

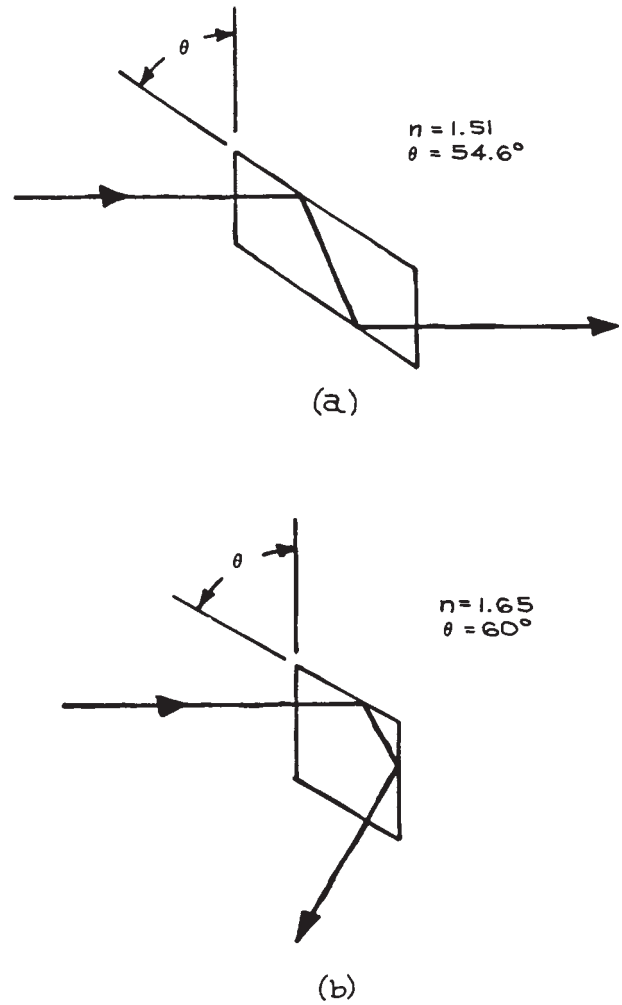

Figure 4.63 Rhomb retarders: (a) Fresnel; (b) Mooney.

4.3.7 Optical Isolators

Optical isolators are devices that allow light to pass through in one direction, but not in the reverse direction. These devices contain two linear polarizers and between them a medium (generally a special glass), which exhibits the Faraday effect. The medium is placed in an axial magnetic field provided by a permanent magnet or magnets. A Faraday-active medium rotates the plane of an input linearly polarized wave, and the direction of rotation depends on the relative direction of light propagation and the magnetic field direction. In an isolator, the optical path length through the Faraday material and the magnetic field strength are selected to provide a 45° rotation of the input linear polarization, which then lines up with the exit polarizer set at 45° to the input polarizer, as shown

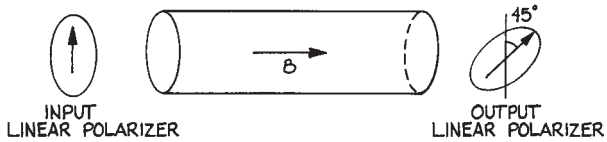

Figure 4.64 Optical isolator that uses two linear polarizers and a Faraday material producing a 45° polarization rotation.

in Figure 4.64. Light passing in the reverse direction has its plane of linear polarization also rotated by 45°, but in a sense that makes it orthogonal to the next polarizer so negligible light emerges. Commercially available Faraday isolators typically provide 30 dB isolation and must be selected for the specific wavelength desired. Both free space and optical-fiber-based devices are available from companies such as AC Photonics, Conoptics, Electro-Optics Technology, Isowave, Leysop, Linos Photonics, Namiki, New Focus, Newport, and OFR (now Thorlabs).

Optical isolators are particularly useful in certain precision experiments using lasers, to avoid *feedback instability*. If some of the light from a laser re-enters the laser, the amplitude and phase of the laser will fluctuate, and this can sometimes be very marked.

4.3.8 Filters

Filters are used to select a particular wavelength region from light containing a broader range of wavelengths than is desired. Thus, for example, they allow red light to be obtained from a white light source, or they allow the isolation of a particular sharp line from a lamp or laser in the presence of other sharp lines or continuum emission. Although filters do not have high resolving power (see Section 4.3.5), they have much higher optical efficiency at their operating wavelength than higher-resolving-power, wavelength-selective instruments, such as prism or grating monochromators. That is, they have a high ratio of transmitted flux to input flux in the wavelength region desired. Filters of several types are available for different applications.

Color Filters. A *color filter* selectively transmits a particular spectral region while absorbing or reflecting others. These simple filters are glasses or plastics containing absorbing materials such as metal ions or dyes, which have characteristic transmission spectra. Such color filters are available from Chance-Pilkington, Corning, CVI, Hoya, Kodak (Wratten filters), Kopp Glass, Melles-Griot (now CVI-Melles-Griot), Newport, Newport Thin Film Laboratory, Omega Optical, Praezisions Glas & Optik, Schott, Rolyn, Rosco, and Sterling Precision Optical. Transmission curves for these filters are available from the manufacturers, and in tabulations of physical and chemical data.[7,46]

Care must be taken when color filters are being used to block a strong light signal, such as a laser. These filters may fluoresce, so although the primary incident light is blocked, a weak, longer-wavelength fluorescence can occur. We have seen this phenomenon quite strongly when using orange plastic to block a blue/green laser.

Band-Pass Filters. A *band-pass filter* is usually a *Fabry–Perot etalon* of small thickness. Although etalons will be discussed in further detail in Section 4.7.4, a brief discussion is in order here.

In its simplest form, the Fabry–Perot etalon consists of a plane, parallel-sided slab of optical material of refractive index n and thickness d with air on both sides. In normal incidence the device has maximum transmission for wavelengths for which the thickness of the device is an integral number of half wavelengths. In this case, from Equation (4.110):

$$Z''_3 = Z'_3 = Z'_1 \tag{4.184}$$

and there is zero reflection. For incidence at angle θ, regardless of the polarization state of the light, there is maximum transmission for wavelengths (*in vacuo*) that satisfy:

$$m\lambda_0 = 2d\cos\theta_2 \tag{4.185}$$

where θ_2 is the angle of refraction in the etalon.

A Fabry–Perot etalon is a "comb" filter. (Figure 4.159 shows an example of a transmission characteristic of such a device.) If the thickness of the etalon is small, the transmission peaks are broad. In a typical band-pass filter operated as an etalon, all the transmission peaks but the desired one can be suppressed by additional absorbing or multilayer reflective layers. The spectral width of the transmission peak of the filter can be reduced by stacking

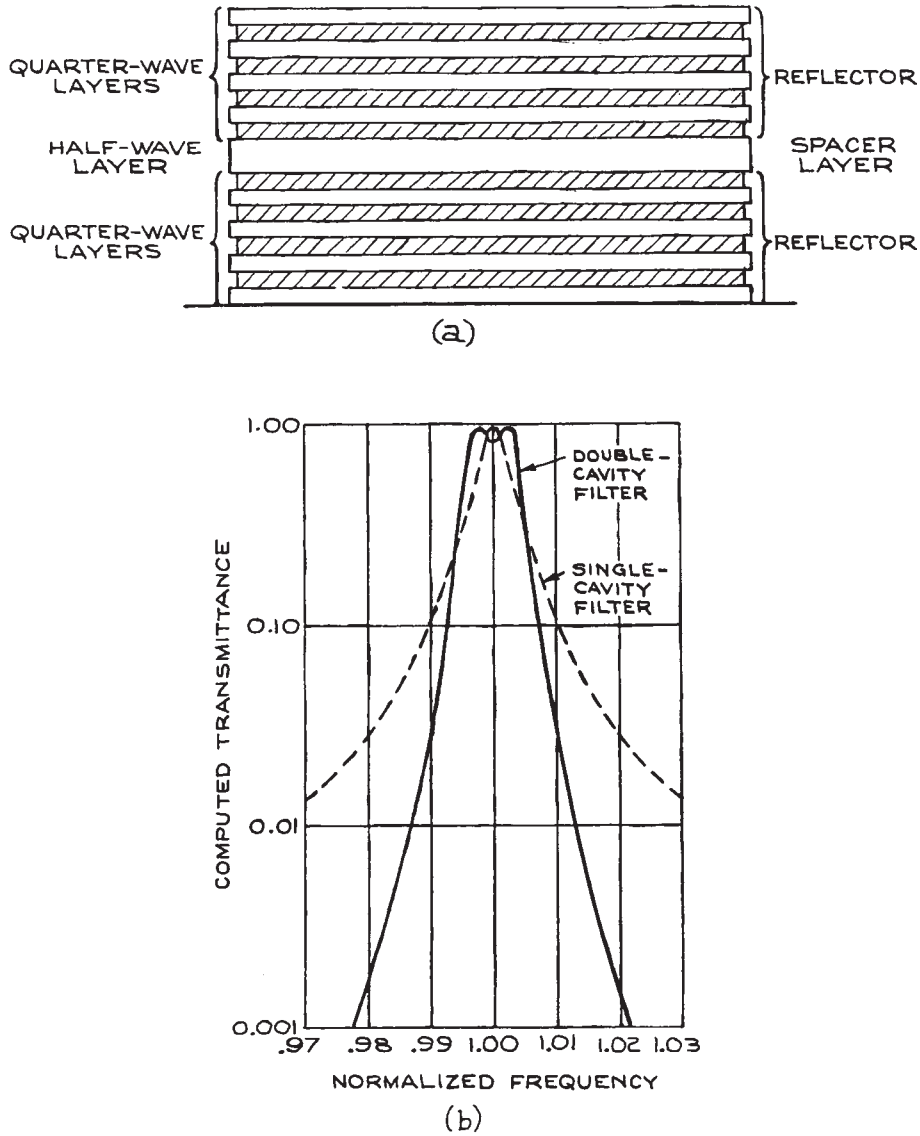

Figure 4.65 (a) Construction of an all-dielectric single-cavity Fabry–Perot interference filter; (b) theoretical transmittance characteristics of single- and double-cavity filters. (From *Handbook of Lasers*, R. J. Pressley (Ed.), CRC Press, Cleveland, 1971; by permission of CRC Press, Inc.)

individual etalon filters in series. A single etalon filter might consist, for example, of two multilayer reflective stacks separated by a half-wavelength-thick layer, as shown in Figure 4.65(a), while a two-etalon filter would have two half-wavelength-thick layers bounded by multilayer reflective stacks. Commercially available band-pass filters for use in the visible usually have a passband ranging from below 1 nm to 50 nm (full width at half maximum

transmission). The narrowest band-pass filters are frequently called "spike filters." Filters to transmit particular wavelengths, such as 632.8 nm (He-Ne laser), 514.5 and 488 nm (argon ion laser), 404.7, 435.8, 546.1, 577.0, and 671.6 nm (mercury lamp), 589.3 nm (sodium lamp), and other wavelengths, are available as standard items.[31] Filters at nonstandard wavelengths can be fabricated as custom items. Band-pass filters for use in the ultraviolet usually have lower transmittance, typically 20%, than filters in the visible, whose transmittance usually ranges from 40% to 70%, being lowest for the narrowest passband. Infrared band-pass filters are also readily obtained, at least out to about 10 μm, and have good peak transmittance. The typical available band-pass for a filter whose peak transmission is λ_{peak} can usually be estimated as $\lambda_{peak}/50$, although narrower band-pass filters can be obtained at higher cost. Band-pass filters are available from many suppliers, including Andover Optical, LOT-Oriel, Melles Griot, Newport, Omega Optical, Spectrogon, Spectrum Thin Films, and Sterling Precision Optical.

Band-pass filters are usually designed for use in normal incidence. Their peak of transmission can be moved to shorter wavelengths by tilting the filter, although the sharpness of the transmission peak will be degraded by this procedure. If a filter designed for peak wavelength λ_0 is tilted by an angle θ, its transmission maximum will shift to a wavelength:

$$\lambda_s = \lambda_0 \sqrt{1 - \frac{\sin^2 \theta}{n^2}} \tag{4.186}$$

where n is the refractive index of the half-wavelength-thick layer of the filter. For small tilt angles:

$$\lambda_0 - \lambda_s = \frac{\lambda_0 \sin^2 \theta}{2n^2} \tag{4.187}$$

Thus, a band-pass filter whose peak-transmission wavelength is somewhat longer than desired can be optimized by tilting.

Long- and Short-Wavelength-Pass Filters. A *long-wavelength-pass filter* is one that transmits a broad spectral region beyond a particular cutoff wavelength, λ_{min}. A *short-wavelength-pass filter* transmits in a broad spectral region below its cutoff wavelength λ_{max}. A combination of a long-wavelength-pass and a short-wavelength-pass filter can be used to produce a band-pass filter, as shown in Figure 4.66. Although long-and short-wavelength-pass filters usually involve multilayer dielectric stacks, the inherent absorption and transmission characteristics of materials can be utilized. Semiconductors exhibit fairly sharp long-wavelength-pass behavior beginning at the band gap energy. For example, germanium is a long-pass filter with $\lambda_{min} = 1.8$ μm.

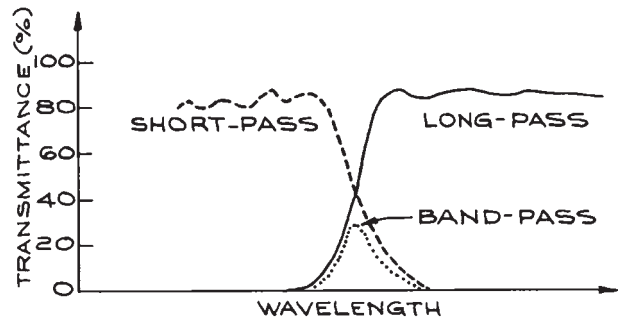

Figure 4.66 Schematic transmission of long- and short-pass optical filters showing the band-pass transmission characteristics of the two in combination.

Holographic Notch Filters. These filters are special diffractive structures that reflect a narrow range of wavelengths (~5 nm) very strongly, and consequently they reduce transmitted light substantially (40–60 dB) over the same narrow range. These filters are ideal for rejection of laser light in experiments where a weaker light signal – fluorescence or Raman scattering – is being studied, and some scattering or reflection of the excitation laser light is occuring. These filters are available from Andor Technology, Del Mar Ventures, Kaiser Optical Systems, MK Photonics, and Semrock.

Rugate Filters. Rugate filters are notch interference filters with high rejection of a narrow band of wavelengths. In contrast to conventional multilayer dielectric interference filters, in which the refractive index variation from layer to layer is a square wave, *rugate filters* use a sinusoidally variable refractive index throughout the oxide film layers. They can provide a single notch band without harmonics, as shown in

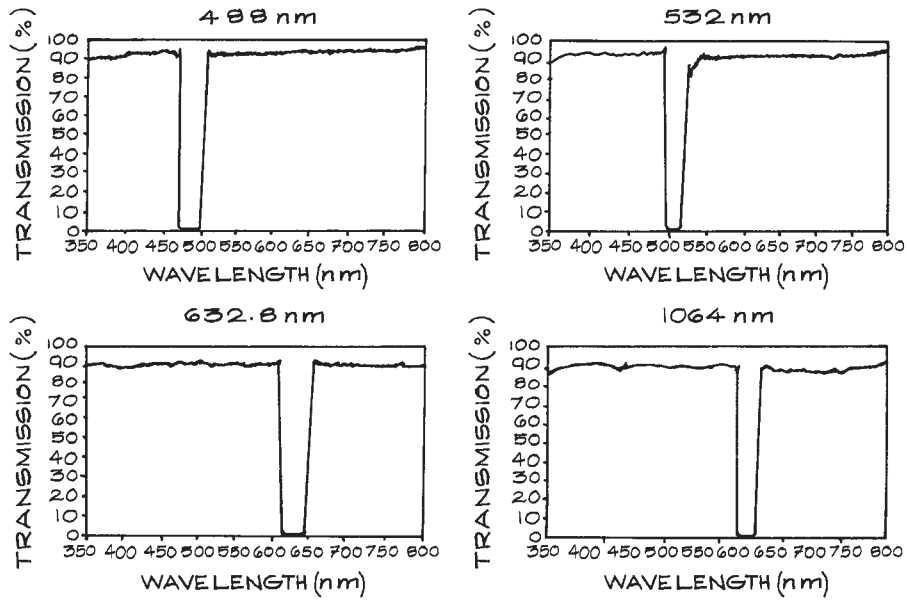

Figure 4.67 Transmission characteristics of some rugate filters.

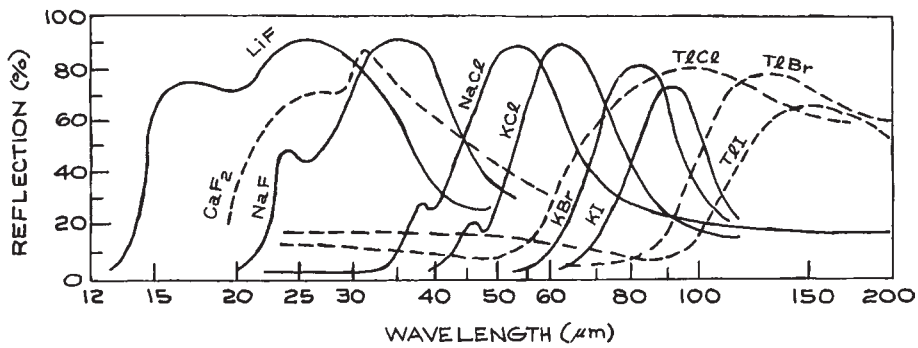

Figure 4.68 Reststrahlen filters. (Courtesy of Harshaw Chemical Co.)

Figure 4.67. A rugate filter can look almost completely colorless and transparent, and yet reject laser light at a specified wavelength very efficiently. They are available from Advanced Technology Coatings, Barr Associates, Edmund Optics, Gist Optics, and Rugate Technologies.

Reststrahlen Filters. When ionic crystals are irradiated in the infrared, they reflect strongly when their absorption coefficient is high, and their refractive index changes sharply. This high reflection results from resonance between the applied infrared frequency and the natural vibrational frequency of ions in the crystal lattice. The characteristic reflected light from different crystals, termed *Reststrahlen*, allows specific broad spectral regions to be isolated by reflection from the appropriate crystal. Some examples of Reststrahlen filters are given in Figure 4.68.

Christiansen Filters. In the far infrared, the alkali halides exhibit anomalous dispersion: at certain wavelengths their refractive indices pass through unity.

(Normal dispersion involves an increase of refractive index with wavelength.) Thus a powdered alkali halide, which would generally attenuate a transmitted wave severely because of scattering, will transmit well at wavelengths where its refractive index is the same as that of air. Filters using such an alkali halide powder held between parallel plates are called Christiansen filters and provide sharp transmission peaks at certain wavelengths listed in Table 4.4.

Neutral-Density Filters. *Neutral-density (ND) filters* are designed to attenuate light uniformly over some broad spectral region. The ideal neutral-density filter should have a transmittance that is independent of wavelength. These filters are usually made by depositing a thin metal layer on a transparent substrate. The layer is kept sufficiently thin that some light is transmitted through it. The optical density D of a neutral-density filter is defined as:

$$D = \log_{10}(1/T) \tag{4.188}$$

where T is the transmittance of the filter. T is controlled both by reflection from and by absorption in the metal film. If such filters are stacked in series, the optical density of the combination is the sum of the optical densities of the individual filters, provided the filters are positioned so that multiple reflection effects do not occur between them in the direction of interest.

Neutral-density filters are used for calibrating optical detectors and for attenuating strong light signals falling on detectors to ensure that they respond linearly. Because neutral-density filters usually reflect and transmit light, they can be used as beamsplitters and beamcombiners for any desired intensity ratio. There are many suppliers.[31] Variable ND filters are available from HB Optical, Melles Griot, Nova Phase, Reynard, and Singh-Ray.

Light Traps. If a beam of light must be totally absorbed (for example, in an application where any reflected light from a surface could interfere with some underlying weak emission), a light trap can be constructed. The two types illustrated in Figure 4.69 work well: the Wood's horn, in

Table 4.4 Christiansen filters

Crystal	Wavelength of Maximum Transmission (μm)
LiF	11.2
NaCl	32
NaBr	37
KCl	37
RbCl	45
NaI	49
CsCl	50
KBr	52
CsBr	60
TlBr	64
KI	64
RbBr	65
RbI	73
TlI	90

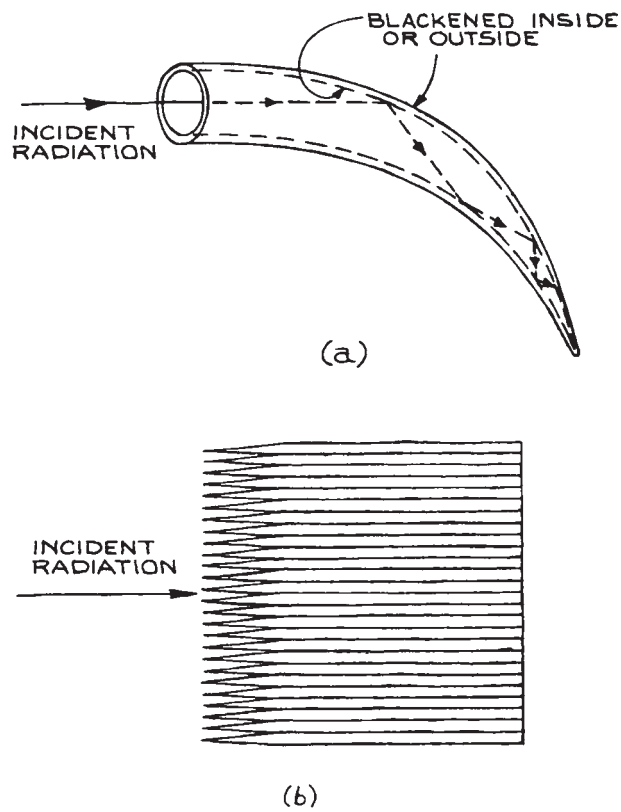

Figure 4.69 Light traps: (a) Wood's horn; (b) stacked razor blades.

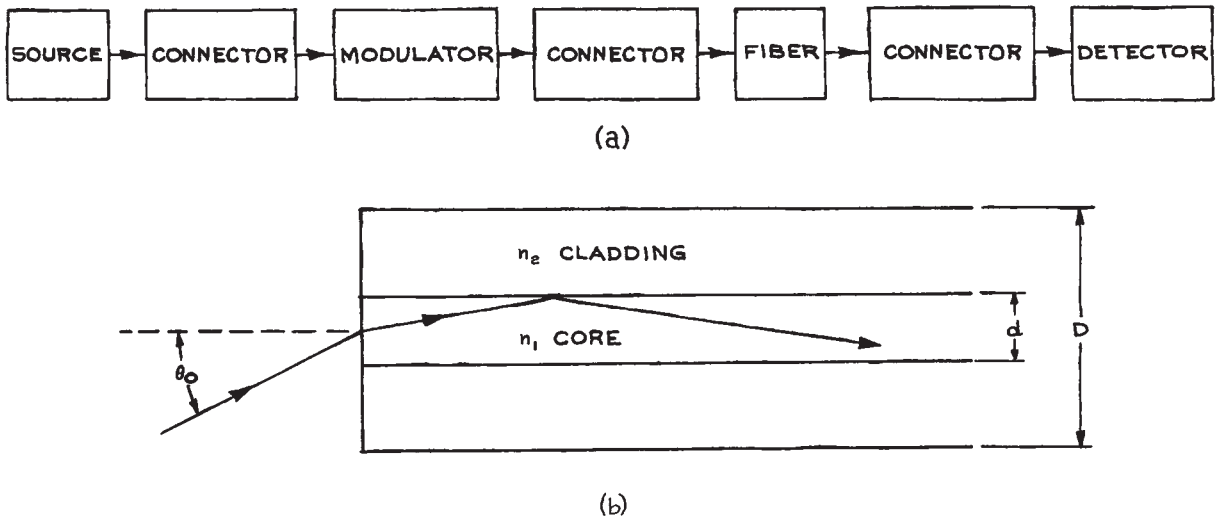

Figure 4.70 (a) Fundamental components of a fiber-optic data link; (b) meridional section through a step-index optical fiber. The core refractive index is n_1; the cladding refractive index is n_2. The core and cladding diameters are d and D, respectively. A ray entering the fiber will be totally internally reflected provided its angle of incidence is less than θ_0, where $\sin \theta_0 = \text{NA}$.

which a beam of light entering the trap is gradually attenuated by a series of reflections at an absorbing surface made in the form of a curved cone (usually made of glass); and a stack of razor blades, which absorbs incident light very efficiently.

4.3.9 Fiber Optics

As is well known, the use of optical fibers has become widespread in the telecommunications field. Consequently, there are numerous suppliers of the various components and subsystems involved.[31] The use of optical fibers in scientific research can be a very valuable technique, and one that is not particularly complicated. For example, in experiments where radio frequency (rf) interference, pickup, and ground loops are a problem, an experimental signal can be used to modulate a small light-emitting diode or laser. The modulated optical signal is then passed along an optical fiber to the observation location, where the original electrical signal can be recovered with a photodiode. Complete analog transmission systems of this kind are available from A.A. Lab Systems, Alcatel, Analog Modules, Force, JDS Uniphase, Luxlink, and Metrotek Industries. A schematic diagram of the various components of such a system is shown in Figure 4.70(a). The source may be supplied fabricated directly onto a fiber. The modulator is frequently unnecessary, as the source itself can be directly amplitude-modulated. The detector may also be supplied fabricated directly onto the end of the fiber. A few specific points are worthy of note for the experimentalist who may wish to utilize this technology.

For certain laboratory applications the construction of a fiber system without any connectors is straightforward. Light from the source is focused into the end of the fiber with a microscope objective. Light emerging from the other end of the fiber is focused onto the detector in a

similar way. A convenient range of microscope objectives for this purpose is available from Newport, who also supply a wide range of components for holding and positioning fibers. The choice of lens focal length and placement is governed by the *numerical aperture* (NA) of the fiber. The meaning of this parameter can be understood with reference to Figure 4.70(b), which shows a meridional section through a so-called step-index fiber. In this composite fiber the cylindrical core has refractive index n_1, and the surrounding cladding has index n_2, where for total internal reflection of rays to occur in the core, $n_1 > n_2$. Light entering the fiber at angles $\leqslant \theta_o$ will totally internally reflect inside the core. The NA is:

$$\sin\theta_o = \sqrt{n_1^2 - n_2^2} \tag{4.189}$$

Commercially available fibers typically have a smoothly varying radial index profile, but the NA is still the appropriate parameter for determining the acceptance angle. Two specific types of fiber are in most common use: single-mode and multimode. Single-mode fibers typically have core diameters on the order of 10 μm and cladding diameters of 125 μm. They require very precise connectors and are only needed in specialized experiments, for example in high data rate optical communications, where the ability of the fiber to support only a single propagating mode is important. Multimode fibers have larger core diameters, from 50 μm to above 1 mm, and cladding diameters somewhat larger than their respective core diameters. These fibers are easy to use: the larger sizes are frequently used to channel light for illumination into positions that are difficult to access, or to collect light from one location and channel it to a detector somewhere else. Large fibers that are suitable for these purposes are available from AFL Telecommunications, Berkshire Photonics, Edmund Optics, Fiberguide Industries, Newport, Polymicro Technologies, and 3M Speciality Optical Fibers.

Fibers can be cut to provide a flat end face with the aid of specialist cleaving tools of varying degrees of precision and complexity, available from suppliers such as Newport and York. In simple experimental setups an adequate cleaved flat face can be obtained in the following way:

(1) Remove the outer plastic protective coating from the cladding in the region that is to be cut by using a fiber-stripping tool or by immersing this part of the fiber in methylene chloride (the active ingredient in most proprietary paint and varnish strippers). To clean a fiber that has been stripped of its cladding use Kimwipes or lens tissue moistened with pure isopropyl alcohol. Do not wipe the bare fiber with dry tissue.
(2) Lightly scratch the cladding with a cleaving tool (slightly more precise than a conventional glass cutter).
(3) Fasten one half of the fiber to a flat surface with masking tape, and pull the other half of the fiber axially away, keeping the fiber flat on the surface.

This procedure usually gives a flat enough face for use with a microscope objective. If fibers are to be cut and fitted with connectors, they must be cut and polished according to the instructions supplied with the connector.

Fiber Optic Connectors. If two identical fibers are to be joined together, this can be done with mechanical coaxial connectors, with a mechanical splice, or the fibers can be fused together with a fusion splicer. In all cases the flat, cleaved faces of the two fibers to be joined must be brought together so that the two faces are in close proximity, are parallel, and the fibers are coaxial. Proper alignments for orthogonal and angle cleaves are shown in Figure 4.71(a) and (b), respectively. Any lateral or tilt offset of the fibers when they are joined will reduce coupling efficiency. Precision mechanical optical fiber connectors are able to couple two fibers together with losses in the range 0.1–0.2 dB. Sometimes the connector contains a small amount of index-matching gel that is squeezed in the gap between the fibers.

Mechanical fiber splices are an inexpensive way to join fibers. They generally have a sleeve-like construction into which the two fibers are pushed and then glued or clamped in place. Better yet, a *fusion splicer* can be used to fuse fibers together; this is, however, an expensive device. A good fusion splice can have a loss

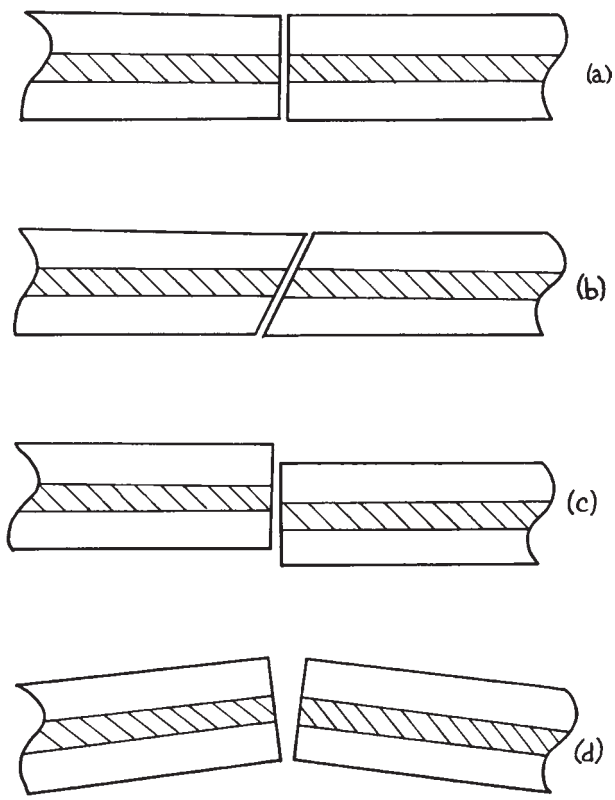

Figure 4.71 Alignment of optical fibers for optical connection: (a) correct alignment for perpendicular-cleaved fibers; (b) correct alignment for angle-cleaved fibers; (c) lateral misalignment; (d) angle misalignment.

below 0.1 dB. After two fibers are fused together, a *splice protector* should be included if the joined fiber is to be protected from failure of the splice.

The use of optical fiber devices is much simplified if these devices are purchased with appropriate fiber optic connectors already attached. A convenient way to obtain a connectorized fiber where access to one free end is required is to buy a fiber *jumper*, which is the optical equivalent of patch cord or coaxial cable. By cutting the jumper cable, a length of fiber with a connector on one end is easily obtained. Fiber jumpers with various kinds of connectors, different fiber optic cables, and of various lengths are readily available (Cableorganizer.com, Datamax Technologies, Fiberall, Fiber.com, Fiber Optic Cable Shop, L-Com, Optica, Stonewall Cable, and Unicom). Fiber optic connectors come in many types for both single-mode and multimode fibers: FC, LC, SMA, ST, SC, MT-RJ, MU, 50/125, D4, E2000, 62.5/125, 9/125, and Opto-clips. For special applications, angle-cleaved connectors are available, which reduce the inevitable small reflection that occurs at a fiber connector. A comprehensive discussion of practical fiber optics can be found in Goff.[47]

Polarization-maintaining (PM) fiber will preserve the polarization state of launched light (to about 1% purity). Special connectors and splicing techniques are needed for PM fiber, as the azimuthal orientation of the two fibers is now important.

4.3.10 Precision Mechanical Movement Systems

It is frequently necessary to be able to position components in an optical system with high precision. The type of stage with which this is done depends on the scale of movement, the accuracy, repeatability resolution, and freedom from backlash that is required. There are a large number of suppliers of stages, including translation, rotation, tilting, multi-axis positioning and combinations of these including Aerotech, Daedal, Melles Griot, Newport, New Focus, Optosigma, Thor Labs, and Velmex. Both manual and motor-driven stages are available. Although precision mechanical stages can be built in the laboratory, they are widely available commercially. It is not likely that an experimentalist will save money by building rather than buying a precision stage.

The accuracy of adjustment is the difference between the actual and desired positions. Repeatability refers to the ability to reproduce a desired position after a movement of a stage to a different position. In a fair comparison of stages this should involve significant, comparable movements away from, and then back to a desired position. Resolution is the smallest motion that a stage can make, which for a screw-driven device will be limited by factors such as the number of threads per inch in the lead screw, and friction. A

precision micrometer might, for example, have a resolution of about 1/10 of the smallest scale graduation around the micrometer head. Another factor of importance is creep. After a stage has been set to a desired position does it stay there, or does removal of stress from a positioning screw cause it to relax? Absence of creep means that a mount, once positioned, holds its position for a long period. It is our experience that stainless-steel mounts are less susceptible to creep than aluminum mounts.

Resolution alone as a specification does not mean much without additional specification of accuracy, repeatability, and stability. The long-term stability of a mount is also influenced by the thermal stability and expansion of the materials from which the stage is made. The convenient materials of construction are aluminum alloy and stainless steel.

Aluminum has a higher coefficient of thermal expansion (24×10^{-6}/K) compared with stainless steel ($10–16 \times 10^{-6}$/K), but aluminum has a higher thermal conductivity and reaches thermal equilibrium more quickly, which minimizes thermally induced strain. Aluminum takes a poor thread and usually brass threaded inserts must be used for brass or stainless-steel positioning screws.

The thermal stability of an optical mount can be improved by using mounting assemblies constructed with two dissimilar metals whose thermal expansions offset each other. Commercially available mounts of the highest precision may include this technology. The manufacturer's technical specifications should be consulted.

It is convenient to divide the movement scales available into three broad categories.

(1) *Medium* – the scale of movement provided by manual micrometer drives or precision lead screws. Typical micrometer drives provide up to 50 mm travel with accuracy on the order of 1 μm. Some commercial drives claim a resolution below 0.1 μm, but, in practice, such claims must be reviewed with skepticism, since the backlash, creep and repeatability of all mechanical, screw-based, stages is likely to be worse than this.

(2) *Fine* – The scales of movement, precision, and repeatabily provided by motor-driven stages, which may be driven either by a stepping motor or dc motor. For repeatability, some form of encoding of the position is needed, or feedback based on the characteristics of the state. Position encoding is usually done with either a shaft encoder, which tells the drive motor on the lead screw exactly what its angular position is, or with a linear encoder. A linear encoder gives a more precise, repeatable measure of the actual location of the object being moved. Precision drives incorporating encoders are available from Griffin Motion, Newport, Physik Instrumente (PI), Quater, and Thorlabs. Precise motor-driven stages are also available from Aerotech, J.A. Noll, Daedal, Melles-Griot, Newport, and New Focus.

(3) *Nanoscale* – positioning down to 1 nm resolution, with varying degrees of repeatability. Positioning on this scale requires the use of piezoelectric or electrostatic transducers. Piezoelectric transducers generally use a ceramic material such as lead zirconate titanate (PZT), which changes its shape in an applied electric field. Typical PZT transducers provide mechanical motion on the order of a few hundreds of nanometers for applied voltages on the order of 1 kV. They provide resolution of 10 nm or less, but do exhibit hysteresis, as shown in Figure 4.72, unless some absolute position encoding scheme is used. Individual PZT transducers are generally available either in the form of tubes or disks,

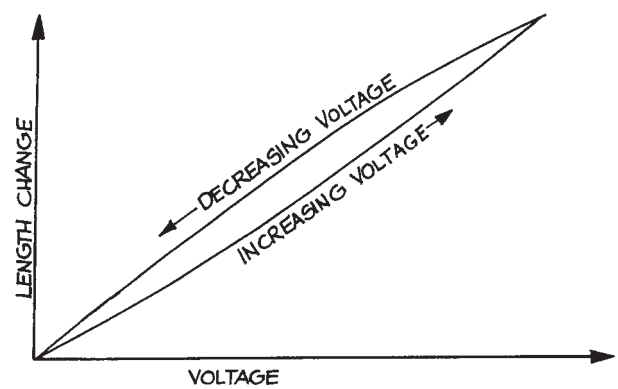

Figure 4.72 Hysteresis in the length change of a piezoelectric element with applied voltage.

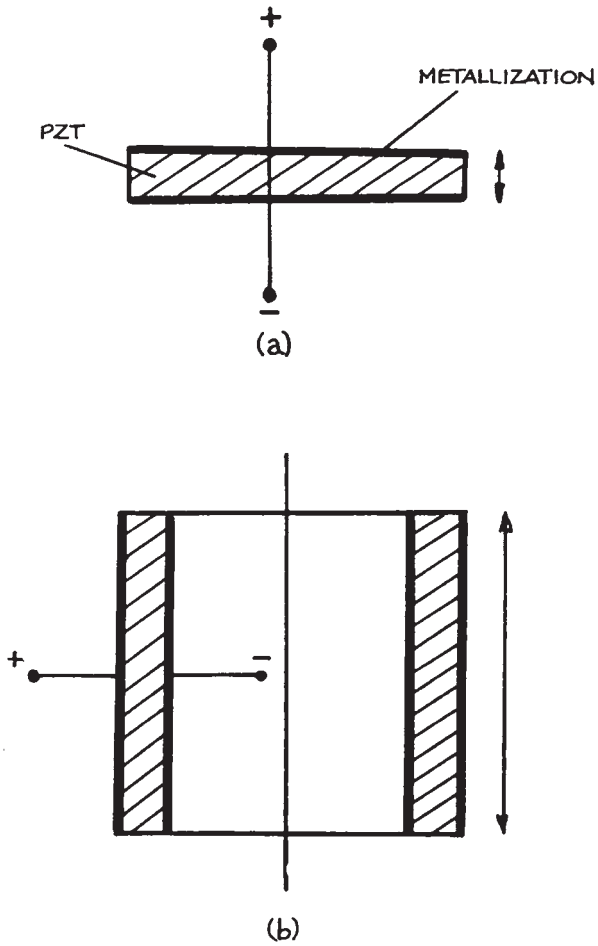

Figure 4.73 Simple piezoelectric elements: (a) slab; (b) cylinder.

as shown in Figure 4.73. Larger motions can be obtained by stacking transducers in either a bimorph or polymorph arrangement. In a bimorph, two slabs of PZT are driven so that one slab extends while the other gets shorter, which causes the bimorph to bend, as shown in Figure 4.74.

In a slab transducer, voltage is applied across the narrow dimension of the slab, which will then change its thickness with applied voltage. In a cylindrical transducer, voltage is

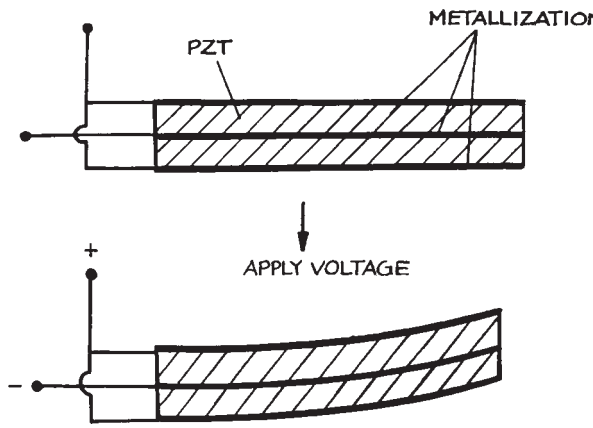

Figure 4.74 Operation of a bimorph piezoelectric element in a *parallel* configuration.

applied between the inner and outer metallized cylindrical surface of the tube, which then changes its length in the axial direction. Nanoscale precision piezoelectric drives are available commercially from Attocube, Mad City Labs, Melles Griot, Queensgate Instruments, Polytec, Physik Instrumente, and Thorlabs, among others. Bimorphs are available from FDK Products and Morgan Electro Ceramics.

Small scale (~10 μm) precision motion in each of three orthogonal axes can be accomplished inexpensively with a modified piezotube. A typical piezotube is on the order of 30 mm long by 10 mm, and is generally supplied with a metal coating on its inner and outer cylindrical surfaces. The outer metallization should be removed in four segements approximately 1 mm wide spaced 90° apart on the outer cylindrical surface, as shown in Figure 4.75. The four segements are then driven by a ''bridge'' amplifier current, in which opposite pairs of electrodes are driven in a push-pull configuration, as shown schematically in Figure 4.76. Driving electrodes 1 and 2 produces an x-directed tilt of the tube, electrodes 3 and 4 produce a y-directed tilt of the tube. An additional amplifier drives electrode 5 for z-directed extension of the tube. Because the interelectrode

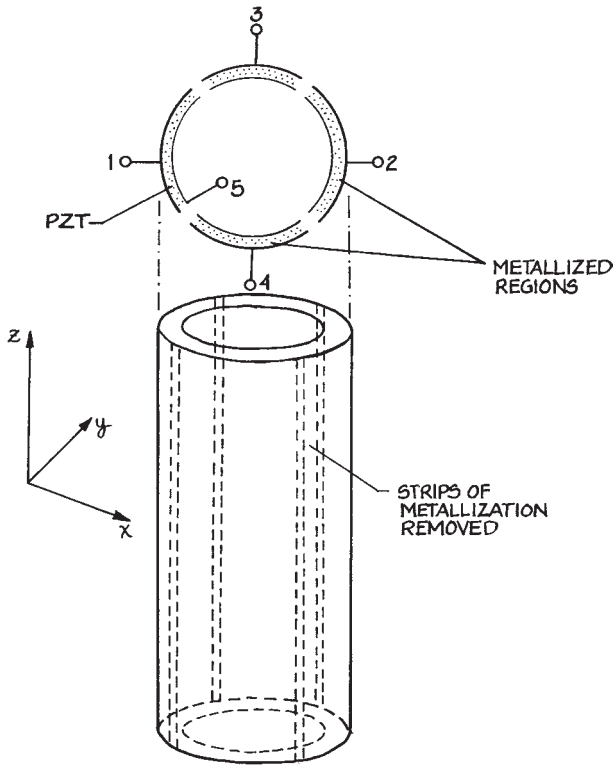

Figure 4.75 A cylindical piezoelectric element with outer quadrant electrodes. The element can be driven to provide axial motion as well as tilt in two orthogonal axes.

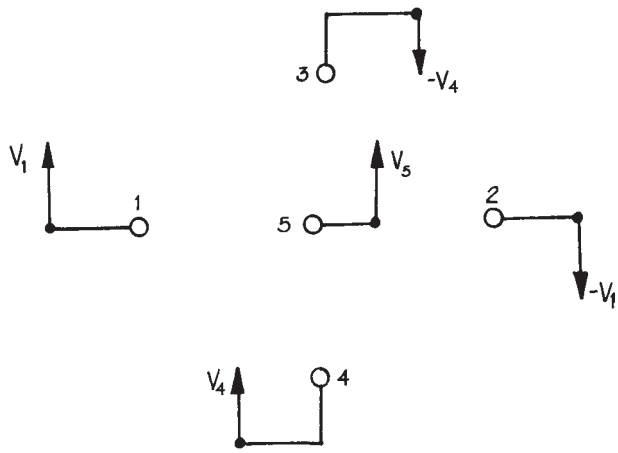

Figure 4.76 Voltage drive scheme for a piezoelectric element such as the one shown in Figure (4.69). Electrodes 1–4 are the quadrant electrodes, Electrode 5 is the inner electrode.

voltages used need to be as large as 1000 V, special op-amps are required. Appropriate amplifers are available from Apex Microtechnology Corporation. Piezo tubes are available from Argillon, APC International, Boston Piezo-Optics, Omega Piezo Technologies, Physik Instrumente (PI), and Sensor Technology.

4.3.11 Devices for Positional and Orientational Adjustment of Optical Components

For positioning a given component, the maximum number of possible adjustments is six: translation along three mutually orthogonal axes and rotation about these (or other) axes. Mounts can be made that provide all six of these adjustments simultaneously. Usually, however, they are restricted and have no more degrees of freedom than are necessary. Thus, for example, a translation stage is usually designed for motion in only one dimension; independent motion along other axes can then be obtained by stacking one-dimensional translation stages. Orientation stages are usually designed for rotation about one axis (polar rotation) or two orthogonal axes (mirror mounts or tilt tables). Once again, such mounts can be stacked to provide additional degrees of freedom. It is often unnecessary for angular adjustment to take place about axes that correspond to translation directions.

The ideal optical mount provides independent adjustment in each of its degrees of freedom without any interaction with other potential degrees of freedom. It should be sturdy, insensitive to extraneous vibrational disturbances, (such as air- or structure-borne acoustic vibrations), and free of backlash during adjustment. Generally it should be designed on kinematic principles (see Section 1.7.1). The effect of temperature variations on an optical mount can also be reduced, if desired, by constructing the mount from

low-coefficient-of-expansion material, such as Invar, or by using thermal-expansion compensation techniques. Very high ridigity in an optical mount generally implies massive construction. When weight is a limitation, honeycombed material or material appropriately machined to reduce excess weight can be used. Most commercially available mounts are not excessively massive, but represent a compromise between size, weight, and rigidity. Generally, mounts do not need to be made any more rigid than mechanical considerations involving Young's modulus and likely applied forces on the mount would dictate.

The design of optical mounts on kinematic principles involves constraining the mount just enough so that, once adjusted, it has no degrees of freedom. Some examples will illustrate how kinematic design is applied to optical mounts.

Two-Axis Rotators. Within this category the commonest devices are adjustable mirror or grating mounts and tilt tables used for orienting components such as prisms. Devices that adjust orientation near the horizontal are usually called tilt adjusters. Mirror holders, on the other hand, involve adjustment about a vertical or near-vertical axis. A basic device of either kind involves a fixed stage equipped with three spherical or hemispherical ball bearings, which locate, respectively, in a V-groove, in a conical hole, and on a plane surface machined on a movable stage. A typical device is shown in Figure 4.77. The movable stage makes contact with the three balls on the fixed stage at just six points – sufficient to prevent motion in its six degrees of freedom – and is held in place with tension springs between the fixed and movable stages. Adjustment is provided by making two of the locating balls the ends of fine-thread screws or micrometer heads. Suitable micrometer heads for this purpose are manufactured by Brown and Sharpe, Mitutoyo, Moore and Wright, Shardlow, and Starrett, and are available from most wholesale machine-tool suppliers. The ball of the micrometer should be very accurately centered on the spindle. The adjustment of the mount shown in Figure 4.77 is about two almost orthogonal axes. There is some translation of the center of the movable

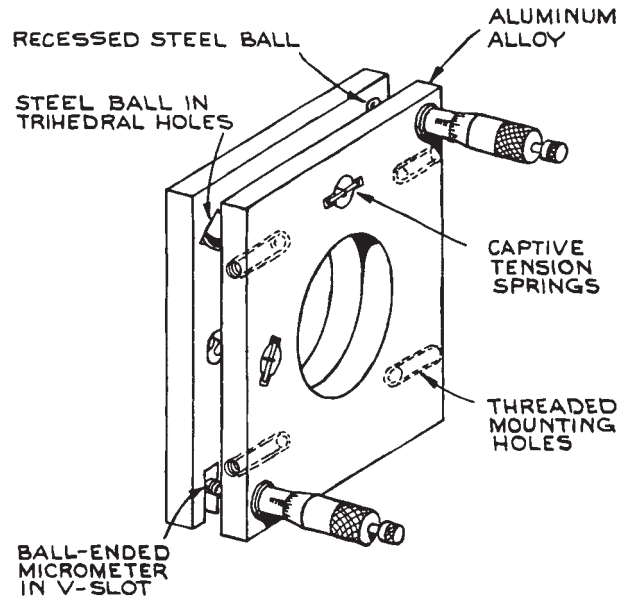

Figure 4.77 Kinematic double-hinge mirror mount.

stage during angular adjustment, which can be avoided by the use of a true gimbal mount.

A few of the constructional details of the mount in Figure 4.77 are worthy of note. Stainless steel, brass, and aluminum are all suitable materials of construction; an attempt to reduce the thermal expansion of the mount by machining it from a low-expansion material such as Invar may not meet with success. Extensive machining of low-expansion-coefficient alloys generally increases the coefficient, unless they are carefully annealed afterward. Putting the component in boiling water and letting it gradually cool will lead to partial annealing. True kinematic design requires ball location in a trihedral hole, in a V-slot, and on a plane surface (or in three V-slots, but this no longer permits angular adjustment about orthogonal axes) (see also Section 1.7.1). If the mount is made of aluminum, the locating hole, slot, and plane on the movable stage should be made of stainless steel, or some other hard material, shrunk-fit into the main aluminum body. A true trihedral slot can be made with a punch, as shown in

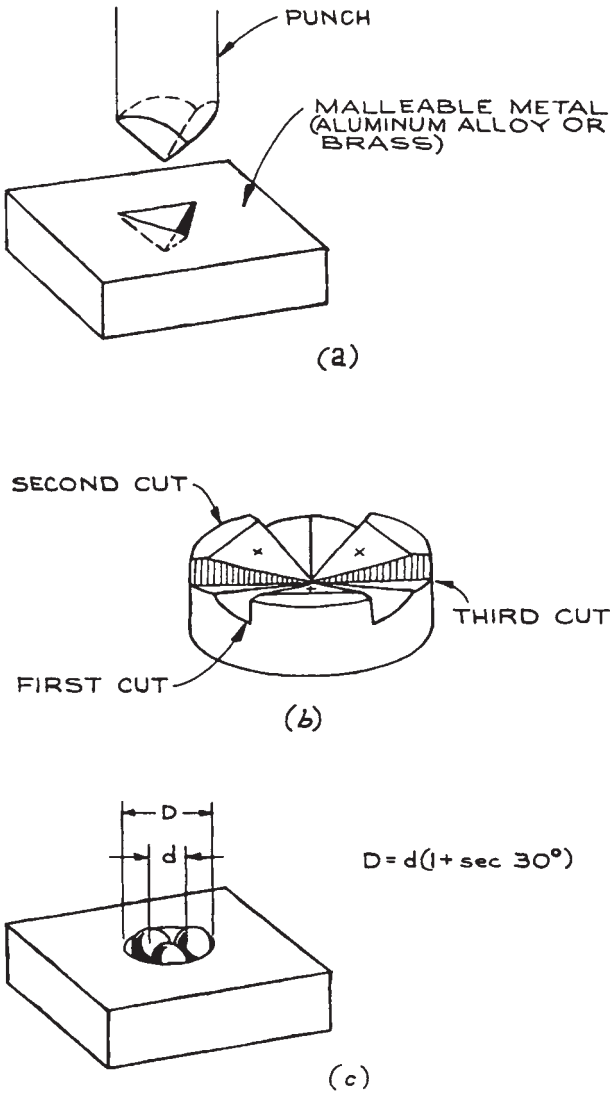

Figure 4.78 Methods for making trihedral locating holes for kinematic design; (a) trihedral steel punch; (b) trihedral hollow machined with 45° milling tool; (c) steel balls fitting tightly in a hole.

Figure 4.78(a), or it can be machined with a 45° milling cutter as shown in Figure 4.78(b). A conical hole is not truly kinematic; a compromise design is shown in Figure 4.79.

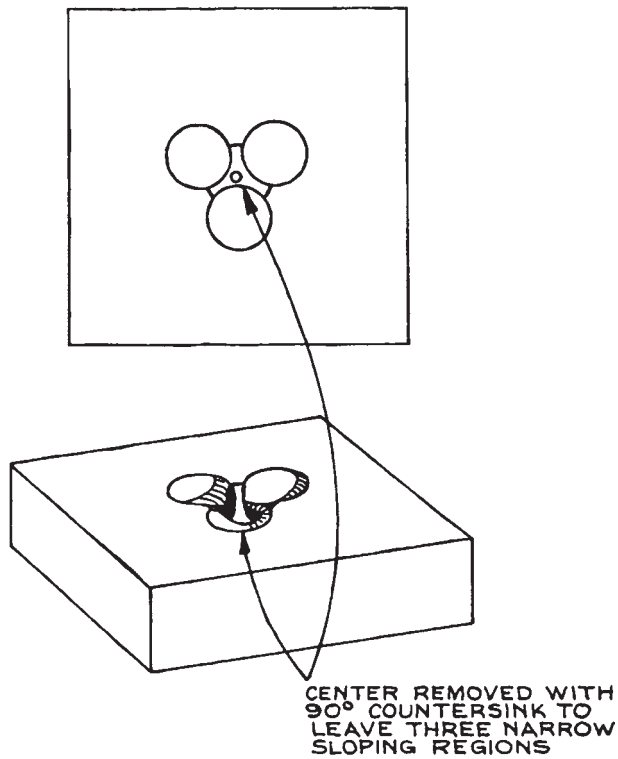

Figure 4.79 Compromise design for kinematic trihedral hole.

Although motion of the mount in Figure 4.77 results from direct micrometer adjustment, various commercial mounts incorporate a reduction mechanism to increase the sensitivity of the mount. Typical schemes that are used involve adjustment of a wedge-shaped surface by a moving ball, as shown in Figure 4.80, or the use of a differential screw drive. The two or more movable stages of an adjustable mount can be held together with captive tension springs, as in Figure 4.77. Designs involving only small angular adjustment can utilize the bending of a thin section of material, as shown in Figure 4.81. The design of such mounts, called *flexures*, is discussed in detail in Section 1.7.6.

The basic principle of a gimbal mount for two-axis adjustment is shown in Figure 4.82. True orthogonal motion about two axes can be obtained in such a design

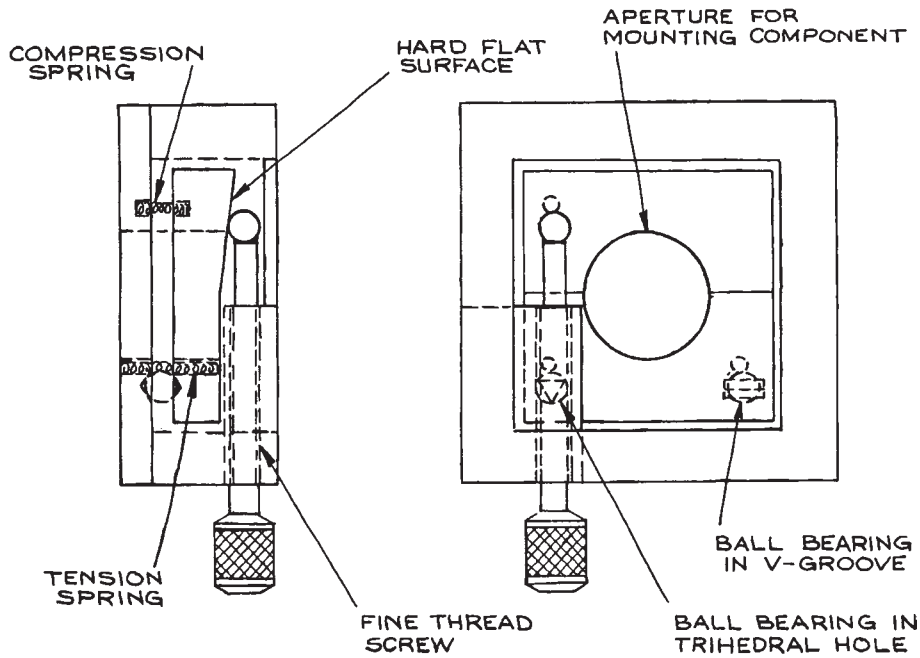

Figure 4.80 Cutaway views of a kinematic, single-axis rotator incorporating a reduction mechanism involving a ball bearing on an angled surface. Two rotators of this kind could be incorporated in a single mount to give two-axis gimbal adjustment.

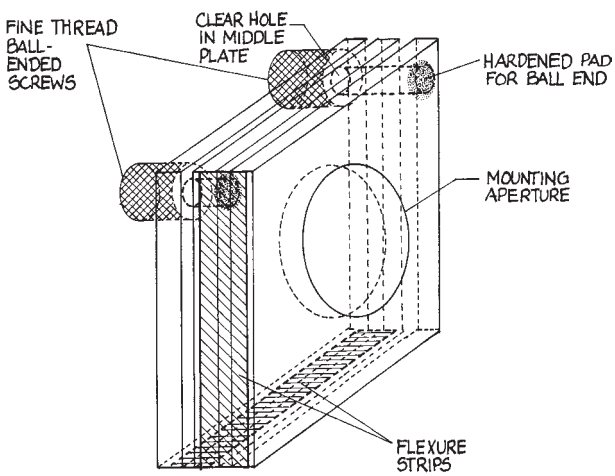

Figure 4.81 Flexure type double-hinge mirror design.

without translation of the center of the adjusted component. A kinematically designed gimbal mount is, however, much more complicated in construction than the mount shown in Figure 4.82. Precision gimbal mounts should be purchased rather than built. Very many companies manufacture adequate devices with a variety of designs, and their prices are lower than the cost of duplicating such devices in the laboratory. Suppliers of gimbal mounts include Aerotech, Daedal, New Focus, Newport, J. A. Noll, Standa, and Thorlabs. Most of these manufacturers also manufacture good nongimbal mounts similar to the one shown in Figure 4.77.

Translation Stages. Translation stages are generally designed to provide linear motion in a single dimension and can be stacked to provide additional degrees of freedom. Mounts for centering optical components, particularly lenses, incorporate motion in two orthogonal (or

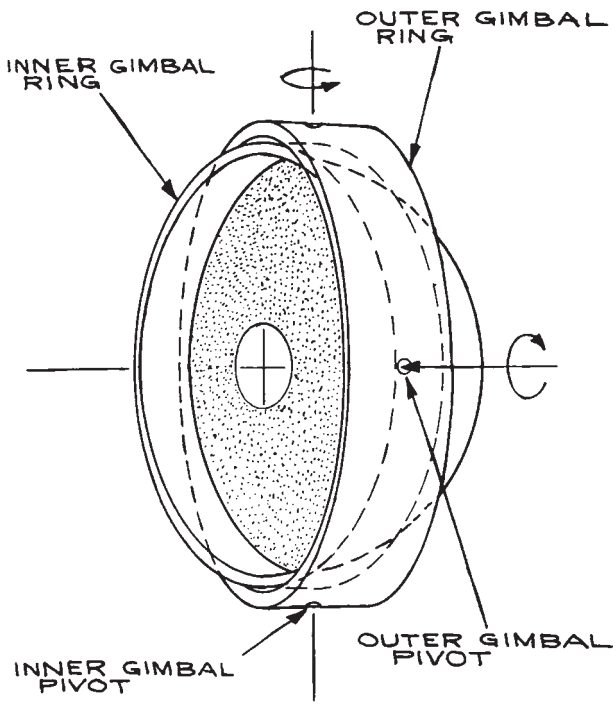

Figure 4.82 Schematic diagram of a true two-axis gimbal mount. The center of the mounted component does not translate during rotation.

near-orthogonal) axes in a single mount. The simplest translation stages usually involve some sort of dovetail groove arrangement, as shown in Figure 4.83(a). Greater precision can be obtained with ball bearings captured between V-grooves with an arrangement to prevent adjacent balls from touching, as shown in Figure 4.83(b), or with crossed-roller bearings, as shown in Figure 4.83(c). A simple ball-bearing groove design is shown in Figure 4.84, although variants are possible. Suppliers of precision, roller bearing translators include Aerotech, Daedal, Melles Griot, Newport, OptoSigma, and Thorlabs. Vertical translators using a fine-thread screw drive are available from Newport. Stages can be built to provide short-range, highly stable, frictionless precision movement by using flexures, as shown in Figure 4.85. Typical travel of a flexure stage is on the order of 10% to 15% of the dimensions of the stage.

Less precise, but generally adequate, nonball-bearing translation stages are available from Newport and Velmex. Mounts for centering optical components such as lenses are available from Aerotech, Ealing, and Newport, among others. A simple kinematic design for a centering mount is illustrated in Figure 4.86.

Rotators and Other Mounts. Rotators are used, for example, for orienting polarizers, retardation plates, prisms, and crystals. They provide rotation about a single axis. Precision devices using ball bearings are available from Aerotech, New Focus, Newport, OptoSigma, and Thorlabs, among various other suppliers.

There are numerous more complicated optical mounts than those described in the previous sections, which provide in a single mount any combination of degrees of freedom desired. Motor-driven and computer-controllable versions of all these mounts are generally available. For

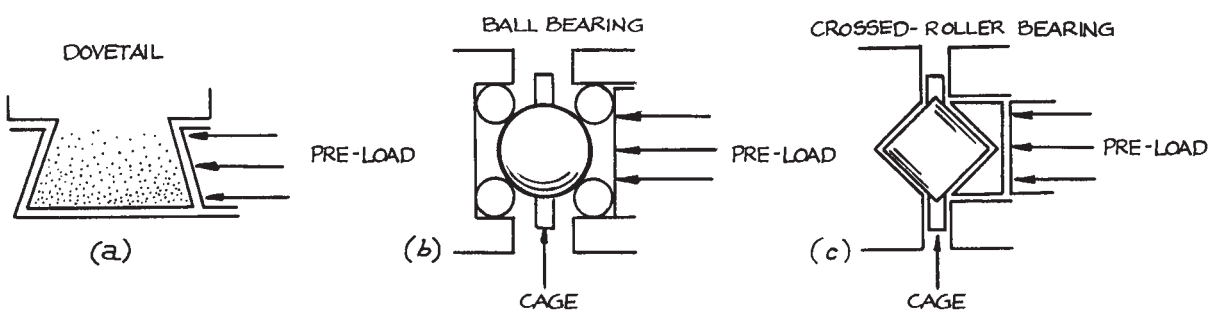

Figure 4.83 Groove mounting arrangements for linear transation stages: (a) dovetail V-groove; (b) ball bearing; (c) crossed-roller bearing.

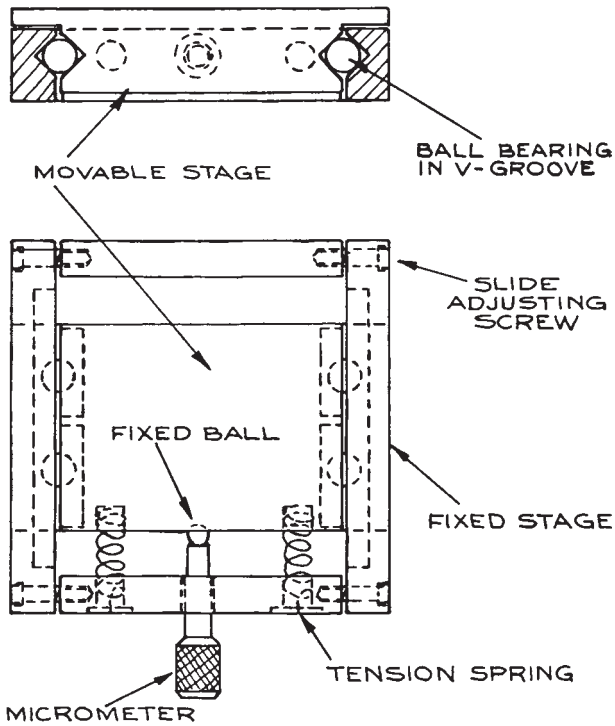

Figure 4.84 Section drawings of a simple 1-D translation stage.

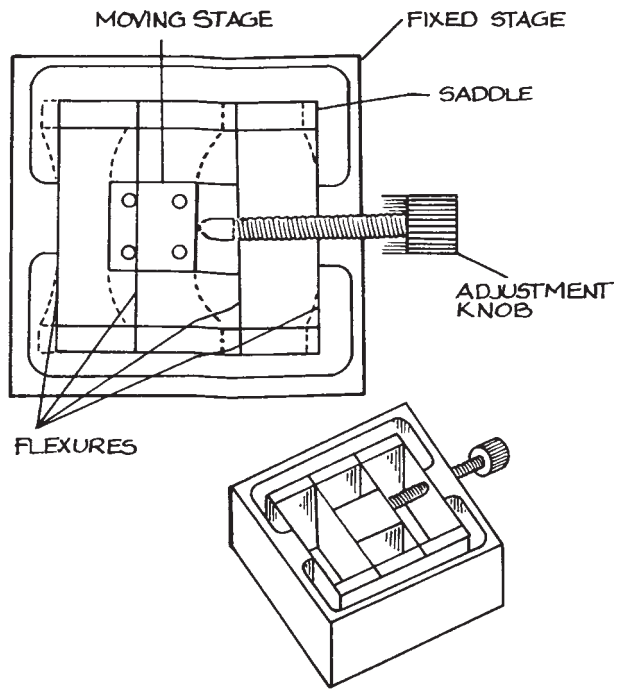

Figure 4.85 Linear translation stage using flexure mounts.

details, the catalogs of the manufacturers previously mentioned should be consulted.

Optical Benches and Components. For optical experiments that involve the use of one or more optical components in conjunction with a source and/or a detector in some sort of linear optical arrangement, construction using an optical bench and components is very convenient, particularly in breadboarding applications. The commonest such bench design is based on the equilateral triangular bar developed by Zeiss and typically machined from lengths of stabilized cast iron. Aluminum benches of this type are also available, but are less rigid. Components are mounted on the bench in rod-mounted holders that fit into carriers that locate on the triangular bench. A cross-sectional diagram of a typical bench and carrier is shown in Figure 4.87.

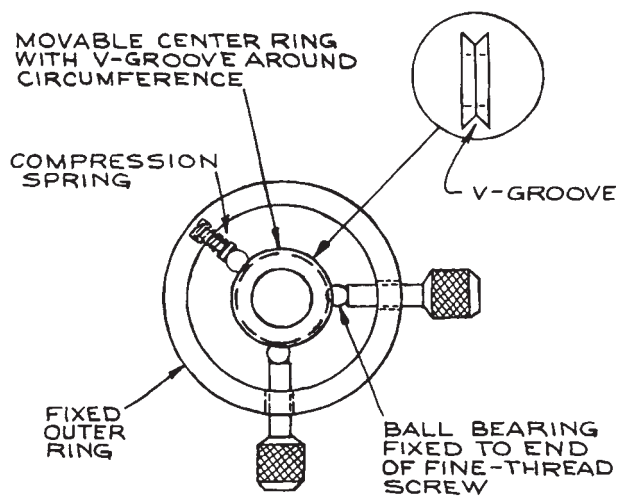

Figure 4.86 A simple precision centering stage.

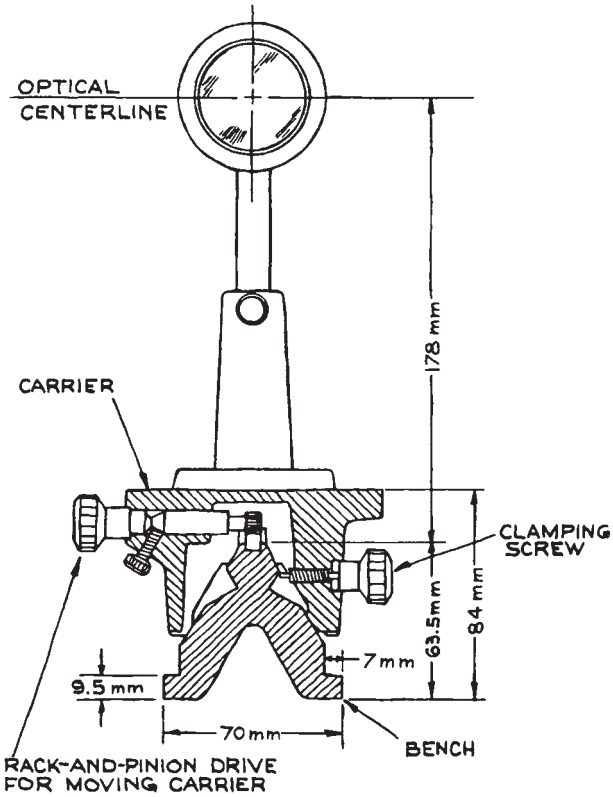

Figure 4.87 Typical dimensions of a Zeiss triangular optical bench with carrier and mounted optical component. (Courtesy of Ealing Corporation).

Coarse adjustment along the length of the bench is provided by moving the carrier manually. On many benches this is accomplished with a rack-and-pinion arrangement. A wide range of mounts and accessories are available, providing for vertical, lateral, and longitudinal adjustment of mounted-component positions. Holders for filters, for centering lenses, and for holding and rotating prisms and polarizers are readily obtained. Precision gimbal mounts, translators, and rotators can be readily incorporated into the structure. Examples of devices that lend themselves well to optical-bench construction are telescopes, collimators, laser-beam expanders and spatial filters, optical isolators, and electro-optic light modulators. Optical benches and accessories are available from Edmund Optics, Lasico, Linos Photonics, Melles Griot, and Newport. Optical benches are no longer as commonly used or available as they once were because of the wide availability of optical tables and mounts, and the additional flexibility provided by their use.

Piezoelectric Transducers. Most PZTs are made from ferroelectric ceramics, such as lead zirconate titanate or barium titanate, but polymers such as polyvinylidene fluoride (PVF) are also used. Simple ceramic transducers are usually supplied as flat discs with a metalized layer on each flat face, or as short hollow cylinders, in which case the metalized electrodes are deposited on the inner and outer cylindrical surfaces. The flat discs change their thickness with applied voltage, the cylindrical types change their axial length. Typical length changes are on the order of 10^{-9} mV. Therefore, these devices are particularly suitable for very fine (submicron) positioning. Much larger motions can be obtained with bimorph PZTs. Bimorphs can be stacked to provide macroscopic motions for modest applied voltages. Excursions of several millimeters can be obtained for voltages of 1 kV. Even larger motions can be obtained with Inchworm transducers, available from EXFO-Burleigh and Sensor Technology. Basic ceramic transducer elements are available from EDO Electro-Ceramic Products, Physik Instrumente (PI), Piezo Systems, CTS Piezoelectric Products, Polytec, and Queensgate Instruments. PVF transducers are available from Atochem North America (formerly Pennwalt). Complete transducer assemblies are available from EXFO-Burleigh, Newport/Klinger, and Polytec Optronics.

Voice Coil Actuators. Voice coil actuators are a convenient way to generate linear movement in the range between micrometers and tens of millimeters, with zero hysteresis, and up to audio frequencies. They are essentially the same as the mechanism in a loudspeaker that moves the diaphragm to generate sound. They are direct drive linear actuators that incorporate magnets and an electrical coil. The voice coil itself is a noncommutated, two-terminal device. It has linear control characteristics, zero hysteresis, zero backlash, and infinite position sensitivity. It has short mechanical and electrical time constants and a high output power-to-weight ratio. A voice coil is generally operated in a control loop where a control signal is provided from a position readout device. Voice coil

actuators are available from Airex, BEI Kimco, Equipment Solutions, H2W Technologies, Innotics, and Orlin.

4.3.12 Optical Tables and Vibration Isolation

A commercially made optical table provides the perfect base for construction of an optical system. Such tables have tops made of granite, steel, Invar, Superinvar (very expensive), or ferromagnetic or nonmagnetic stainless steel. When vibrational isolation of the table top is required, the top is mounted on pneumatic legs. Such an arrangement effectively isolates the table top from floor vibrations above a few Hertz. To minimize acoustically driven vibrations of the table top itself, the better metal ones employ a laminated construction with a corrugated or honeycomb metal cellular core bonded with epoxy to the top and bottom table surfaces.

Granite table tops are very much less intrinsically resonant than metal tops and represent the ultimate in dimensional stability and freedom from undesirable vibrational modes. Complete pneumatically isolated optical table systems, nonisolated tables, and table tops alone are available from Kinetic Systems, Melles Griot, Newport, Standa, Thorlabs, and TMC. In selecting a table, points of comparison to look for include the following:

(1) The overall flatness of the table top (flatness within 50 μm is good, although greater flatness can be obtained)
(2) The low-frequency vibration isolation characteristics of the pneumatic legs
(3) The rigidity of the table top (how much it deforms with an applied load at the center or end)
(4) The isolation from both vertical and horizontal vibrations
(5) The frequencies and damping of the intrinsic vibrational modes
(6) Are the threaded holes in the table top sealed so that liquid spills do not disappear into the interior honeycombs of the table?

Other criteria, such as cost and table weight, may be important. Typical sizes of readily available tops range up to 5 × 12 ft (larger tables are also available) and in thickness from 8 in. to 2 ft. The thicker the table, the greater its rigidity and stability. Most commercial tables are available with 1/4-20 threaded holes spaced on 1 in. centers over the surface of the table. Better designs use blind holes of this type so that liquids spilt on the table do not vanish into its interior. Ferromagnetic table tops permit the use of magnetic hold-down bases for mounting optical components. Such mounts are available from numerous optical suppliers. It is cheaper, and just as satisfactory, to buy magnetic bases designed for machine-tool use from a machine-tool supply company.

Steel and granite surface plates that can be used as small, nonisolated optical tables are available from machine-tool supply companies. If it is desired to construct a vibration-isolated table in the laboratory, a 2 in. thick aluminum plate resting on underinflated automobile-tire inner tubes works rather well, although the plate will have resonant frequencies. Very flat aluminum plate, called *jig plate*, can be obtained for this application at a cost not much greater than ordinary aluminum plate. Just mounting a heavy plate on dense polyurethane foam also works surprisingly well. In fact, the vibrational isolation of a small optical arrangement built on an aluminum plate and mounted on a commercial optical table is increased by having a layer of thick foam between plate and table top.

Even the best-constructed precision optical arrangement on a pneumatic isolation table is subject to airborne acoustic disturbances. A very satisfactory solution to this problem is to surround the system with a wooden particle-board box lined with acoustic absorber. Excellent absorber material, a foam–lead–foam–lead–foam sandwich called Hushcloth DS, is available from American Acoustical Products.

4.3.13 Alignment of Optical Systems

Small helium–neon lasers are now so widely available and inexpensive that they must be regarded as the universal tool for the alignment of optical systems. Complex systems of lenses, mirrors, beamsplitters, and so on can be readily aligned with the aid of such a laser: even visible-opaque infrared components can be aligned in this way by the use of reflections from their surfaces. Fabry–Perot interferometers, perhaps the optical instruments most difficult to align, are easily aligned with the aid of a laser. The laser beam is shone orthogonally through the first mirror of the interferometer (easily accomplished by observing part of the laser

beam reflect back on itself), and the second interferometer mirror is adjusted until the resultant multiple-spot pattern between the mirrors coalesces into one spot.

4.3.14 Mounting Optical Components

A very wide range of optical devices and systems can be constructed using commercially available mounts designed to hold prisms, lenses, windows, mirrors, light sources, and detectors. Some commercially made optical mounts merely hold the component without allowing precision adjustment of its position. Many of the rod-mounted lens, mirror, and prism holders designed for use with standard optical benches fall into this category, although they generally have some degree of coarse adjustability; however, a wide range of commercially available optical mounts allow precision adjustment of the mounted component.

The construction of a complete optical system from commercial mounts can be very expensive, while providing in many cases unnecessary, and consequently undesirable, degrees of freedom in the adjustment and orientation of the various components of the system. Although extra adjustability is often desirable when an optical system is in the ''breadboard'' stage, in the final version of the system it reduces overall stability. An adjustable mount can never provide the stability of a fixed mount of comparable size and mass. Stability in the mounting of optical components is particularly important in the construction of precision optical systems for use, for example, in interferometry and holography.

A custom-made optical mount must allow the insertion and stable retention of the optical component without damage to the component, which is usually made of some fragile (glassy or single-crystal) material. If possible, the precision surface or surfaces of the component should not contact any part of the mount. The component should be clamped securely against a rigid surface of the mount. It should not be clamped between two rigid metal parts: thermal expansion or contraction of the metal may crack the component or loosen it. The clamping force should be applied by an intermediary rubber pad or ring. Some examples of how circular mirrors or windows can be mounted in this way are shown in Figure 4.88. If a precision polished surface of the component must contact part of the mount (for example, when a precision lens, window, mirror, or prism is forming a vacuum-tight seal), the metal surface should be finely machined: the edges of the mounting surface must be free of burrs. Ideally, the metal with which the component is in contact should have a lower hardness than

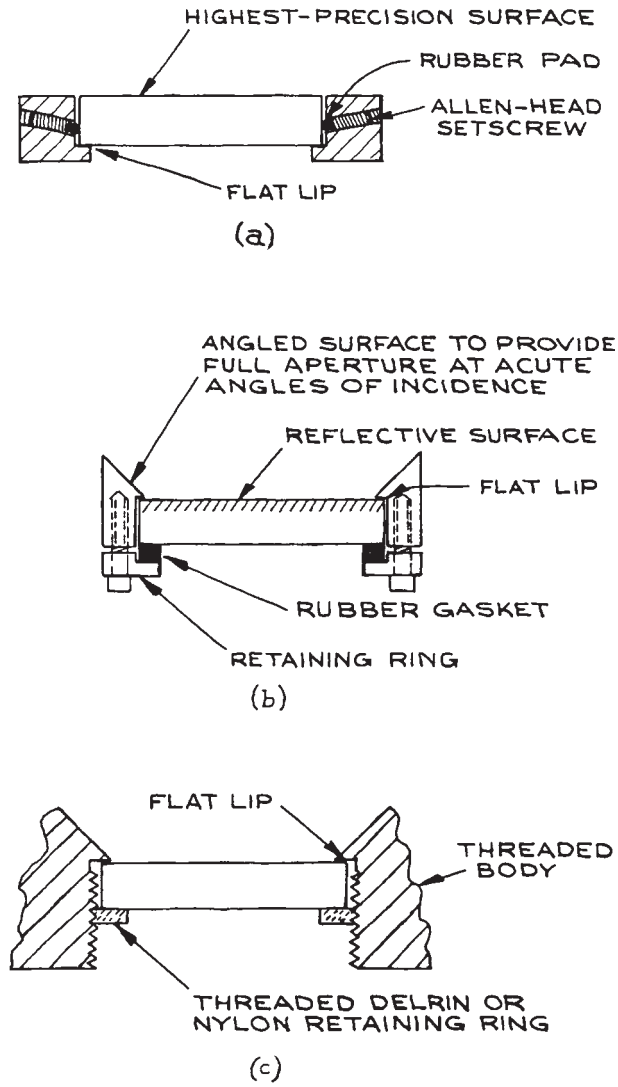

Figure 4.88 Ways for mounting delicate optical components: (a) no contact between precision surface of component and mount; (b) precision surface in minimal contact with mount and held in place with retaining ring; (c) precision surface in minimal contact with bottom of recess in mount and held in place with threaded plastic ring.

the component. A thin piece of paper placed between the component and metal will protect the surface of the component without significantly detracting from the rigidity of the mounting.

Generally speaking, unless an optical component has one of a few standard shapes and sizes, it will not fit directly in a commercial mount and a custom adaptor will need to be made.

It is often necessary to mount a precision optical component (usually a flat window or mirror, but occasionally a lens or spherical mirror) so that it provides a vacuum- or pressure-tight seal. There are two important questions to be asked when this is done: can the component, of a certain clear aperture and thickness, withstand the pressure differential to which it will be subjected, and will it be distorted optically either by this pressure differential or the clamping forces holding it in place?

There are various ways of mounting a circular window so that it makes a vacuum- or pressure-tight seal. Demountable seals are generally made by the use of rubber O-rings (see Section 3.5.2) for vacuum, or flat rubber gaskets for pressure. More-or-less permanent seals are made with the use of epoxy resin, by running a molten bead of silver chloride around the circumference of the window where it sits on a metal flange, or in certain cases by directly soldering or fusing the window in place. Some crystalline materials, such as germanium, can be soldered to metal; many others can be soldered with indium if they, and the part to which they are to be attached, are appropriately treated with gold paint beforehand.[48] If a window is fused in place, its coefficient of expansion must be well matched to that of the part to which it is fixed. Suitably matched glass, fused silica, and sapphire windows on metal are available. Either the glass and metal are themselves matched, or an intermediate graded seal is used (see Section 2.2.4). To decide what thickness-to-unsupported-diameter ratio is appropriate for a given pressure differential, it must be determined whether the method of mounting corresponds to Figure 4.89(a) or (b). In either case, the maximum stress in the window must be kept below the modulus of rupture Y of the window by an appropriate safety factor S_f. A safety factor of four is generally adequate for determining a safe window thickness, but a larger factor may be necessary to avoid deformation of the window that would lead to distortion

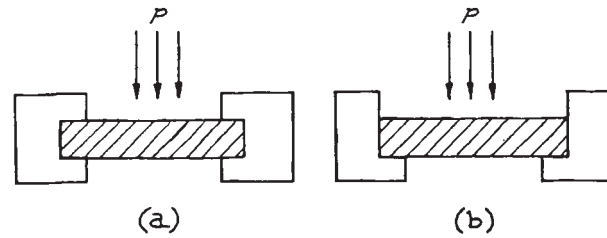

Figure 4.89 Window mounting arrangements: (a) clamped or fixed edge (maximum stress at edge); (b) unclamped or freely supported edge (maximum stress at center).

of transmitted wavefronts. The desired thickness-to-free-diameter ratio for a pressure differential p is found from the formula:

$$\frac{t}{D} = \sqrt{\frac{KpS_f}{4Y}} \tag{4.190}$$

where K is a constant whose value can be taken as 0.75 for a clamped edge and 1.125 for a free edge (see also Sections 1.6.3 and 3.6.3).

A window mounted with an O-ring in a groove, as shown in Figure 4.90, may not provide an adequate seal at moderately high pressures, say above 7MPa[h], unless the clamping force of the window on the ring is great enough to prevent the pressure differential deforming the ring in its grooves and creating a leak. A better design for high-pressure use, up to about 50MPa, is shown in Figure 4.90(b): the clamping force and internal pressure act in concert to compress the ring into position. Clamping an optical-quality window or an O-ring seal of the sort shown in Figure 4.90(a) may cause slight bending of the window.

If an optical window has been fixed ‘‘permanently’’ in place with epoxy resin, it may be possible to recover the window, if it is made of a robust material, by heating the seal to a few hundred degrees or by soaking it in methylene chloride or a similar commercial epoxy remover.[49]

If optical windows are to be used in pressure cells where there is a pressure differential of more than 500 bars ($\simeq$ 7000 psi), O-rings are no longer adequate and special window-mounting techniques for very high pressures must be used.[50–52] Optical cells for use at pressures up to 3 kbar are available from ISS, Inc.

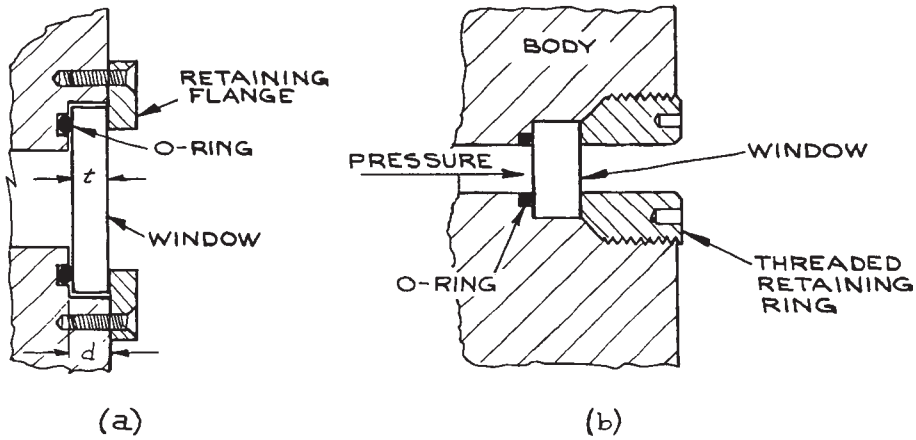

Figure 4.90 Mounting arrangements for optical windows in vacuum and pressure applications: (a) simple vacuum window; (b) high-pressure window.

4.3.15 Cleaning Optical Components

It is always desirable for the components of an optical system to be clean. At the very least, particles of dust on mirrors, lenses, and windows increase scattering; organic films lead to unnecessary absorption, possible distortion of transmitted wavefronts, and – in experiments with ultraviolet light sources – possible unwanted fluorescence. In optical systems employing lasers, dust and films will frequently lead to visible, undesirable interference and diffraction effects. At worst, dirty optical components exposed to high-intensity laser beams can be permanently damaged, as absorbing dust and films can be burnt into the surface of the component.

The method used for cleaning optical components, such as mirrors, lenses, windows, prisms, and crystals, will depend on the nature of both the optical component and the type of contaminant to be removed. For components made of hard materials, such as borosilicate glass, sapphire, quartz, or fused silica, gross amounts of contamination can be removed by cleaning in an ultrasonic tank. The tank should be filled with water and the components to be cleaned placed in a suitable pure solvent, such as acetone or trichloroethylene, contained in a clean glass or plastic beaker. If trichloroethylene is used, the operation should be performed inside a fume hood because there is evidence that this solvent is a human carcinogen. The ultrasonic cleaning is accomplished by placing the beaker in the tank of water. Dust can be removed from the surface of hard materials, including most modern hard dielectric reflecting and antireflecting coatings, by brushing with a soft camels-hair brush. Suitable brushes are available from most photographic stores. Lens tissue and solvent can be used to clean contaminants from both hard and medium-hard surfaces, provided the correct method is used. The category of medium-hard materials includes materials such as arsenic trisulfide, silicon, germanium, gallium arsenide, KRS-5, and tellurium. Information about the relative hardness of these and other materials is contained in Table 4.5. Dust should first be removed from the component by wiping, very gently, in one direction only, with a folded piece of dry lens tissue. The tissue should be folded so that the fingers do not come near any part of the tissue that will contact the surface. Better still, if a cylinder of dry nitrogen is available, dust can be blown from the surface of the component. Because the gas can itself contain particles, it should be passed through a suitable filter, such as fine sintered glass, before use. Clean gas can be used in this way to remove dust from the surface of even very delicate components, such as aluminum- and gold-coated mirrors, and diffraction gratings. The use of gas jets for dust removal requires caution: delicate structures have been damaged by the force of the gas. Commercial ‘‘dust-off’’ sprays are available that use a liquified propellant gas that vaporizes on leaving the spray-can nozzle. These sprays

Table 4.5 Characteristics of optical materials

Material	Useful Transmission Range (⩾ 10% transmission) in 2 mm Thickness	Index of Refraction [wavelength (μm) in parentheses]	Knoop Hardness	Melting Point (°C)
LiF	0.104–7	1.60(0.125), 1.34(4.3)	100	870
MgF_2	0.126–9.7	$n_o = 1.3777$, $n_e = 1.38950(0.589)^f$	415	1396
CaF_2	0.125–12	1.47635(0.2288), 1.30756(9.724)	158	1360
BaF_2	0.1345–15	1.51217(0.3652), 1.39636(10.346)	65	1280
Sapphire(Al_2O_3)	0.15–6.3	$n_o = 1.8336(0.26520)$,[f] n_o=1.5864(5.577)[f], n_e slightly less than n_o	1525-2000[c]	2040 ± 10
Fused silica (SiO_2)	0.165–4[d]	1.54715(0.20254), 1.40601(3.5)	615	1600
Pyrex 7740	0.3–2.7	1.474(0.589), ≃ 1.5(2.2)	≃600	820[g]
Vycor 7913	0.26–2.7	1.458(0.589)	—	1200
As_2S_3	0.6–0.13	2.84(1.0), 2.4(8)	109	300
RIR 2	≃0.4–4.7	1.75(2.2)	≃600	≃900
RIR 20	≃0.4–5.5	1.82(2.2)	542	760
NaF	0.13–12	1.393(0.185), 0.24(24)	60	980
RIR 12	=0.4–5.7	1.62(2.2)	594	≃900
MgO	0.25–8.5	1.71(2.0)	692	2800
Acrylic	0.340–1.6	1.5066(0.4101), 1.4892(0.6563)	—	Distorts at 72
Silver chloride (AgCl)	0.4–32	2.134(0.43), 1.90149(20.5)	9.5	455
Silver bromide (AgBr)	0.45–42	2.313(0.496), 2.2318(0.671)	⩾ 9.5	432
Kel-F	0.34–3.8	—	—	—
Diamond (type IIA)	0.23–200+	2.7151(0.2265), 2.4237(0.5461)	5700–10400[c]	
NaCl	0.21–25	1.89332(0.185), 1.3403(22.3)	18	803
KBr	0.205–25	1.55995(0.538), 1.46324(25.14)	7	730
KCl	0.18–30	1.78373(0.19), 1.3632(23)	—	776
CsCl	0.19– ≃30	1.8226(0.226), 1.6440(0.538)	—	646
CsBr	0.21–50	1.75118(0.365), 2.55990(39.22)	19.5	636
KI	0.25–40	2.0548(0.248), 1.6381(1.083)	5	723
CsI	0.235–60	1.98704(0.297), 1.61925(53.12)	—	621
$SrTiO_3$	0.4–7.4	2.23(2.2), 2.19(4.3)	620	2080
SrF_2	0.13–14	1.438(0.538)	130	1450
Rutile (TiO_2)	0.4–7	$n_o = 2.5(1.0)$, $n_e = 2.7(1.0)^f$	880	1825
Thallium bromide (TlBr)	0.45–45	2.652(0.436), 2.3(0.75)	12	460
Thallium bromoiodide (KRS-5)	0.56–60	2.62758(0.577), 2.21721(39.38)	40	414.5
Thallium chlorobromide (KRS-6)	0.4–32	2.3367(0.589), 2.0752(24)	39	423.5
ZnSe	0.5–22	2.40(10.6)	150	—
Irtran 2 (ZnS)	0.6–15.6	2.26(2.2), 2.25(4.3)	354	800
Si	1.1–15[e]	3.42(5.0)	1150	1420
Ge	1.85–30[e]	4.025(4.0), 4.002(12.0)	692	936
GaAs	1–15	3.5(1.0), 3.135(10.6)	750	1238
CdTe	0.9–16	2.83(1.0), 2.67(10.6)	45	1045
Te	3.8–8+	$n_o = 6.37(4.3)$, $n_e = 4.93(4.3)^f$	—	450
$CaCO_3$	0.25–3	$n_o = 1.90284(0.200)$, $n_e = 1.57796(0.198)^f$	—	—
		$n_o = 1.62099(2.172)$, $n_e = 1.47392(3.324)$	135	894.4[b]

Table 4.5 *(cont.)*

Material	Thermal-Expansion Coefficient (10^{-6}/K)	Solubility in Water [g/(100 g), 20°C]	Soluble in	Comments
LiF	9	0.27	HF	Scratches easily
MgF_2	16	7.6×10^{-3}	HNO_3	—
CaF_2	25	1.1×10^{-3}	NH_4 salts	Not resistant to thermal or mechanical shock
BaF_2	26	0.12	NH_4Cl	Slightly hygroscopic, sensitive to thermal shock
Al_2O_3	6.66,[a] 5.0[b]	9.8×10^{-5}	NH_4 salts	Very resistant to chemical attack, excellent material
SiO_2	0.55	0.00	HF	Excellent material
Pyrex	3.25	0.00	HF, hot H_2PO_4	Excellent mechanical, optical properties
Vycor	0.8	0.00	HF, hot H_2PO_4	Excellent mechanical, optical properties
As_2S_3	26	5×10^{-5}	Alcohol	Nonhygroscopic
RIR 2	8.3	0.00	1% HNO_3	Good mechanical, optical properties
RIR 20	9.6	—	—	Good mechanical, optical properties
NaF	36	4.2	HF	Lowest ref. index of all known crystals
RIR 12	8.3	—	—	Good mechanical and optical properties
MgO	43	6.2×10^{-4}	NH_4 salts	Nonhygroscopic; surface scum forms if stored in air
Acrylic	110–140	0.00	Methylene chloride	Easily scratched, available in large sheets
AgCl	30	1.5×10^{-4}	NH_4OH, KCN	Corrosive, nonhygroscopic, cold-flows
AgBr	—	12×10^{-6}	KCN	Cold-flows
Kel–F	—	—	—	Soft,easily scratched
Diamond	0.8	0.00	—	Hardest material known; thermal conductivity 6 × Cu at room temp., chemically inert
NaCl	44	36	H_2O, glycerine	Corrosive, hygroscopic
KBr	—	65.2	H_2O, glycerine	Hygroscopic
KCl	—	34.35	H_2O, glycerine	Hygroscopic
CsCl	—	186	Alcohol	Very hygroscopic
CsBr	48	124	H_2O	Soft, easily scratched, hygroscopic
KI	—	144.5	Alcohol	Soft, easily scratched, hygroscopic, sensitive to thermal shock
CsI	50	160	Alcohol	Soft, easily scratched, very hygroscopic
$SrTiO_3$	9.4	—	—	Refractive index $\simeq \sqrt{5}$
SrF_2	—	1.17×10^{-2}	Hot HCl	Slightly sensitive to thermal shock
TiO_2	9	0.00	H_2SO_4	Nonhygroscopic, nontoxic
TlBr	—	0.0476	Alcohol	Flows under pressure, toxic
KRS-5	51	<0.0476	HNO_3, aqua regia	Cold-flows, nonhygroscopic, toxic
KRS-6	60	0.32	HNO_2, aqua regia	Cold-flows, nonhygroscopic, toxic
ZnSe	8.5	0.001	—	Very good infrared materials, also transparent to some visible light
ZnS	—	6.5×10^{-5}	HNO_3, H_2SO_4	—
Si	4.2	0.00	HF + HNO_3	Resistant to corrosion, must be highly polished to reduce scattering losses at surface
Ge	5.5	0.00	Hot H_2SO_4, aqua regia	

Table 4.5 *(cont.)*

Material	Thermal-Expansion Coefficient (10^{-6}/K)	Solubility in Water [g/(100 g), 20°C]	Soluble in	Comments
GaAs	5.7	0.00	—	Very good high-power infrared-laser window material
CdTe	4.5	—	—	—
Te	16.8	0.00	H_2SO_4, HNO_3	Poisonous, soft, easily scratched
$CaCO_3$	—	1.4×10^{-3}	Acids, NH_4Cl	—
	—	—	—	—

[a] Parallel to c-axis.
[b] Perpendicular to c-axis.
[c] Depends on crystal orientation.
[d] Depends on grade.
[e] Long-wavelength limit depends on purity of material.
[f] Birefringent.
[g] Softening temperature.
[h] Decomposition temperature.

are not recommended for cleaning delicate or expensive components. They can exert considerable force at close range and can also deposit unvaporized propellant on the component, or condense water vapor into the surface of a hygroscopic material.

There are two good methods for cleaning hard and medium-hard components with lens tissue and solvent. The lens tissue should be folded as indicated previously, and a few drops of solvent placed on the tissue in the area to be used for the cleaning. The tissue should be wiped just once in a single direction across the component and then discarded. Fingers should be kept away from the solvent-impregnated part of the tissue, and it may be desirable to hold the component to be cleaned with a piece of dry tissue to avoid the transmission of finger grease to its surface. Hemostats, available from surgical supply stores, are very convenient for holding tissue during cleaning operations. To clean a single, fairly flat optical surface, such as a dielectric coated mirror or window, place a single lens tissue flat on the surface. Put one drop of clean solvent (spectroscopically pure grades are best) on the tissue over the component. Then draw the tissue across the surface of the component so that the dry portion of the tissue follows the solvent-soaked part and dries off the surface.

Several suitable solvents exist for these cleaning operations, such as acetone, trichloroethylene, and methyl, ethyl, and isopropyl alcohols. Diethyl ether is a very good solvent for cleaning laser mirrors, but its extreme flammability makes its use undesirable.

If there is any doubt as to the ability of an optical component to withstand a particular solvent, the manufacturer should be consulted. This applies particularly to specially coated components used in ultraviolet and some infrared systems. Some delicate or soft components cannot be cleaned at all without running the risk of damaging them permanently, although it is usually safe to remove dust from them by blowing with clean, dust-free gas. It is worth noting that diffraction gratings frequently look as though they have surface blemishes. These blemishes frequently look much worse than they actually are and do not noticeably affect performance. Never try to clean diffraction gratings. It is also very difficult to clean aluminum- or gold-coated mirrors that are not overcoated with a hard protective layer such as silicon monoxide. Copper mirrors are soft and should be cleaned with extreme care.

Most optical components used in the visible and near-ultraviolet regions of the spectrum are hard; soft materials are often used in infrared systems. In this region several soft crystalline materials such as sodium chloride, potassium chloride, cesium bromide, and cesium iodide are commonly used. These materials can be cleaned,

essentially by repolishing their surfaces. For sodium and potassium chloride windows this is particularly straightforward. Fold a piece of soft, clean muslin several times to form a large pad. Place the pad on a flat surface – a piece of glass is best. Stretch the pad tight on the surface and fix it securely at the edges with adhesive tape. Dampen an area of the pad with a suitable solvent such as trichloroethylene or alcohol. Place the window to be polished on the solvent-soaked area, and work it back and forth in a figure-eight motion. Gradually work the disc onto the dry portion of the pad. This operation can be repeated as many times as necessary to restore the surface of the window. Do not attempt to clean windows of this kind, which are hygroscopic, by wiping them with solvent-soaked tissue. The evaporation of solvent from the surface will condense water vapor onto it and cause damage. The above recommended cleaning procedure is quite satisfactory for cleaning even laser windows. Small residual surface blemishes and slightly foggy areas do not detract significantly from the transmission of such windows in the middle infrared and beyond – which in any case is the only spectral region where they should be used. For removing slightly larger blemishes and scratches from such soft windows, very fine aluminum oxide powder (available from Adolf Meller) can be mixed with the cleaning solvent on the pad in the first stages of polishing. Perhaps the best way of all for cleaning hard and medium-hard optical components is to vapor-degrease them. This is a very general procedure for cleaning precision components. Place some trichloroethylene or isopropyl alcohol in a large beaker (500 ml or larger) to a depth of about 1 cm. Suspend the components to be cleaned in the top of the beaker so that their critical surfaces face downward. An improvised wire rack is useful for accomplishing this. Cover the top of the beaker tightly with aluminum foil. Place the beaker on an electric hot plate, and heat the solvent until it boils. The solvent vapor thus produced is very pure. It condenses on, and drips off, the suspended item being cleaned, effectively removing grease and dirt. If large items are being cleaned, it may be necessary to blow air on the aluminum foil with a small fan. At the end of several minutes turn off the heat and remove the clean items while they are still warm. This cleaning procedure is recommended for components that must be extremely clean, such as laser Brewster windows.

4.4 OPTICAL MATERIALS

The choice of materials for the various components of an optical system such as windows, prisms, lenses, mirrors, and filters is governed by several factors:

(1) Wavelength range to be covered
(2) Environment and handling that components must withstand
(3) Refractive-index considerations
(4) Intensity of radiation to be transmitted or reflected
(5) Cost.

4.4.1 Materials for Windows, Lenses, and Prisms

For the purposes of classification, the characteristics of various materials for use in transmissive applications will be considered in three spectral regions:

(1) Ultraviolet, 100–400 nm
(2) Visible and near infrared, 400 nm–2 μm
(3) Middle and far infrared, 2–1000 μm.

There are, of course, many materials that can be used in part of two or even three of these regions. Table 4.5 summarizes the essential characteristics of all the common, and most of the rarely used, materials in these three regions. The useful transmission range given for each material is only a guide; the transmission at the ends of this range can be increased and the useful wavelength range of the component extended by using thinner pieces of material – if this is possible. The refractive index of all these materials varies with wavelength, as is illustrated for several materials in Figure 4.91. The Knoop hardness[53] is a static measure of material hardness based on the size of impression made in the material with a pyramidal diamond indenter under specific conditions of loading, time, and temperature. Roughly speaking, a material with a Knoop hardness above about 60 is hard enough to withstand the cleaning procedures described in Section 4.3.15.

Transmission curves for many of the useful optical materials summarized in Table 4.5 are collected together in Figures 4.92 – 4.101. Most of these materials are available from several suppliers. Some of the materials listed in Table 4.5 are worthy of brief extra comment.

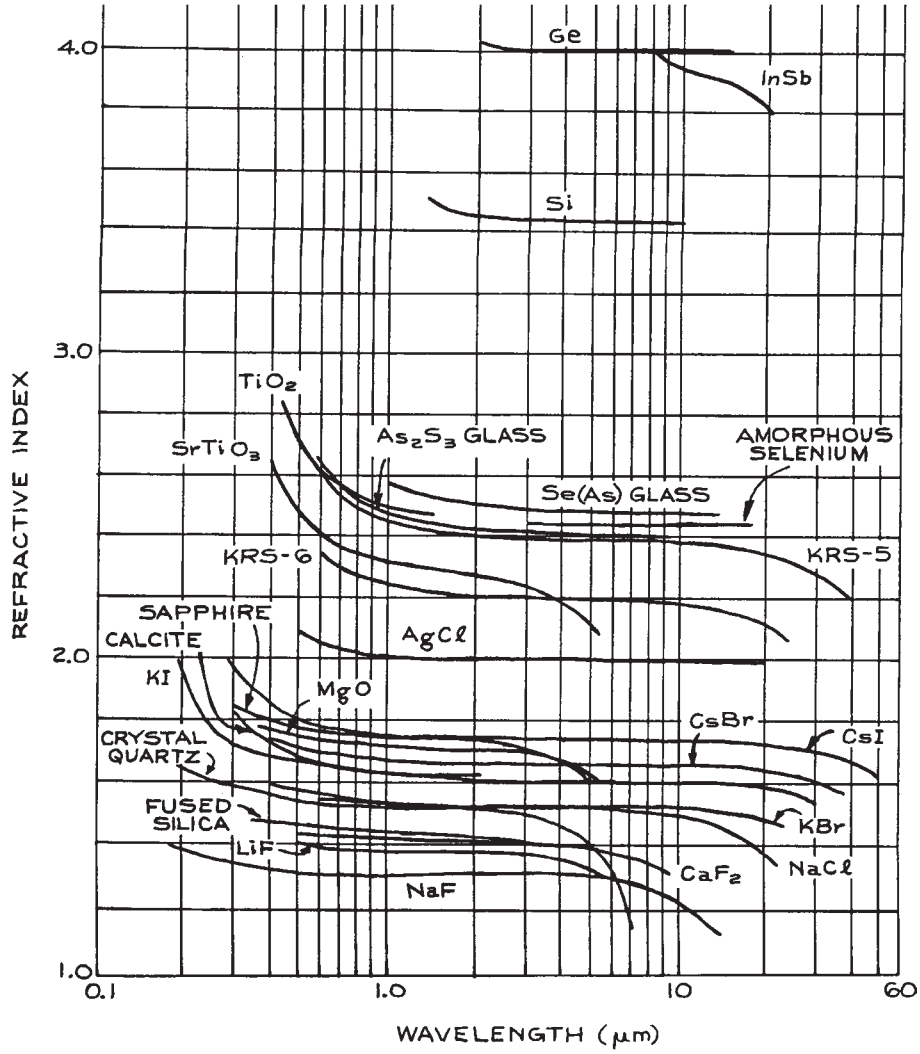

Figure 4.91 The refractive indices of various optical materials. [Adapted, with permission, from W. C. Wolfe and S. S. Ballard, *Optical Materials, Films and Filters for Infrared Instrumentation,* Proceedings of the IRE, **47**, 1540-1546, 1959. © 1959 IRE (now IEEE).]

Ultraviolet Transmissive Materials. The following are suitable for use in the UV region.

(i) Lithium fluoride. Lithium fluoride (LiF, Figure 4.92) has useful transmittance further into the vacuum ultraviolet than any other common crystal. The transmission of vacuum-ultraviolet quality crystals is more than 50% at 121.6 nm for 2 mm thickness, and thinner crystals have useful transmission down to 104 nm. The short-wavelength transmission of the material deteriorates on exposure to atmospheric moisture or high-energy radiation. Moisture does not affect the infrared transmission, which extends to 7 μm. Several grades of LiF are available. Vacuum-ultraviolet-grade material is soft, but visible-grade material is hard.

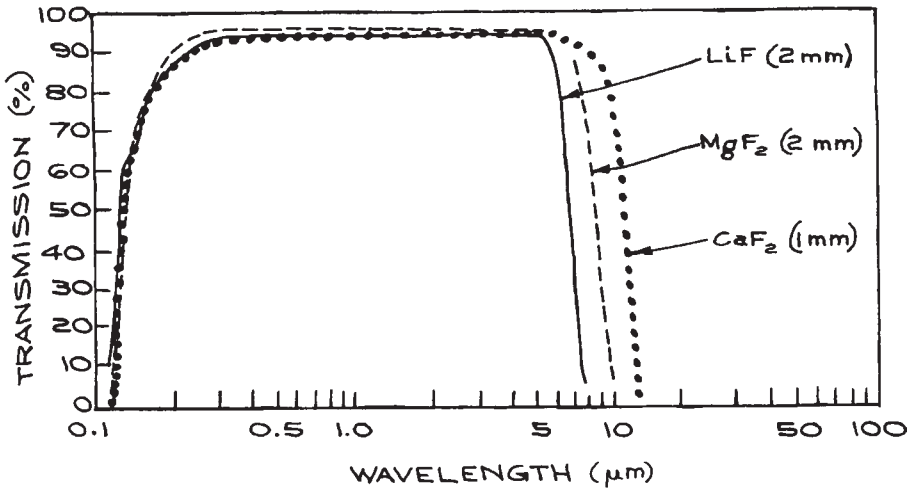

Figure 4.92 Transmission curves of lithium fluoride, magnesium fluoride, and calcium fluoride windows of specified thicknesses.

LiF can be used as a vacuum-tight window material by sealing with either silver chloride or a suitable epoxy.

(ii) Magnesium fluoride. Vacuum-ultraviolet-grade magnesium fluoride (MgF_2, Figure 4.92) transmits farther into the ultraviolet than any common material except LiF. The transmission at 121.6 nm is 35% or more for a 2 mm thickness. MgF_2 is recommended for use as an ultraviolet-transmissive component in space work, as it is only slightly affected by ionizing radiation. MgF_2 is birefringent and is used for making polarizing components in the ultraviolet. Irtran 1 is a polycrystalline form of magnesium fluoride manufactured by Kodak, which is not suitable for ultraviolet or visible applications. Its useful transmission extends from 500 nm to 9 μm.

(iii) Calcium fluoride. Calcium fluoride (CaF_2, Figure 4.92) is an excellent, hard material that can be used for optical components from 125 nm to beyond 10 μm. Vacuum-ultraviolet-grade material transmits more than 50% at 125.7 nm for a 2 mm path length. Calcium fluoride is not significantly affected by atmospheric moisture at ambient temperature. Calcium fluoride lenses are available from Argus, Janos Technology, Linos Photonics, Meller Optics, Melles Griot, Newport, Optovac, Newport/Oriel and Precision Optical. Irtran 3 is a polycrystalline form of CaF_2, which is not suitable for ultraviolet or visible applications, but transmits in the infrared to 11.5 μm.

(iv) Barium fluoride. Although barium fluoride (BaF_2, Figure 4.93) is slightly more water soluble than calcium or magnesium fluoride, it is more resistant than either of these to ionizing radiation. It is a good general-purpose optical material from ultraviolet to infrared. It has excellent transmission to beyond 10 μm, and windows that are not too thick (< 2 mm) can be used in CO_2 laser applications, except at very high energy densities. Barium fluoride lenses are available from Infrared Optical Products and International Scientific Products.

(v) Synthetic sapphire. Synthetic sapphire (corundum, Al_2O_3; Figure 4.93) is probably the finest optical material available in applications from 300 nm to 4 μm. It is very hard, strong, and resistant to moisture and chemical attack (even HF below 300 °C). The useful transmissive range extends from 150 nm to 6 μm, the transmission of a 1 mm thickness being 21% and 34%, respectively, at these two wavelengths. Sapphire optical components are available from many suppliers.[31]

Sapphire is also resistant to ionizing radiation, has high thermal conductivity, and can be very accurately fabricated in a variety of forms. It has low dispersion, however, and is not very useful as a prism material. Chromium-doped Al_2O_3 (ruby) is used in laser applications.

(vi) Fused silica. Fused silica (SiO_2, Figure 4.94) is the amorphous form of crystalline quartz. It is almost as good

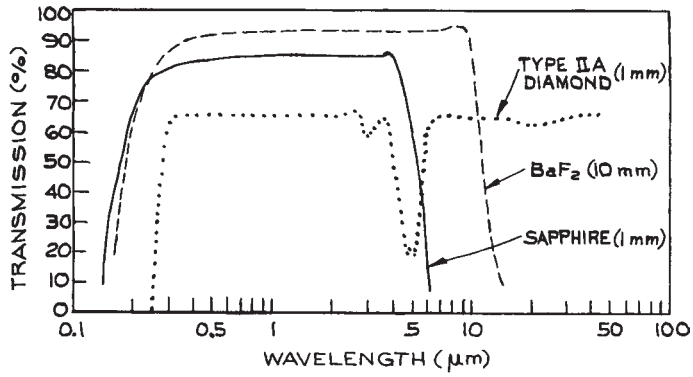

Figure 4.93 Transmission curves of sapphire, barium fluoride, and type IIA diamond windows of specified thicknesses.

an optical material as sapphire and is much cheaper. Its useful transmission range extends from about 170 nm to about 4.5 μm. Special ultraviolet-transmitting grades are manufactured (such as Spectrosil and Suprasil), as well as infrared grades (such as Infrasil) from which undesirable absorption features at 1.38, 2.22, and 2.72 μm, due to residual OH radicals, have been removed. Fused silica has a very low coefficient of thermal expansion, 5×10^{-7}/K in the temperature range from 20 to 900 °C, and is very useful as a spacer material in applications such as Fabry–Perot etalons and laser cavities. Fused-silica optical components such as windows, lenses, prisms, and etalons are readily available. Crystalline quartz is birefringent and is widely used in the manufacture of polarizing optics, particularly quarter-wave and half-wave plates.

Very pure fused silica is also the material of which most optical fibers are made. In fiber optic applications the index gradient inside the fiber is generally produced by germania (GeO_2) doping. The pure silica used in optical fibers is most transparent in the infrared, generally near 1.55 μm.

(vii) Diamond. Windows made of type-IIA diamond (Figure 4.93) have a transmittance that extends from 230 nm to beyond 200 μm, although there is some absorption between 2.5 and 6.0 μm. The high refractive index of diamond, $n = 2.4$, over a very wide band, leads to a reflection loss of about 34% for two surfaces. Diamond windows are extremely expensive, ($10,000–20,000 for a 1 cm diameter, 1 mm thick window); however, some properties of diamond are unique: its thermal conductivity is six times that of pure copper at 20 °C, and it is the hardest material known, very resistant to chemical attack, with a low thermal-expansion coefficient and high resistance to radiation damage.

Visible- and Near-Infrared-Transmissive Materials. The materials so far considered as ultraviolet-transmitting are also excellent for use in the visible and near infrared. There are, however, several materials that transmit well in the visible and near infrared, but are not suitable for ultraviolet use.

(i) Glasses. There is an extremely large number of types of glass used in the manufacture of optical components. They are available from many manufacturers, such as Chance, Corning, Hoya, Ohara, and Schott.

Two old classifications of glass into *crown* and *flint* glasses can be related to the glass chart. Crown glasses are glasses with a V value greater than 55 if $n_d < 1.6$ and $V > 50$ if $n_d > 71.6$. The flint glasses have V values below these limits. The rare earth glasses contain rare earths instead of SiO_2, which is the primary constituent of crown and flint glasses. Glasses containing lanthanum contain the symbol La.

A few common glasses are widely used in the manufacture of lenses, windows, prisms, and other components. These include the borosilicate glasses Pyrex, BK7/A, and crown (BSC), as well as Vycor, which is 96% fused quartz. Transmission curves for Pyrex No. 7740 and Vycor No.

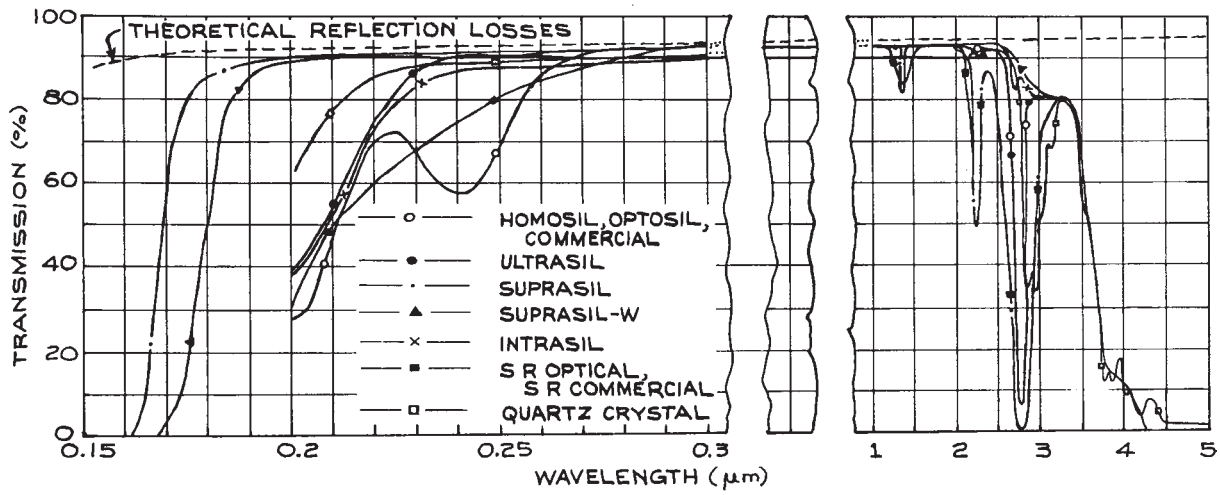

Figure 4.94 Transmission characteristics of various grades of fused silica; all measurements made on 10 mm thick materials. (Courtesy of Heraeus-Amersiol, Inc.)

7913 are shown in Figure 4.95. These glasses are not very useful above 2.5 μm, their transmission at 2.7 μm is down to 20% for a 10 mm thickness. In the spectral region between 350 nm and 2.5 μm, however, they are excellent transmissive materials. They are inexpensive, hard, and chemically resistant, and can be fabricated and polished to high precision. Special glasses for use further into the infrared are available from Hoya and Corning. In window applications these glasses do not appear to offer any particular advantages over more desirable materials such as infrared-grade fused silica or sapphire; however, in specialized applications, such as infrared lens design, their higher refractive indices are useful.

For special applications, many colored filter glasses can be obtained. Glasses that transmit visible but not infrared, or vice versa, or that transmit some near ultraviolet, but no visible,

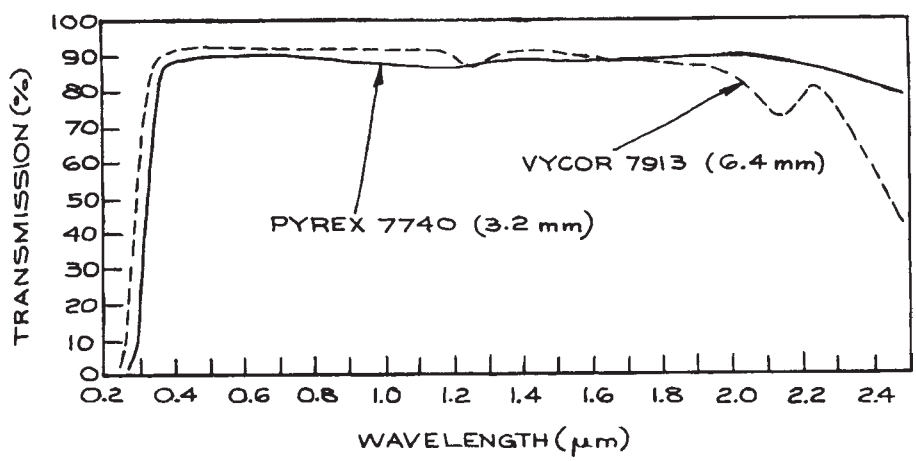

Figure 4.95 Transmission curves for Pyrex 7740 and Vycor 7913.

and many other combinations are available. The reader should consult the catalogs published by the various manufacturers and suppliers such as Chance-Pilkington, Corning, CVI, Hoya, Kopp Glass, Melles-Griot (now CVI-Melles-Griot), NPraezisions Glas & Optik, Schott, and Rolyn.

Special glasses whose expansion coefficients match selected metals can be made because the composition of glass is continuously variable,. These glasses are useful for sealing to the corresponding metals in order to make windows on vacuum chambers. Corning glass No. 7056 is often used in this way, as it can be sealed to the alloy Kovar. Vacuum-chamber windows of quartz or sapphire are also available,[54] but their construction is complex, and consequently they are costly. Various grades of flint glass are available that have high refractive indices and are therefore useful for prisms. For a tabulation of the types available the reader is referred to Kaye and Laby.[7] The refractive indices available range up to 1.93 for Chance-Pilkington Double Extra Dense Flint glass No. 927210, but this and other high-refractive-index glasses suffer long-term damage such as darkening when exposed to the atmosphere.

(ii) Plastics. In certain noncritical applications, such as observation windows, transparent plastics such as polymethylmethacrylate (Acrylic, Plexiglas, Lucite, Perspex) or polychlorotrifluoroethylene (Kel-F) are cheap and satisfactory. They cannot be easily obtained in high optical quality (with very good surface flatness, for example) and are easily scratched. The useful transmission range of Acrylic windows 1 cm thick runs from about 340 nm to 1.6 μm. A transmission-versus-wavelength curve for this material is shown in Figure 4.96. One important application of Acrylic is in the manufacture of Fresnel lenses (see Section 4.3.3). Kel-F (polychlorotrifluoroethylene) is useful up to about 3.8 μm, although it shows some decrease in transmission near 3 μm. It is similar to polytetrafluoroethylene (Teflon) and is very resistant to a wide range of chemicals – even gaseous fluorine.

(iii) Arsenic trisulfide. Arsenic trisulfide (As_2S_3, Figure 4.97) is a red glass that transmits well from 800 nm to 10 μm. Its usefulness stems from its relatively low price, ease of fabrication, nontoxicity, and resistance to moisture. Although primarily an infrared-transmissive material, it is also transmissive in the red, which facilitates the alignment

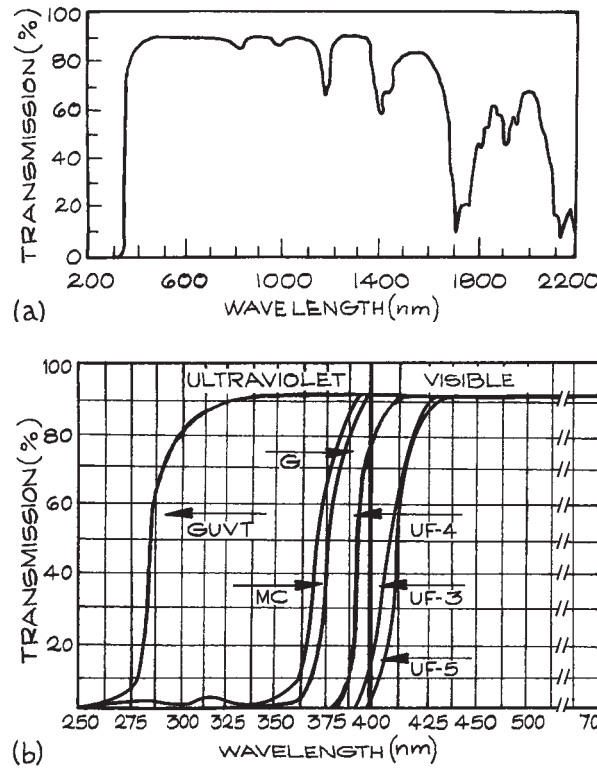

Figure 4.96 (a) Transmission curve for 3.175 mm thick acrylic. (Courtesy of Melles Griot, Inc.); (b) Transmission curve of various grades of acrylic available from Altumax International.

of optical systems containing it. As_2S_3 is relatively soft and will cold-flow over a long period of time. A wide range of As_2S_3 lenses are available from Amorphous Materials, OFR (Thorlabs), Recon Optical, and REFLEX Analytical.

Middle- and Far-Infrared-Transmissive Materials.

The following are useful well into the IR region.

(i) Sodium chloride. Sodium chloride (NaCl, Figure 4.98) is one of the most widely used materials for infrared-transmissive windows. Although it is soft and hygroscopic, it can be repolished by simple techniques and maintained exposed to the atmosphere for long periods without damage simply by maintaining its temperature higher than ambient.

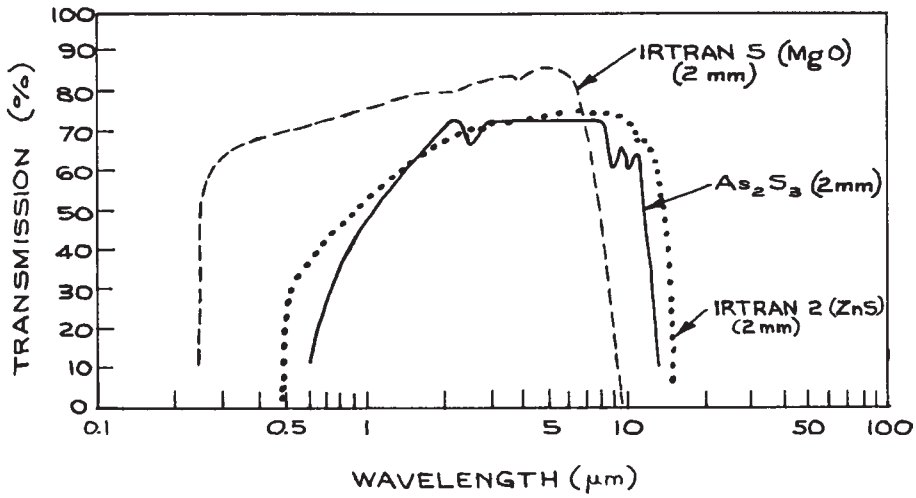

Figure 4.97 Transmission curves for Irtran 2 (ZnS), Irtran 5 (MgO), and As_2S_3 windows of specified thicknesses.

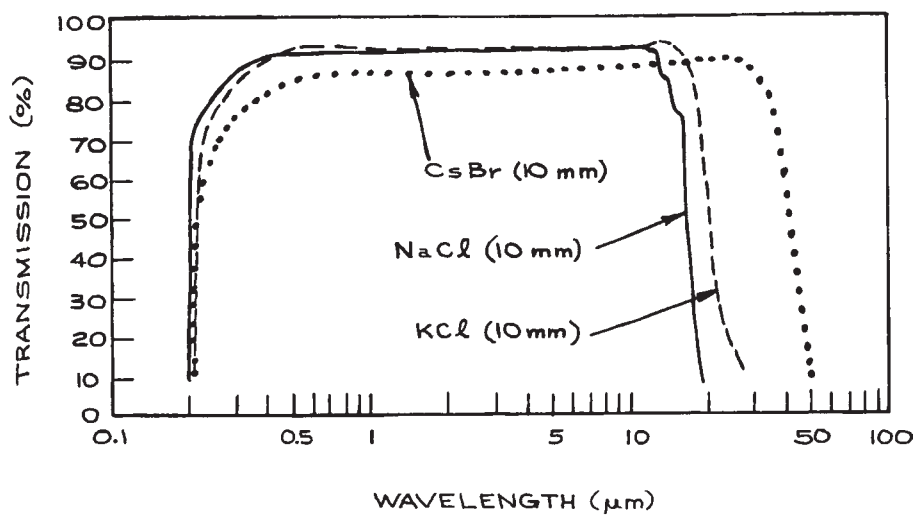

Figure 4.98 Transmission curves for cesium bromide, potassium chloride, and sodium chloride windows of specified thickness.

Two simple ways of doing this are to mount a small tungsten-filament bulb near the window, or to run a heated wire around the periphery of small windows. High-precision sodium chloride windows are in widespread use as Brewster windows in high-energy, pulsed CO_2 laser systems.

(ii) Potassium chloride. Potassium chloride (KCI, Figure 4.98) is very similar to sodium chloride. It is also an excellent material for use as a Brewster window in pulsed CO_2 lasers, as its transmission at 10.6 μm is slightly greater than that of sodium chloride.

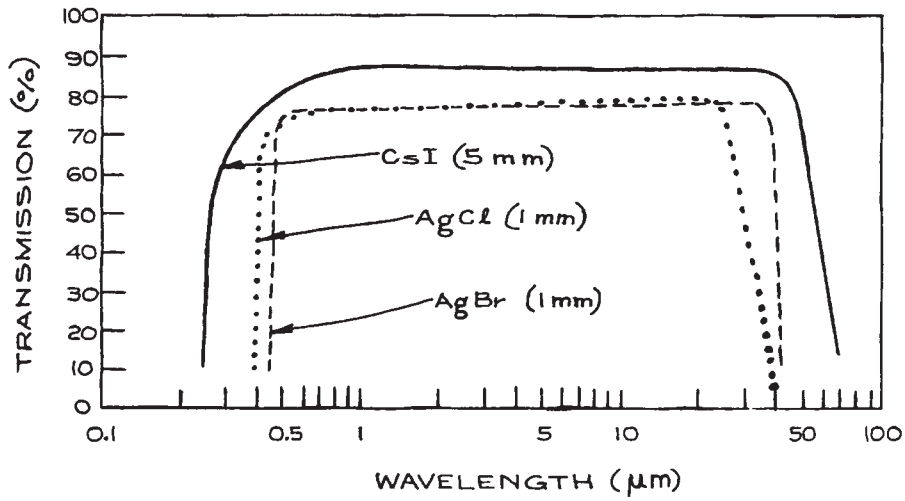

Figure 4.99 Transmission curves for cesium iodide, silver bromide, and silver chloride windows of specified thicknesses.

(iii) Cesium bromide. Cesium bromide (CsBr, Figure 4.98) is soft and extremely soluble in water, but has useful transmission to beyond 40 μm. It will suffer surface damage if the relative humidity exceeds 35%.

(iv) Cesium iodide. Cesium iodide (CsI, Figure 4.99) is used for both infrared prisms and windows; it is similar to CsBr, but its useful transmission extends beyond 60 μm.

(v) Thallium bromoiodide (KRS-5). Thallium bromoiodide (Figure 4.100), widely known as KRS-5, is an important material because of its wide transmission range in the infrared – from 600 nm to beyond 40 μm for a 5-mm thickness – and its low solubility in water. KRS-5 will survive atmospheric exposure for long periods of time and can even be used in liquid cells in direct contact with aqueous solutions. Its refractive index is high: reflection losses at 30 μm are 30% and it has a tendency to cold-flow. KRS-5 lenses are available from Almaz Optics, Infrared Optical Products, ISP Optics, and Janos Technology.

(vi) Zinc selenide. Chemical-vapor-deposited zinc selenide (ZnSe, Figure 4.100) is used widely in infrared-laser applications. It is transmissive from 500 nm to 22 μm. Zinc selenide is hard enough that it can be cleaned easily. It is resistant to atmospheric moisture and can be fabricated into precision windows and lenses. Its transmissive qualities in the visible (it is orange-yellow in color) makes the alignment of infrared systems using it much more convenient than in systems using germanium, silicon, or gallium arsenide. Irtran 4 is a polycrystalline form of zinc selenide originally developed by

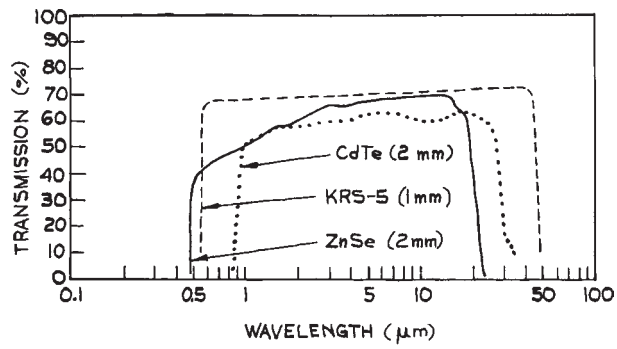

Figure 4.100 Transmission curves for zinc selenide, cadmium telluride, and KRS-5 windows of specified thicknesses.

Kodak, which is available from Harrick Scientific and Perkin Elmer.

(vii) Plastic films. Several polymer materials are sold commercially in film form, including polyethylene (Polythene, Polyphane, Poly-Fresh, Dinethene, etc.), polyvinylidene chloride copolymer (Saran Wrap), polythylene terephthalate (Mylar, Melinex, Scotchpar), and polycarbonate (Lexan). These plastic materials can be used to wrap hygroscopic crystalline optical components to protect them from atmospheric moisture. If the film is wrapped tightly, it will not substantially affect the optical quality of the wrapped components in the infrared. Care should be taken to use a polymer film that transmits the wavelength for which the protected component is to be used. For example, several commercial plastic food wraps can be used to wrap NaCI or KCI windows for use in CO_2-laser applications. Not all will prove satisfactory, however, and a particular plastic film should be tested for transmission before use. A note of caution: plastic films contain plasticizers, the vapor from which may be a problem.

(viii) Plastics and other materials for far-infrared use. Plastics are widely used for windows, beamsplitters, and light guides in the far-infrared. A Mylar film is widely used as the beam-splitting element in far-infrared Michelson interferometers, and polyethylene, polystyrene, nylon, and Teflon are used as windows in far-infrared spectrometers and lasers. Black polyethylene excludes visible and near-infrared radiation, but transmits far-infrared. Lenses and stacked-sheet polarizers for far-infrared use can be made from polyethylene. Several crystalline and semiconducting materials, although they absorb in the middle infrared, begin to transmit again in the far infrared. A 1 mm thick quartz window has 70% transmission at 100 μm and more than 90% transmission from 300 to 1000 μm. The alkali and alkaline-earth halides such as NaF, LiF, KBr, KCI, NaCl, CaF_2, SrF_2, and BaF_2 show increasing transmission for wavelengths above a critical value that varies from one crystal to another but is in the 200–400 μm range. Further details of the specialized area of far-infrared materials and instrumentation are available in the literature.[55–57]

Semiconductor Materials. Several of the most valuable infrared optical materials are semiconductors. In very pure form these materials should be transmissive to all infrared radiation with wavelengths longer than that corresponding to the band gap. In practice the long-wavelength transmission will be governed by the presence of impurities – a fact that is put to good use in the construction of infrared detectors. Semiconductors make very convenient "cold mirrors," as they reflect visible radiation quite well but do not transmit it.

(i) Silicon. Silicon (Si, Figure 4.101) is a hard, chemically resistant material that transmits wavelengths beyond about 1.1 μm. It does, however, show some absorption near 9 μm, so it is not suitable for CO_2-laser windows. It has a high refractive index (the reflection loss for two surfaces is 46% at 10 μm), but can be antireflection-coated. Because of its high refractive index it should always be highly polished to reduce surface scattering. Silicon has a high thermal conductivity and a low thermal expansion coefficient, and it is resistant to mechanical and thermal shock. Silicon mirrors can therefore handle substantial infrared-laser power densities. Silicon lenses are available from II-VI Infrared, ISP Optics, Lambda Research Optics, Laser Research Optics, Meller Optics, and V.A. Optical.

(ii) Germanium. Germanium (Ge, Figure 4.101) transmits beyond about 1.85 μm. Very pure samples can be transparent into the microwave region. It is somewhat brittle, but is still one of the most widely used window and lens materials in infrared-laser applications. It is chemically inert and can be fabricated to high precision. Germanium

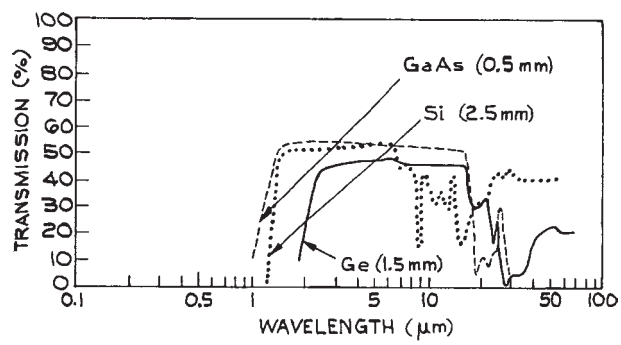

Figure 4.101 Transmission curves for the semiconductor materials germanium, gallium arsenide, and silicon.

has good thermal conductivity and a low coefficient of thermal expansion; it can be soldered to metal. In use, its temperature should be kept below 40 °C, as it exhibits thermal runaway – its absorption increases with increasing temperature. A wide range of germanium lenses are available from Lambda Research Optical, Laser Research Optics, Meller Optics, Umicore, and V.A. Optical.

(iii) Gallium arsenide. Gallium arsenide (GaAs, Figure 4.101) transmits from 1 to 15 μm. It is a better, although more expensive, material than germanium, particularly in CO- and CO_2-laser applications. It is hard and chemically inert, and maintains a very good surface finish. It can handle large infrared power densities because it does not exhibit thermal runaway until it reaches 250 °C. It is also used for manufacturing infrared-laser electro-optic modulators. Gallium arsenide lenses are available from Infrared Optical Products ISP Optics, Lambda Research Optics, and REFLEX Analytical.

(iv) Cadmium telluride. Cadmium telluride (CdTe, Figure 4.100) is another excellent material for use between 1 and 15 μm. It is quite hard, chemically inert, and takes a good surface finish. It is also used for manufacturing infrared-laser electro-optic modulators. Irtran 6 is a polycrystalline form of cadmium telluride available from Kodak; it transmits to 31 μm. Cadmium telluride lenses are available from ISP Optics and REFLEX Analytical.

(v) Tellurium. Tellurium is a soft material that is transparent from 3.3 μm to beyond 11 μm. It is not affected by water. Its properties are highly anisotropic; it can be used for second harmonic generation with CO_2-laser radiation. Tellurium should not be handled, as it is toxic and can be absorbed through the skin.

4.4.2 Materials for Mirrors and Diffraction Gratings

Metal Mirrors. The best mirrors for general broadband use have pure metallic layers, vacuum-deposited or electrolytically deposited on glass, fused-silica, or metal substrates. The best metals for use in such reflective coatings are aluminum, silver, gold, and rhodium. Solid metal mirrors with highly polished surfaces made of metals such as stainless steel, copper, zirconium-copper, and molybdenum are also excellent, particularly in the infrared. The reflectance of a good evaporated metal coating exceeds that of the bulk metal. Flat solid-metal mirrors can be made fairly cheaply by machining the mirror blank, surface-grinding it, and finally polishing the surface. If precision polishing facilities are not available, there are numerous optical component suppliers who will undertake the polishing of such surface-ground blanks to flatnesses as good as $\lambda/10$ in the visible. Finished flat and spherical solid-metal mirrors are available from II-VI Infrared, OptiForms, Space Optics Research Labs (SORL), and Spawr. Solid-metal mirrors are most valuable for handling high-power infrared laser beams when metal-coated mirrors cannot withstand the power dissipation in the slightly absorbing mirror surface. Water-cooled copper mirrors for handling very intense infrared laser beams are available from Spawr and Umicore Laser Optics Ltd.

The spectral reflectances in normal incidence of several common metal coatings are compared in Figure 4.102. Several points are worthy of note. Gold and copper are not good for use as reflectors in the visible region. Unprotected gold, silver, copper, and aluminum are very soft. Aluminum rapidly acquires a protective layer of oxide after deposition; this significantly reduces the reflectance in the vacuum ultraviolet and contributes to increased scattering throughout the spectrum. Aluminum and gold are frequently supplied commercially with a thin protective dielectric layer, which increases their resistance to abrasion without significantly affecting their reflectance, and also protects the aluminum from oxidation. The protective layer is usually a $\lambda/2$ layer (at 550 nm) of SiO for aluminum mirrors used in the visible region of the spectrum. Aluminum coated with a thin layer of MgF_2 can be used as a reflector in the vacuum ultraviolet, although the reflectance is substantially reduced below about 100 nm, as shown in Figure 4.103. Many optical instruments operating in the vacuum ultraviolet, including some spectrographs, have at least one reflective component. Above 100 nm, coated aluminum is almost always used for this reflector. Below 100 nm, platinum and indium have superior reflectance to aluminum. At very short wavelengths, below about 40 nm, the reflectance of platinum in normal incidence is down to

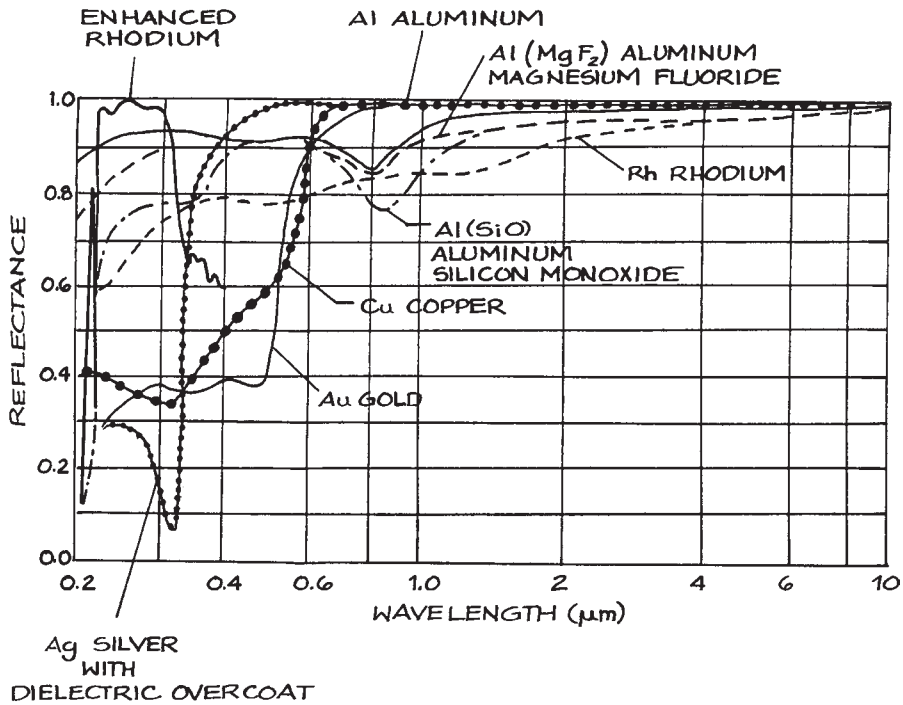

Figure 4.102 Reflectance of freshly deposited films of aluminum, copper, gold, rhodium, and coated silver, aluminum and rhodium as a function of wavelength from 0.2 to 10 μm.

only 10%, as shown in Figure 4.103. Therefore, reflective components in this wavelength region are generally used at grazing incidence, as the reflectance under these conditions can remain high. For example, at 0.832 nm the reflectance of an aluminum film at a grazing angle of 0.5° is above 90%.

Freshly evaporated silver has the highest reflectance of any metal in the visible; however, it tarnishes so rapidly that it is rarely used except on internal reflection surfaces. In this case the external surface is protected with a layer of Inconel or copper and a coat of paint.

Multilayer Dielectric Coatings. Extremely high-reflectance mirrors (up to 99.99%) can be made by using multilayer dielectric films involving alternate high- and low-refractive-index layers, ranging around $\lambda/4$ thick, deposited on glass, metal, or semiconductor substrates. The layers are made from materials that are transparent in the wavelength region where high reflectance is required. Both narrow-band and broad-band reflective-coated mirrors are available commercially. Figure 4.34(a) shows an example of each. Multilayer or single-layer dielectric-coated mirrors having almost any desired reflectance at wavelengths from 150 nm to 20 μm are also commercially available.[31]

Substrates for Mirrors. The main factors influencing the choice of substrate for a mirror are: (1) the dimensional stability required; (2) thermal dissipation; (3) mechanical considerations such as size and weight; and (4) cost. Glass is an excellent substrate for most totally reflective mirror applications throughout the spectrum, except where high thermal dissipation is necessary. Glass is inexpensive and strong, and takes a surface finish as good as $\lambda/200$ in the

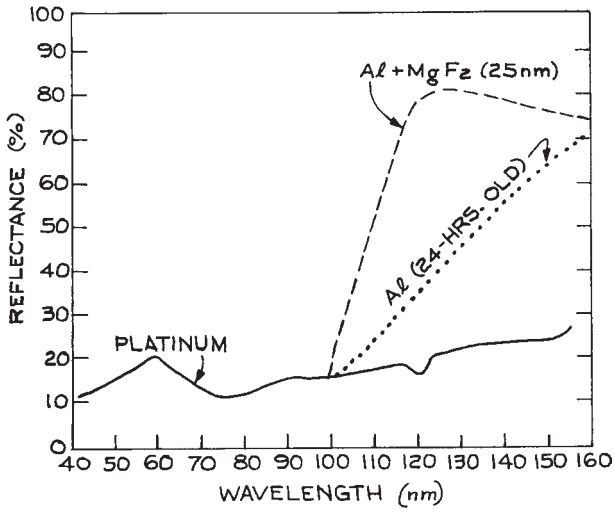

Figure 4.103 Normal-incidence reflectance of platinum, aluminum with a 25 nm thick overcoat of MgF_2, and unprotected aluminum 24 hours after film deposition.

visible. Fused silica and certain ceramic materials such as *Zerodur* (available from Schott Glass) are superior, but more expensive, alternatives to glass when greater dimensional stability and a lower coefficient of thermal expansion (CTE) are required. Fused silica has the lowest CTE, ~5 $\times$ 10^{-7}/K of any readily available material. The ceramic Zerodur has a CTE that can be 10 times smaller. The alloy Superinvar has a CTE similar to quartz, but generally over a restricted temperature range. Machining or polishing of low CTE materials can produce stresses in them and increase their expansion coefficients. Metal mirrors are frequently used when a very high light flux must be reflected, but even the small absorption loss in the reflecting surface necessitates cooling of the substrate. Metals are, however, not so dimensionally stable as glasses or ceramics, and their use as mirrors should be avoided in precision applications, particularly in the visible or ultraviolet.

Partially reflecting, partially transmitting mirrors are used in many optical systems, such as interferometers and lasers. In this application the substrate for the mirror has to transmit in the spectral region being handled. The substrate material should possess the usually desirable properties of hardness and dimensional stability, plus the ability to be coated. For example, germanium, silicon, and gallium arsenide are frequently used as partially transmitting mirror substrates in the near infrared. Only the least expensive partially reflecting mirrors use thin metal coatings. Such coatings are absorbing, and multilayer, dielectric-coated reflective surfaces are much to be preferred.

There are numerous suppliers of totally and partially reflecting mirrors.[31] The experimentalist need only determine the requirements and specify the mirror appropriately.

Mirrors that reflect visible radiation and transmit infrared *(cold mirrors)* or transmit visible radiation and reflect infrared *(hot mirrors)* are available as standard items from several suppliers.[31]

Diffraction Gratings. Diffraction gratings are generally ruled on glass, which may then be coated with aluminum or gold for visible or infrared reflective use, respectively. Many commercial gratings are replicas made from a ruled master, although high-quality holographic gratings are available from several suppliers.[31] For high-power infrared-laser applications, gold-coated replica gratings are unsatisfactory and master gratings ruled on copper should be used. Such gratings are available from Diffraction Products, Jobin-Yvon, and Richardson Grating Laboratory (through Newport).

4.5 OPTICAL SOURCES

Optical sources fall into two categories: *incoherent sources* such as mercury or xenon arc, tungsten filament, and sodium lamps; and *coherent sources* (lasers). There are many different types of laser, of which some exhibit a high degree of coherence and others are not significantly more coherent than a line source, such as a low-pressure mercury lamp.

Incoherent sources fall into two broad categories: *line sources* and *continuum sources*. Line sources emit most of their radiation at discrete wavelengths, which correspond to strong spectral emission features of the excited atom or ion that is the emitting species in the source. *Continuum sources* emit over some broad spectral region, although their radiant intensity varies with wavelength.

4.5.1 Coherence

There are two basic coherence properties of an optical source. One is a measure of its relative spectral purity. The other depends on the degree to which the wavefronts coming from the source are uniphase or of fixed spatial phase variation. A wavefront is said to be *uniphase* if it has the same phase at all points on the wavefront. The Gaussian TEM_{00} mode emitted by many lasers has this property.

The two types of coherence are illustrated by Figure 4.104. If the phases of the electromagnetic field at two points, *A* and *B*, longitudinally separated in the direction of propagation, have a fixed relationship, then the wave is said to be *temporally coherent* for times corresponding to the distance from *A* to *B*. The existence of such a fixed phase relationship could be demonstrated by combining waves extracted at points separated like *A* and *B* and producing an interference pattern. The Michelson interferometer (see Section 4.7.6) demonstrates the existence of such a fixed phase relationship. The maximum separation of *A* and *B* for which a fixed phase relationship exists is called the *coherence length* of the source l_c. The coherence length of a source is related to its *coherence time* τ_c by:

$$l_c = c\tau_c \tag{4.191}$$

Conceptually l_c is the average length of the uninterrupted wave trains from the source between random phase interruptions. Fourier theory demonstrates that the longer in time a sinusoidal wave train is observed, the narrower is its frequency spread. Thus the *spectral width* of a source can be related to its coherence time by writing:

$$\Delta\nu \simeq 1/\tau_c \tag{4.192}$$

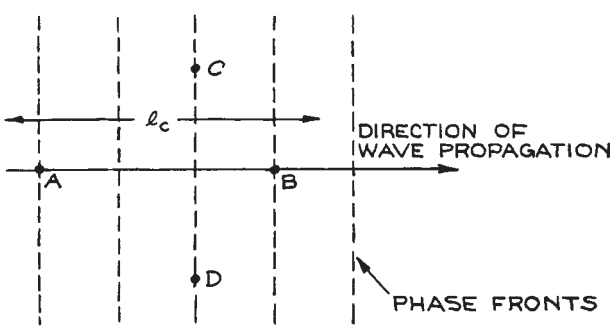

Figure 4.104 Temporal and spatial coherence.

The most coherent conventional lamp sources are stabilized low-pressure mercury lamps, which can have τ_c ranging up to about 10 ns. Lasers, however, can have τ_c ranging up to at least 1 ms.

Spatial coherence is a measure of phase relationships in the wavefront transverse to the direction of wave propagation. In Figure 4.104, if a fixed phase relationship exists between points *C* and *D* in the wavefront, the wave is said to be spatially coherent over this region. The *area of coherence* is a region of the wavefront within which all points have fixed phase relationships. Spatial coherence can be demonstrated by placing pinholes at different locations in the wavefront and observing interference fringes. Temporally incoherent sources can exhibit spatial coherence. Small sources (so-called point sources) fall into this category. The light from a star can be spatially coherent.

Extended, temporally incoherent sources have a low degree of spatial coherence because light coming from different parts of the source has different phases. Lasers emitting a TEM_{00} (fundamental) mode have very good spatial coherence over their whole beam diameter.

4.5.2 Radiometry: Units and Definitions

Radiometry deals with the measurement of amounts of light. In radiometric terms the characteristics of a light source can be specified in several ways.

Radiant power, *W*, measured in watts, is the total amount of energy emitted by a light source per second. The spectral variation of radiant power can be specified in terms of the radiant power density per unit wavelength interval, W_λ. Clearly:

$$W = \int_0^\infty W_\lambda \mathrm{d}\lambda \tag{4.193}$$

If a light source emits radiation only for some specific duration – which may be quite short in the case of a flashlamp – it is more useful to specify the source in terms of its *radiant energy output*, Q_e, measured in joules. If the source emits radiation for a time *T*, we can write:

$$Q_e = \int_0^T W(t)\mathrm{d}t \tag{4.194}$$

The amount of power emitted by a source in a particular direction per unit solid angle is called *radiant intensity* I_e, and is measured in watts per steradian. In general:

$$W = I_e(\omega)\mathrm{d}\omega \tag{4.195}$$

where the integral is taken over a closed surface surrounding the source. If I_e is the same in all directions, the source is said to be an isotropic radiator. At a distance r from such a source, if r is much greater than the dimensions of the source, the radiant flux crossing a small area ΔS is:

$$\phi_e = \frac{I_e \Delta S}{r^2} \tag{4.196}$$

The *irradiance* at this point, measured in W/m^2, is:

$$E_e = \frac{I_e}{r^2} \tag{4.197}$$

which is equal to the average value of the Poynting vector measured at the point. The radiant flux emitted per unit area of a surface (whether this be emitting or merely reflecting and scattering radiation) is called the *radiant emittance* M_e, and it is measured in W/m^2. For an extended source, the radiant flux emitted per unit solid angle per unit area of the source is called its *radiance* or *brightness* L_e:

$$L_e = \frac{\delta I_e}{\delta S_n} \tag{4.198}$$

where the area δS_n is the projection of the surface element of the source in the direction being considered. When the light emitted from a source or scattered from a surface has a radiance that is independent of viewing angle, the source or scatterer is called a perfectly diffuse or *Lambertian radiator*. Clearly, for such a source, the radiant intensity at an angle θ to the normal to the surface is:

$$I_e(\theta) = I_e(0)\cos\theta \tag{4.199}$$

as illustrated in Figure 4.105.

The total flux emitted per unit area of such a surface is its radiant emittance, which in this case is:

$$M_e = \pi I_e(0) \tag{4.200}$$

Illuminated diffusing surfaces made of finely ground glass or finely powered magnesium oxide will behave as Lambertian radiators.

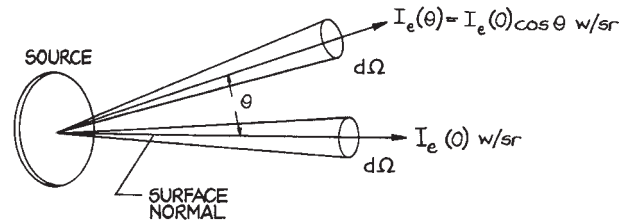

Figure 4.105 Radiant intensity characteristics of a Lambertian radiator.

For plane waves, since all the energy in the wave is transported in the same direction, the concepts of radiant intensity and emittance are not useful. It is customary to specify the radiant flux crossing unit area normal to the direction of propagation, and call this the *intensity* I of the plane wave. Because lasers emit radiation into an extremely small solid angle, they have very high radiant intensity, and it is once again more usual to refer simply to the *intensity* of the laser beam at a point as the energy flux per second per unit area. The total power output of a laser is:

$$W = \int_{\text{beam}} I\mathrm{d}S \tag{4.201}$$

4.5.3 Photometry

Photometry is the measurement of light that is in, or close to, the spectral region where the human eye responds. It is related to radiometry, but its units are weighted by the response of the human eye. The human eye provides a nonlinear and wavelength-dependent subjective impression of radiometric quantities. The response function of the human eye extends roughly from 360 to 700 nm, with a peak at 555 nm for the photopic (light-adapted) eye, where the *cones* are the dominant receptors. The dark-adapted human eye exhibits the *scotopic response*, which comes from the light- (but not color-) sensitive *rods* in the periphery of the retina. The photopic and scotopic response are shown in Figure 4.106. Measures in photometry take into account the so-called photopic spectral luminous efficiency function $V(\lambda)$. Thus, for example, in

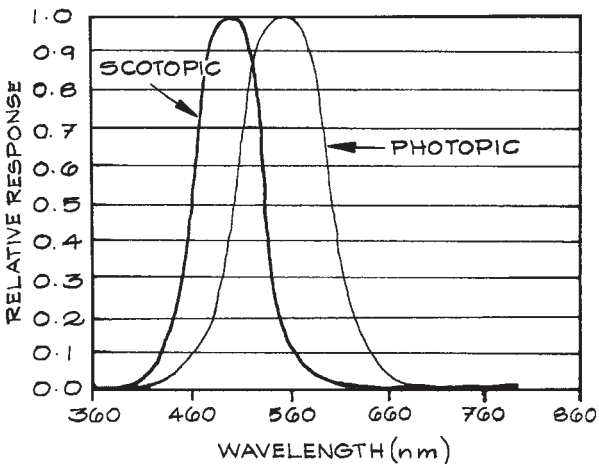

Figure 4.106 The photopic and scotopic spectral response of the human eye.

physiological photometry the *luminous flux F* is related to radiant flux $\phi_e(\lambda)$ by:

$$F = K\int_0^\infty V(\lambda)\phi_e(\lambda)\mathrm{d}\lambda \qquad (4.202)$$

where K is a constant. When F is measured in lumens and $\phi_e(\lambda)$ in watts, $K = 683$ lumen W^{-1}. In practice, the integral in Equation (4.202) need only be evaluated between 360 nm and 830 nm, as $V(\lambda)$ is zero outside this range. Other photometric quantities that may be encountered in specifications of light sources are as follows:

(1) The *luminous intensity* I_v measured as candela (Cd), where:

1 candela = 1 lumen per sr

This is the photometric equivalent of the radiometric quantity radiant intensity. The formal scientific specification of the candela is that it is the luminous intensity, in a given direction, of a source that emits monochromatic radiation of wavelength 550 nm and that has a radiant intensity in that direction of 1/683 watt per steradian.

(2) The *illuminance*, E_v measured in lumen/m^2 ≡ lux; lumen/cm^2 ≡ phot; or lumen/ft^2 ≡ footcandle.

(3) The *luminance* or *brightness*, L_v measured in candela/m^2 ≡ nit; candela/cm^2 ≡ stilb; candela/π ft^2 ≡ footlambert; candela/π m^2 ≡ apostilb; or candela/π cm^2 lambert.

(4) The *luminous energy*, Q_v, measured in lumen seconds ≡ talbot. The correspondences between radiometric and photometric quantities are summarized in Table 4.6.

For a Lambertian source the luminance is independent of the observation direction. Photometric description of the characteristics of light sources should be avoided in strict scientific work, but some catalogs of light sources use photometric units to describe lamp performance. For further details of photometry, and other concepts, such as color in physiological optics, the reader should consult Levi[24] or Fry.[58]

Calibration standards and devices for radiometric and photometric calibration of light sources are available from Gamma Scientific, International Light, Optronic Laboratories, and UDT Instruments (formerly Graseby).

4.5.4 Line Sources

Line sources are used as wavelength standards for calibrating spectrometers and interferometers; as sources in atomic absorption spectrometers; in interferometric

Table 4.6 Correspondence between radiometric and photometric quantities

Radiometric Quantity	Radiometric Unit	Photometric Quantity	Photometric Unit
Radiant power	watt (W)	Power	lumen (lm)
Radiant emittance	Wm^{-2}	Illuminance	lumen m^{-2} = lux (lx)
Radiant intensity	W/sr	Luminous intensity	lumen/sr = candela (cd)
Radiance (Brightness)	$Wm^{-2}sr^{-1}$	Luminance (Brightness)	lm m^{-2} sr^{-1} = cd m^{-2} = nit
Radiant Energy	Joule	Luminous Energy	lm s ≡ talbot

arrangements for testing optical components, such as Twyman–Green interferometers (Section 4.7.6); in a few special cases for optically pumping solid-state and gas lasers; and for illumination.

The emission lines from a line source are not infinitely sharp. Their shape is governed by the actual conditions and physical processes occurring in the source. The variation of the radiant intensity with frequency across a line whose center frequency is ν_0 is described by its *lineshape function* $g(\nu, \nu_0)$, where:

$$\int_{-\infty}^{\infty} g(\nu,\nu_0)\mathrm{d}\nu = 1 \tag{4.203}$$

The extension of the lower limit of this integral to negative frequencies is done for formal theoretical reasons connected with Fourier theory and need not cause any practical problems, since for a sharp line the major contribution to the integral in Equation (4.203) comes from frequencies close to the center frequency ν_0. There are three main types of lineshape function:[59] Lorentzian, Gaussian, and Voigt.

The *Lorentzian lineshape* function is:

$$g_{\mathrm{L}}(\nu,\nu_0) = \frac{2}{\pi\Delta\nu}\frac{1}{1 + [(\nu - \nu_0)/\Delta\nu]^2} \tag{4.204}$$

where $\Delta\nu$ is the frequency spacing between the half-intensity points of the line (the full width at half maximum height, or FWHM). Spectral lines at long wavelengths (in the middle and far infrared) and lines emitted by heavy atoms at high pressures and/or low temperatures frequently show this type of lineshape.

The *Gaussian lineshape* function is:

$$g_{\mathrm{D}}(\nu,\nu_0) = \frac{2}{\Delta\nu_{\mathrm{D}}}\left(\frac{\ln 2}{\pi}\right)^{1/2}\exp\left\{-\left[2\frac{\nu - \nu_0}{\Delta\nu_{\mathrm{D}}}\right]^2 \ln 2\right\} \tag{4.205}$$

where $\Delta\nu_{\mathrm{D}}$ is the FWHM. Spectral calibration lamps are available from Avantes, Cathodeon, Gamma Scientific, Heraus Nobleight, Newport/Oriel, Ocean Optics, Spectral Products, and Resonance. Gaussian lineshapes are usually associated with visible and near-infrared lines emitted by light atoms in discharge-tube sources at moderate pressures. In this case, the broadening comes from the varying Doppler shifts of emitting species, whose velocity distribution in the gas is Maxwellian. Emitting ions in real crystals sometimes have this type of lineshape because of the random variations of ion environment within a real crystal produced by dislocations, impurities, and other lattice defects. A Lorentzian and a Gaussian lineshape are compared in Figure 4.107.

Frequently, the broadening processes responsible for Lorentzian and Gaussian broadening are simultaneously operative, in which case the resultant lineshape is a convolution of the two and is called a *Voigt profile*.[15]

The low-pressure mercury lamp is the most commonly used narrow-line source. These lamps actually operate with a mercury–argon or mercury–neon mixture. The principal lines from a mercury–argon lamp are listed in Table 4.7. Numerous other line sources are also available. In particular, hollow-cathode lamps emit the strongest spectral line of any desired element for use in atomic absorption spectrometry. Such lamps are available from Bulbtronics, GBC Scientific Equipment, Hamamatsu,

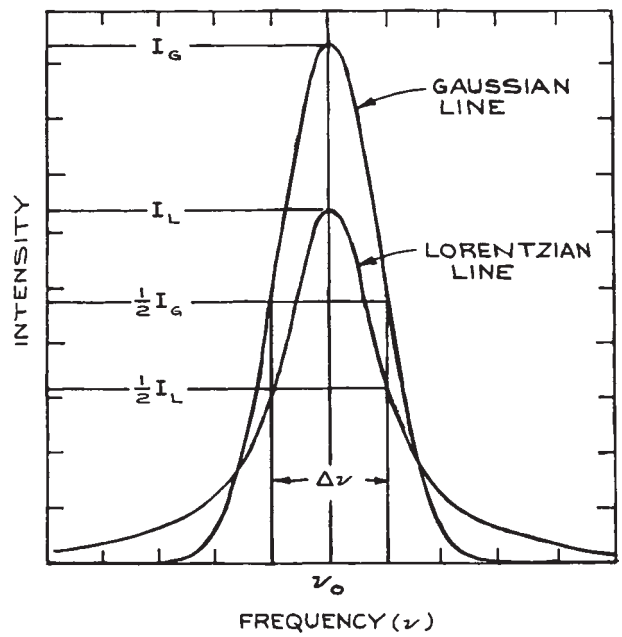

Figure 4.107 Gaussian and Lorentzian lineshapes of the same FWHM, $\Delta\nu$.

Table 4.7 Characteristic lines from a mercury lamp

Wavelength[a] (μm)
0.253652
0.313156
0.313184
0.365015
0.365483
0.366328
0.404656
0.435835
0.546074
0.576960
0.579066
0.69075
0.70820
0.77292
1.0140
1.1287
3.9425

Note: Extensive listings of calibration lines from other sources cab be found in C.R. Harrison *M.I.T. Wavelength Tables,* M.I.T. Press, Cambridge, Mass, 1969; and in A. R. Striganov and N. S. Sventitskii, *Tables of Spectral Lines of Neutral and Ionized Atoms,* IFT/Plenum Press, New York, 1968.

[a] *In vacuo*.

Hellma International, REFLEX Analytical, Semicon Associates, and Vitro Technology, Ltd.

4.5.5 Continuum Sources

A continuum source in conjunction with a monochromator can be used to obtain radiation whose wavelength is tunable throughout the emission range of the source. If the wavelength region transmitted by the monochromator is made very small, not very much energy will be available in the wavelength region selected. Even so, continuum sources find extensive use in this way in absorption and fluorescence spectrometers. Certain continuum sources, called blackbody sources, have very well-characterized radiance as a function of wavelength and are used for calibrating both the absolute sensitivity of detectors and the absolute radiance of other sources.

Blackbody Sources. All objects are continuously emitting and absorbing radiation. The fraction of incident radiation in a spectral band that is absorbed by an object is called its *absorbtivity.* When an object is in thermal equilibrium with its surroundings, it emits and absorbs radiation in any spectral interval at equal rates. An object that absorbs all radiation incident on it is called a *blackbody* – its absorbtivity α is equal to unity. The ability of a body to radiate energy in a particular spectral band compared to a blackbody is its *emissivity.* A blackbody is also the most efficient of all emitters – its emissivity ϵ is also unity. In general, for any object emitting and absorbing radiation at wavelength λ, $\epsilon_\lambda = \alpha_\lambda$. Highly reflecting, opaque objects, such as polished metal surfaces, do not absorb radiation efficiently; nor, when heated, do they emit radiation efficiently.

The simplest model of a blackbody source is a heated hollow object with a small hole in it. Any radiation entering the hole has minimal chance of re-emerging. Consequently, the radiation leaving the hole will be characteristic of the interior temperature of the object. The energy density distribution of this *blackbody radiation* in frequency is:

$$\rho(\nu) = \frac{8\pi h\nu^3}{c^3}\frac{1}{e^{h\nu/kT}-1} \tag{4.206}$$

where $\rho(\nu)d\nu$ is the energy stored (J/m^3) in a small frequency band $d\nu$ at ν. The energy density distribution in wavelength is:

$$\rho(\lambda) = \frac{8\pi hc}{\lambda^5}\frac{1}{e^{hc/\lambda kT}-1} \tag{4.207}$$

This translates into a spectral emittance (the total power emitted per unit wavelength interval into a solid angle 2π by unit area of the blackbody) given by:

$$M_{e\lambda} = \frac{C_1}{\lambda^5(e^{C_2/\lambda T}-1)} \tag{4.208}$$

where $C_1 = 2\pi hc^2$, called the *first radiation constant*, has the value 3.7418×10^{-16} Wm^2/s, and $C_2 = ch/k$, called the *second radiation constant*, has the value 1.43877×10^{-2} mK.

A true blackbody is also a diffuse (Lambertian) radiator. Its radiance is independent of the viewing angle. For such a source:

$$M_{e\lambda} = \pi L_{e\lambda} \tag{4.209}$$

The variation of $L_{e\lambda}$ with wavelength for various values of the temperature is shown in Figure 4.108. The wavelength of maximum emittance, λ_m at temperature T obeys Wien's displacement law:

$$\lambda_m T = 2.8978 \times 10^{-3}\ \text{m K} \tag{4.210}$$

The total radiant emittance of a blackbody at temperature T is:

$$M_e = \int_0^\infty M_{e\lambda} d\lambda = \frac{2\pi^5 k^4}{15c^2h^3} T^4 = \sigma T^4 \tag{4.211}$$

This is a statement of the Stefan–Boltzmann law. The coefficient σ, called the *Stefan–Boltzmann constant*, has a value of 5.6705×10^{-8} W m^{-2} K^{-4}. The known parameters $M_{e\lambda}$ and M_e of a blackbody allow it to be used as an absolute calibration source in radiometry. If a detector responds to photons, the spectral emittance in terms of photons, N_λ, may be useful:

$$N_\lambda = \frac{M_{e\lambda}}{hc/\lambda} \tag{4.212}$$

Curves of N_λ are given by Kruse, McGlauchlin, and McQuistan.[60]

A source whose spectral emittance is identical to that of a blackbody apart from a constant multiplicative factor is called a *graybody*. The constant of proportionality, ϵ, is its emissivity. Several continuum sources, such as tungsten-filament lamps, carbon arcs, and flashlamps, are approximately graybody emitters within certain wavelength regions.

Practical Blackbody Sources. The radiant emittance of a blackbody increases at all wavelengths as the temperature of the blackbody is raised, so a practical blackbody should, ideally, be a heated body with a small emitting aperture that is kept as small as possible. Kruse, McGlauchlin, and McQuistan[60] describe such a source, illustrated in Figure 4.109, that can be operated at

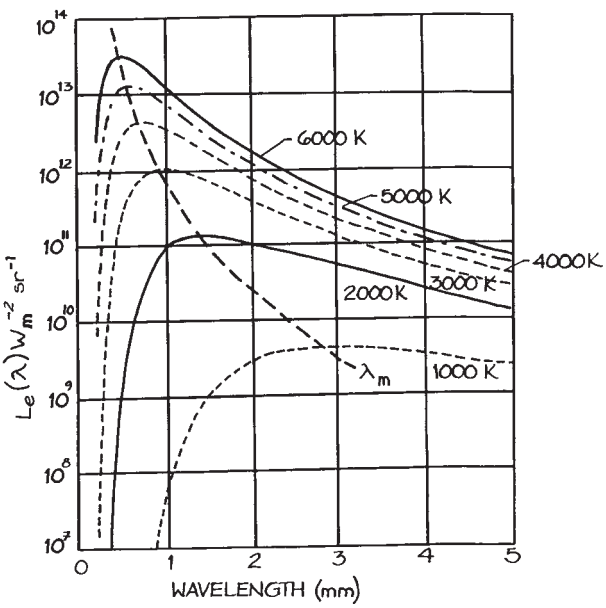

Figure 4.108 Spectral radiance $L_{e\lambda}$ of a blackbody source at various temperatures.

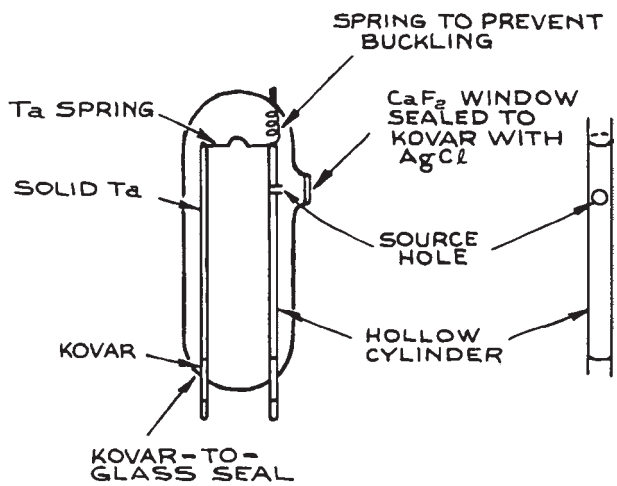

Figure 4.109 Construction details of a simple high-temperature blackbody source. (From P. W. Kruse, L. D. McGlauchlin, and R. B. McQuistan, *Elements of Infrared Technology: Generation, Transmission, and Detection*, John Wiley & Sons, Inc., New York, 1962; by permission of John Wiley & Sons, Inc.)

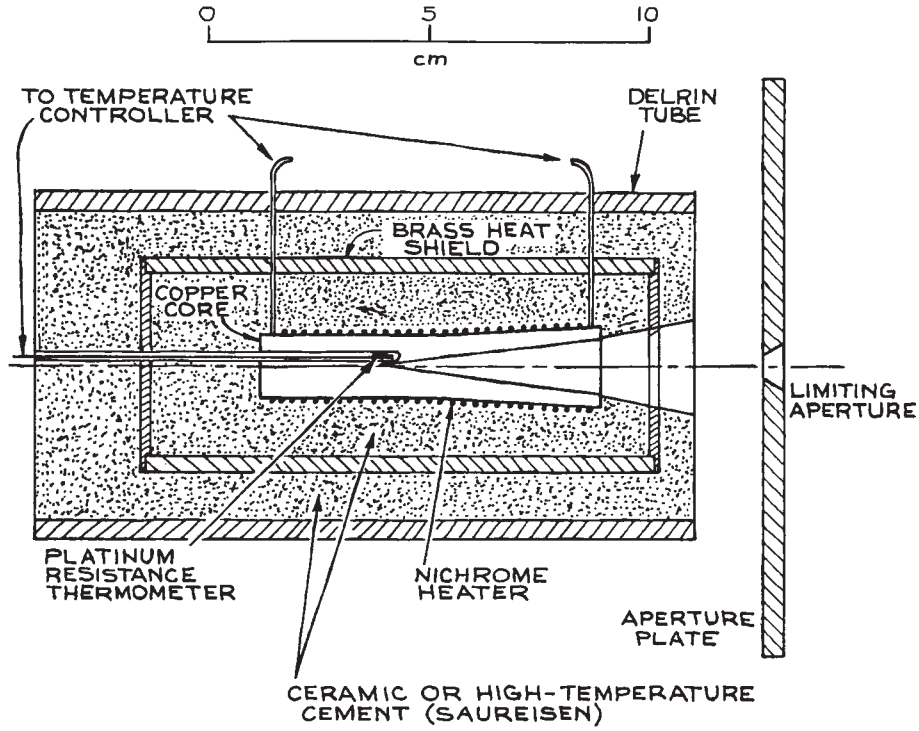

Figure 4.110 Construction details of an NBS-type blackbody source.

temperatures as high as 3000 K. A 25-μm-thick tungsten ribbon 2 cm wide is rolled on a 3-mm-diameter copper mandrel and seamed with a series of overlapping spot welds. A hole about 0.75 mm in diameter is made in the foil, and the copper dissolved out with nitric acid under a fume hood. The resulting cylinder is mounted on 1-mm-diameter Kovar or tungsten rod feedthroughs in a glass envelope and heated from a high-current, low-voltage power supply. The glass envelope should be fitted with a window that is transmissive to the wavelength region desired from the source.

Another design of blackbody source is shown in Figure 4.110. This design is based on a heated copper cylinder, containing a conical cavity of 15° semivertical angle, that is allowed to oxidize during operation (so that it becomes nonreflective and consequently of high emissivity). The cylinder is heated by an insulated heater wire wrapped around its circumference. If nichrome wire is used, the cylinder can be heated to about 1400 K. This assembly is mounted in a ceramic tube (alumina is quite satisfactory) or potted in high-temperature ceramic cement. For high-temperature operation, the whole assembly can be mounted inside a water-cooled block.

A popular blackbody source uses a ''Globar,'' a rod of bonded silicon carbide. In the high-temperature blackbody source supplied by Newport/Oriel this has been replaced by pyrolytic graphite. For further details of the advantages and disadvantages of this and various other blackbody sources, the reader is referred to Hudson.[61] Blackbody sources are available commercially from The Eppley Laboratory, HGH Optronics, Infrared Industries, Isotech, Micron, Omega, and Newport/Oriel.

Tungsten-Filament Lamps. Tungsten-filament lamps are approximately graybodies in the visible with an emittance between 0.45 and 0.5. Such lamps are

frequently described in terms of their *color temperature* T_c, which is the temperature at which a blackbody would have a spectral emittance closest in shape to the lamp's. The color temperature will depend on the operating conditions of the lamp.

Tungsten-filament lamps can most conveniently be operated in the laboratory with a variable transformer. For best stability and freedom from ripple on their output, however, they should be operated from a stabilized d.c. supply. Typical supply requirements range up to a few hundred volts. Lamps with wattage ratings up to 1 kW are readily available.

Small tungsten-filament lamps that can be used as point sources are available from Newport/Oriel. Very-long-life, constant-efficiency tungsten–halogen lamps are available, in which the lamp envelope usually contains a small amount of iodine. In operation, the iodine vaporizes and recombines with tungsten that has evaporated from the filament and deposited on the inside of the lamp envelope. The tungsten iodide thus formed diffuses to the hot filament, where it decomposes, redepositing tungsten on the filament. The constant replacement of the filament in this way allows it to be operated at very high temperature and radiant emittance. Because the lamp envelope must withstand the chemical action of hot iodine vapor and high temperatures, it is made of quartz. Hence such lamps are frequently called quartz–iodine lamps. Such lamps can be quite compact: a 1 kW lamp will have a filament length of about 1 cm. They are available from Bulb Direct and Ocean Optics. The National Institute of Standards and Technology (NIST) standard of spectral irradiance consists of a quartz–iodine lamp with a coiled-coil tungsten filament operating at about 3000 K and calibrated from 250 nm to 2.6 μm against a blackbody source. Such calibrated lamps are available from EG&G and Newport/Oriel. Because they are intense sources of radiant energy, these lamps can also be used for heating. In particular, they are often placed inside complex vacuum systems to bake out internal components that are well insulated thermally from the chamber walls.

Continuous Arc Lamps. High-current electrical discharges in gases, with currents that typically range from 1 to 100 A, can be intense sources of continuum or line emission, and sometimes both at the same time. For substantial continuum emission the most popular such lamps are the high-pressure xenon, high-pressure mercury, and high-pressure mercury–xenon lamps. The arc in these lamps typically ranges up to about 5 cm long and 6.2 mm in diameter (for a 10 kW lamp – 100 V, 100 A input). Because of their small size, arc lamps have much higher spectral radiance (brightness) than quartz–iodine lamps of comparable wattage. In the visible region at 500 nm, a typical xenon arc lamp shows 1.9 times the output of a quartz–iodine lamp; at 350 nm, 14 times; and at 250 nm, 200 times. In addition, because of their small size, high-pressure arc lamps work well in the illumination of monochromator slits in spectroscopic applications. Lower-wattage arc lamps come close to being point sources and are ideal for use in projection systems and for obtaining well-collimated beams.

There are two different kinds of high-pressure arc lamps: those where the discharge is confined to a narrow quartz capillary (which must be water-cooled), and those where the discharge is not confined (which usually operate with forced-air cooling). The former are available from Flashlamps (Verre et Quartz), ILC Technology, Xenon Corp., and Ushio and are used for pumping CW solid-state lasers. (Krypton arc lamps are better than xenon arc lamps for pumping Nd^{3+} lasers, as their emission is better matched to the absorption spectrum of Nd^{3+} ions.)

Because high-pressure arc lamps operate at very high pressures when hot (up to 200 bar), they must be housed in a rugged metal enclosure to contain a possible lamp explosion. The mounting must be such as to allow stress-free expansion during warmup. Generally speaking, commercial lamp assemblies should be used. The power-supply requirements are somewhat unusual. An initial high-voltage pulse is necessary to strike the arc, and then a lower voltage, typically in the range 70–120 V, to establish the arc. When the arc is fully established, the operating voltage will drop to perhaps as low as 10 V. Arcs containing mercury need a further increase in operating voltage as they warm up and their internal mercury pressure increases. Complete lamp assemblies and power supplies are available from several companies, among them, ILC Technology, Newport/Oriel, ORC Lighting Products, Perkin Elmer, and Spectral Energy.

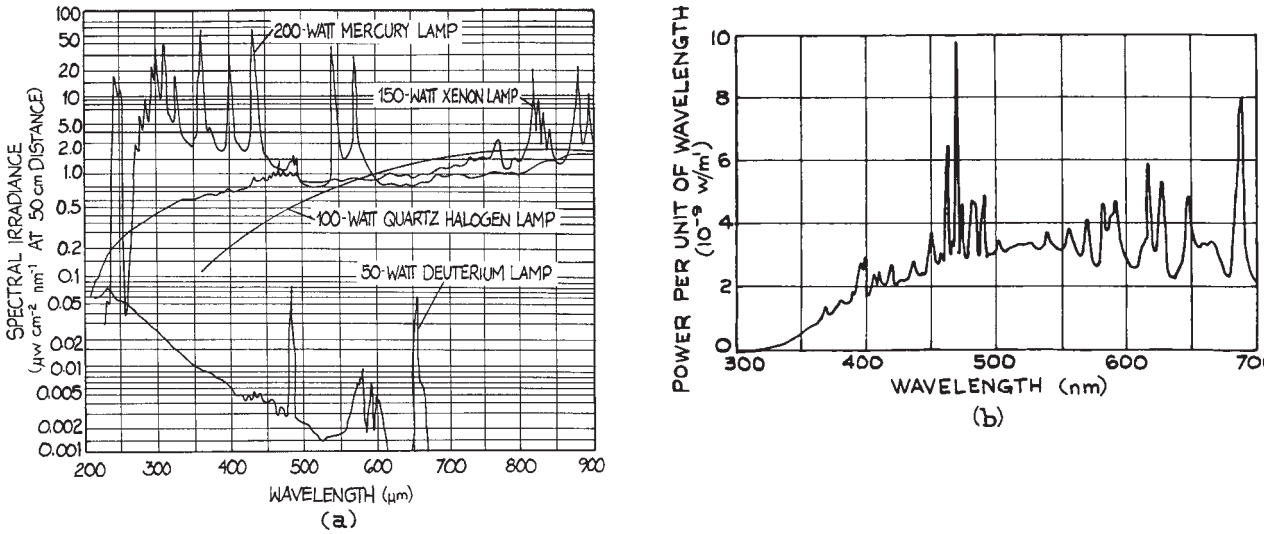

Figure 4.111 (a) Spectral irradiance of various moderate-power gas-discharge lamps (courtesy of Oriel Corporation, Stamford, Conn.); (b) spectral energy distribution for a high-power (10 kW) xenon arc lamp with a long discharge column (from A. A. Kruithof, "Modern Light Sources," in *Advanced Optical Techniques*, A. C. S. Van Heel, Ed., North-Holland, Amsterdam, 1967; by permission of North-Holland Publishing Company).

High-pressure arc lamps give substantial continuum emission with superimposed line structure, as can be seen in Figure 4.111. These lamps are not efficient sources of infrared radiation. They give substantial UV emission, however, and care should be taken in their use to avoid eye or skin exposure. Their UV output will also generate ozone, and provision should be made for venting this safely from the lamp housing. They are available from Bulbtronics, Hamamatsu, Laser Drive, Lighting Technologies International, and Newport/Oriel.

Deuterium lamps are efficient sources of ultraviolet emission with very little emission at longer wavelengths, as shown in Figure 4.111(a). They are available from Catheodeon, Hamamatsu, Newport/Oriel, Ocean Optics, and Spectral Energy. Hollow-cathode lamps, available from Hamamatsu and Hellma, emit stong spectral lines characteristic of the material of which their cathode is made. They can be used as wavelength calibration sources.

Discharges in high-pressure noble gases can also be used as intense continuum sources of vacuum-ultraviolet radiation. This radiation arises from noble-gas excimer emission, which in the case of helium, for example, arises from a series of processes that can be represented as:

$$\begin{aligned} \mathrm{He} + \mathrm{e} &\rightarrow \mathrm{He}^*, \\ \mathrm{He}^* + \mathrm{He} &\rightarrow \mathrm{He}_2^*, \\ \mathrm{He}_2^* &\rightarrow \mathrm{He} + \mathrm{He} + h\nu \end{aligned} \tag{4.213}$$

The spectral regions covered by the excimer continua are He, 105–400 nm; Ar, 107–165 nm; Kr, 124–185 nm; and Xe, 147–225 nm. Because there are no transmissive materials available for wavelengths below about 110 nm, sources below this wavelength are used without windows. Radiation leaves the lamp through a small slit, or through a multicapillary array. The latter is a close-packed array of many capillary tubes, which presents considerable resistance to the passage of gas, but is highly transparent to light. Multicapillary arrays can be obtained from Burle Electro-Optics. To maintain the lamp pressure, gas is continuously admitted. Gas that passes from the lamp into the rest of the experiment (for example a vacuum-ultraviolet monochromator) is continuously pumped away by a high-speed vacuum

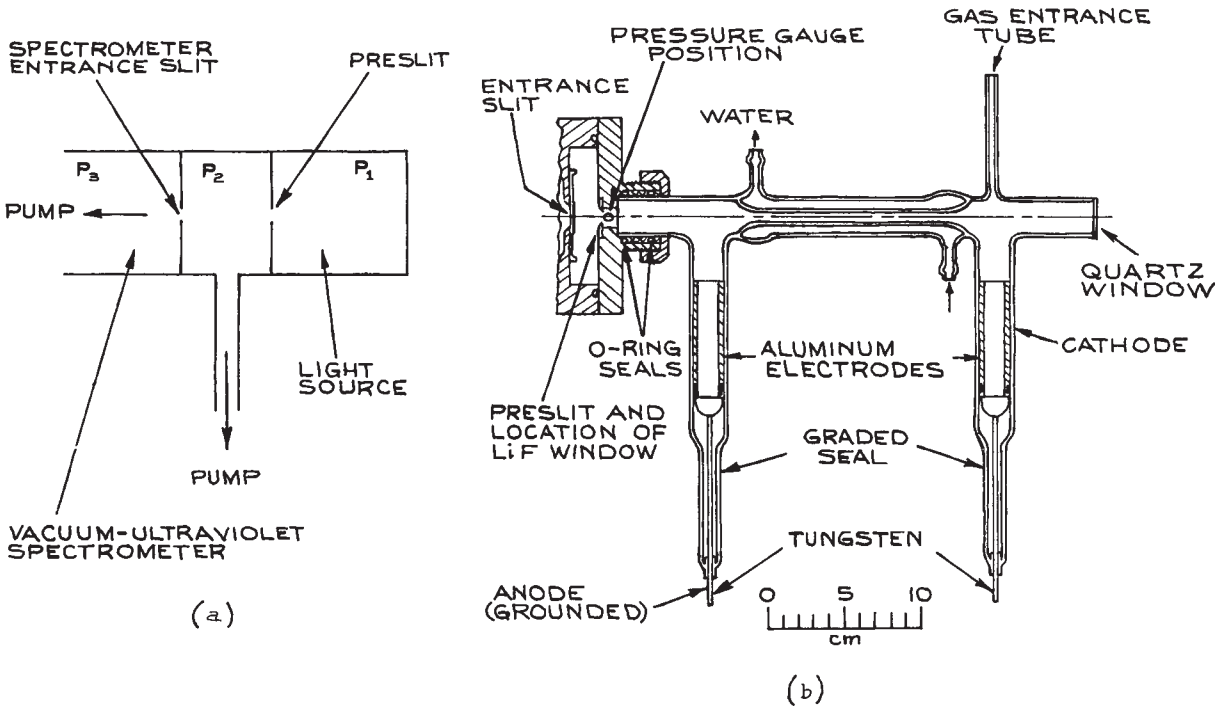

Figure 4.112 (a) Differential pumping arrangement (P_1, P_2, P_3 are the light source, differential pumping unit, and spectrometer operating pressures, respectively); (b) light source for the production of the noble-gas continua – in a differentially pumped mode, no LiF window would be used. (From R. E. Huffman, Y. Tanaka, and J. C. Larrabee, "Helium Continuum Light Source for Photoelectric Scanning in the 600–1100 Å Region," *Appl. Opt.*, **2,** 617–623, 1963; by permission of the Optical Society of America.)

pump, as shown in Figure 4.112. This technique is called *differential pumping* (see Section 3.6.2). For further details of vacuum-ultraviolet sources and technology, the reader is referred to Samson.[62]

Microwave Lamps. Small microwave-driven discharge lamps are very useful where a low-power atomic-emission line source is desired, particularly if the atomic emission is desired from some reactive species such as atomic chlorine or iodine. A small cylindrical quartz cell containing the material to be excited, usually with the addition of a buffer of helium or argon, is excited by a microwave source inside a small tunable microwave cavity, as shown in Figure 4.113. Suitable cavities for this purpose, designed for operation at 2450 MHz, are available from Opthos Instruments; power supplies for these lamps are available from Opthos and Cathodeon.

Flashlamps. The highest-brightness incoherent radiation is obtained from short-pulse flashlamps. By discharging a capacitor through a gas-discharge tube, much higher discharge currents and input powers are possible than in d.c. operation. As the current density or pressure of a flashlamp is increased, the emission from the lamp shifts from radiation that is characteristic of the fill gas, with lines superimposed on a continuum, to an increasingly close approximation to blackbody emission corresponding to the temperature of the discharge gas. Commercial flashlamps can be roughly divided into two categories. In long-pulse lamps, fairly large capacitors (100–10 000 μF),

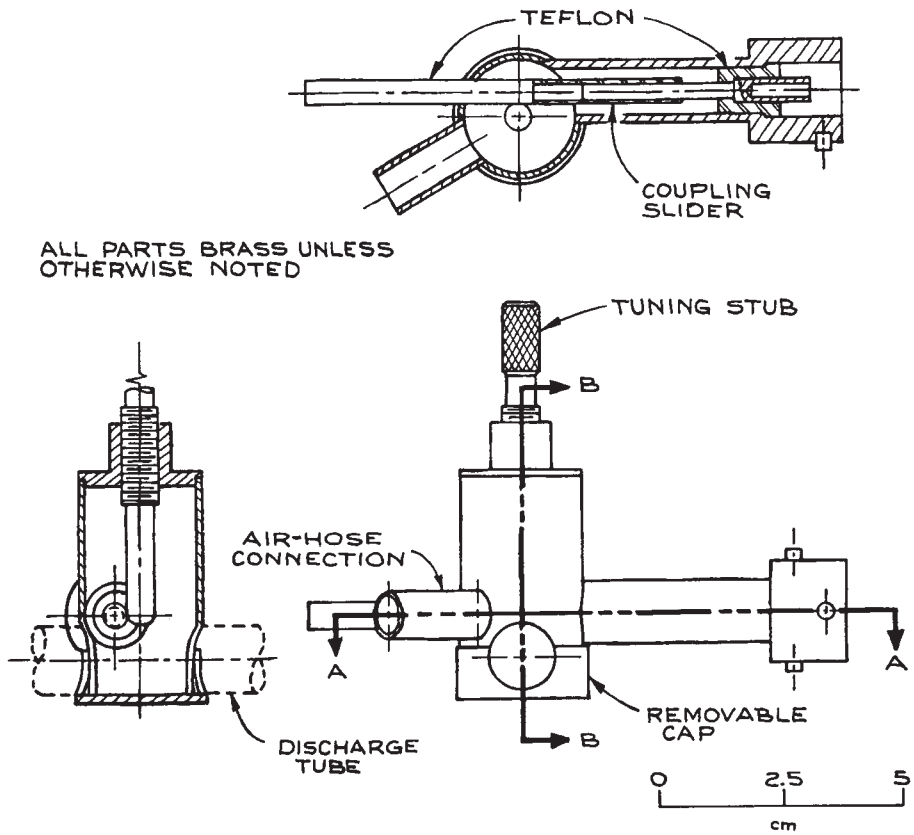

Figure 4.113 Microwave cavity for exciting a gas discharge in a cylindrical quartz tube (design used by Opthos). (After F. C. Fehsenfeld, K. M. Evenson, and H. P. Broida, "Microwave Discharge Cavities Operating at 2450 MHz," *Rev. Sci. Instr.*, **36,** 294–298, 1965; by permission of the American Institute of Physics.)

charged to moderately high voltages (typically up to about 5 kV), are discharged slowly (on time scales from 100 μs to 1 ms) through high-pressure discharge tubes. In short-pulse, high-peak-power lamps, smaller, low-inductance capacitors (typically 0.1–10 μF), charged to high voltages (10–80 kV), are discharged rapidly (on time scales down to 1 μs) through lower-pressure discharge tubes. Suppliers of linear flashlamps include Continuum, Laser SOS Group, New Source Technology, Perkin-Elmer Optoelectronics, and Xenon Corporation.

(i) Long-pulse lamps. Long-pulse lamps are generally filled with xenon,[63] but krypton lamps[64] (for pumping Nd^{3+} lasers) and alkali-metal lamps are also available. Fill pressures are typically on the order of 0.1–1 bar. Although the discharge current in such lamps can run to tens of thousands of A/cm^2, at low repetition frequencies (< 0.1 Hz) ambient cooling is all that is necessary. Three of the most commonly used circuits for operating such lamps are shown in Figure 4.114. In all three of these circuits, the capacitor, or pulse-forming network shown in Figure 4.114 (c), is charged through a resistor R. The capacitor is discharged through the lamp by triggering the flashlamp with one of the trigger circuits shown in Figure 4.115. The lamp itself behaves both resistively and inductively when it is fired. If the inductance and resistance of the lamp are not

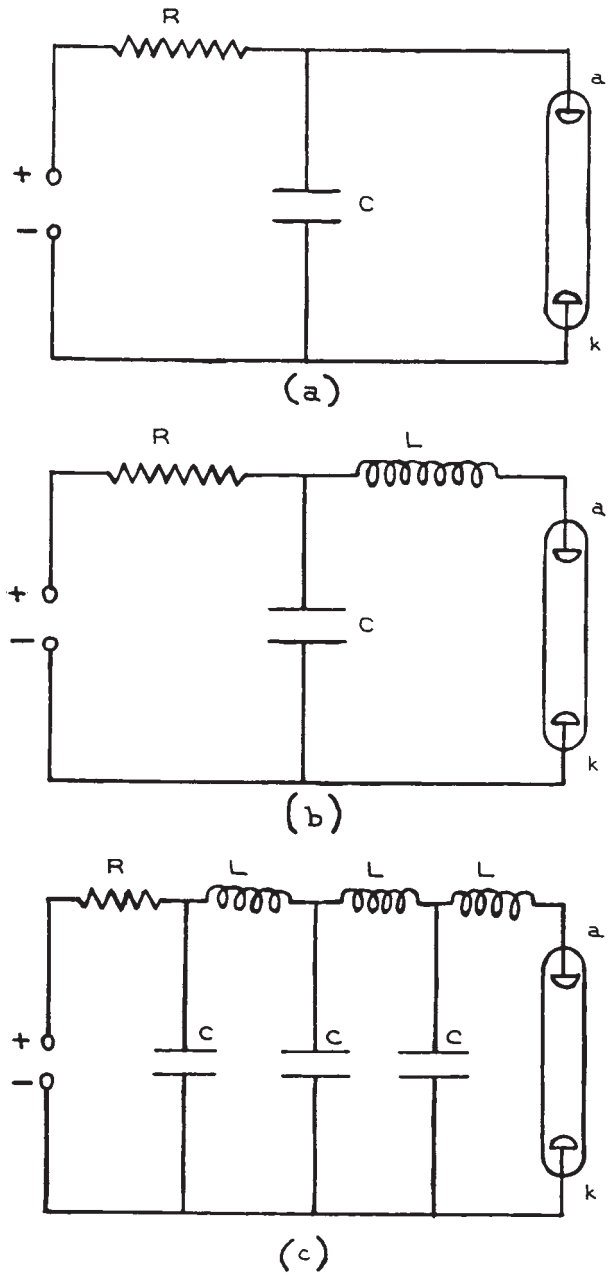

Figure 4.114 Operating circuits for flashlamps (a = lamp anode; k = lamp cathode): (a) RC discharge; (b) RLC critically damped discharge; (c) pulse-forming network.

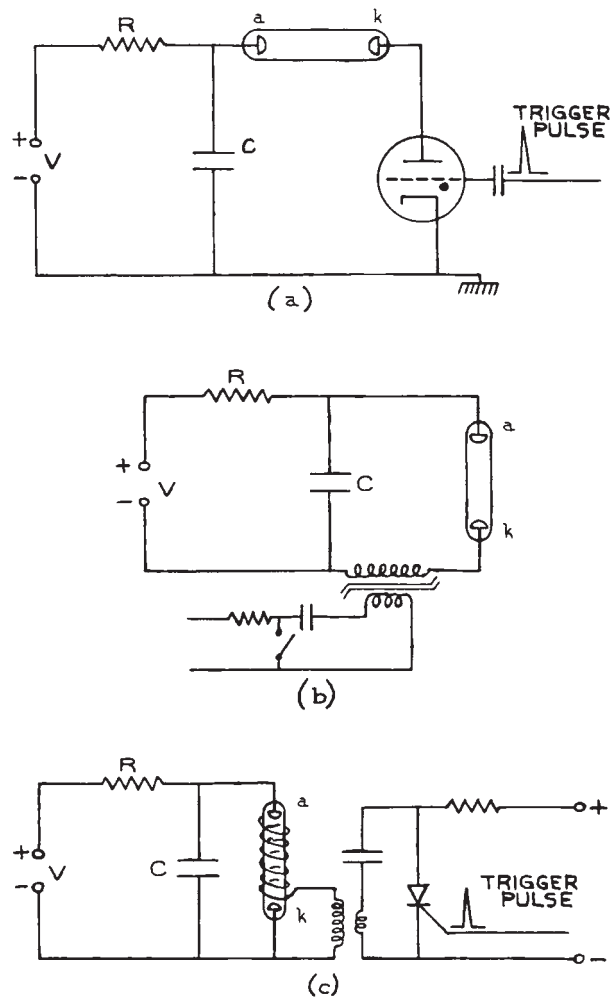

Figure 4.115 Flashlamp triggering schemes (a = lamp anode; k = lamp cathode): (a) overvoltage triggering (V > self-flash voltage of flashlamp; switching is accomplished in this case with a thyratron, but a triggered spark gap or ignitron can also be used); (b) series triggering (a saturable transformer is used with a fast-risetime 10–20 kV pulse with sufficient energy to trigger the lamp and saturate the core); (c) external triggering (the flashlamp is ionized by a trigger wire wrapped around the outside of the lamp and connected to the 5–15 kV secondary of a high-voltage pulse transformer).

sufficiently large, the capacitor may discharge too rapidly, which can lead to damage of both lamp and capacitor. Generally speaking, an additional series inductor will be desirable to control the discharge. The problem of selecting the appropriate inductor for a particular capacitor size and lamp has been dealt with in detail by Markiewicz and Emmett.[65] Slow flashlamps have a nonlinear V-I characteristic, which can be approximated by:

$$V = K_0\sqrt{|I|} \tag{4.214}$$

where the sign of V is taken to be the same as the sign of I. The value of K_0, measured in $\Omega A^{1/2}$, is a parameter specified by a manufacturer for a given lamp. Given this value and the capacitor size to be used, the calculations of Markiewicz and Emmett allow a suitable value of series inductor to be chosen. Other factors must be taken into account in designing the flashlamp circuit: the maximum power loading, usually specified as the explosion energy of the lamp (which will depend on the discharge-pulse duration), and the maximum repetition frequency of the lamp. Usually, the larger the capacitor-stored energy, the lower the permitted repetition frequency will be. As lamps and discharge energies get smaller, repetition frequencies can be extended, to several kilohertz for the smallest low-energy lamps, such as those used in stroboscopes. The explosion energy of the lamp is the minimum input required to cause lamp failure in one shot. To obtain long flashlamp life, a lamp should be operated only at a fraction of its explosion energy. For example, at 50% of the explosion energy the expected lifetime is from 100 to 1000 flashes, while at 20% it is from 10^5 to 10^6 flashes. The lamp should be mounted freely and not clamped rigidly at its ends when it is operated.

The spectral output of a flashlamp varies slightly during the flash. For moderate- and high-power lamps (> 100 J in 1 ms), the spectral output approaches that of a blackbody, as shown in Figures 4.116 and 4.117.[66] Low-power lamps exhibit the spectral feature of their fill gas, as shown in Figure 4.118. Figure 4.116 shows the transition from a spectrum with some line structure to a blackbody continuum as the current density through the lamp is increased.

A word about the triggering schemes shown in Figure 4.115. External triggering, accomplished by switching a high-voltage pulse from a transformer to a trigger wire wrapped around the lamp, is perhaps the simplest scheme; it is used only with long-pulse lamps and does not give quite so good time synchronization as series-spark-gap or thyratron-switched operation. The other methods are more complex, but can be also used with short-pulse, high-power lamps. Series triggering allows the incorporation of triggering and lamp series inductance in a single unit. Trigger transformers of various types are available from EG&G and ILC. EG&G and EEV supply a range of excellent thyratrons.

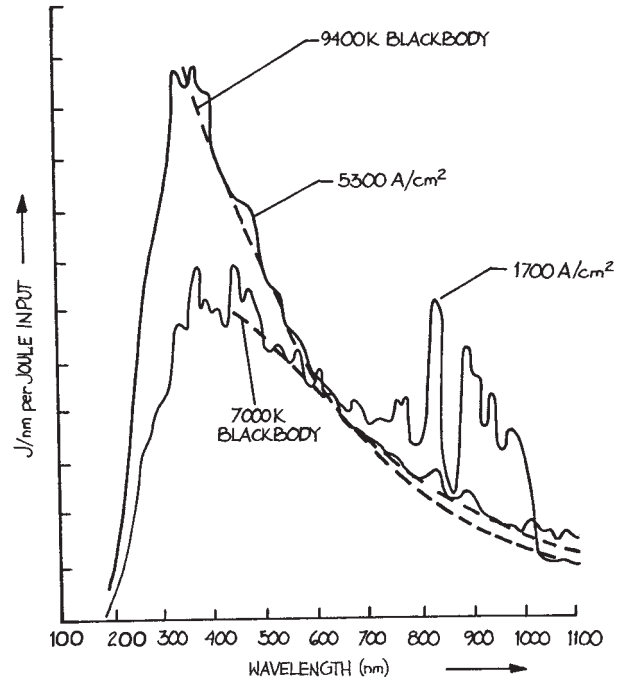

Figure 4.116 Output spectrum of a Perkin-Elmer FX-47A xenon flashlamp (0.4 atm) at two current densities: 1700A/cm^2 and 5300A/cm^2.

(ii) Short-pulse high-power lamps. Flashlamps that can handle the rapid discharge of hundreds of joules on timescales down to a few microseconds are available commercially from Flashlamps (Verre et Quartz), ILC Technology, Perkin Elmer, and Xenon Corporation, among others. To achieve such rapid discharges, these lamps are generally operated in a low-inductance discharge circuit. When these lamps are fired at high-peak-power inputs, a severe shock

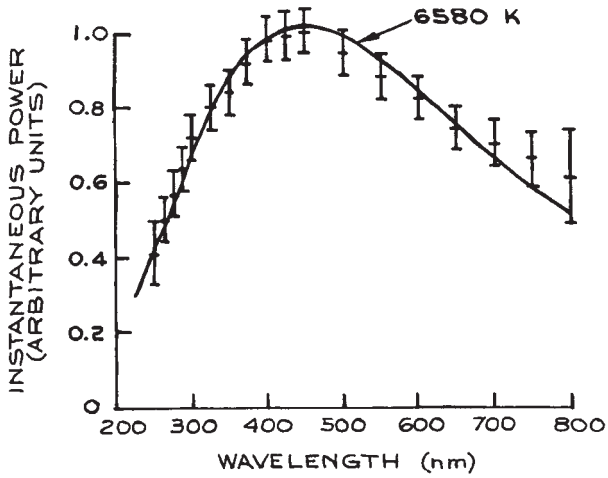

Figure 4.117 Spectral distribution of power radiated by an EG&G FX42 xenon-filled flashlamp (76 mm long by 7 mm bore) operated in a critically damped mode with 500 J discharged in 1 ms. The spectral distribution was observed 0.7 ms from flash initiation. The line is the blackbody radiation curve of best fit. (After J. G. Edwards, "Some Factors Affecting the Pumping Efficiency of Optically Pumped Lasers," *Appl. Opt.*, **6,** 837–843, 1967; by permission of the Optical Society of America.)

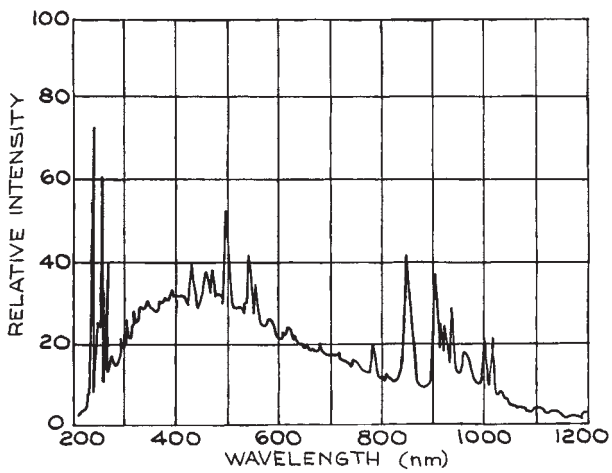

Figure 4.118 Spectral distribution of intensity from an ILC 4L2 xenon flashlamp (51 mm long by 4 mm bore) operated in a critically damped mode with 10 J discharged in 115 μs. (Courtesy of ILC).

wave is generated in the lamp. To withstand the shock wave, the lamps are designed with special re-entrant electrode seals. If lamps designed for long-pulse operation are discharged too rapidly, their electrodes are quite likely to break off because the electrode seals are not shock-resistant.

The spectral emission of short-pulse, high-energy lamps is generally quite close to that of a high-temperature blackbody, perhaps as hot as 30 000 K. The fill pressure in these lamps is often lower than in long-pulse lamps, typically from 0.1 to a few tens of millibars. The fill gas is usually xenon, but other noble gases such as krypton or argon can be used. If a short-pulse lamp has a narrow discharge-tube cross-section, at high power inputs material can ablate from the wall and a substantial part of the emission from the lamp can come from this material. Such lamps can be made with heavy-walled discharge-tube bodies of silica, glass, or even Plexiglas. These lamps can be made fairly simply. A good design described by Baker and King[67] is illustrated in Figure 4.119. It can be operated in a non-ablating or ablating mode (at high or low pressure, respectively). When operated in the ablating regime, such lamps can be filled with air as the nature of the fill gas is unimportant. Figure 4.119 also shows the use of a field-distortion-triggered spark gap for firing the lamp – a spark-gap design that offers quiet, efficient switching of rapid-discharge capacitors. Rapid-discharge (low-inductance) capacitors suitable for fast flashlamp and other applications are available from CSI Technologies, Hipotronics, and Maxwell Energy Products.

4.6 LASERS

Lasers are now so widely used in physics, chemistry, the life sciences, and engineering that they must be regarded as the experimentalist's most important type of optical source. With few exceptions, anyone who wants a laser for an experiment should buy one. This is certainly true in the case of helium–neon, argon–ion, and helium–cadmium gas lasers and all solid-state crystalline, glass, or semiconductor lasers. True, these lasers can be built in the laboratory, but this is the province of the laser specialist and will generally be found time-consuming and unproductive for scientists in other disciplines. On the other hand, there are some lasers, such as nitrogen, Exciplex,

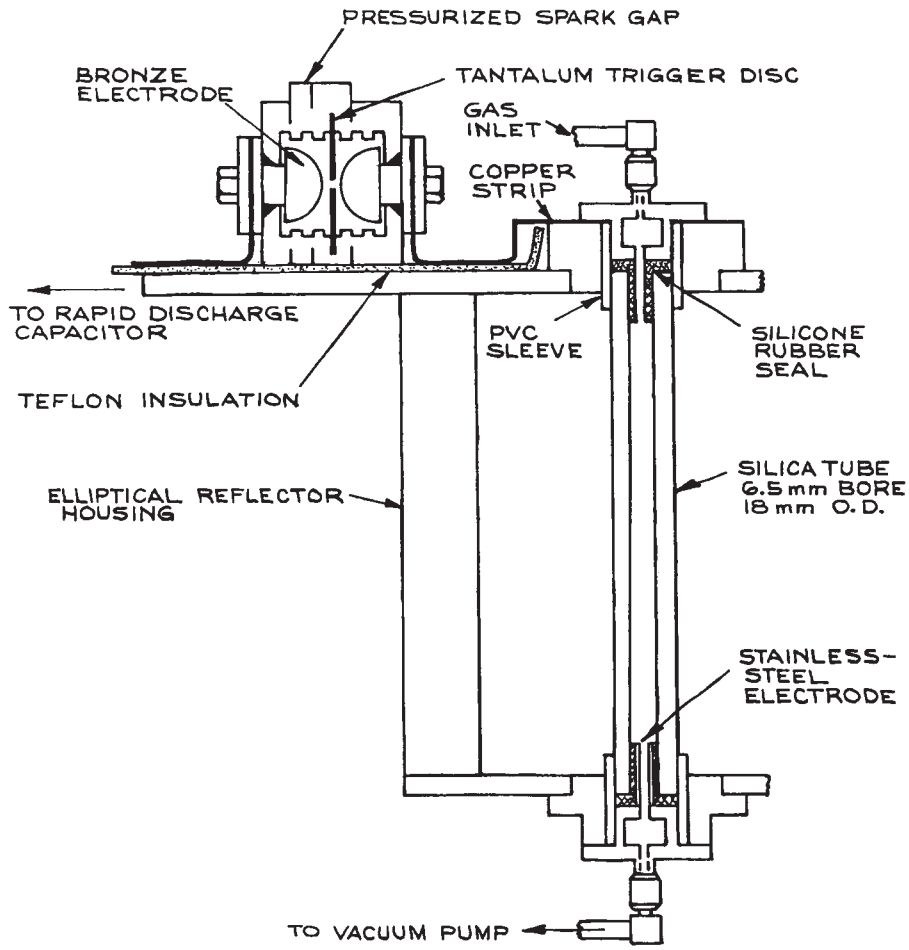

Figure 4.119 High-pulse-energy, fast flashlamp design for conventional or ablation-mode operation. (From H. J. Baker and T. A. King, "Optimization of Pulsed UV Radiation from Linear Flashtubes," *J. Phys. E.: Sci. Instr.*, **8,** 219–223, 1975. Copyright 1975 by the Institute of Physics, used with permission).

CO_2, and CO gas lasers, and dye lasers, that it might occasionally pay to build for oneself, even though models are available commercially. A detailed discussion of how to construct all these lasers will not be given here, but, to illustrate how it is accomplished, design features of some specific systems will be discussed.

Table 4.8 lists the primary wavelengths available from the more commonly used lasers presently available commercially. For more detailed information about suppliers and specifications consult a trade reference, such as the Laser Focus or Photonics Spectra Buyers Guides. Laser suppliers come and go, as does the availability of specific types of laser. Before briefly describing some of these laser systems, some background material will be presented that is pertinent to a discussion of lasers in general. More detailed information regarding the physics of laser operation is given in the books by Davis,[15] Silfvast,[68] Saleh and Teich,[69] Yariv,[14] and Siegman.[70]

Table 4.8 Wavelengths available from important lasers

CW Gas Lasers	
Type	Operating Wavelengths (nm)
Ar ion	229
	244[a]
	348[a]
	257[a]
	275[a]
	333.4
	333.6
	351.1[b]
	363.8[b]
	454.5
	457.9
	465.8
	476.5
	488.0[b]
	496.5
	50.17
	514.5[b]
	528.7
	1092.3
Kr ion	337.5
	350.7
	356.4
	406.7
	413.1
	461.9
	468.0
	476.2
	482.5
	530.9[b]
	568.1[b]
	647.0
	676.4
	752.5
	793.1
	799.3
He–Ne	543
	594.1
	612
	632.8[c]
	1152
	3392
	5400
	11552
He-Cd	325.0
	441.6
CO	5–6.5[d]
CO_2	9–11[d]
	10.6[e]

Table 4.8 *(cont.)*

Pulsed Gas Lasers	
Type	Operating Wavelengths (nm)
Excimer	
ArF	193.3
KrF	248.4–249.1
XeCl	307–308.43
XeF	348.8–354
Cu vapor	510.54 570 578.2
F_2	157
N_2	337.1
Type	Operating Wavelengths (μm)
CO_2	10.6 9–11
CW Solid-State Lasers	
Type	Operating Wavelengths (μm)
Alexandrite	365 0.370 0.730 0.760
Nd:YAG	266.8[f] 355[g] 0.532[h] 1.064 (This is the primary line, Nd:YLF gives 1.047 μm and 1.053 μm, Nd:YVO4 also gives 1064 nm) 1.318
Ti:Sapphire	0.7–1.02 Tunable
Pulsed Solid-State Lasers	
Type	Operating Wavelengths (μm)
Alexandrite	0.720–0.780 (tunable, can also provide 2nd, 3rd and 4th harmonic wavelengths)
Er:fiber lasers	1.2–2.0
Er:glass	1.534
Er:YAG	2.940
Er:glass	1.534
Ho:YAG	2.1
Nd:glass	0.266[f] 0.355[g] 0.532[h] 1.06[i]

Table 4.8 *(cont.)*

Pulsed Solid-State Lasers *(Cont.)*	
Type	Operating Wavelengths (μm)
Ti:Sapphire	0.68–1 Tunable
Nd:YAG	0.213[j] 0.265[f] 0.355[g] 0.53[h] 1.064
Ruby	0.6943
Ytterbium:glass	1.030

Diode-Pumped Solid-State Lasers	
Type	Operating Wavelengths (nm)
	266[f] 355[g] 460 473 488 515 532 670 1064 1030 1480 1535–1565

CW Tunable Dye Lasers
(pumped with ion lasers, frequency-doubled Nd:YAG lasers at 530nm, or frequency tripled Nd:YAG laser at 355 nm)
Tuning range (μm)
0.4–1.1 (The tuning range depends on the dye used. A typical dye provides 50–100 nm of tuning)

Pulsed Tunable Dye Lasers
Tuning Range (μm)
0.197–1.036

[a] Produced by second harmonic generation of blue-green argon ion laser lines.
[b] Strongest lines.
[c] Most readily available wavelength.
[d] Molecular lasers that offer discrete tunability over several lines.
[e] Strongest line. Industrial CO_2 lasers generally operate only at 10.6 μm.
[f] Frequency quadrupled from 1.06 μm output.
[g] Frequency tripled from 1.06 μm output.
[h] Frequency doubled from 1.06 μm output.
[i] Phosphate glass gives 1.05 μm. Nd:YLF gives 1.053 μm
[j] Fifth harmonic from1.06 μm output.

The lasers listed in the table fall into two categories: pulsed and CW (continuous wave). Many can be operated in both ways, with the exception of nitrogen, copper vapor, and excimer lasers, which can only operate in a pulsed mode. These three laser types are *self-terminating*: once they lase they destroy their own population inversion, and a period of time must elapse before the upper laser level can be re-excited.

For pulsed lasers, the available energy outputs per pulse can be classified as low (< 10 mJ) medium (10 mJ–1 J), high (1 J–100 J), and very high (> 100 J). Pulse lengths depend on the type of laser and its mode of operation. Almost all pulsed solid-state lasers operate in a *Q-switched* mode,[15] which typically provides a pulse length in the 10 ns range, but varies somewhat from manufacturer to manufacturer. Non Q-switched long-pulse (LP) solid-state lasers have pulse lengths > 0.1 ms. Solid-state and dye lasers are frequently operated in a mode-locked (ML) configuration, which provides pulse lengths in the 0.1–10 ps range. A given laser can often be operated in ML, Q, and LP modes. The energy output per pulse will decrease as LP > Q > ML.

Continuous wave lasers can be classified by output power as low (< 10 mW), medium (10 mW–1 W), high (1–10 W), very high (10–100 W), and industrial (> 100 W). Continuous wave gas lasers, in particular, provide power outputs at many different wavelengths, and the available power varies from line to line. These lasers are generally supplied to operate in a specific wavelength range with discrete tunability within that range. Ultraviolet gas lasers, for example, are equipped with special optics, so do not generally operate in the visible range as well.

The energy outputs available from pulsed lasers, together with their available pulse-repetition rates and pulse lengths, cover a very wide range. The highest available energy outputs are generally available only at the lowest pulse-repetition rates. In the case of CW lasers, available power outputs vary from line to line and from manufacturer to manufacturer. To the intended purchaser of a laser system, we recommend the following questions:

(1) What fixed wavelength or wavelengths must the laser supply?
(2) Is tunability required?
(3) What frequency and amplitude stability are required?
(4) What laser linewidth is required?
(5) What power or pulse energy is required?
(6) Are high operating reliability and long operating lifetime required?
(7) For time-resolved experiments, what pulse length is needed?
(8) Is the spatial profile of the output beam important?

The desirable attributes in each of these areas are unlikely to occur simultaneously. For example, frequency tunability is not readily available throughout the spectrum without resorting to the specialized techniques of nonlinear optics.[14,15,71–75]

In Table 4.8 the various categories of laser: CW gas, pulsed gas, CW solid-state, pulsed solid state, CW dye and pulsed dye frequently show tuning ranges and wavelengths that are obtained from these lasers by the use of nonlinear optics. For example, shorter wavelengths from argon ion, Nd:YAG, Ti:sapphire, and CO_2 can be obtained by frequency doubling (tripling or even quadrupling) by the use of a nonlinear crystal. The nonlinear crystal is generally external to the primary laser, although it may be housed in its own resonant structure. Generating second or third harmonic light from a sufficiently powerful laser is not especially difficult, although this is still a relatively specialized endeavor.

New frequency generation from a primary pump laser can also be obtained by the use of an optical paramatic oscillator (OPO). In such a device an appropriate nonlinear crystal is pumped with a frequency ν_p and in this process generates two new frequencies ν_s and ν_i, called the *signal* and *idler* frequencies, respectively. In this process photon energy must be conserved, so:

$$\nu_p = \nu_s + \nu_i \tag{4.215}$$

High-energy and high-power lasers are generally less stable, both in amplitude and in frequency, and will generally be less reliable and need more ‘‘hands on’’ attention than their low-energy or low-power counterparts. When a decision is made to purchase a laser system, compare the specifications of lasers supplied by different manufacturers; discuss the advantages and disadvantages of different systems with others who have purchased them previously. Reputable laser manufacturers are generally very willing to supply the names of previous purchasers.

To some experimental scientists a laser is merely a rather monochromatic directional lightbulb; for others, detailed knowledge of its operating principles and characteristics is essential. Certain aspects of laser designs and operating characteristics, however, are very general and are worthy of some discussion.

4.6.1 General Principles of Laser Operation

A laser is an optical-frequency oscillator: in common with electronic circuit oscillators, it consists of an amplifier with feedback. The optical-frequency amplifying part of a laser can be a gas, a crystalline or glassy solid, a liquid, or a semiconductor. This medium is maintained in an amplifying state, either continuously or on a pulsed basis, by pumping energy into it appropriately. In a gas laser the input energy comes from electrons (in a gas discharge or an electron beam), or from an optical pump (which may be a lamp or a laser). Solid-state crystalline or glassy lasers receive their pumping energy from continuous or pulsed lamps, and in more and more cases from semiconductor lasers. Liquid lasers can be pumped with a flashlamp or, on a continuous or pulsed basis, by another laser. Semiconductor lasers are *p-n* junction devices and are operated by passing pulsed or continuous electrical currents though them.

The amplifying state in a laser medium results if a population inversion can be achieved between two sublevels of the medium. The energy *sublevels* of a system are single states with their own characteristic energy. A set of sublevels having the same energy is called an energy *level*. This can be seen with reference to Figure 4.120, which shows a schematic partial energy-level diagram of a typical laser system. Input energy excites ground-state particles (atoms, molecules, or ions) of the medium into the state (or states) indicated as 3. These particles then transfer themselves or excite other particles preferentially to sublevel 2. In an ideal system, negligible excitation of particles into sublevel 1 should occur. If the populations of the sublevels 2 and 1 are n_2 and n_1, respectively, and $n_2 > n_1$, this is called a *population inversion*. The medium then becomes capable of amplifying radiation of frequency:

$$\nu = \frac{E_2 - E_1}{h} \tag{4.216}$$

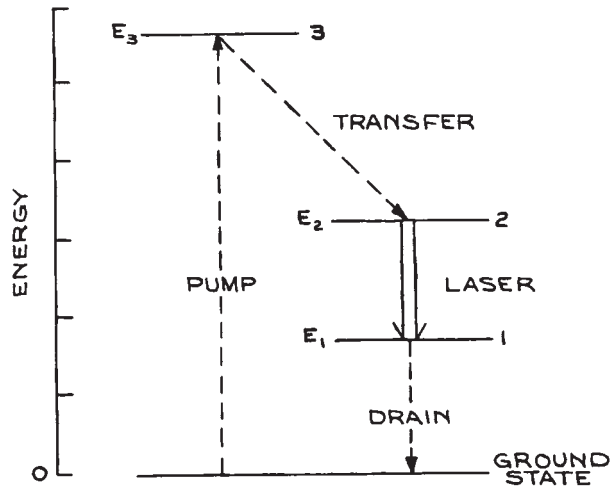

Figure 4.120 Schematic partial energy-level diagram of a laser system.

where h is Planck's constant. In practice, energy levels of real systems are of finite width, so the medium will amplify radiation over a finite bandwidth. The gain of the amplifier varies with frequency in this band and is specified by a gain profile $g(\nu)$, as shown in Figure 4.121. Actual laser oscillation occurs when the amplifying medium is placed in an optical resonator, which provides the necessary positive feedback to turn the amplifier into an oscillator. Most optical resonators consist of a pair of concave mirrors, or one concave and one flat mirror, placed at opposite ends of the amplifying medium and aligned parallel. A laser resonator is in essence a Fabry–Perot (see Section 4.7.4), generally of large spacing. The radii and spacing of the mirrors will determine, to a large degree, the type of Gaussian beam that the laser will emit. At least one of the mirrors is made partially transmitting, so that useful output power can be extracted. The choice of optimum mirror reflectance depends on the type of laser and its gain.

Low-gain lasers such as the helium–neon have high-reflectance mirrors, (98–99%), while higher-gain lasers such as pulsed nitrogen, CO_2, or Nd^{3+}:YAG can operate with much lower reflectance values. In certain circumstances, when their gain is very high, lasers will emit laser radiation without any deliberately applied feedback.

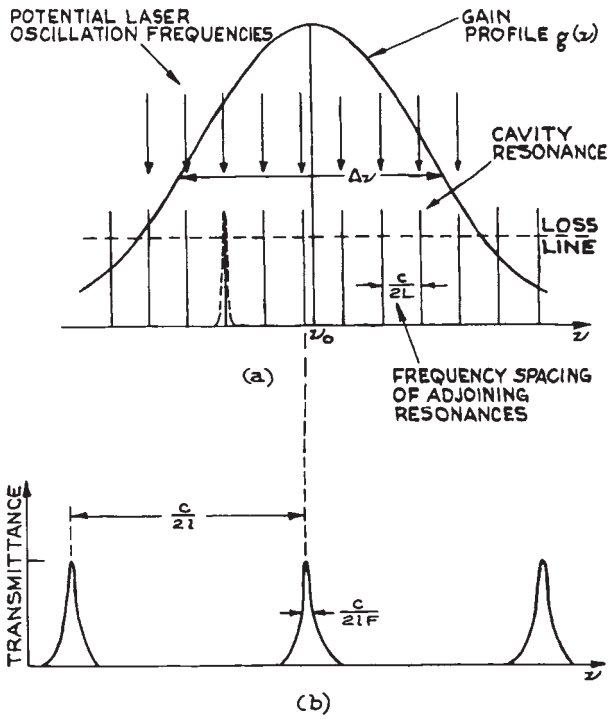

Figure 4.121 (a) Laser gain profile showing position of cavity resonances and potential laser oscillation frequencies near cavity resonances where gain lies above loss (L is length of laser cavity); (b) transmission characteristic of intracavity etalon, on same frequency scale as (a), for single-mode operation (l is the etalon thickness and F its finesse).

Lasers that operate in this fashion are generally operating in an *amplified spontaneous emission* (ASE) mode. Such lasers are just amplifying their own spontaneous emission very greatly in a single pass.

4.6.2 General Features of Laser Design

Even though the majority of laser users do not build their own, an awareness of some general design features of laser systems will help the user to understand what can and cannot be done with a laser. It will also assist the user who wishes to make modifications to a commercial laser system to increase its usefulness or convenience in a particular experimental situation. Figure 4.122 shows a schematic diagram of a typical gas laser, which incorporates most of the desirable design features of a precision system. The amplifying medium of a gas laser is generally a high- or low-pressure gas excited in a discharge tube. The excitation may be pulsed (usually by capacitor discharge through the tube), d.c., or occasionally a.c. Some gas lasers are also excited by electron beams, by radiofrequency energy, or by optical pumping with either a lamp or another laser. Far-infrared lasers, in particular, are frequently pumped with CO_2 lasers. Depending on the currents that must be passed through the discharge tube of the laser, it can be made of Pyrex, quartz, beryllium oxide, graphite, or segmented metal. These last three have been used in high-current-density discharge tubes for CW ion lasers. Several types of pulsed high-pressure or chemical lasers, such as CO_2, HF, DF, and HCI, can be excited in structures built of Plexiglas or Kel-F.

Because most gas lasers are electrically inefficient, a large portion of their discharge power is dissipated as heat. If ambient or forced-air cooling cannot keep the discharge tube cool enough, water cooling is used. This can be done in a closed cycle, using a heat exchanger. Some lasers need the discharge tube to run at temperatures below ambient. In such cases a refrigerated coolant such as ethylene glycol can be used. Many gas lasers use discharge tubes fitted with windows placed at Brewster's angle. This permits linearly polarized laser oscillation to take place in the direction indicated in Figure 4.122; light bouncing back and forth between the laser mirrors passes through the windows without reflection loss. Mirrors fixed directly on the discharge tube can also be used – this is common in commercial He–Ne lasers. In principle, such lasers should be unpolarized, although in practice various slight anisotropies of the structure often lead to at least some polarization of the output beam. The two mirrors that constitute the laser resonator, unless these are fixed directly to the discharge tube, should be mounted in kinematically designed mounts and held at fixed spacing ℓ by a thermally stable resonator structure made of Invar or quartz. In this structure an important parameter is the *optical length*, L, of the structure. For a laser in which the whole space between the two resonator mirrors is filled with a medium of refractive index n, the optical length is $L = n\ell$. For a composite structure with regions of different refractive index this result is easily generalized. Because the laser generates one or more output frequencies which are close to integral

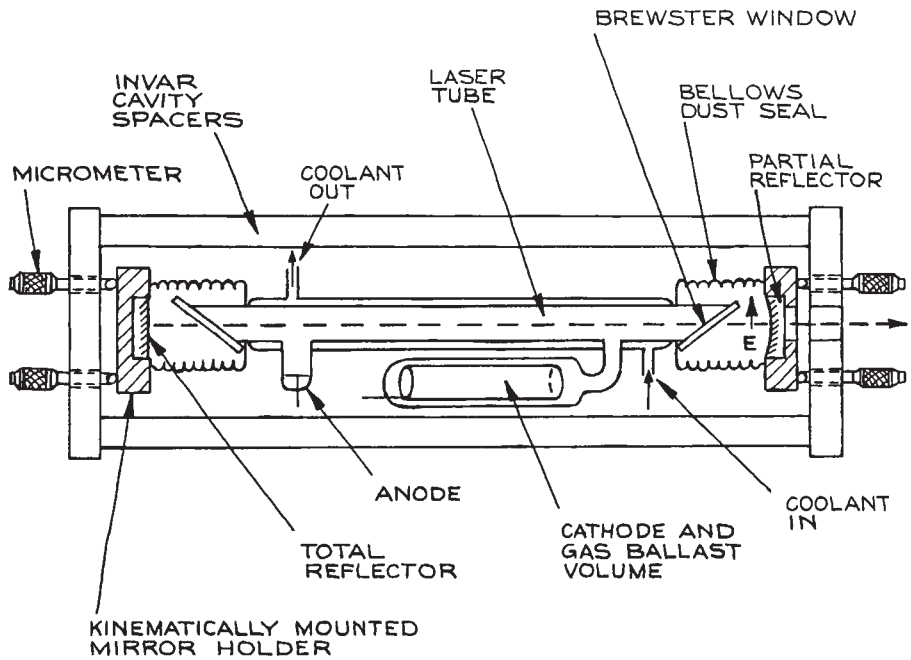

Figure 4.122 Schematic diagram of a typical gas laser showing some of the desirable features of a well-engineered research system. In high-discharge-current systems, some form of internal or external gas-return path from cathode to anode must be incorporated into the structure.

multiples of $c/2L$, any drift in mirror spacing L causes changes in output frequency v. This frequency change Δv satisfies:

$$\frac{\Delta v}{v} = \frac{\Delta L}{L} \tag{4.217}$$

For a laser 1 m long, even with an Invar-spaced resonator structure, the temperature of the structure would need to be held constant within 10 mK to achieve a frequency stability of only 1 part in 10^8. The discharge tube should be thermally isolated from the resonator structure unless the whole forms part of a temperature-stabilized arrangement.

If single-frequency operation is desired, the laser should be made very short – so that $c/2L$ becomes larger than Δv in Figure 4.121 – or operated with an intracavity etalon (see Sections 4.6.4 and 4.7.4). Visible lasers that have the capability of oscillating at several different wavelengths are generally tuned from line to line by replacing one laser mirror with a Littrow prism whose front face is set at Brewster's angle and whose back face is given a high-reflectance coating, as shown in Figure 4.123(a). Alternatively, as shown in Figure 4.123(b), one can use a separate intracavity prism, designed so the intracavity beam passes through both its faces at Brewster's angle. Infrared gas lasers that can oscillate at several different wavelengths are tuned by replacing one resonator mirror with a gold-coated or solid metal diffraction grating mounted in Littrow, as shown in Figure 4.123(c). The laser oscillation wavelength then satisfies:

$$m\lambda = 2d \sin\theta \tag{4.218}$$

where d is the spacing of the grating grooves, θ is the angle of incidence, and m is an integer.

A laser will oscillate only if its gain exceeds all the losses in the system, which include mirror transmission losses, absorption and scattering at mirrors and windows,

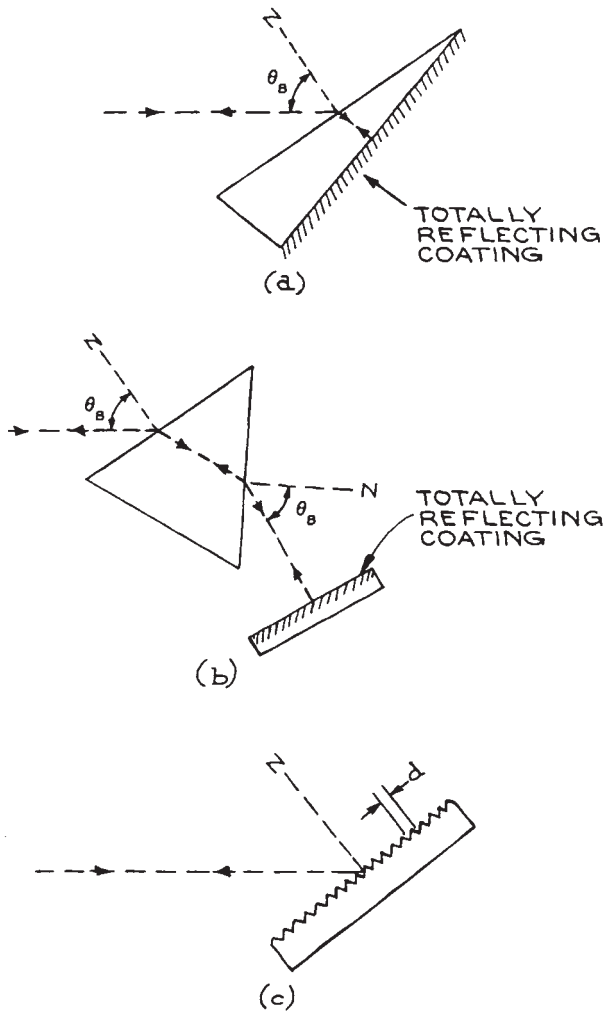

Figure 4.123 Methods for wavelength-selective reflection in laser systems: (a) Brewster's-angle Littrow prism; (b) intracavity Brewster's-angle prism; (c) reflective diffraction grating. N = surface normal.

and any inherent losses of the amplifying medium itself – the last generally being significant only in solid-state, liquid, and semiconductor lasers. Consequently, it is particularly important to keep the mirrors and windows of a laser system clean and free of dust. Most commercial systems incorporate a flexible, sealed enclosure between Brewster windows and mirrors to exclude contaminants.

Figure 4.124 shows some design features of a simple lamp-pumped solid-state laser oscillator. This design incorporates a linear pulsed or continuous lamp and a crystalline or glass laser rod with Brewster windows mounted inside a metal elliptical reflector, which serves to reflect pumping light efficiently into the laser rod. Although such solid-state lasers are rarely used in experiments where extreme frequency stability and narrow linewidth operation are required, it is still good practice to incorporate features such as stable, kinematic resonator design and thermal isolation of the hot lamp from the resonator structure. Elliptical reflector housings for solid-state lasers (and flashlamp-pumped dye lasers) can be made in two halves by horizontally milling a rectangular aluminum block with the axis of rotation of the milling cutter set at an angle of $\arccos(a/b)$, where a and b are the semiminor and semimajor axes of the ellipse. This process is repeated for a second aluminum block. The two halves are then given a high polish, or plated, and joined together with locating dowel pins. For further details of solid-state laser design and particulars of other arrangements for optical pumping the reader should consult Röss[76] or Koechner.[77] Flashlamp-pumped dye lasers share some design features with solid-state lasers. The main difference is that the former require excitation of short pulse duration ($< 1\,\mu s$) with special flashlamps in low-inductance discharge circuitry.[78–81]

4.6.3 Specific Laser Systems

Gaseous Ion Lasers. Gaseous ion lasers, of which the argon, krypton, and helium–cadmium are the most important, generate narrow-linewidth, highly coherent visible and ultraviolet radiation with powers in the range from milliwatts to a few tens of watts CW. Pulsed ion lasers operate at high current densities, but have low duty cycles, so that ambient cooling is adequate. These lasers are not in widespread experimental use. Helium–cadmium lasers use low-current-density (a few A/cm^2) air-cooled discharge structures, which in many respects are similar to those of helium–neon lasers. They are limited to a few tens of milliwatts in conveniently available output power. They do, however, provide UV output at 325 nm. Argon and krypton ion lasers use very high-current-density discharges (100–2000 A/cm^2) in special refractory discharge structures

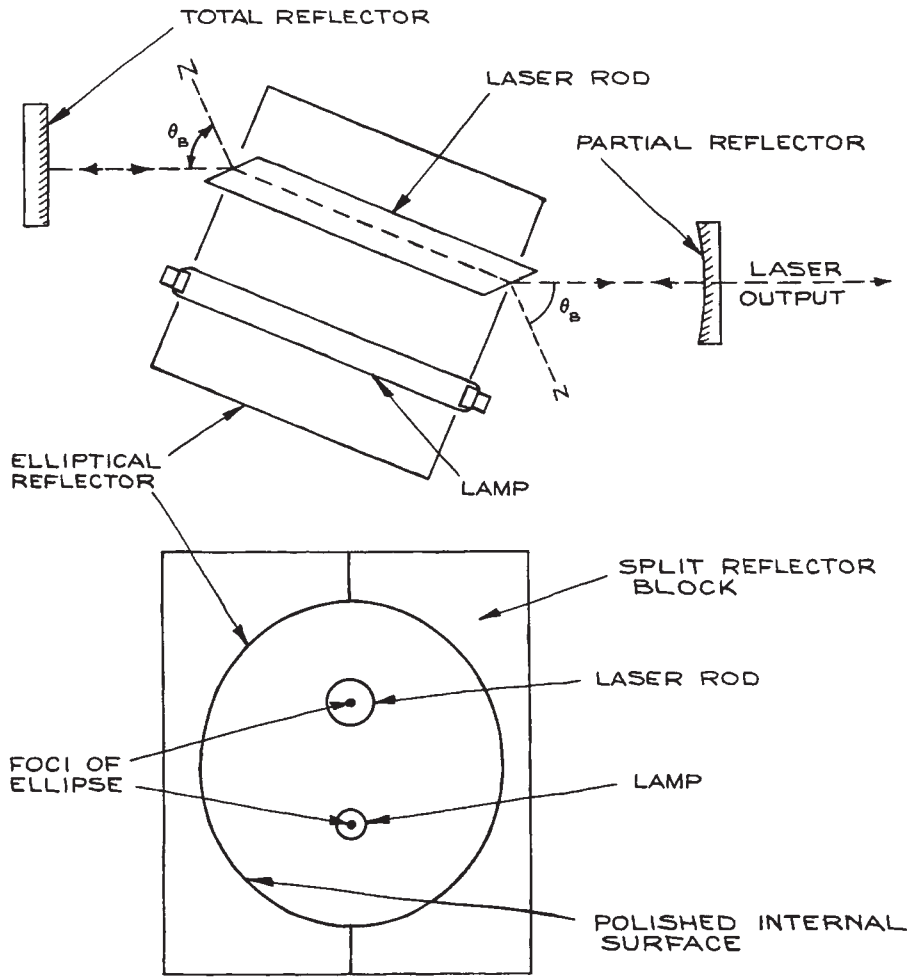

Figure 4.124 Schematic diagram of a simple solid-state laser system.

usually made of tungsten disks with ceramic spacers, as shown in Figure 4.125. In operation, these disks cool themselves by radiating through an outer fused-silica envelope surrounded by coolant water. Commercially available powers range up to a few tens of watts, but outputs up to 1 kW in the visible have been reported. Low power (< 100 mW) argon ion lasers can be forced-air cooled. Comprehensive information about ion lasers can be found elsewhere.[82,83] Argon and krypton ion lasers are available commercially from Coherent, JSC Plasma, JDSU, Melles Griot, and Spectra Physics (Newport Corporation). Argon and krypton ion lasers have in the past been widely used for pumping CW dye lasers and Ti:sapphire lasers. They are, however, rapidly being replaced in these applications by frequency-doubled Nd lasers, which are more and more likely to be pumped themselves by semiconductor diode lasers. Because of the large currents at which they operate, argon and krypton ion lasers regularly need their plasma tubes to be replaced (typically evey few thousand hours of operation), which is an expensive business. It appears

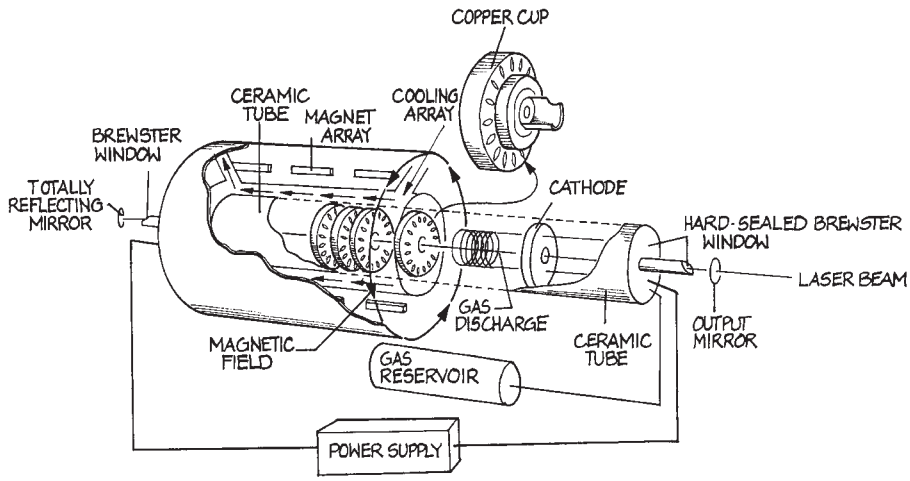

Figure 4.125 Construction of a high-power, water-cooled ion laser.

likely that these lasers will disappear from use and be universally replaced by diode-pumped solid-state (DPSS) lasers.

Helium–Neon Lasers. Of all types of laser, helium–neon lasers come closest to being the ideal classical monochromatic source. They can have very good amplitude ($\simeq 0.1\%$) and frequency stability (1 part in 10^8 without servo frequency control). Servo-frequency-controlled versions are already in use as secondary frequency standards, and have excellent temporal and spatial coherence.[84] Typical available power outputs range up to 50 mW. Single-frequency versions with power outputs of 1 mW, which are ideal for interferometry and optical heterodyne experiments, are available from Spectra-Physics and Aerotech. Although 632.8 nm is the routinely available wavelength from He–Ne lasers, other wavelengths, such as 543 nm or 1.15 or 3.39 μm are also available. Helium–neon lasers of low power are very inexpensive, costing from about $100, and are ideal for alignment purposes. Because of their superior spectral qualities compared to semiconductor lasers that can operate at the same wavelength, they remain a valuable source in applications such as interferometry and metrology. Other suppliers include Newport/Spectra Physics, Meles Griot, and Micro-Controle.

Helium–Cadmium Lasers. These lasers are similar in many ways to helium–neon lasers. They operate at relatively low current densities and use discharge tube structures that do not require water cooling. They are quite important in applications requiring deep blue and ultraviolet light at powers of ten of milliwatts. They operate at 325 nm and 441.6 nm. These wavelengths, especially 325 nm, are useful in applications where a photochemically active source is required. They are widely used in photolithography. Helium–cadmium lasers are available from Kimmon Electric Co. and Melles Griot.

CO_2 Lasers. Both pulsed and CW CO_2 lasers are easy to construct in the laboratory. A typical low-pressure CW version would incorporate most of the features shown in Figure 4.122. A water-cooled Pyrex discharge tube of internal diameter 10–15 mm, 1–2 m long, and operating at a current of about 50 mA, is capable of generating tens of watts output at 10.6 μm. The best operating gas mixture is CO_2–N_2–He in the ratio 1:1:8 or 1:2:8, at a total pressure of about 25 mbar in a 10 mm diameter tube. ZnSe is the best material to use for the Brewster windows, as it is transparent to red light and permits easy mirror alignment. The optimum output mirror reflectance depends on the ratio of the tube length to diameter, L/d, roughly according to:[85]

$$R \simeq 1 - L/500d \tag{4.219}$$

The output mirror is usually a dielectric-coated germanium, gallium arsenide, or zinc selenide substrate. Such mirrors are available from Janos, Laser Optics, Coherent, Infrared Industries, Laser Research Optics, Unique Optical, and II-VI Infrared, and Rocky Mountain Instruments, among others. The total reflector can be gold-coated in lasers with outputs of a few tens of watts. For tunable operation, gratings are available from American Holographic, Gentec, Jobin-Yvon, Perkin-Elmer, Richardson Grating Laboratory, and Rochester Photonics. When a grating is used to tune a laser with Brewster windows, the grating should be mounted so that the *E* vector of the laser beam is orthogonal to the grating grooves. An excellent review of low-pressure CW CO_2 gas lasers has been given by Tyte.[85]

Continuous wave CO_2 lasers can also be operated in a waveguide configuration, in which a much higher pressure gas mixture is excited in a small size discharge capillary.[86] These lasers provide substantially greater power output per volume than the low pressure variety. They can be excited by direct current, but r. f. excitation is now popular, and has now solved the unreliability problems that afflicted early commercial versions. Current suppliers of these compact lasers are Access Laser, Coherent, Edinburgh Instruments, Infrared Optical Products, Rofin-Sinar, Synrad, Trumpf, and Universal Laser Systems.

Transversely excited atmospheric-pressure (TEA) CO_2 lasers are widely used when high-energy, pulsed infrared energy near 10 μm is required. These lasers operate in discharge structures where the current flow is transverse to the resonator axis through a high-pressure ($\geqslant 0.5$ bar) mixture of CO_2, N_2, and He, typically in the ratio 1:1:5. To achieve a uniform, pulsed glow discharge through a high-pressure gas, special electrode structures and preionization techniques are used to inhibit the formation of localized spark discharges. Many very-high-energy types utilize electron-beam excitation. Discharge-excited TEA lasers are relatively easy to construct in the laboratory. A device with a discharge volume 60 cm long $\times$ 5 cm wide with a 3 cm electrode spacing excited with a 0.2 μF capacitor charged to 30 kV, will generate several joules in a pulse about 150 ns long. There are very many different designs for CO_2 TEA lasers; particulars of various types can be found in the *IEEE Journal of Quantum Electronics* and the *Journal of Applied Physics*. A particularly good design that is easy to construct is derived from a vacuum-ultraviolet photopreionized design described by Seguin and Tulip.[87] A diagram of the discharge structure is shown in Figure 4.126, together with its associated capacitor-discharge circuitry. The cathode is an aluminum Rogowski $2\pi/3$ profile;[88] the anode is a brass mesh, beneath which is a section of double-sided copper-clad printed circuit board machined into a matrix of separate copper sections on its top side. This printed circuit board provides a source of very many surface sparks for photopreionization of the main discharge. The laser is fitted with two separate capacitor banks: each circuit-board spark channel is energized by a 3600 pF Sprague or similar ''doorknob'' capacitor, while the main discharge is energized with a 0.2 μF low-inductance capacitor. Such capacitors are available from CSI Technologies, Hi Voltage Components, and Maxwell Labs. Both capacitor banks are switched with a single spark gap, which incorporates a Champion marine spark plug for triggering. The end of the spark plug, which has an annular gap, is ground down to its ceramic insulator and is triggered by an EG&G Model TM-11A Trigger generator. A good double Rogowski TEA laser design has been given by Seguin, Manes, and Tulip.[89] TEA lasers based on the multiple-pin-discharge design first described by Beaulieu[90] are also easy to construct, but they do not give output energies comparable to those of volume-excited designs. They do, however, lend themselves well to laser oscillation in many different gases – for example, HF formed by discharge excitation of H_2–F_2 mixtures.

CO Lasers. Continuous wave CO lasers are essentially similar in construction to CO_2 lasers except that the discharge tube must be maintained at low temperatures – certainly below 0 °C. They operate in a complex mixture of He, CO, N_2, O_2, and Xe with (for example) 21 mbar He, 0.67 mbar N_2, 0.013 mbar O_2, and 0.4 mbar Xe. They are available from Access Laser and Edinburgh Instruments.

Exciplex (Excimer) Lasers. Exciplex lasers operate in high-pressure mixtures such as Xe–F_2, Xe–Cl_2, Kr–Cl_2, Kr–F_2, and Ar–F_2. They are commonly also called ''excimer'' lasers, although this is not strictly correct scientific terminology except in the case of the F_2^* laser. Both discharge TEA and E-beam-pumped configurations are used.

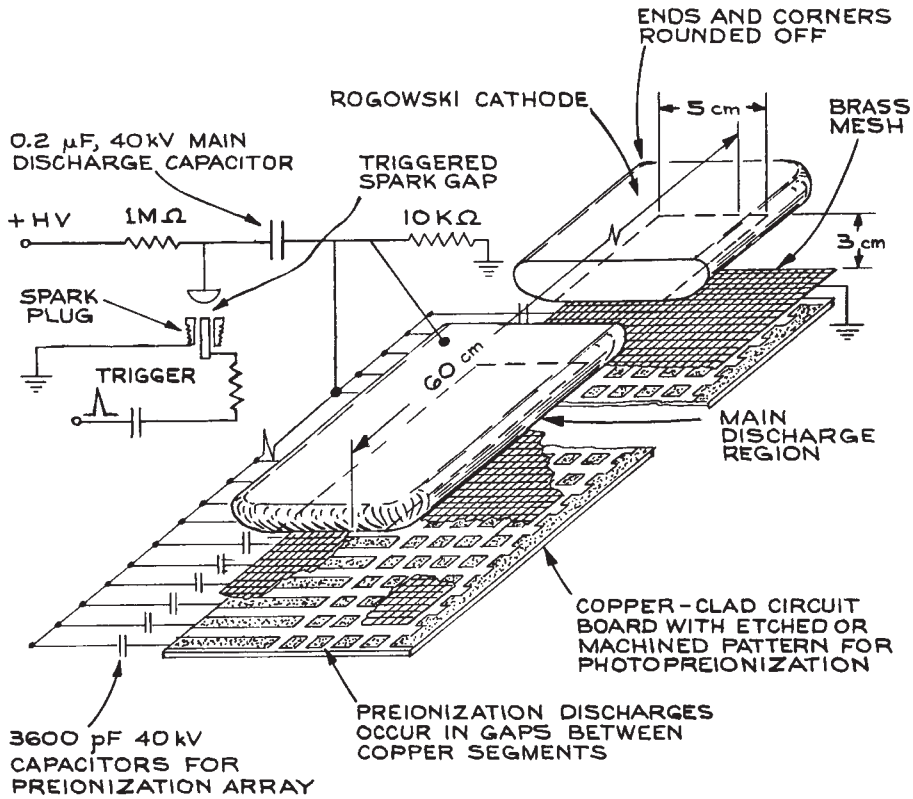

Figure 4.126 Cutaway view of vacuum-ultraviolet photopreionized Rogowski TEA laser structure.

Under electron bombardment, a series of reactions occur that lead to the formation of an excited complex (exciplex) such as XeF^*, which is unstable in its ground state and so dissociates immediately on emitting light. Excimer lasers available commercially are sources of intense pulsed ultraviolet radiation. The radiation from these lasers is not inherently of narrow linewidth, because the laser transition takes place from a bound to a repulsive state of the exciplex, and therefore is not of well-defined energy. Excimer lasers are attractive sources for pumping dye lasers and whenever intense pulsed UV radiation is required in, for example, photolithography or photochemistry.

The beam quality from an excimer laser is not normally very high. These are ''multimode'' lasers, with often a rectangular output beam profile. These lasers are widely available commercially from companies such as Gam Laser, JP Sercel Associates (JPSA), Lambda Physik (now Coherent), Optec, MPB Communications, and SOPRA.

Excimer lasers share technological design features in common with both CO_2 TEA lasers and nitrogen lasers. They use rapid pulsed electrical discharges through the appropriate high-pressure gas mixture. The discharge design must be of low inductance and the excitation is generally faster than is necessary to operate a CO_2 TEA laser. Because these lasers use toxic gases, such as fluorine and chlorine, appropriate gas-handling safety precautions must be taken in their use. The gases used, which are usually diluted mixtures of a halogen in a noble gas, should be housed in a vertical gas cabinet and exhaust gases from the laser should be sent through a chemical ''scrubber'' or filter cartridge before venting into the atmosphere.

Nitrogen (N_2) Lasers. Molecular-nitrogen lasers are sources of pulsed ultraviolet radiation at 337.1 nm. Commercially available low-energy devices usually operate on a flowing nitrogen fill at pressures of several tens of mbar, and generate output powers up to about 1 MW in pulses up to about 10 ns long. These lasers are reliable and easy to operate, and are widely used for pumping low-energy pulsed dye lasers. Nitrogen lasers, by virtue of their internal kinetics, only operate in a pulsed mode. They use very rapid transversely excited discharges, usually between two parallel, rounded electrodes energized with small, low-inductance capacitors charged to about 20 kV. The whole discharge arrangement must be constructed to have very low inductance. Special care must be taken with insulation in these devices; the very rapidly changing electric fields present can punch through an insulating material to ground under circumstances where the same applied d.c. voltage would be very adequately insulated. There are several good N_2-laser designs in the literature.[91–96] These designs fall into two general categories: Blumlein-type distributed-capacitance discharge structures, and designs based on discrete capacitors. The latter, although they do not give such high-energy outputs from a given laser as the very rapid-discharge Blumlein-type structures, are much easier to construct in the laboratory and are likely to be much more reliable. The capacitors used in these lasers need to be of low inductance and capable of withstanding the high voltage reversal and rapid discharge to which they will be subjected. Suitable capacitors for this application can be obtained from Murata or Sprague.

The output beam from a transversely excited N_2 laser is by no means Gaussian. It generally takes the form of a rectangular beam, typically $\simeq$ 0.5 cm $\times$ 3 cm, with poor spatial coherence. Such a beam can be focused into a line image with a cylindrical lens for pumping a dye cell in a pulsed dye laser. Nitrogen lasers are available commercialy from LTB Lasertechnik and Spectr-Physics (now Newport).

Copper Vapor Lasers. These are high-pulse-repetition-frequency (prf) pulsed gas lasers that operate using high-temperature gas mixtures of copper vapor in a helium or neon buffer gas. With individual pulse energies up to several millijoules and prf up to 20 kHz, these lasers provide average powers up to several watts. They are used for pumping pulsed dye lasers. The principal operating wavelengths are 510.6 and 578.2 nm. Suppliers include Laser Consultants and Oxford Laser. Pulsed gold vapor lasers are also available commercially, which are similar in most respects. They operate at 627.8 nm.

Continuous wave Solid-State Lasers. The most important laser in this category is the Nd:YAG laser, where YAG (yttrium aluminum garnet $Y_3Al_5O_{12}$) is the host material for the actual lasing species – neodymium ions, Nd^{3+}. Other host materials are also used: YLF (yttrium lithium fluoride, $LiYF_4$), YVO_4 (yttrium vanadate), YALO (yttrium aluminum oxide $YAlO_3$) and GSGG (scandium-substituted gadolinium gallium garnet, $Gd_3Sc_2Ga_3O_{12}$). The principal neodymium output wavelength is 1.06 μm, but other infrared wavelengths, especially 1.32 μm, are available. There are many suppliers.[31] The 1.06 μm can be efficiently doubled to yield a CW source of green radiation. This source of green radiation has replaced the argon-ion laser in many applications, especially since the neodymium laser itself can be pumped so conveniently with appropriate semiconductor lasers.

Ti:sapphire is an attractive laser material for generating tunable radiation in the 700–1060 nm range. These lasers are generally pumped by argon-ion lasers on frequency-doubled neodymium lasers. Suppliers include Coherent, Inc., Continuuum, Photonics Industries International, and Quantronix.

Fiber lasers use a gain medium that is a fiber doped with rare-earth ions such as erbium (Er^{3+}), neodymium (Nd^{3+}), ytterbium (Yb^{3+}), thulium (Tm^{3+}), or praseodymium (Pr^{3+}). They are pumped by one or more semiconductor laser diodes.[97] A simple schematic of how they are constructed is shown in Figure 4.127. In practice, the pump light may be coupled in through the cladding of the fiber. Very high-power fiber lasers with powers above 100 W are increasingly being used in industrial applications. Suppliers include B&W Tek, Fibercore, Fibertek, IPG Photonics, Micro-Controle, Newport, Nufren, and Toptica. Fiber lasers can be mode-locked to generate very short pulses (< 1 ps) in the infrared. Pulsed Er^{3+} fiber lasers are available from Calmar Optcom, PriTel, and IPG Phtonics. Pulsed Yb^{3+} lasers are available from Calmar Optcom, Clark-MXR, IPG Photonics, Laser Photonics, and Quantel.

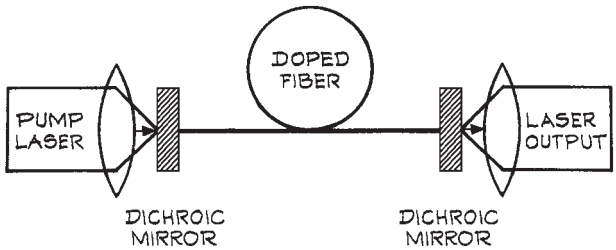

Figure 4.127 Schematic construction of a fiber laser.

An important application of erbium-doped fiber is in erbium-doped optical fiber amplifiers (EDFAs), widely used in fiber optic communication networks to amplify 1.55 μm semiconductor laser radiation.

F-center lasers[98] are doped-crystal lasers that are pumped with argon, krypton, or dye lasers. They provide tunable operation in two regions: between 1.43 and 1.58 μm and between 2.2 and 3.3 μm, but are somewhat inconvenient, because the crystal must be cooled with liquid nitrogen. They no longer appear to be available commercially.

Pulsed Solid-State Lasers. Three lasers are most important in this category Nd:YAG, Nd:glass, and ruby. Nd:YAG and Nd:glass lasers oscillate at the same principal wavelength, 1.06 μm. Nd:YAG is generally used in high-pulse-repetition-rate systems and/or where good beam quality is desired. High-energy Nd laser systems frequently incorporate an Nd:YAG oscillator and a series of Nd:glass amplifiers. There are many suppliers.[31] Ruby lasers, despite being the first laser to be demonstrated, are little used in research. They have medical applications because they provide a high-energy pulsed deep-red output (694.3 nm). They are available from Continuum.

All these pulsed solid-state lasers use fairly long flash excitation (≃ 1 ms). Unless the laser pulse output is controlled, they generate a very untidy optical output, consisting of several hundred microseconds of random optical pulses about 1 μs wide, spaced a few microseconds apart. This mode of operation, called *spiking*, is rarely used. Usually the laser is operated in a *Q*-switched mode. In this mode the laser cavity is blocked with an optical shutter such as an electro-optic modulator or Kerr cell, as illustrated in Figure 4.128. An appropriate time after flashlamp ignition, after the population inversion in the laser rod has had time to build to a high value, the shutter is opened. This operation, which changes the *Q* of the laser cavity from a low to a high value, causes the emission of a very large short pulse of laser energy. The *Q*-switched pulse can contain nearly as much energy as would be emitted in the "spiking" mode and is

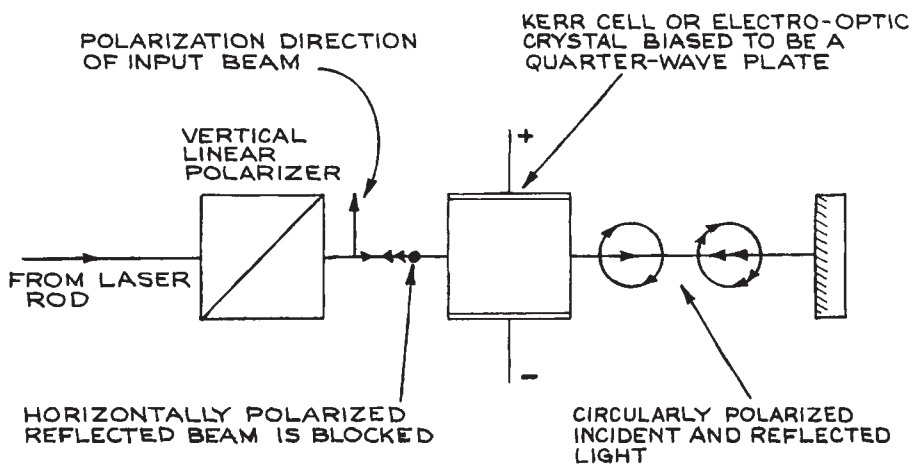

Figure 4.128 Schematic arrangement for *Q*-switching. Laser oscillation occurs when the voltage bias on the Kerr cell or electro-optic crystal is removed, thereby allowing the reflected beam to remain linearly polarized in the vertical direction.

typically 10–20 ns long. Passive *Q*-switching can also be accomplished with a "bleachable" dye solution placed in an optical cell inside the laser cavity. The dye is opaque at low incident light intensities and inhibits the buildup of laser oscillation. When, however, the laser acquires enough gain to overcome the intracavity dye absorption loss, laser oscillation begins, the dye bleaches, and a *Q*-switched pulse results. A bleachable dye cell with a short relaxation time, placed close to one of the laser mirrors, will frequently lead to mode-locked operation[99–101] within the *Q*-switched pulse (see Section 4.6.4).

Semiconductor Lasers. Five principal types of semiconductor laser are available commercially:

(1) Wide bandgap semiconductor lasers based on GaN/AlGaN, which, depending on stoichiometry, can emit down to 375 nm. These UV, blue, and green diode lasers have power outputs of several milliwatt and above. The developer of the shortest wavelength laser diodes based on GaN is Nichia, other manufacturers include Coherent, Cree, Koheras, Micro Laser Systems, Sony, and Toptica. Wavelengths above 375 nm are obtained from diodes with elements such as indium, aluminum, gallium, or nitrogen added, which produces laser diodes with wavelengths from 480 to 520 nm. The availability of short wavelength diode and diode-pumped solid-state lasers has significantly reduced the market and applications for visible and UV gas lasers such as argon ion, helium–cadmium, helium–neon, and krypton ion.

(2) GaAs or GaAlAs lasers, which operate at fixed wavelengths in the region between 0.75 and 0.9 μm. These lasers are very inexpensive and reliable; they are widely used in communication and information-processing systems, and in compact-disk players. High-power versions are used as the pumping source in DPSS lasers.

(3) InGaAsP lasers operate principally in the 1.3 and 1.55 μm regions for telecommunications applications. They have been developed to operate at the optimum wavelengths for minimum dispersion and lowest loss in optical-fiber communication systems. Near infrared semiconductor lasers are described in detail in many specialized texts.[102–110]

(4) Tunable diode lasers, which utilize lead-salt semiconductors such as PbSSe, PbSnSe, and PbSnTe can provide tunable operation over limited regions anywhere between 3 and 30 μm. The tunable lead-salt diode lasers are now commonly used in high-resolution spectroscopy.[111] They generally emit several modes, which, because of the very short length of the laser cavity, are spaced far enough in wavelength for a single one to be isolated by a monochromator. The output laser linewidths that are obtainable in this way are about $10^{-4}/cm^{1}$ (3 MHz). Scanning is accomplished by changing the temperature of the cryogenically cooled semiconductor or the operating current. Complete tunable-semiconductor-laser spectroscopic systems are available from Quantum Associates or Spectra-Physics (Laser Analytics).

(5) Quantum cascade lasers[112] can provide tunable operation over specific limited spectral regions within a range from 3 to 211 μm. The wavelength range varies from manufacturer to manufacturer. These lasers use multiple quantum wells, a so-called *superlattice*, to provide laser operation between *sub-bands* in the conduction bands of the structure. These lasers do not use *p-n* junctions for their operation. Quantum cascade lasers are available from Alpes, Boston Electronics, Cascade Technologies, and Sacher Lasertechnik.

Semiconductor Laser Properties. Only researchers involved in semiconductor laser development will fabricate these lasers. Their laser performance is, however, strongly influenced by their generally small size, and device structure. Figures 4.129–4.132 give examples of some

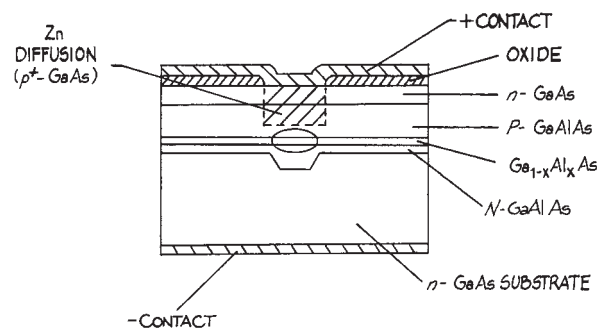

Figure 4.129 Double heterostructure laser diode design using a stripe excitation region confined by an oxide layer and deep zinc diffusion.

representative structures that are used in current semiconductor diode lasers. The basic laser structure involves a *p-n* junction through which a drive current flows. In all these structures the current flow through the device is controlled so that a specific volume of the active region is excited. This region is generally very small. The active length is not generally more than 1–2 mm. The lateral dimensions of the active region are generally in the 5–10 μm range, however, in single quantum well (SQW) and multiple quantum well (MQW) lasers, the dimension of the active region in the direction of current flow can be as small as 10–100 nm.

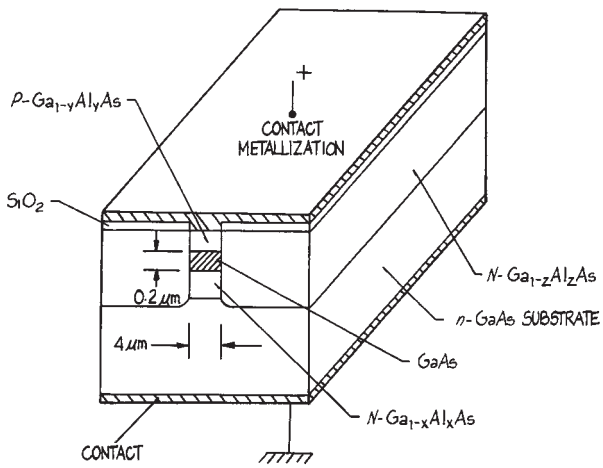

Figure 4.130 Double heterostructure laser of a buried stripe design.

Laser oscillation occurs in a resonant Fabry–Perot structure made up of the two end facets of the laser. The active region acts like a waveguide to confine the laser beam, which ideally emerges from the emitting facet as an elliptical Gaussian beam. This is a Gaussian beam whose spot sizes w_x, w_y are different in the two orthogonal (x, y) directions perpendicular to the z propagation direction of the laser beam. The smaller spot size is generally in the direction perpendicular to the junction. This asymmetry of the laser beam causes its beam divergence to be larger in the direction perpendicular to the junction than it is in the orthogonal direction, as shown schematically in Figure 4.133. Commercial diode lasers are often supplied with an *anamorphic* beam expander, which circularizes the laser beam and equalizes its orthogonal beam divergence angles, however, in general the beam quality from any semiconductor laser is

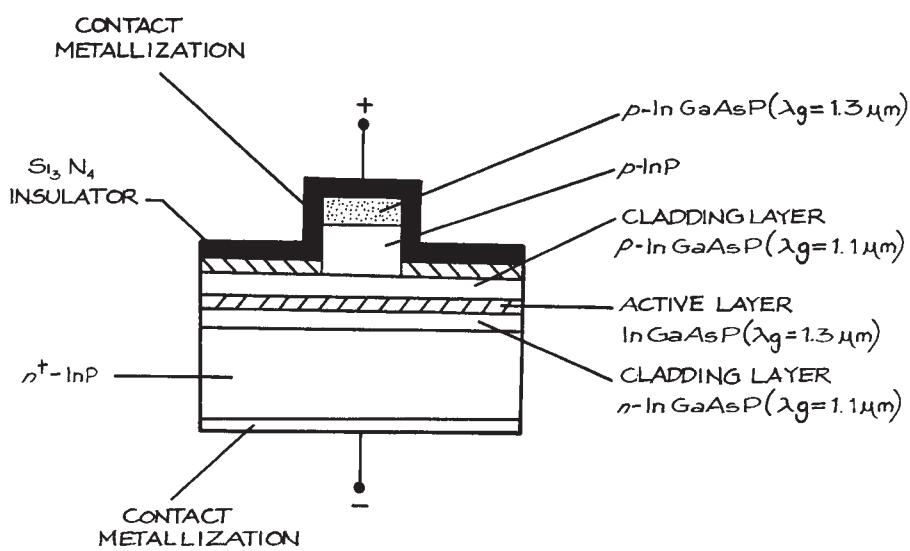

Figure 4.131 Cladded ridge double heterostructure semiconductor laser design.

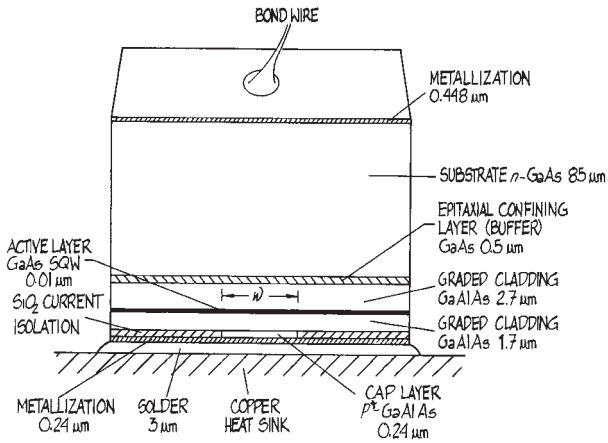

Figure 4.132 Graded index separate confinement heterostructure (GRINSCH) semiconductor laser design. Typical dimensions of the various layers are indicated. For a narrow stripe laser $w \sim 5$ μm, for a broad stripe laser $w \sim 60$ μm.

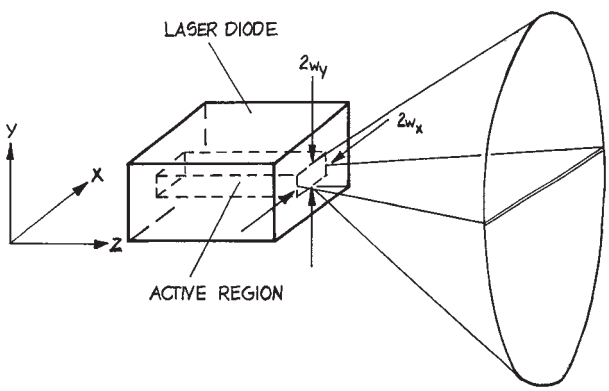

Figure 4.133 Schematic diagram of how a semiconductor laser emits a quasi-elliptical output beam because of asymmetrical beam confinement in two orthogonal directions inside the laser structure.

inferior to that from most gas lasers. A circular, clean, output beam can be obtained from a fiber-coupled diode laser. Vertical cavity surface emitting lasers (VCSELs) also provide circular output beams.

The spectral purity of Fabry–Perot semiconductor lasers is generally inferior to helium–neon lasers or diode-pumped solid-state lasers. Semiconductor laser linewidths are typically several MHz or more, so their coherence lengths are short. This makes them less suitable in most interferometric applications than most gas lasers or diode-pumped solid-state (DPSS) lasers. Narrower linewidth semiconductor lasers use an external cavity incorporating a grating structure, or have a Bragg grating structure incorporated into the semiconductor material itself: so-called distributed feedback (DFB) or distributed Bragg reflection (DBR) lasers. Suppliers include Agere, AMS Technologies, EXFO, Infineon, Lasermate, Sacher Lasertechnik, and Toptica. These lasers are mostly available at the telecommunications wavelengths of 1300 nm and 1550 nm.

Diode lasers have achieved their greatest commercial importance in telecommunications systems, but the availability of diode lasers at many discrete wavelengths from 375 nm to beyond 2 μm[31] has increased their use in spectroscopic applications. They can provide some degree of tunability by changing their operating temperature or drive current. Suppliers include Applied Optronics, Coherent, DILAS, Laser Diode, Lasermate Group, Lasertel, Melles Griot, New Focus, Newport, Opton, Photonic Products, Point Source, and QPC Lasers. Manufacturers' data sheets should be consulted for wavelengths, mode quality (single or multimode), beam quality (circular or elliptical), powers, and operational currents.[31] Many of these lasers can be obtained coupled to an optical fiber, which provides a clean, circular beam.

Some of the commonly available wavelengths (in nm) from diode lasers are: 375, 405, 408, 440, 635, 640, 650, 670, 690, 730, 780, 808, 830, 915, 940, 980, 1300, 1370, 1470, 1550, 1720, 1850, 1907, 1950, 2004, and 2350.

High-power diode lasers are available with powers up to and beyond 1 kW. They are widely used as pump sources in diode-pumped solid-state lasers; however, as far as spectroscopy purity is concerned they are closer in character to a light-emitting diode than they are to high-coherence lasers such as helium–neon, helium–cadmium or diode-pumped Nd:YAG.

Diode-Pumped CW Solid-State Lasers. Because of a fortuitous coincidence between the output of GaAlAs semiconductor lasers working near 809 nm and a strong absorption of the neodymium ions (Nd^{3+}) in YAG, YLF, or YVO_4, it is very efficient to optically pump Nd^{3+} lasers

with diode lasers. These lasers have become widely available commercially. They can also be efficiently frequency doubled to 530 nm, so have begun to replace ion lasers in applications where intense green light is required. Green output powers up to 70 W are available.

Diode-pumped lasers in which the semiconductor lasers are arranged to inject their pump radiation through the cylindrical faces of a laser rod are in many ways akin to lamp-pumped lasers of the same kind. Because of the high electrical efficiency of GaAlAs laser diodes (>10%) the overall electrical-to-optical conversion efficiency of these lasers is very high, approaching 10%. If the diode laser pump radiation is injected along the axis and matched to the transverse mode geometry of the solid-state laser then very stable, narrow linewidth laser oscillation can be obtained: Figure 4.134 shows the clever monolithic Nd:YAG laser design of Kane and Byer.[113] In this laser the magneto-optical properties of YAG are used to obtain unidirectional amplification of a traveling wave in the laser cavity. This prevents the spatial hole-burning that can occur in a standing wave homogeneously broadened laser, which can allow multiple longitudinal modes to oscillate.[15]

Frequency doubling of a DPSS laser is generally carried out with an intracavity nonlinear crystal such as BBO (beta-BaB_2O_4), PPLN (periodically poled lithium niobate), or PPKTP [periodically poled potassium titanium oxide phosphate ($KTiOPO_4$)], or with an external resonant cavity containing a nonlinear crystal. Figure 4.135 shows how intracavity frequency doubling is done with a Nd:YVO_4 coherent Verdi laser. This use of a ring laser resonator with unidirectional laser oscillation provides single longitudinal mode operation and a narrow linewidth. Frequency-tripled operation of diode-pumped Nd^{3+} laser at 355 nm is available at powers in excess of 3 W, frequency-quadrupled operation at 266 nm provides powers up to 500 mW. There are many suppliers of diode-pumped Nd^{3+} lasers, including A-B Lasers, Alphalas, Cobolt AB, Coherent, Continuum, Lee Laser, Lightwave Electronics, Melles Griot, Quantronix, Spectra-Physics, TecOptics, and TRUMPF, among others.[31] Diode-pumped solid-state lasers are also available at other wavelengths, notably 2.1 μm in holmium (Ho^{3+}), 1.6 μm and 2.8 μm in erbium (Er^{3+}) and 2.3 μm in thulium (Tm^{3+}).

The principal advantages of this type of laser are reliability, narrow linewidth, and single-frequency operation.

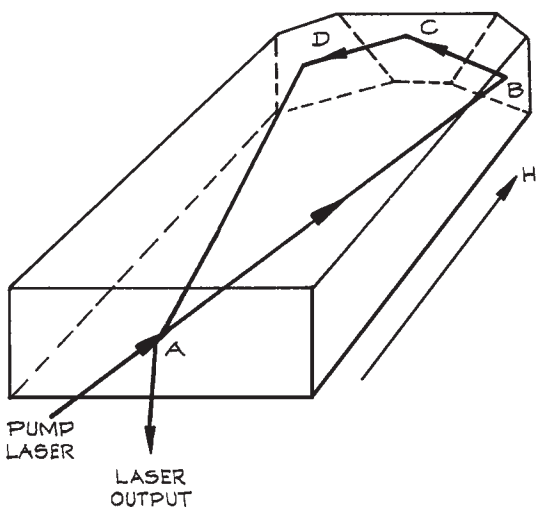

Figure 4.134 The "MISER" ring laser design of Kane and Byer.

Continuous Wave Dye Lasers. Continuous wave dye lasers usually take the form of a planar jet of dye solution continuously sprayed at Brewster's angle from a slit nozzle, collected, and recirculated. The jet stream is in a spherical mirror laser cavity, where it is pumped by the focused radiation of a CW ion laser or frequency-doubled Nd:YAG laser, as shown in Figure 4.136. These lasers can generally be regarded as wavelength converters – they have essentially the linewidth, frequency, and amplitude stability of the pumping source. For example, narrow-linewidth operation requires an etalon-controlled single-frequency ion laser. Continuous wave dye lasers are quite efficient at converting the wavelength of the pump laser; at pump powers far enough above threshold, the conversion efficiency ranges from 10 to 45%. Laser dyes are available from Exciton Lambda Physik and Radiant Dyes Laser Accessories, among others. Dye lasers are rapidly being replaced, wherever possible, with tunable solid-state devices. The dyes used photodegrade and liquid spills are common. The laboratories of most dye-laser users are stained with the dyes that they use! For further details of CW-dye-laser operation consult Schafer.[78] Continuous wave dye lasers are available from Big Sky Laser Technologies, Coherent, Quantel, and Spectra-Physics.

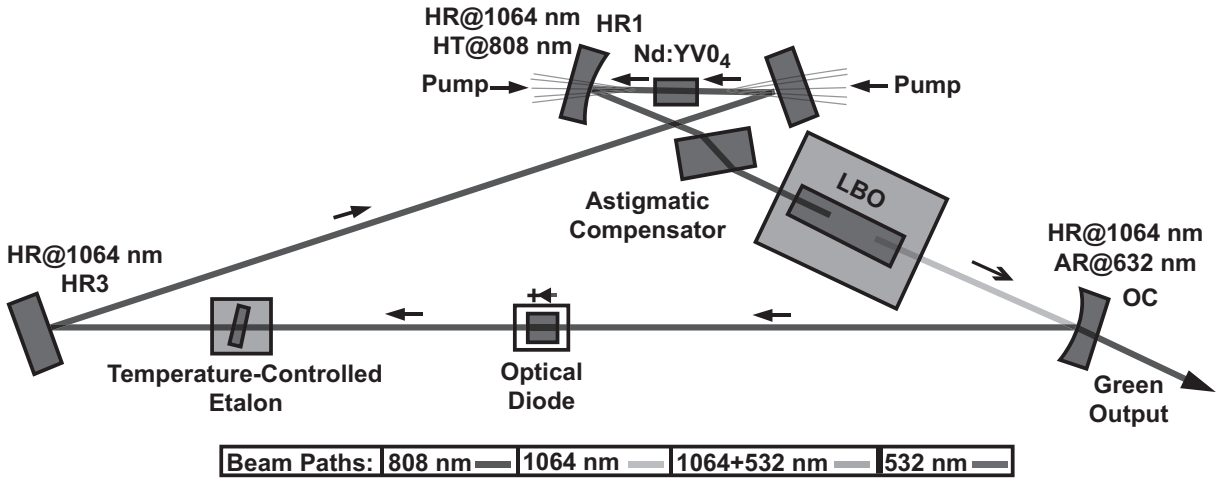

Ring Cavity Resonator of Coherent, Inc. Verdi Green DPSS Laser

Figure 4.135 The layout of the Coherent, Inc. "Verdi" laser where intracavity frequency doubling with a lithium triborate LiB_3O_5 (LBO) crystal is used to generate 530 nm from 1.06 μm. The initial laser oscillation is at 1.064 μ using a neodymium-doped yttrium vanadate (Nd:YVO_4) crystal pumped with an 808 nm diode laser. In the diagram HR – high reflectance mirror; OC – output coupling mirror.

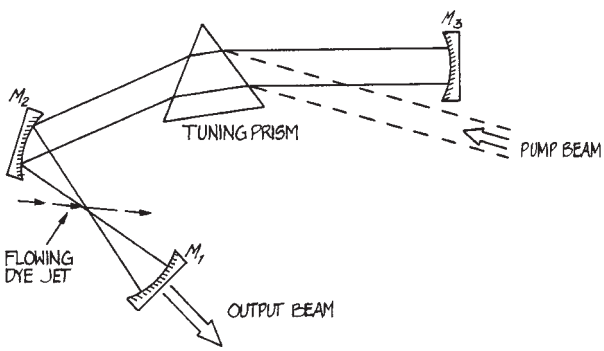

Figure 4.136 Layout of a CW dye laser using a flowing dye jet.

Pulsed Dye Lasers. Continuous wave dye lasers are not as frequently constructed in the laboratory as are pulsed dye lasers. In its simplest form, a pulsed dye laser consists of a small rectangular glass or quartz cell placed on the axis of an optical resonator and excited with a focused line image from a pump laser. Two simple geometrics are shown in Figure 4.137.

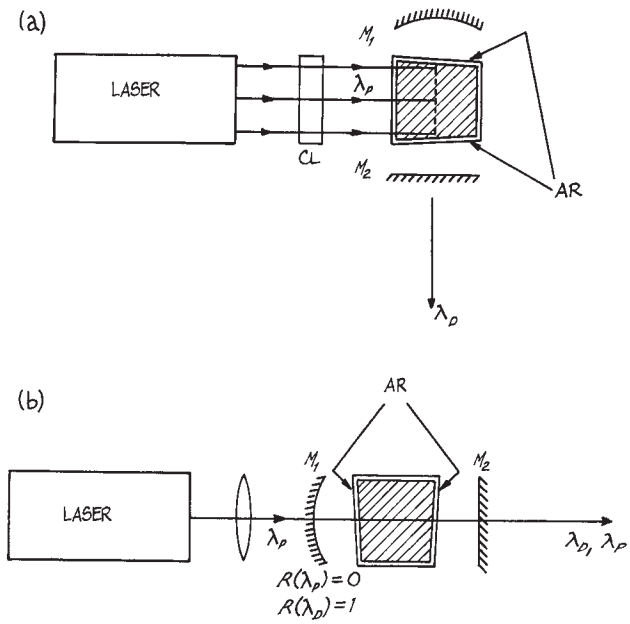

Figure 4.137 Two simple pulsed dye laser arrangements: (a) transverse pumping; (b) longitudinal pumping.

The most commonly used pump lasers are N_2 and frequency-doubled Nd:YAG, although ruby, excimer and copper-vapor lasers are also used. In its simplest form, this type of pulsed dye laser will generate a broad-band laser output (5–10 nm). Various additional components are added to the basic design to give tunable, narrow-linewidth operation. A very popular design that incorporates all the desirable features of a precision-tunable visible source has been described by Hänsch.[114] The essential components of a Hänsch-type pulsed dye laser are shown in Figure 4.138.

The pump laser is focused, with a cylindrical and/or a spherical lens, to a line image in the front of a dye cell. The line of excited dye solution (for example a 5×10^{-3} molar solution of Rhodamine 6G in ethanol) is the gain region of the laser. The laser beam from the gain region is expanded with a telescope in order to illuminate a large area of a high dispersion, Littrow-mounted echelle grating. Rotation of the grating tunes the center wavelength of the laser. Without the telescope, only a small portion of the grating is illuminated, high resolution is not achieved, and the laser linewidth will not be very narrow. With telescope and grating alone, the laser linewidth will be on the order of 0.005 nm at 500 nm ($\simeq 0.2\ \text{cm}^{-1}$). Even narrower linewidth can be achieved by including a tilted Fabry–Perot etalon in the cavity. A suitable etalon will have a finesse of 20 and a free spectral range (see Section 4.7.4) below about $1\ \text{cm}^{-1}$ in this case. Line widths as narrow as 4×10^{-4} nm can be achieved. A few experimental points are worthy of note: the laser is tuned by adjusting grating and/or etalon; alignment of the telescope to give a parallel beam at the grating is quite critical; the dye should be contained in a cell with slightly skewed faces to prevent spurious oscillation; the dye solution can remain static when low-power (10–100 kW) pump lasers are used, magnetically stirred when pump lasers up to about 1 MW are used, or continuously circulated from a reservoir when higher-energy or high-repetition-rate pump lasers are used. Suitable dye cells are available from Anderson Lasers, Esco, Hellma Cells and NSG Precision Cells. Cells can be constructed from stainless steel with Brewster window faces when end-on pumping with a high-energy laser is used (as shown in Figure 4.139). The dye can be magnetically stirred by placing a small Teflon-coated stirring button in the bottom of the dye cell. When continuous circulation of dye is used, suitable

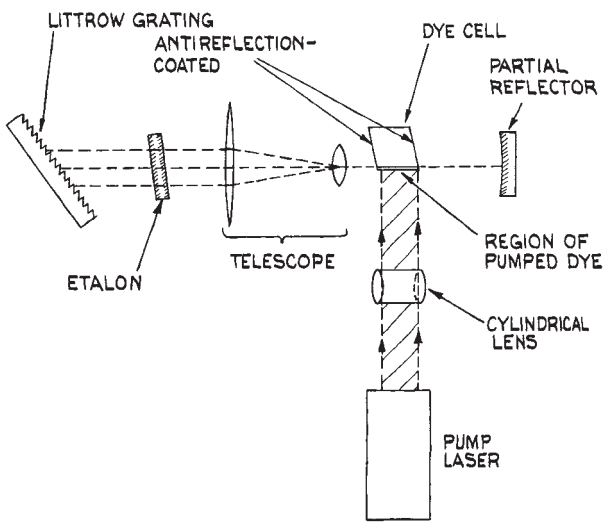

Figure 4.138 Hänsch-type pulsed dye laser.

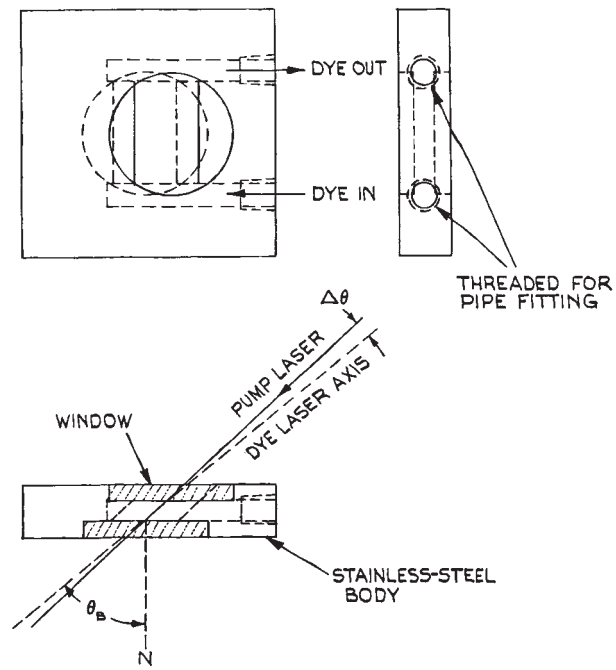

Figure 4.139 Flowing dye cell for end-pumped operation. N = normal to windows; θ_B = Brewster's angle, approximately the same for both pump and dye laser wavelengths; $\Delta\theta$ = a small angle. Dye solution flows laminarly in the channel between the windows.

pumps are available from Fluid-o-Tech and Micropump Corporation.

Once a narrow-linewidth pulsed-dye-laser oscillator has been constructed, its output power can be boosted by passing the laser beam through one or more additional dye cells, which can be pumped with the same laser as the oscillator. In a practical oscillator-amplifier configuration, 10% of the pump power will be used to drive the oscillator and 90% to drive the amplifier(s). Further details of Hänsch-type dye-laser construction are available in several publications.[115–119]

Two other approaches to achieving narrow-linewidth laser oscillation are worthy of note. The intracavity-telescope beam expander can be replaced, by a multiple-prism beam expander (see Section 4.3.4), which expands the beam onto the grating in one direction only. Such an arrangement does not need to be focused. An alternative, simple approach described by Littman[118,119] is to eliminate the beam expander and instead use a Littrow-mounted holographic grating in grazing incidence, as shown in Figure 4.140. Linewidths below 0.08 cm can be obtained without the additional use of an intracavity etalon.

Optical Parametric Oscillators. At one time, *optical parametric oscillators* (OPOs) were not readily available commercially, and were tricky to use. This has changed. Optical parametric oscillators provide tunable radiation typically in the range 210–5000 nm. They operate by using nonlinear optical processes in a crystal.[15,120–124] The OPO requires a *pump* laser of frequency ν_P, which is passed through a nonlinear crystal such as PPLN. Two new frequencies are generated in this process, a *signal* of frequency ν_S, and an *idler* of frequency ν_I. Energy is conserved in this process so that $\nu_S = \nu_P - \nu_I$. Tunability results by changing the angle of the pump beam with respect to the optic axis of the crystal, or by changing the temperature of the crystal. One or more of the three frequencies, pump, signal, or idler, is resonated inside a resonant structure that surrounds the nonlinear crystal. Figure 4.141 shows a schematic of an OPO with a resonant signal beam. An OPO generally generates tunable radiation with relatively broad linewidths (>1 cm). Special techniques are needed to generate narrow linewidths.[125] Optical parametric oscillators are available from Coherent, Continuum, EKSPLA, Linos Photonics, Opotek, Quantel, Radiantis, and Spectra Physics. Pulsed OPOs are more readily available than CW OPs and have larger tuning ranges. They can also generate very short (femtosecond) pulses.

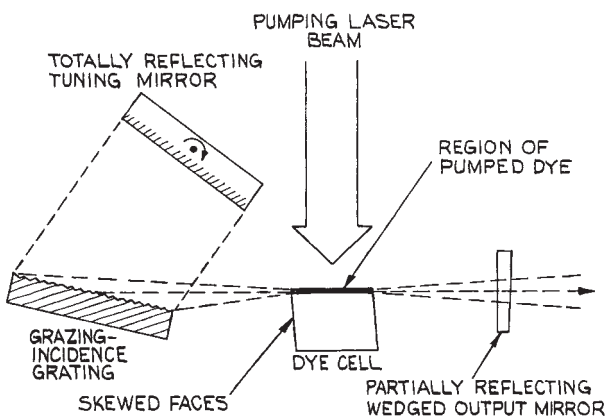

Figure 4.140 Littman-type dye laser.

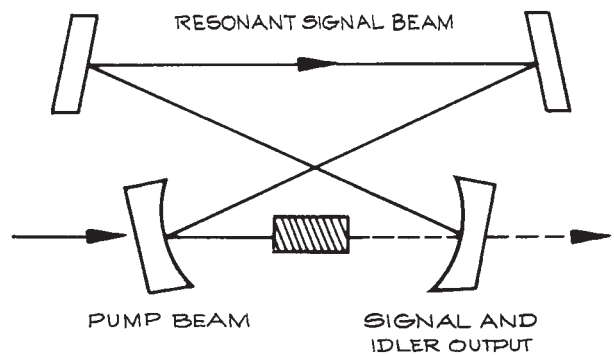

Figure 4.141 Schematic layout of an optical parametric oscillator (OPO).

4.6.4 Laser Radiation

Laser radiation is highly monochromatic in most cases, although flashlamp-pumped dye lasers in a worst case may have linewidths as large as 100 cm^{-1} (2.5 nm at 500 nm). The spectral characteristics of the radiation vary from laser to laser, but will be specified by the manufacturer. Lasers are usually specified as *single-mode lasers* or *multimode lasers*.

A *single-mode* laser emits a single-frequency output. Continuous wave CO_2 lasers and other middle- and far-infrared lasers usually operate in this way, and helium–neon and argon–ion lasers can also be caused to do so. The single output frequency will itself fluctuate randomly, typically over a bandwidth of 100 kHz–1 MHz, unless special precautions are taken to stabilize the laser – usually by stabilizing the spacing between the two mirrors that constitute its resonant cavity.

Multimode lasers emit several modes, called longitudinal modes, spaced in frequency by $c_0/2L$, where c_0 is the velocity of light *in vacuo* and L is the optical path length between the resonator mirrors. In a medium of refractive index n and geometric length l, $L = nl$. There may, in fact, be several superposed combs of equally spaced modes in the output of a multimode laser if it is not operating in a single transverse mode. The transverse modes specify the different spatial distributions of intensity that are possible in the output beam. The most desirable such mode, which is standard in most good commercial lasers, is the fundamental TEM_{00} mode, which has a Gaussian radial intensity distribution (see Section 4.2.4). A laser will generally operate on multiple longitudinal modes if the linewidth Δv of the amplifying transition is much greater than $c_0/2L$. In this case, the output frequencies will span a frequency range on the order of Δv. In short-pulse lasers the radiation oscillating in the laser cavity may not be able to make many passes during the duration of the laser pulse, and (particularly if the linewidth of the amplifying transition is very large) the individual modes may not have time to become well characterized in frequency. This is the situation that prevails in pulsed dye and excimer lasers. Additional frequency-selective components must be included in such lasers, such as etalons and/or diffraction gratings, to obtain narrow output linewidths.

Laser radiation is highly collimated: beam divergence angles as small as 1 mrad are quite common. This makes a laser the ideal way to align an optical system, far superior to traditional methods using point sources and autocollimators. As mentioned previously, lasers are highly coherent. Single-mode lasers have the highest temporal coherence – with coherence lengths that can extend to hundreds of kilometers. Fundamental-transverse-mode lasers have the highest spatial coherence.

In multimode lasers, the many output frequencies lie underneath the gain profile, as shown in Figure 4.121. Laser oscillation can be restricted to a single transverse mode by appropriate choice of mirror radii and spacing. Then, the available output frequencies are uniformly spaced longitudinal modes a frequency $c_0/2L$ apart, where L is the optical spacing of the laser mirrors. Laser oscillation can be restricted to a single one of these longitudinal modes by placing an etalon inside the laser cavity. The etalon should be of such a length l that its free spectral range $c/2l$ is greater than the width of the gain profile, Δv. Its finesse should be high enough so that $c/2lF \leqslant c_0/2L$. The etalon acts as a filter that allows only one longitudinal mode to pass without incurring high loss.

Many lasers can be operated in a *mode-locked* fashion. Then the longitudinal modes of the laser cavity become locked together in phase and the output of the laser becomes a train of uniformly spaced, very narrow pulses. The spacing between these pulses corresponds to the round-trip time in the laser cavity, $c_0/2L$. The temporal width of the pulses is inversely proportional to the gain bandwidth; thus, the broader the gain profile, the narrower the output pulses in mode-locked operation. For example, an argon-ion laser with a gain profile 5 GHz wide can yield mode-locked pulses 200 μs wide. A mode-locked dye laser with a linewidth of 100 cm (3×10^{12} Hz) can, in principle, give mode-locked pulses as short as about 0.3 ps.

Even shorter pulses than this can be obtained with ring-dye lasers, with mode-locked Ti:sapphire lasers, or with colliding pulse mode-locking techniques,[15] which, with pulse compression techniques, can generate pulses a few tens of femtoseconds (10^{-15} s) long. Ultrafast laser systems are available from Big Sky Laxer, Clark-MXR, Coherent, Quantronix, and Spectra Physics (now Newport).

Pulse compressors are available from Calmar Optcom, Femtochrome Research, and Swamp Optics.

4.6.5 Coupling Light from a Source to an Aperture

A common problem in optical experiment design involves either the delivery of light from a source to a target, or

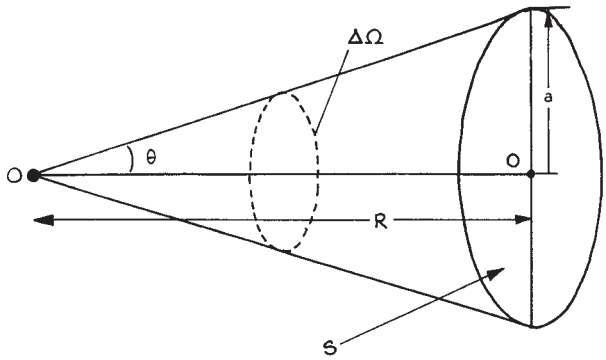

Figure 4.142 Geometry used to determine the collection efficiency of an aperture when it is illuminated by light from a point source.

collection of light from a source and delivery of the light to a collection aperture. The collection aperture might be the active area of a photodetector, the entrance slit of a spectrometer, or the facet of an optical fiber. A problem of specific importance is the focusing of a laser beam to a small spot. Sometimes the solution to one of these problems will involve a imaging system, but it might also involve a nonimaging light collector.

(1) *Collection of light from a point source and its delivery to a target aperture*. This situation is illustrated in Figure 4.142. The solid angle $\Delta\Omega$ subtended by a circular aperture $S = \pi a^2$ at distance R from the source is:

$$\Delta\Omega = 2\pi(1 - \cos\theta) \tag{4.220}$$

which for $R >> a$ can be written as:

$$\Delta\Omega = \frac{S}{R^2} \tag{4.221}$$

If the radiant power of the source is P watts then the power, collected by the aperture is:

$$P' = P\frac{\Delta\Omega}{4\pi} \tag{4.222}$$

To increase the light delivered to the aperture S, a lens system can be placed between O and O′ as shown in Figure 4.143. To maximize light collection, the lens used should have a small *f*/number (*f*/#). The point

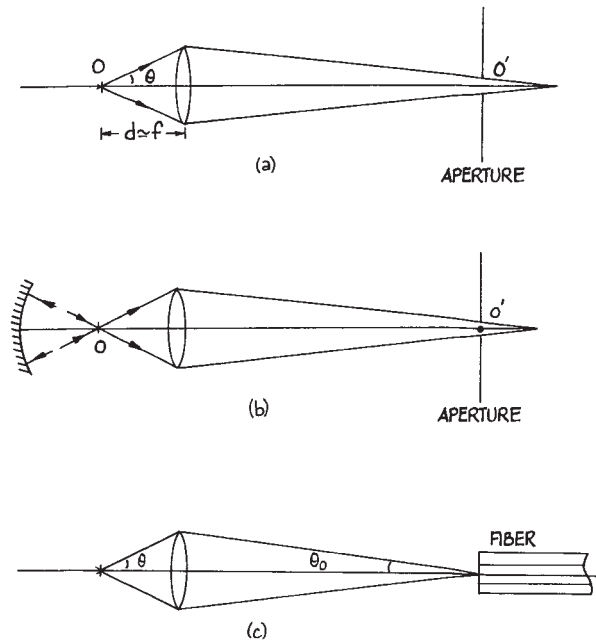

Figure 4.143 Optical arrangements for optimizing coupling of a point source to an aperture: (a) lens coupling; (b) lens and spherical mirror coupling; (c) coupling of a point source to an optical fiber.

source is placed close to the focal point of the lens, so that:

$$\cos\theta \simeq f/\sqrt{a^2 + f^2} \tag{4.223}$$

and

$$P' = \frac{P}{2}\left(1 - \frac{f}{\sqrt{a^2 + f^2}}\right) \tag{4.224}$$

Since the *f*/number is:

$$f/\# = \frac{f}{2a} \tag{4.225}$$

Equation (4.224) becomes:

$$P' = P\left(\frac{1}{2} - \frac{f/\#}{\sqrt{1 + 4f/\#}}\right) \tag{4.226}$$

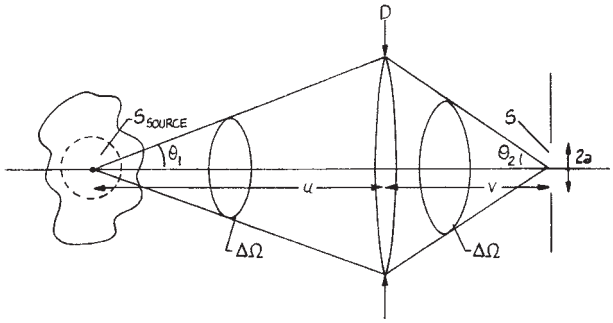

Figure 4.144 Geometry of an extended source and collection aperture used to describe the collection efficiency.

With an *f*/1 lens

$$P' = P\left(\frac{1}{2} - \frac{1}{\sqrt{5}}\right) = 0.053P \tag{4.227}$$

In practice an aspheric lens should be used in this application, especially if the aperture S is of small size. If a spherical reflector is placed behind the source, as shown in Figure 4.143(b), so that the source lies at its center of curvature, then the collection efficiency can be doubled.

(2) *Coupling light from a point source to an optical fiber.* Whether the source is actually a point source or is of small finite size relative to other distances in the geometry of Figure 4.143(c) is not very important. For coupling light to a fiber, the source must be imaged onto the front end of the cleaved fiber, but the light rays must remain within the numerical aperture of the fiber: $\sin\theta_0 \leqslant \text{NA}$. In principle, this can be accomplished by placing the source close to the focal point of the lens so that linear magnification (v/u) is large. In practice, the maximum magnification that can be used will be limited by the core diameter of the fiber and the finite size of the source.

(3) *Collection of light from an extended source and its delivery to a aperture.* This situation is shown in Figure 4.144. It is not possible in this case to image the extended source to a point, the best that can be done is to image as large an area of the source as possible onto the aperture S. If an axial point on the source is imaged to the center of the aperture S, then the area of the source that can be imaged onto the aperture S is

$$S_{\text{source}} = \frac{S}{m^2} \tag{4.228}$$

since $m = (v/u)$ is the linear magnification of the system. A high-quality imaging system would need to be used in this situation, especially if the aperture S is small, otherwise, aberrations will affect the size of the image.

If the brightness of the extended source in Figure 4.144 is $B_1(\text{Wm}^{-2}\,\text{sr}^{-1})$, then the power collected by the lens is, approximately:

$$P_1 = 2\pi B_1 S_{\text{source}}(1 - \cos\theta_1) \tag{4.229}$$

This light is imaged onto the collection aperture of area S where it occupies a solid angle $\Delta\Omega_2$ determined by the angle θ_2, where:

$$\Delta\Omega_2 = 2\pi(1 - \cos\theta_2) \tag{4.230}$$

The brightness of the image is:

$$\begin{aligned} B_2 &= \frac{P_1}{2\pi S(1 - \cos\theta_2)} \\ &= \frac{B_1 S_{\text{source}}}{S}\frac{(1 - \cos\theta_1)}{(1 - \cos\theta_2)} \end{aligned} \tag{4.231}$$

which gives:

$$B_2 = \frac{B_1}{m^2}\frac{\sin^2(\theta_1/2)}{\sin^2(\theta_2/2)} \tag{4.232}$$

For a paraxial system $\sin(\theta_1/2) \simeq (\theta_1/2)$, so:

$$B_2 = \frac{B_1}{m^2}\frac{(\theta_1^2)}{(\theta_2^2)} \tag{4.233}$$

The ratio $\left(\dfrac{\theta_2}{\theta_1}\right)$ is the angular magnification, m', of the system. Therefore, since $mm' = 1$:

$$B_2 = B_1 \tag{4.234}$$

This is an example of the *brightness* theorem, which states that the brightness of an image can not be greater than the brightness of the object.[k]

4.6.6 Optical Modulators

In many optical experiments, particularly those involving the detection of weak light signals or weak electrical signals generated by some light-stimulated phenomenon, the signal-to-noise ratio can be considerably improved by the use of phase-sensitive detection. The principles underlying this technique are discussed in Section 6.8.2. To modulate the intensity of a weak light signal falling on a detector, the signal must be periodically interrupted. This is most easily done with a mechanical chopper. Weak electrical signals that result from optical stimulation of some phenomenon can also be modulated in this way by chopping the radiation from the stimulating source.

Modulation of narrow beams of light such as laser beams, or of extended sources that can be focused onto a small aperture with a lens, is easily accomplished with a tuning-fork chopper. Such devices are available from Boston Electronics, Electro-Optical Products, and Scitec Instruments. The region chopped can range up to several millimeters wide and a few centimeters long at frequencies from 5 Hz to 3 kHz. For chopping emission from extended sources, or over large apertures, rotating chopping wheels are very convenient. The chopping wheel can be made of any suitable rigid, opaque material and should have radially cut apertures of one of the forms indicated in Figure 4.145. This form of aperture ensures that the mark-to-space ratio of the modulated intensity is independent of where the light passes through the wheels. By cutting very many slots in the wheel, very high modulation rates can be achieved – for example, up to 100 kHz with a 20 000 rpm motor and a wheel with 300 slots. The chopping wheel should usually be painted or anodized matt black. For chopping intense laser beams (in excess of perhaps 1 W), it may be better to make the wheel reflective so that unwanted beam energy can be reflected into a beam dump. Reflective glass chopping wheels can be used at low speeds in experiments where a light beam must be periodically routed along two different paths.

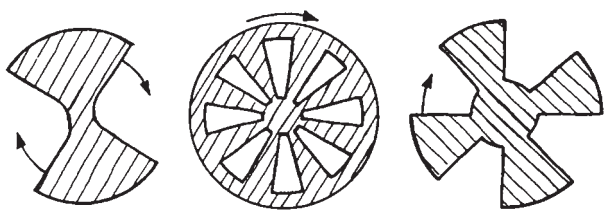

Figure 4.145 Some chopping-wheel designs.

To obtain an electrical reference signal that is synchronous with a mechanical chopping wheel, a small portion of the transmitted beam, if the latter is intense enough, can be reflected onto a photodiode or phototransistor. Alternatively, an auxiliary tungsten filament lamp and photodiode can be mounted on opposite sides of the wheel. If these are mounted on a rotatable arm, the phase of the reference signal they provide can be adjusted mechanically. Chopping wheels with built-in speed control and electrical rotation reference signals are available commercially from Boston Electronics, DL Instrument, EG&G Princeton Applied Research, Electro-Optical Products Corp., New Focus, Stanford Research Systems, and Thorlabs.

Electro-optic modulators (*Pockel's cells*) can also be used in special circumstances, particularly for modulating laser beams, or when mechanical vibration is undesirable. The operation of these devices is shown schematically in Figure 4.146. Light passing through the electro-optic crystal is plane-polarized before entry and then has its state of polarization altered by an amount that depends on the voltage applied to the crystal. The effect is to modulate the intensity of the light transmitted through a second linear polarizer placed behind the electro-optic crystal. By choosing the correct orientation of the input polarizer relative to the axes of the electro-optic crystal and omitting the output polarizer, the device becomes an optical phase modulator. For further details of these electro-optic amplitude and phase modulators the reader is referred to the books by Yariv,[14] Kaminow,[125] and Davis.[15] Electro-optic modulators are available from Cleveland Crystals, Conoptics, II-VI, JDS Uniphase, Meadowlark Optics, New Focus, and Quantum Technology, among others.

Acousto-optic modulators which operate by diffraction effects induced by sound-wave-produced periodic density variations in a crystal are also available.[126,127] The most widely used materials for these devices are $LiNbO_3$, TeO_2, and fused quartz. In their operation a radio-frequency (r.f.) sound wave is driven through the material from a piezoelectric transducer, usually fabricated from $LiNbO_3$ or ZnO. A schematic diagram of how such an acousto-optic modulator works is given in Figure 4.147. Incident light

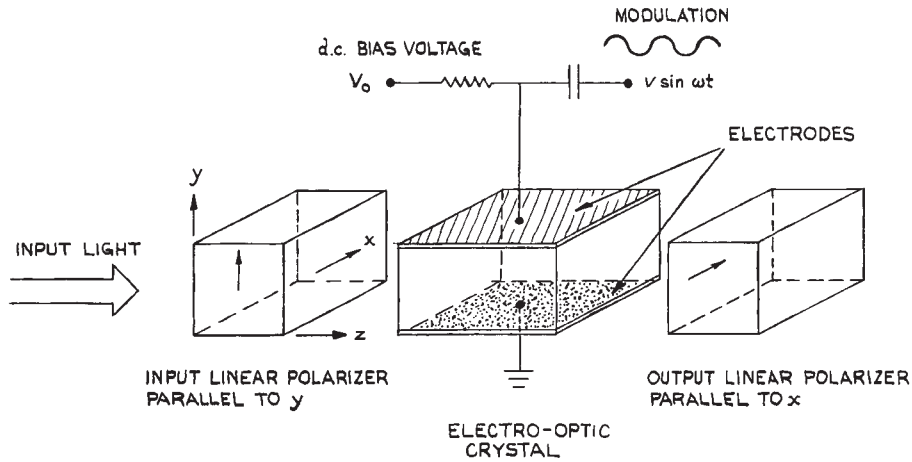

Figure 4.146 An electro-optic amplitude modulator using a transversely operated electro-optic crystal. The d.c. bias voltage can be used to adjust the operating point of the modulator so that, in the absence of modulation, the output intensity is a maximum, a minimum, or some intermediate value.

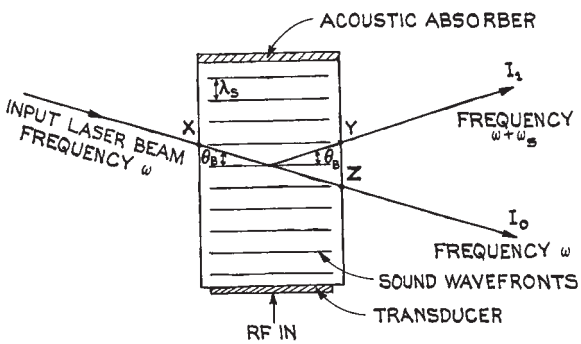

Figure 4.147 Schematic diagram showing the operation of an acousto-optic device in the Bragg regime. For simplicity, the refraction of the laser beam at *X*, *Y*, and *Z* is not shown.

that makes an appropriate angle θ_B, with the sound wavefronts will be diffracted if it simultaneously satisfies the condition for constructive interference and reflection from the sound wavefronts. This condition is $\sin \theta_B = \lambda/\lambda_s$, where λ is the laser wavelength in the acousto-optic material, and λ_s is the sound wavelength. The device is used as an amplitude modulator by amplitude-modulating the input r.f., which will be set to a specific optimum frequency for the device being used. Increase of drive power increases the diffracted power I_1 and reduces the power of the undeviated beam I_0 and vice versa. The device also functions as a frequency shifter. In Figure 4.147 the laser beam reflects off a moving sound wave and is Doppler shifted so that the beam I_1 is at frequency $\omega + \omega_s$, where ω_s is the frequency of the sound wave. Acousto-optic devices are available from many suppliers, including Crystal Technology, Electro-Optical Products, IntraAction, Isomet, and NEOS Technologies. Further details about these devices can be found in References 15, 126, and 127.

Very many liquids become optically active on application of an electric field; that is, they rotate the plane of polarization of a linearly polarized beam passing through them. This phenomena is the basis of the *Kerr cell*, which can be used as a modulator, but is more commonly used as an optical shutter (for example, in laser *Q*-switching applications as discussed in Section 4.6.3). A typical Kerr cell uses nitrobenzene placed between two plane electrodes across which a high voltage is applied. This voltage is typically several kilovolts and is sufficient to rotate the plane of polarization of the incident light passing between the plates by 45 or 90°. Kerr cells are rarely used these days and have been superseded by electro-optic modulators.

Closely related to optical modulators are optical deflectors, which can be used for the spatial scanning or switching of light beams. Two principal types are commonly used: electromechanical devices that utilize small mirrors mounted on galvanometer suspensions (available from Cambridge Technology, GSI Lumonics, and NEOS Technologies) and beam deflectors that utilize the acousto-optic effect. In the latter the deflection angle shown in Figure 4.147 is controlled by changing the r.f. drive frequency. These devices are available from Crystal Technology, IntraAction, Isomet, and NEOS Technologies. Electro-optic scanners are also available, but are less widely used. These devices are generally designed for small deflections. They are available from Conoptics.

Spatial light modulators are multiple element devices, which generally use liquid crystals, work in transmission, and can modify the characteristics of an entire wavefront in a pixellated fashion. They are available from Display Tech and Meadowlark Optics.

4.6.7 How to Work Safely with Light Sources

Light sources, whether coherent or incoherent, can present several potential safety hazards in the laboratory. The primary hazard associated with the use of home-built optical sources is usually their power supply. Lasers and flashlamps in particular, generally operate with potentially lethal high voltages, and the usual safety considerations for constructing and operating such power supplies should be followed in their design:

(1) Provide a good ground connection to the power supply and light-source housing.
(2) Screen all areas where high voltages are present.
(3) Install a clearly visible indicator that shows when the power supply is activated.
(4) HV power supplies, particularly those that operate with pulsed power, can remain dangerous even after the power is turned off, unless energy-storage capacitors are automatically shunted to ground. Always short the capacitors in such a unit to ground after the power supply is turned off before working on the unit.
(5) As a rule of thumb, keep a gap of about 25 mm for every 10 kV between high-voltage points and ground.
(6) To avoid excessive corona at voltages above about 20 kV, make sure that high-voltage components and connections have no sharp edges. Where such points must be exposed, corona can be reduced by installing a spherical metal corona cap on exposed items such as bolts or capacitor terminals. Resistor and diode stacks can be potted in epoxy or silicone rubber to prevent corona.
(7) Sources that are powered inductively or capacitively with r.f. or microwave power can burn fingers that come too close to the power source, even without making contact.

Commercial optical sources are generally fairly safe electrically and are likely to be equipped with safety features, such as interlocks, which the experimentalist may not bother to incorporate into home-built equipment. *Caveat emptor.* Remember the maxim ''it's the volts that jolts but it's the mills that kills.''

Other general precautions with regard to electric shock include the following:

(1) Avoid wearing metallic objects such as watches, watchbands, and rings.
(2) If any operations must be performed on a line circuit, wear well-insulated shoes and, if possible, use only one hand – ''Always keep one hand in your pocket.''
(3) Keep hands dry; do not handle electrical equipment if you are sweating.
(4) Learn rescue and resuscitation procedures for victims of electric shock: Turn off the equipment, remove the victim by using insulated material; if the victim is not breathing, start mouth-to-mouth resuscitation; if there is no pulse, begin CPR procedures immediately; summon medical assistance; continue resuscitation procedures until relieved by a physician. If the victim is conscious, but continues to show symptoms of shock, keep the person warm. Always call for professional help. (Dial 911 in the USA.)

Other hazards in the use of light sources include the possibility of eye damage, direct burning (particularly, by exposure to the beam from a high-average-power laser), and the production of toxic fumes. The last is most important in the use of high-power CW arc lamps, which can generate substantial amounts of ozone. The lamp housing should be suitably ventilated and the ozone discharged into a fume

hood or into the open air. Some lasers operate using a supply of toxic gas, such as hydrogen fluoride and the halogens. Workers operating such systems must be sufficiently experienced to work safely with these materials. The *Matheson Gas Data Book*, published by Matheson Gas Products, is a comprehensive guide to laboratory gases, detailing the potential hazards and handling methods appropriate to each.

The potential eye hazard presented by most incoherent sources is not great. If a source appears very bright, one should not look at it, just as one should not look directly at the Sun. Do not look at sources that emit substantial ultraviolet radiation; at the least, severe eye irritation will result – imagine having your eyes full of sand particles for several days! Long-term exposure to UV radiation should be kept below 0.5 $\mu W/cm^2$. Ordinary eyeglasses will protect the eyes from ultraviolet exposure to some extent, but plastic goggles that wrap around the sides are better. Colored plastic or glass provides better protection than clear material. The manufacturer's specification of ultraviolet transmission should be checked, since radiation below 320 nm must be excluded from the cornea.

The use of lasers in the laboratory presents an optical hazard of a different order. Because a laser beam is generally highly collimated and at least partially coherent, if the beam from a visible or near-infrared laser enters the pupil of the eye it will be focused to a very small spot on the retina (unless the observer is very short-sighted). If this focused spot happens to be on the optic nerve, total blindness may result: if it falls elsewhere on the retina, an extra blind spot may be generated. Although the constant motion of the human eye tends to prevent the focused spot from remaining at a particular point on the retina for very long, always obey the following universal rule: *Never look down any laser beam either directly or by specular reflection*. In practice, laser beams below 1 mW CW are probably not an eye hazard, but they should still be treated with respect. A beam must be below about 10 μW before most workers would regard it as really safe.

The safe exposure level for CW laser radiation depends on the exposure time. For pulsed lasers, however, it is the maximum energy that can enter the eye without causing damage that is the important parameter. In the spectral region between 380 and 1.5 μm, where the interior material of the eye is transparent, the maximum safe dose is on the order of 10^{-7} J/cm^2 for *Q*-switched lasers and about 10^{-6} J/cm^2 for non-*Q*-switched lasers. If any potential for eye exposure to a laser beam or its direct or diffuse reflection exists, it is advisable to carry out the experiment in a lighted laboratory: in a darkened laboratory, the fully dark-adapted human eye with a pupil area of about 0.5 cm^2 presents a much larger target for accidental exposure. The Laser Institute of America publishes a guide that shows the maximum permitted exposure in terms of power and direction for a range of laser wavelengths.[128]

Infrared laser beams beyond about 1.5 μm are not a retinal hazard, as they will not penetrate to the retina. Beams between 1.5 and 3 μm penetrate the interior of the eye to some degree. Because its energy is absorbed in a distributed fashion in the interior of the eye, 1.55 μm is one of the safest laser wavelengths. Lasers beyond 3 μm are a burn hazard, and eye exposure must be avoided for this reason. CO_2 lasers, for example, which operate in the 10 μm region, are less hazardous than equivalent-intensity argon-ion or neodymium lasers. Neodymium lasers represent a particularly severe hazard: they are widely used, emit substantial powers and energies, and operate at the invisible wavelength of 1.06 μm. This wavelength easily penetrates to the retina, and the careless worker can suffer severe eye damage without any warning. The use of safety goggles is strongly recommended when using such lasers. These goggles absorb or reflect 1.06 μm, but allow normal transmission in at least part of the visible spectrum. Laser safety goggles are available commercially from several sources, such as Bollé, Control Optics, Glendale, Kentek, Lase-R Shield, Melles Griot, Newport, NOIR, Thorlabs, and UVEX. The purchaser must usually specify the laser wavelength(s) for which the goggles are to be used.

Unfortunately, one problem with goggles prevents their universal use. Because the goggles prevent the laser wavelength from reaching the eyes, they prevent the alignment of a visible laser beam through an experiment by observation of diffuse reflection of the beam from components in the system. When such a procedure must be carried out, we recommend caution and the operation of the laser at its lowest practical power level during alignment. Frequently, a weak, subsidiary alignment laser can be used to check the potential path of a high-power beam before this is turned on – a strongly recommended procedure. For infrared laser beams, thermal sensor cards are available that will reveal the location of an infrared laser beam through thermally activated fluorescence or fluorescence quenching. They are

available from Applied Scintillation Technology, Laser S.O.S., Macken Instruments, Newport, and Solar TII. Some of these sensor cards or plates, especially for CO_2 laser beam location, require illumination with a UV source. Where an infrared laser beam strikes the illuminated surface a dark spot appears. Used Polaroid film and thermally sensitive duplicating paper are also useful for infrared-beam tracking.

The beam from an ultraviolet laser can generally be tracked with white paper, which fluoresces where the beam strikes it. A potential burn and fire hazard exists for lasers with power levels above about 1 W/cm^2, although the fire hazard will depend on the target. Black paper burns most easily. Very intense beams can be safely dumped onto pieces of firebrick. Pulsed lasers will burn at output energies above about 1 J/cm^2.

In the United States, commercial lasers are assigned a rating by the FDA Center for Devices and Radiological Health, which identifies their type, power output range, and potential hazard. It must be stressed, however, that lasers are easy to use safely: accidents of any sort have been rare. Their increasing use in laboratories requires that workers be well-informed of the standard safety practices. For further discussion of this and all aspects of laser safety and related topics, we recommend both the book by Sliney and Wolbarsht[129] and a series of articles on laser safety in the *CRC Handbook of Laser Science and Technology*, Vol. 1.[130]

4.7 OPTICAL DISPERSING INSTRUMENTS

Optical dispersing instruments allow the spectral analysis of optical radiation or the extraction of radiation in a narrow spectral band from some broader spectral region. In this general category we include interference filters, prism and grating monochromators, spectrographs and spectrophotometers, and interferometers. Interferometers have additional uses over and above direct spectral analysis – including studies of the phase variation over an optical wavefront, which allow the optical quality of optical components to be measured. Spectrometers, or *monochromators* as they are generally called, are optical filters of tunable center wavelength and bandwidth. The output narrow-band radiation from these devices is generally detected by a photon or thermal detector, which generates an electrical signal output. *Spectrographs*, on the other hand, record the entire spectral content of an extended bandwidth region either photographically, or more commonly these days with a linear detector area. *Spectrophotometers* are complete commercial instruments, which generally incorporate a source or sources, a dispersing system (which may involve interchangeable prisms and/or gratings), and a detector. They are designed for recording ultraviolet, visible, or infrared absorption and emission spectra.

Spectrofluometers are instruments to record fluorescence spectra. In such an application two principal modes of spectral usage exist. The emission fluorescence spectrum is the spectral distribution of emission produced by a particular monochromatic excitation wavelength. The excitation spectrum is the total fluorescence emission recorded as the wavelength of the excitation source is scanned.

Before giving a discussion of important design considerations in the construction of various spectrometers and interferometers, it is worthwhile mentioning two important figures of merit that allow the evaluation and comparison of the performance of different types of optical dispersing instruments. The first is the resolving power, ($\Re = \lambda/\Delta\lambda$, which has already been discussed in connection with diffraction gratings (Section 4.3.5). The second is the luminosity, which is the flux collected by a detector at the output of a spectrometer when the source at the input has a radiance of unity. The interrelation between resolving power and luminosity for spectrometers using prisms, gratings, and Fabry–Perot etalons has been dealt with in detail by Jacquinot.[131]

Prism spectrometers have almost disappeared from use in recent years, however, because of their simple mode of operation they serve as an archetype in discussing spectrometer performance.

Figure 4.148, which shows the essential components of a prism monochromator, will serve to illustrate the points made here. High resolution is clearly obtained in this arrangement by using narrow entrance and exit slits. The maximum light throughput of the spectrometer results when the respective angular widths W_1, W_2 of the input and output slits θ_1, θ_2 satisfy:

$$W_1 = W_2 \tag{4.235}$$

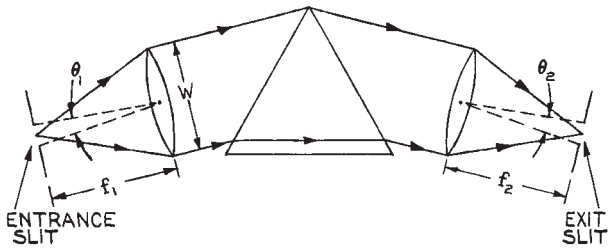

Figure 4.148 Basic elements of a prism monochromator.

where

$$W_1 = \frac{\theta_1}{(\mathrm{d}\alpha/\mathrm{d}\lambda)_\delta}, \quad W_2 = \frac{\theta_2}{(\mathrm{d}\delta/\mathrm{d}\lambda)_\alpha} \tag{4.236}$$

The angles α are the same as those used in Figure 4.47. The input and output dispersions $(\mathrm{d}\alpha/\mathrm{d}\lambda)_\delta$ and $(\mathrm{d}\delta/d\lambda)_\alpha$ are only equal in a position of minimum deviation, or with a prism (or grating) used in a Littrow arrangement. If diffraction at the slits is negligible, the intensity distribution at the output slit when a monochromatic input is used is a triangular function, as shown in Figure 4.149, where W is the spectral width of the slits given by:

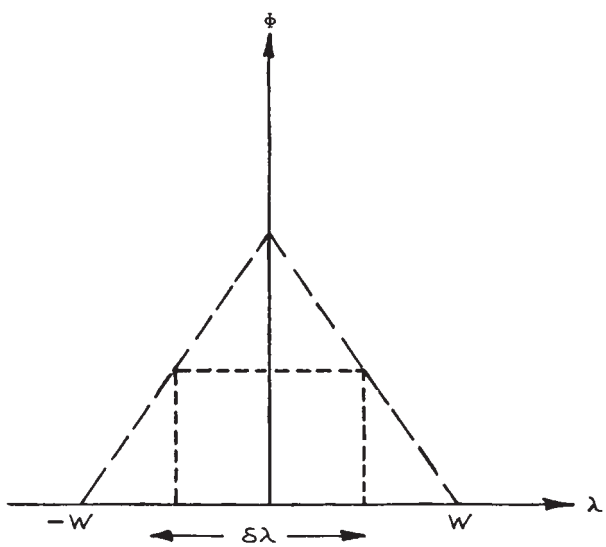

Figure 4.149 Intensity distribution at the output slit of a monochromator whose entrance and exit slits have the same spectral width W.

$$W = W_1 = W_2 \tag{4.237}$$

The limit of resolution of the monochromator is:

$$\delta\lambda = W = \frac{\theta_2}{(\mathrm{d}\delta/\mathrm{d}\lambda)_\alpha} \tag{4.238}$$

The maximum flux passing through the output slit is:

$$\Phi = TE_\mathrm{e}(\lambda)Sl\theta_2/f_2 \tag{4.239}$$

where S is the normal area of the output beam, T is the transmittance of the prism (or efficiency of the grating in the order used) at the wavelength being considered, l is the height of the entrance and exit slits (equal), and $E_e(\lambda)$ is the radiance of the monochromatic source of wavelength λ illuminating the entrance slit. $l\theta_2/f_2$ is the solid angle that the exit slit subtends at the output focusing lens. Equation (4.239) can be written as:

$$\Phi = \frac{TE_\mathrm{e}(\lambda)Sl\lambda(\mathrm{d}\delta/\mathrm{d}\lambda)_\alpha}{f_2\Re} \tag{4.240}$$

which clearly shows that the output flux is inversely proportional to the resolving power [for a continuous source at the entrance slit, Equation (4.240) is multiplied by an additional factor $\lambda/\Re$]. The efficiency E of the monochromator is defined by the equation:

$$E = \frac{TSl}{f}\left(\frac{\mathrm{d}\delta}{\mathrm{d}\lambda}\right)_\alpha \tag{4.241}$$

where we have assumed the usual case in which $f_1 = f_2 = f$.

To collect all the light from the collimating optics in the arrangement of Figure 4.148, the prism or grating should have a normal area at least as large as the aperture of the collimating optics. Thus, the height of the prism (or diffraction grating) should be $h \geqslant W$. The ratio f/W, which is a measure of the light-gathering power of the monochromator, defines its f/number. The most efficient way to use a spectrometer of any kind is to send the input radiation into the entrance slit within the cone of angles defined by the f/number. The maximum resolution is obtained if the input f/number matches the spectrometer f/number. If radiation enters the spectrometer with an f/number that is too small, this radiation overfills the dispersing element and some is wasted. This can be

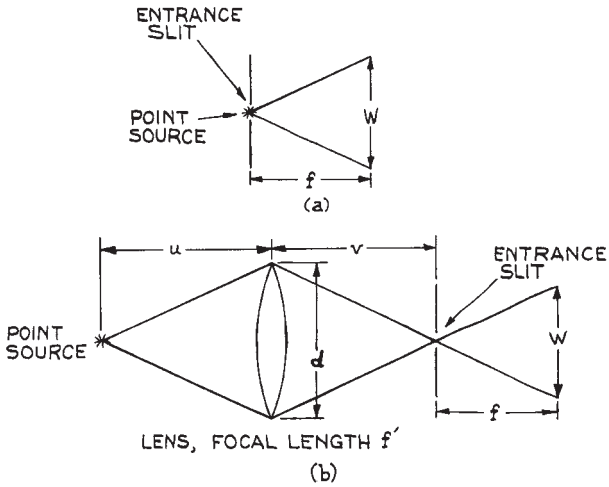

Figure 4.150 Schematic diagrams illustrating geometrical factors involved in optimizing light-collection efficiency by a spectrometer of aperture *W*: (a) point source directly at entrance slit; (b) remote point source imaged on entrance slit with a lens.

illustrated with the aid of Figure 4.150, which shows the use of a point source directly at the entrance slit. In Figure 4.150(b) a point source is imaged on the entrance slit using a lens that matches the input radiation to the *f*/number of the spectrometer. In Figure 4.150(a) the fractional useful light collection from the source is:

$$\phi_1 \simeq \frac{\pi W^2}{4f^2} = \frac{\pi}{4F^2} \tag{4.242}$$

where F is the *f*/number of the spectrometer. In contrast, in Figure 4.150(b) it is approximately:

$$\phi_2 \simeq \frac{\pi d^2}{4u^2} \tag{4.243}$$

which can be written as:

$$\phi_2 = \frac{\pi d^2 (v-f)^2}{4f^2 v^2} \tag{4.244}$$

and substituting $v/d = F$, $f/d = F'$ (the *f*/number of the lens), we have:

$$\phi_2 = \frac{\pi (F/F' - 1)^2}{4F^2} \quad (F' \leqslant F) \tag{4.245}$$

Thus, equally efficient light gathering to that which would be obtained with the point source at the entrance slit results if:

$$F' = F/2 \tag{4.246}$$

More efficient light gathering results if F' is less than this value, but, if the lens and point source are incorrectly positioned so that $v/d < F$, then not all the light collected by the lens reaches the dispersing element of the spectrometer.

It is quite common for spectrometers to be used with a fiber optic light-delivery system. If the NA of the fiber is too large and the fiber optic is placed at the entrance of the spectrometer, then overfilling of the dispersing element will occur. In this case correction optics must be included to match the fiber to the *f*/number of the spectrometer.

4.7.1 Comparison of Prism and Grating Spectrometers

Following Jacquinot,[131] we use Equation (4.240) to compare prism and grating instruments. Assume identical values of l and f_2, since, for a given degree of aberration of the system, their values are identical for prisms and gratings. Blazed-grating efficiencies can be high, so T is assumed to be similar for prism and grating. Thus, the comparison of luminosity under given operating conditions of wavelength and resolution depends solely on the quantity $S(\mathrm{d}\delta/\mathrm{d}\lambda)_\alpha$ for a prism and $S(\mathrm{d}\beta/\mathrm{d}\lambda)_\alpha$ for a grating.

For the prism:

$$\frac{\mathrm{d}\delta}{\mathrm{d}\lambda} = \frac{t}{W}\frac{\mathrm{d}n}{\mathrm{d}\lambda} \tag{4.247}$$

where, for maximum dispersion, the whole prism face is illuminated, so that t is the width of the prism base. $S = hW$ and $th = A$, the area of the prism base, and so:

$$S\frac{\mathrm{d}\delta}{\mathrm{d}\lambda} = A\frac{\mathrm{d}n}{\mathrm{d}\lambda} \tag{4.248}$$

For the grating:

$$\frac{\mathrm{d}\beta}{\mathrm{d}\lambda} = \frac{m}{d\cos\beta} \tag{4.249}$$

$S = A\cos\beta$, where A is the area of the grating. If it is assumed that the grating is used in Littrow, then $m\lambda = 2d \sin\beta$, and therefore:

$$S\frac{\mathrm{d}\beta}{\mathrm{d}\lambda} = \frac{2A\sin\beta}{\lambda} \tag{4.250}$$

Table 4.9 Main characteristics of optical dispersing elements

Element	Advantages	Disadvantages
Multilayer dielectric interference filter	High throughput at center frequency, ≃50%. Tunable to some extent by tilting.	Low resolution – minimum bandwidth ≃1 nm. None available at short wavelengths ⩽ 200 nm.
Prism spectrometer	Dispersion and resolution increase near absorption edge of prism (however, transmission falls).	Cannot be used below 120 nm (with LiF prism).
	No ghosts.	Resolution not as good as grating spectrometer, best ≃0.01 nm.
	Scattered light can be lower than in grating spectrometer.	Resolution particularly poor in infrared
	No order sorting necessary.	.
Grating spectrometer	Resolution can be high (⩽0.001 nm). Can be used from vacuum UV to far IR.	Ghosts can be a problem. Expensive if really low scattered light required – may need double- or triple-grating instrument.
	Dispersion independent of wavelength.	Need to remove unwanted orders (not necessarily a serious problem).
	Luminosity depends on blaze angle, but generally much higher than for prism spectrometer.	
Fabry–Perot interferometer	Very high light throughput – much higher than for grating spectrometer. Very high resolution – tens of MHz at optical frequencies (⩾10^{-5} nm).	Many orders generally transmitted simultaneously. Cannot be used at short wavelengths (⩽200 nm). Transmission maximum can be scanned only over narrow range. Most difficult dispersing element to use.

The ratio of luminosities for a prism and grating of comparable size is therefore:

$$\rho = \frac{\Phi(\text{prism})}{\Phi(\text{grating})} = \frac{\lambda \mathrm{d}n/\mathrm{d}\lambda}{2\sin\beta} \qquad (4.251)$$

This ratio can be improved by a factor of two if the prism is also used in Littrow. For a typical value of 30° for β, Equation (4.251) predicts that a grating is always superior to a prism instrument. Except for a few materials in restricted regions of wavelength where $\mathrm{d}n/\mathrm{d}\lambda$ becomes large and ρ may reach 0.2–0.3, a grating is more luminous than a prism by a factor of 10 or more. The only potential advantage of a prism instrument over a grating is the absence of overlapping orders. A grating instrument illuminated simultaneously with 300 and 600 nm, for example, will transmit both at the same angular position; a prism instrument will not. This minor problem is easily solved with an appropriate order-sorting color or interference filter.

Jacquinot[131] has demonstrated that a Fabry–Perot etalon or interferometer (see Section 4.7.4) used at a high or moderate resolving power is superior in luminosity to a grating instrument by a factor that can range from 30 to 400 or more. In general, an etalon cannot be used alone, because of its many potential overlapping orders. It is usual to couple it with a grating or prism monochromator in high-resolution spectroscopic applications, except in those cases where the source is already highly monochromatic.

Table 4.9 gives a comparison of the performance characteristics of prism and grating monochromators and

Fabry–Perot interferometers. From the vacuum ultraviolet (prism instruments cannot be used below about 1200 Å) to the far infrared, grating instruments are much superior to comparable-size prism instruments in both resolving power and luminosity. In recent years, the advantages of grating instruments over prism instruments has virtually eliminated the latter. This has primarily resulted because of improvements in grating fabrication. Holographic plane gratings have fewer and weaker ghosts than metal gratings, and holographic curved gratings have allowed aberration reduction in spectrometers. Apart from the minor inconvenience of potential overlapping orders, grating instruments are almost always to be preferred over prism instruments. There is one exception worth noting: when a monochromator is being used to observe some weak optical emission in the simultaneous presence of a strong laser beam, unless the optical emission is too close in wavelength to the laser for prism resolution to be adequate. In this application, a prism avoids the problems of ghost emission or grating scattering. A good prism has very low scattered light. It is common to predisperse a light beam with a prism before sending the beam into the entrance slit of a monochromator, in order to avoid both the overlapping-order problem and spurious signals from a very strong light signal at another wavelength. Fabry–Perot interferometers have very high resolution and luminosity, but require careful and regular adjustment to maintain high performance. They are used only where their very high resolution is essential, frequently in conjunction with a grating monochromator for pre-isolation of a narrow spectral region.

A final point to note with regard to the use of grating spectrometers: these instruments are polarization sensitive. If unpolarized light strikes a grating, the diffracted light will be partially polarized because the grating efficiency is wavelength-, and *S* and *P* polarization-dependent.

4.7.2 Design of Spectrometers and Spectrographs

The construction of monochromators and spectrographs is a specialized undertaking. The availability of good commercial instruments generally makes it unnecessary for anyone but the enthusiast to contemplate their construction in the laboratory. On the other hand, the principles that underlie good design in a dispersing instrument are not complex. Some essential features of such instruments can be illustrated with reference to particular designs that are used both in laboratory and commercial instruments. Attention will be restricted to monochromators; spectrographs are similar, apart from having an array detector or photographic plate instead of an exit slit, as shown in Figure 4.151. Spectrographs are also simpler in construction because wavelength scanning is not required and all optical components of the system remain fixed. The discussion here should also allow intelligent evaluation and comparison of commercial instruments. For further details of the many different instrument designs that have been used for the construction of monochromators, spectrographs and spectrophotometers, References[132,133], *The Photonics Design and Applications Handbook*[134], and the catalogs of instrument manufacturers should be consulted.

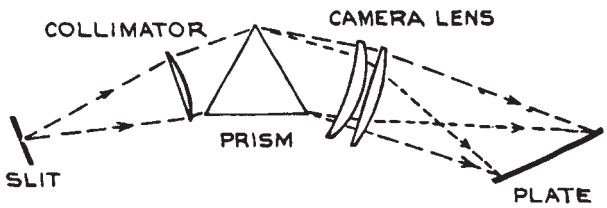

Figure 4.151 Schematic diagram of a simple prism spectrograph. (From R.J. Meltzer, "Spectrographs and Monochromators," in *Applied Optics and Optical Engineering*, Vol. 5, R. Kingslake (Ed.), Academic Press, New York, 1969; by permission of Academic Press.)

Figure 4.152 shows a Littrow prism monochromator. The light from the input slit is collimated with an off-axis paraboloidal mirror. The output wavelength is changed by rotating the Littrow mirror. If the output wavelength must change uniformly with rotation of a drive shaft, then the rotation of the mirror requires a cam. Figure 4.153 shows a Czerny–Turner prism configuration. The collimating mirrors are spherical. In the geometry of Figure 4.153(a), the coma of one mirror compensates that of the other, while in Figure 4.153(b) these comas are additive. The wavelength is changed by rotating the prism.

In any of these spectroscopic instruments, the optical arrangement should be enclosed in a light-tight enclosure

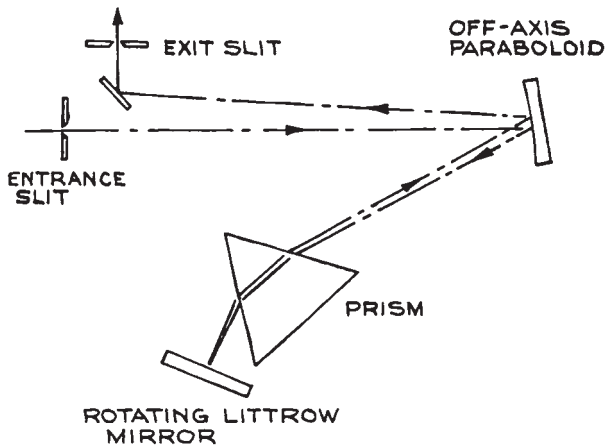

Figure 4.152 Littrow monochromator. (From R.J. Meltzer, "Spectrographs and Monochromators," in *Applied Optics and Optical Engineering*, Vol. 5, R. Kingslake (Ed.), Academic Press, New York, 1969; by permission of Academic Press.)

painted on its interior with black nonreflective paint. Table 4.10 lists the various "black" coatings that are available for this purpose and in any application where broad reflection over a range of angles from a surface must be minimized. This helps to minimize scattered light. It is essential that light passing through the entrance slit is not able to reach the exit slit without going through the illuminating optics and prism. To this end, it is common practice to incorporate internal blackpainted baffles in the monochromator enclosure. The most likely source of scattered light is overillumination of the input collimator: input radiation should not enter with an *f*/number smaller than that of the monochromator. To check for stray light, visual observation through the exit slit in a darkened room when the entrance slit is illuminated with an intense source will reveal where additional internal baffles would be helpful. Stray light is more likely to be a problem in a Littrow arrangement than in a straight-through type, such as the Czerny–Turner.

In the visible and near infrared, lens collimating optics can be used, as, for example, in the design shown in Figure 4.151. Good lenses, such as camera lenses, should be used. Mirror collimating optics are useful over a much broader wavelength region. For ultraviolet use they

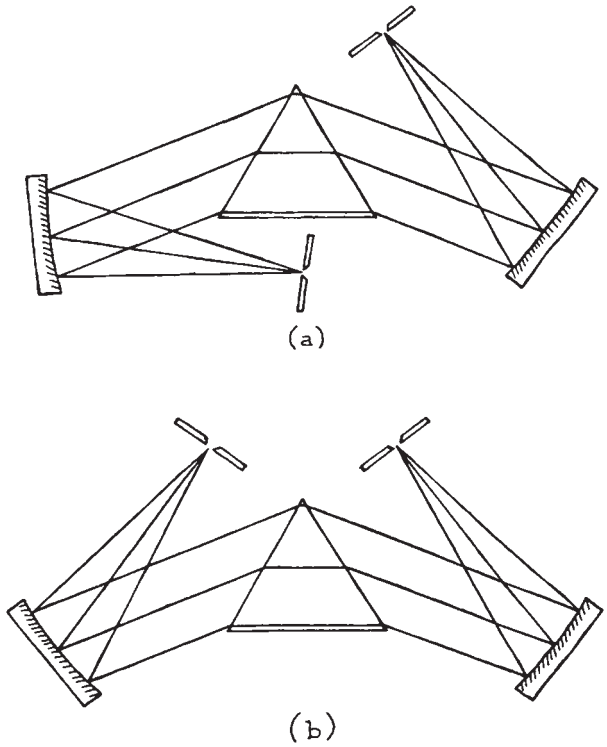

Figure 4.153 Czerny–Turner monochromator arrangements; (a) coma of one mirror compensates that of the other; (b) comas are additive.

should be aluminum overcoated with MgF_2, and they are frequently of this type, even in instruments designed for longer wavelengths.

Slit design is important in achieving high resolution. Entrance and exit slits of equal width are generally used. If the source is small, having a height much less than the height of the prism or grating, parallel-sided slits are adequate. Adjustable versions are available from Melles Griot, Newport, and OptoSigma. Fixed slits can be easily made using razor blades or purchased from Melles Griot or National Aperture. If the source is high compared to the height of the dispersing element, a straight entrance slit produces a curved image at the exit slit. In the case of a prism, this happens because light passing through the prism at an angle inclined to the meridian plane suffers slightly more deviation than light in the meridian plane.

Table 4.10 Black materials and coatings

Material	Absorptivity
Anodized black	0.88
Carbon lampblack	0.84
Chemglaze black paint Z306	0.91
Delrin black plastic	0.87
Electro-optical industries Mid-temperature black coating (up to 200 °C)	0.965
Electro-optical industries High-temperature black coating (up to 1400 °C)	0.93
Martin black velvet paint	0.94
3M black velvet paint	0.91
Parsons black paint	0.91
Polyethylene black plastic	0.92
Anodized aluminum	0.84

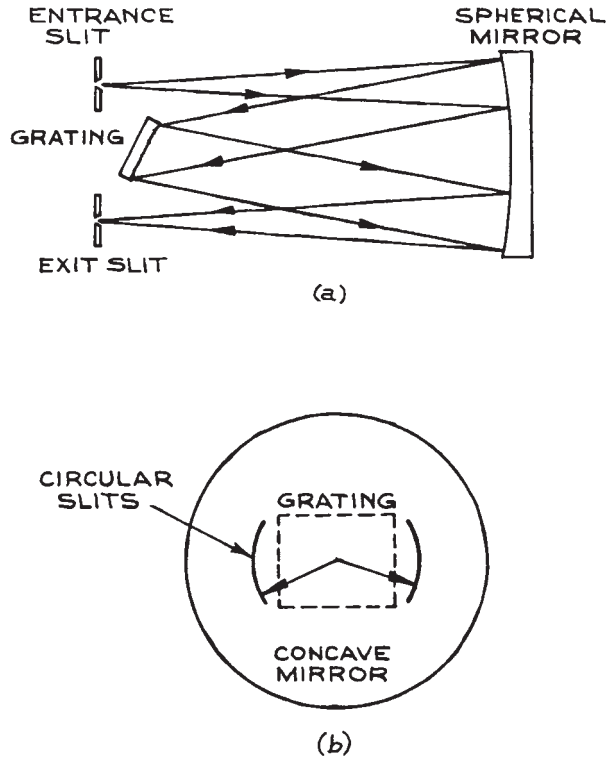

Figure 4.154 (a) Ebert–Fastie monochromator; (b) curved entrance- and exit-slit configuration for use with the above.

Light striking a grating in a plane that is not perpendicular to the grating grooves sees an apparently smaller groove spacing, and is consequently deviated more than light in the plane perpendicular to the grating. To maintain high resolution in the presence of image curvature, curved entrance and exit slits should be used, each with a radius equal to the distance of the slit from the axis of the system. This slit arrangement is shown in Figure 4.154, which also shows a very good, and widely used, grating monochromator design due to Fastie[135] (based on a design originally described by Ebert[136] for use with a prism). It is also quite common for the single spherical mirror in Figure 4.154 to be replaced by a pair, in which case the design becomes the Czerny–Turner one. Such an arrangement is shown in Figure 4.155. In either case the wavelength is tuned by rotating the grating. The wavelength variation at the exit slit is much more nearly linear with grating rotation than with prism rotation. If linearity is required, a cam, sine-drive, or other such arrangement is used for rotating the grating or prism.[133] In a Czerny–Turner grating instrument the entrance and exit slits are generally arranged asymmetrically with respect to the grating, as this allows coma to be corrected in the working wavelength range. Czerny–Turner monochromators are available from Edmund Optics, Genesis Laboratory Systems (who now manufacture the former Jarrel-Ash line of spectrometers), Horiba Yobin Yvon, McPherson, Minuteman Laboratories, Ocean Optics, Princeton Intruments/Acton, and Thorlabs.

Grating monochromators for use in the vacuum ultraviolet generally have a concave grating. Such a grating, which has equally spaced grooves on the chord of a spherical mirror, combines both dispersion and focusing in one element. For maximum resolution, both the object and image formed by a concave grating must be on a circle called the *Rowland circle*, whose diameter is the principal radius of the spherical surface on which the grating is ruled, as shown in Figure 4.156. The use of a concave-grating monochromator (or spectrograph) entails mounting grating and slits (or grating, slits, and photographic plate) on a Rowland circle. Adjustment of the instrument will involve moving the grating, slits, or plate on the

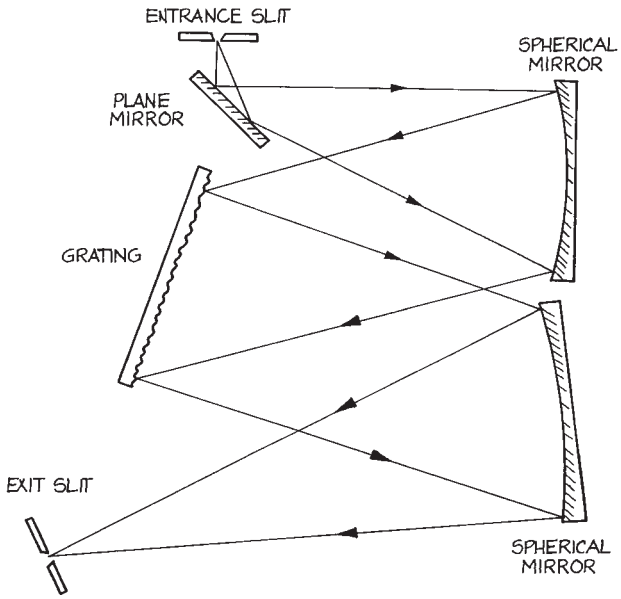

Figire 4.155 Arrangement of a Czerny–Turner grating monochromator.

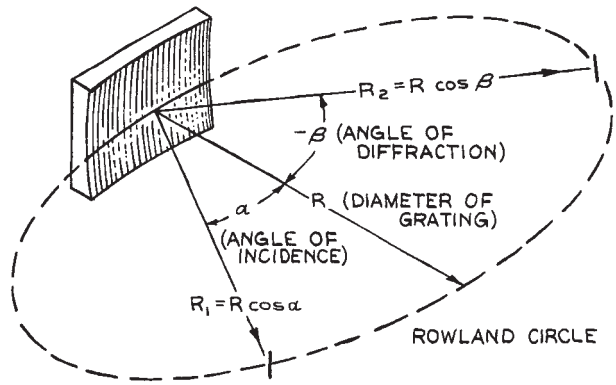

Figure 4.156 Rowland circle of a concave diffraction grating. For maximum resolution, both object and image must be on the Rowland circle. R = object (entrance-slit) distance: R_2 = image (exit-slit) distance. (From R. J. Meltzer, "Spectrographs and Monochromators," in *Applied Optics and Optical Engineering*, Vol. 5, R. Kingslake (Ed.), Academic Press, New York, 1969; by permission of Academic Press.)

circle. Various mounting configurations, such as the Abney, Eagle, Paschen, Rowland, and Wadsworth, and grazing-incidence mounting have been used to accomplish this.

A convenient concave-grating design widely used in vacuum-ultraviolet monochromators is the Seya–Namioka,[137,138] shown in Figure 4.157. In this arrangement, by judicious choice of slit distances from the grating and slit angular separation, the only adjustment needed for wavelength adjustment is rotation of the grating. In comparison with an ideal Rowland-circle mounting, only a small resolution loss results over a wide wavelength range. Vacuum-ultraviolet instruments possess the added complication that all interior adjustments of the instrument must be transmitted through the walls of the vacuum chamber that houses the optical arrangement. Various kinds of rotary-shaft and bellows seals and magnetically coupled drives exist for this purpose.[139] See also Section 3.5.4.

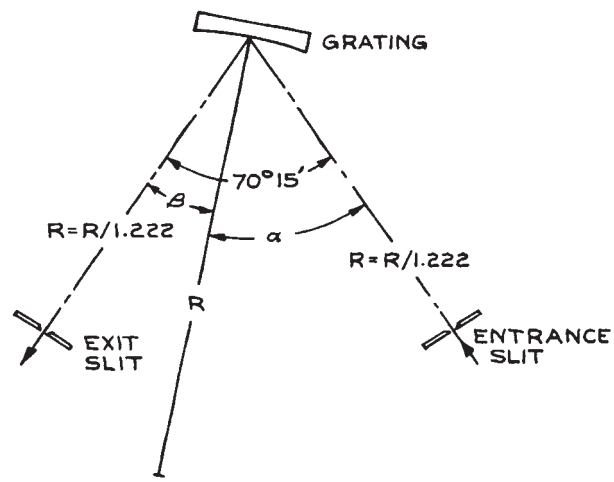

Figure 4.157 Layout of the Seya–Namioka monochromator.

Multiple monochromators use multiple dispersing elements in series to obtain greater dispersion and/or lower scattered light. For example, in a double-grating monochromator, two diffraction gratings move simultaneously; the desired diffracted wavelength from the first grating is diffracted once again from the second grating before being focused on the exit slit. The considerable reduction in scattered light that can be obtained with multiple

monochromators makes them particularly useful for analyzing weak emissions close in wavelength to a strong emission, as in Raman spectroscopy. Instruments with as many as four gratings in series are available commercially. Grating monochromators, spectrographs, and spectrophotometers are available from many manufacturers,[31] including American Holographic, Coherent Scientific, CVI Spectral Products, Horiba Jobin-Yvon (formerly Spex or Instruments SA), Minuteman Laboratories, Newport/Oriel, Olis, Princeton Instruments/Acton, and Thermo Scientific (which incorporates the old companies Jarrell-Ash, Aminco-Bowman, Unicam, and Varian Associates). Fiber-coupled spectrometers are manufactured by Ocean Optics, Photon Control, and Stellar Net. These instruments either consist of a complete spectrometer on a PC card or are compact units connected to a computer through a USB port. McPherson, Minuteman Laboratories, and Princeton Instruments/Acton are noted for their vacuum instruments, Coherent Scientific, Horiba Jobin-Yvon, and Princeton Instruments/Acton for their multiple grating spectrometers, and Genesis Laboratory Systems for their high-resolution spectrometers and spectrographs.

Imaging Spectrographs [sometimes called optical multichannel analysers (OMAs)] image an entire spectrum onto either a linear photodiode area (PDA) or onto a linear CCD. These instruments often have the capability for recording complete spectra from several sources at once. Manufacturers include Horiba Jobin-Yvon, Instrument Systems GmbH, Olis, Nomadics, Princeton Instruments/Acton, and Roper Scientific. Note that CCD arrays are approximately 100 times more sensitive than PDAs, so are best used for the lowest light-level applications. Change-coupled devices must be used with appropriate shutters or light modulation otherwise image ''smear'' will occur. This happens if new light falls on the array while the previous deposited charge distribution is being read out.

Wavemeters are optical devices that are designed to provide direct electronic readout of the wavelength of monochromatic radiation that is directed into them. They are most frequently used in conjunction with a tunable laser system. These convenient instruments incorporate a Fabry–Perot or Fizeau interferometer. Manufacturers include Bristol Instruments, Elliott Scientific, Holo-Spectra, MK Photonics, and Specialise Instruments Marketing.

4.7.3 Calibration of Spectrometers and Spectrographs

To calibrate the wavelength scale of a spectrometer or spectrograph, the entrance slit is illuminated with a reference source that has characteristic spectral features of accurately known wavelength. It is quite common to mount a small reference lamp – mercury, neon, and hollow-cathode iron lamps are the most popular – near the entrance slit and use a small removable mirror or beamsplitter to superimpose the spectrum of the reference on the unknown spectrum under study. To calibrate a grating instrument through its various orders, a helium–neon laser is ideal. If the slits are set to their narrowest position and a low-power (< 1 mW) He–Ne laser is directed at the entrance slit, the various grating settings that transmit a signal (which can be safely observed by eye at the exit slit) correspond to the wavelengths 0, 632.8 nm, 632.8×2 nm, 632.8×3 nm, and so on. By interpolation between the observed values, a reliable calibration curve can be obtained even for instruments operating far into the infrared.

The efficiency of the instrument at a given wavelength can be determined with any suitable detector. A laser or other narrow-band source at the desired wavelength illuminates the entrance slit, or a duplicate of it, and the transmitted power is measured with the detector placed directly behind the slit. A similar measurement is then made at the exit slit of the whole instrument. The relative spectral efficiency can be determined by illuminating the entrance slit with a blackbody source. A lens should not be used for focusing light on the entrance slit, as its collection and focusing efficiency will vary with wavelength. The signal at the output slit is then measured as a function of wavelength with a spectrally flat detector, such as a pyroelectric detector, thermopile, or Golay cell (see Section 7.10), and normalized with respect to the blackbody distribution.

4.7.4 Fabry–Perot Interferometers and Etalons

Fabry–Perot interferometers and etalons are optical filters that operate by multiple-beam interference of light reflected and transmitted by a pair of parallel flat or coaxial spherical reflecting interfaces. In its simplest form, an *etalon* consists of a flat, parallel-sided slab of transparent

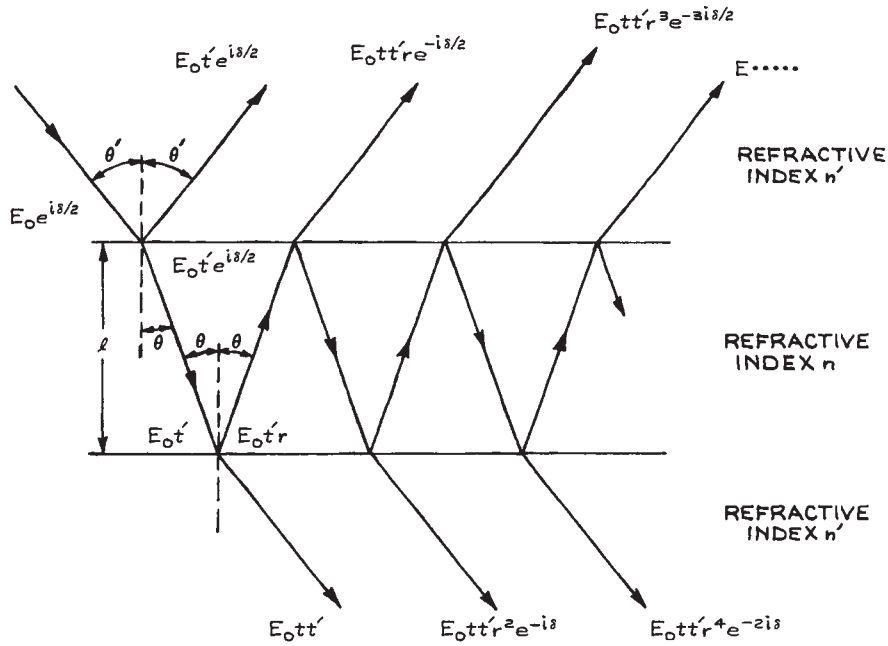

Figure 4.158 Paths of transmitted and reflected rays in a Fabry–Perot etalon. The complex amplitude of the fields associated with the rays at various points is shown.

material, which may or may not have semireflecting coatings on each face. An etalon may also consist of a pair of parallel, air-spaced flat mirrors of fixed spacing. If the reflective surfaces have adjustable spacing, or if their effective optical spacing can be adjusted by changing the gas pressure between the surfaces, the device is called a *Fabry–Perot interferometer*. These devices can be analyzed by the impedance concepts discussed in Section 4.2.6, but it is instructive to discuss their operation from the standpoint of multiple-beam interference.

Figure 4.158 shows the successive reflected and transmitted field amplitudes of a plane electromagnetic wave striking a plane-parallel Fabry–Perot etalon or interferometer at angle of incidence θ'. Although the reflection coefficients at the two reflecting interfaces may be different, only the case where they are equal will be analyzed. Almost all practical devices are built this way. The optical-path difference between successive transmitted waves is $2nl\cos\theta$, where l is the interface spacing and n is the refractive index of the medium between these interfaces (air, glass, quartz, or sapphire, for example). If refraction occurs at the reflecting interfaces, θ and θ' will be related by Snell's law. The phase difference between successive transmitted waves is:

$$\delta = 2kl\cos\theta + 2\epsilon \tag{4.252}$$

where:

$$k = \frac{2\pi}{\lambda} = \frac{2\pi n}{\lambda_0} = \frac{2\pi nv}{c_0} \tag{4.253}$$

and ϵ is the phase change (if any) on reflection.

The total resultant transmitted complex amplitude is:

$$\begin{aligned} E_T &= E_0tt' + E_0tt'r^2e^{-i\delta} + E_0tt'r^4e^{-2i\delta} + \ldots \\ &= \frac{E_0tt'}{1 - r^2e^{-i\delta}} \end{aligned} \tag{4.254}$$

Here r and t are the reflection and transmission coefficients of the waves passing from the medium of refractive index n to that of refractive index n' at each interface, r' and t' are the corresponding coefficients for passage from n' to n, and E_0 is the amplitude of the incident electric field.

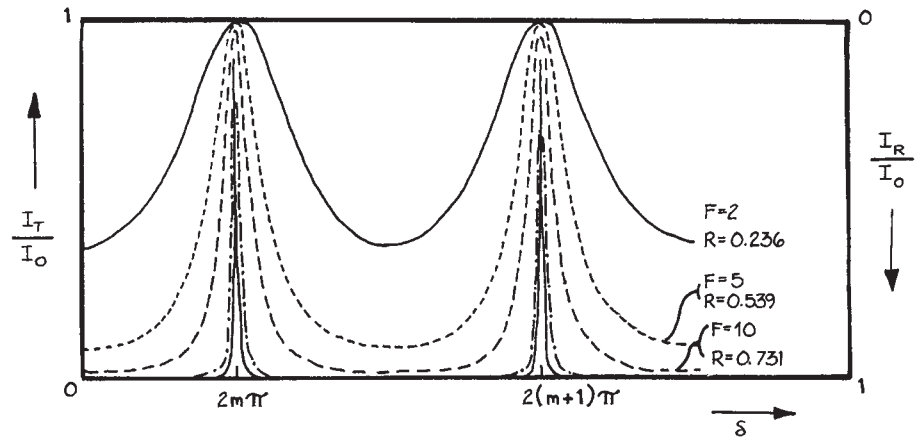

Figure 4.159 Transmission and reflection characteristics of a Fabry-Perot etalon.

The total transmitted intensity is:

$$I_T = \frac{|E_T|^2}{2Z} = \frac{I_0|tt'|^2}{|1 - r^2 e^{-i\delta}|^2}. \tag{4.255}$$

Here $|tt'| = T$ and $|r|^2 = |r'|^2 = R$, where T and R are the transmittance and reflectance of each interface. If there is no energy lost in the reflection process:

$$T = 1 - R \tag{4.256}$$

If the etalon had slightly absorbing reflective layers, this would no longer be true; if each layer absorbed a fraction A of the incident energy, then:

$$T = 1 - R - A \tag{4.257}$$

If $A = 0$, Equation (4.255) gives:

$$\frac{I_T}{I_0} = \frac{1}{1 + \frac{4R}{(1-R)^2}\sin^2\frac{\delta}{2}} \tag{4.258}$$

This variation of transmitted intensity with δ is called an Airy function and is illustrated in Figure 4.159 for several values of R. The variation of reflected intensity with δ is just the inverse of Figure 4.159, since:

$$\frac{I_R}{I_0} = 1 - \frac{I_T}{I_0} \tag{4.259}$$

If $A \neq 0$, Equation (4.258) becomes:

$$\frac{I_T}{I_0} = \frac{\left(\frac{T}{1-R}\right)^2}{1 + \frac{4R}{(1-R)^2}\sin^2\frac{\delta}{2}} \tag{4.260}$$

In either case, maximum transmitted intensity results when:

$$\delta = 2m\pi \tag{4.261}$$

where m is an integer. If the phase change on reflection is neglected, this reduces to:

$$2l\cos\theta = m\lambda \tag{4.262}$$

where λ is the wavelength of the light in the medium between the two reflecting surfaces (plates). In normal incidence, transmission maxima result when:

$$l = m\lambda/2 \tag{4.263}$$

Even if the phase change on reflection is included, the adjustment in spacing necessary to go from one transmission maximum to the next is one half-wavelength. Thus, for example, the transmitted intensity as a function of plate separation when a Fabry–Perot interferometer is illuminated normally with plane monochromatic light is also as shown in Figure 4.159. In an ideal Fabry–Perot device,

the overall transmittance at a transmission-intensity maximum is unity, whereas in a practical device, which will invariably have some losses, the maximum overall transmittance is reduced by a factor $[T/(1-R)]^2$. As is clear from Figure 4.159, the transmission peaks of the device become very sharp as R approaches unity.

Free Spectral Range, Finesse, and Resolving Power. If a particular transmission maximum for fixed I occurs for normally incident light of frequency v_0, then:

$$v_0 = \frac{mc}{2l} \tag{4.264}$$

where c is the velocity of light in the material between the plates. Of course, the device will also show transmission maxima at all frequencies $v_0 \pm pc/2l$ as well, where p is an integer. The frequency between successive transmission maxima is called the *free spectral range*:

$$\Delta v = \frac{c}{2l} \tag{4.265}$$

When R is close to unity, all phase angles δ within a transmission maximum differ from the value $2m\pi$ by only a small angle. Thus, we can write:

$$\delta = \frac{4\pi v l}{c} = \frac{4\pi v_0 l}{c} + \frac{4\pi(v - v_0)l}{c} \tag{4.266}$$

which can be written in the form:

$$\delta = 2m\pi + \frac{2\pi(v - v_0)}{\Delta v} \tag{4.267}$$

Equation (4.258) becomes:

$$\frac{I_T}{I_0} = \frac{1}{1 + \dfrac{4R\pi^2}{(1-R)^2}\left(\dfrac{v - v_0}{\Delta v}\right)^2} \tag{4.268}$$

Writing $\pi\sqrt{R}/(1-R) = F$, where F is called the *finesse*, the shape of a narrow transmission maximum can be written as:

$$\frac{I_T}{I_0} = \frac{1}{1 + \left[2(v - v_0)/\Delta v_{1/2}\right]^2} \tag{4.269}$$

Here $\Delta v_{1/2}$, the full width at half maximum transmission of the transmission peak, is given by:

$$\Delta v_{1/2} = \Delta v/F \tag{4.270}$$

The *resolving power* of a Fabry–Perot device is a measure of its ability to distinguish between two closely spaced monochromatic signals. A good criterion for determining this is the *Rayleigh criterion*, which recognizes two closely spaced lines as distinguishable if their half-intensity points on opposite sides of the two line shapes are coincident, as shown in Figure 4.160. Thus, for a Fabry–Perot device the resolving power is:

$$\Re = \frac{v}{\Delta v_{1/2}} = \frac{Fv}{\Delta v} \tag{4.271}$$

It would appear that very high resolving powers can be obtained by the use of high-reflectance plates (and consequent high finesse values, as illustrated in Table 4.11) and/or large plate spacings (and consequent small free spectral ranges). Additional practical considerations limit how far these approaches to high resolution can actually be used.

Practical Operating Configurations and Performance Limitations of Fabry–Perot Systems. The use of very high reflectance values to obtain improved resolving power is limited by the ability of the optical polisher to achieve ultraflat optical surfaces. Very good-quality plates for use in the visible can be obtained with flatnesses of $\lambda/200$ over regions a few

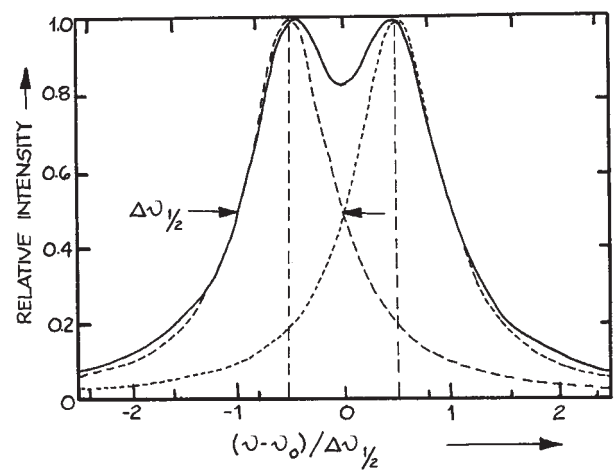

Figure 4.160 Two monochromatic spectral lines just resolved according to the Rayleigh criterion.

Table 4.11 Properties of Fabry-Perot etalons

Plate Separation l (cm)	Reflectance R (%)	Free Spectral Range $\Delta\upsilon = c/2Z$ Hz	Finesse $\mathrm{F} = \pi\sqrt{\frac{R}{(1-R)}}$	Resolving Power $R = F\upsilon/\Delta\upsilon$
0.1	80	1.5×10^{11}	14	5.6×10^{4}
0.1	90	1.5×10^{11}	30	1.2×10^{5}
0.1	95	1.5×10^{11}	61	2.44×10^{5}
0.1	99	1.5×10^{11}	313	1.25×10^{6}
1.0	80	1.5×10^{10}	14	5.6×10^{5}
1.0	90	1.5×10^{10}	30	1.2×10^{6}
1.0	95	1.5×10^{10}	61	2.44×10^{6}
1.0	99	1.5×10^{10}	313	1.25×10^{7}
10.0	80	1.5×10^{9}	14	5.6×10^{6}
10.0	90	1.5×10^{9}	30	1.2×10^{7}
10.0	95	1.5×10^{9}	61	2.44×10^{7}
10.0	99	1.5×10^{9}	313	1.25×10^{8}

Note: Properties shown are at 500 nm (600 THz).

centimeters in diameter. Some claims of flatness in excess of $\lambda/200$ are also seen. These should be viewed with skepticism – such a degree of flatness is extremely difficult to verify. If the plates have surface roughness Δs, the average error in plate spacing is $\sqrt{2}\Delta s$. This gives rise to a spread in the frequency of transmission maxima equal to:

$$\Delta v_s \simeq \frac{mc\Delta s}{\sqrt{2}l^2} \simeq \sqrt{2}v_0\frac{\Delta s}{l} \tag{4.272}$$

Thus the flatness-limited finesse is:

$$F_s = \frac{\Delta v}{\Delta v_s} = \frac{1}{\sqrt{2}}\left(\frac{\Delta v}{v_0}\right)\frac{l}{\Delta s} = \frac{\lambda}{2\sqrt{2}\Delta s} \tag{4.273}$$

For example, two plates with surface roughness of $\lambda/200$ would have a flatness-limited finesse of about 71. The use of super mirrors has allowed finesse values to 30 000 to be achieved. In practice, Fabry–Perot plates may not be randomly rough, and their stated flatness figure may represent the average deviation from parallelism of the two plates. In this case, the parallelism-limited finesse is:

$$F_\rho = \frac{\lambda}{2\Delta s} \tag{4.274}$$

where Δs is the deviation from parallelism over the used aperture of the system. Thus, for example, with a 1 cm aperture, a 1/100 arc-second deviation from parallelism would imply $\Delta s = 4.84$ nm and a parallelism-limited finesse of only 56 at 546 nm. Depending on the definition of what is meant by surface roughness and deviation from parallelism, Equations (4.273) and (4.274) may take slightly different forms.[139]

Fabry–Perot plates must be held very nearly parallel to achieve high resolution. Also, their separation should not be allowed to drift. A random variation of Δs will limit the finesse, as predicted by Equation (4.273). A fractional length change of 10^{-6} in a 1 cm spacing Fabry–Perot device will limit the finesse to only about 27. Thus it must be isolated from vibrational interference to achieve high finesse. Further, if the frequencies of the transmission maxima are not to drift, the change in plate spacing due to thermal expansion must be minimized by constructing the device of low-expansion materials such as Invar,[141] Superinvar,[142] fused silica,[143] or special ceramics.[144]

The resolving power of a Fabry–Perot system is also limited by the range of angles that can be transmitted through the instrument. One popular configuration is shown in Figure 4.161. A small source, or light from an extended source that passes through a small aperture, is collimated by a lens, passes through the interferometer, and is focused onto a second small aperture in front of a detector. The maximum angular spread of rays passing through the system will be governed by the aperture sizes W_1 and W_2 and the two focal lengths f_1 and f_2. In the paraxial-ray

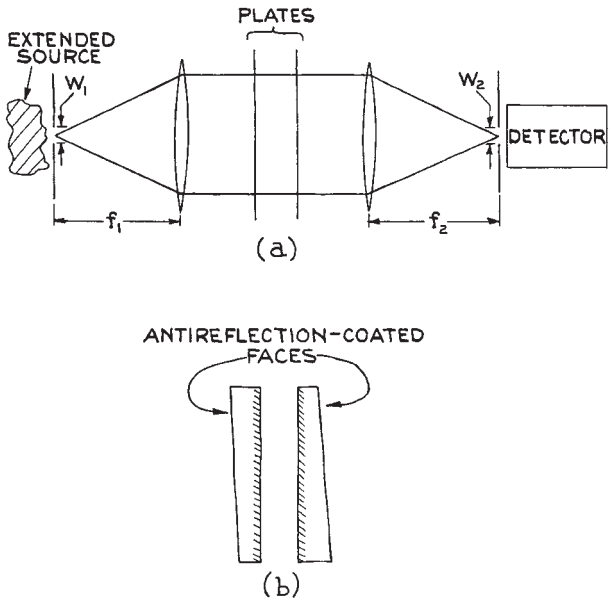

Figure 4.161 (a) Operating scheme for a Fabry–Perot interferometer, using collimated light; (b) detail of typical plate configuration (the wedge angle of the reflecting plates is exaggerated).

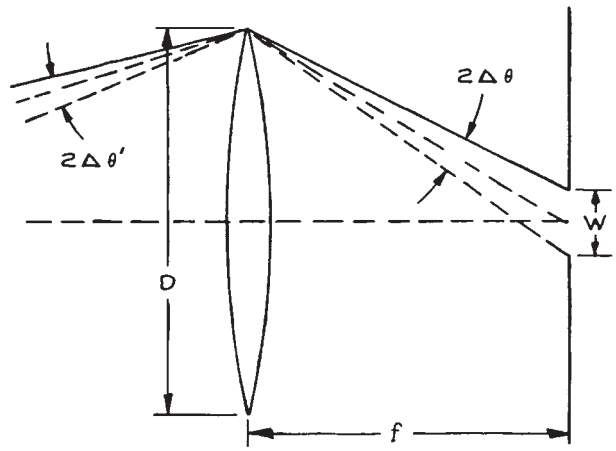

Figure 4.162 Angular factors involved in the collection of light transmitted through a Fabry–Perot interferometer by a circular aperture. In the paraxial-ray approximation, $\Delta\theta' = \Delta\theta$.

approximation, the angular width $2\Delta\theta$ of the paraxial-ray bundle that comes from, or is delivered to, an aperture of diameter W is equal to the angular width $2\Delta\theta'$ that traverses the system, as illustrated in Figure 4.162. In this case:

$$\Delta\theta \simeq W/2f \tag{4.275}$$

In Figure 4.161 the resolving power will be limited by W_1/f_1 or W_2/f_2, whichever is the larger. The transmitted frequency spread associated with an angular spread $\Delta\theta$ around the normal direction is, from Equations (4.262) and (4.264):

$$\Delta\nu_{1/2} = \nu_0(\Delta\theta)^2/2 \tag{4.276}$$

The corresponding aperture-limited finesse is:

$$F_{\mathrm{A}} = \frac{\lambda}{l(\Delta\theta)^2} = \frac{4\lambda f^2}{lW^2} \tag{4.277}$$

For example, using a 1 mm diameter aperture, a 10 cm focal-length lens, and a 1-cm air-spaced Fabry–Perot device at 546.1 nm, the aperture-limited finesse is 218. The operating conditions of a Fabry–Perot system should be arranged so that F_{A} is at least three times larger than the desired operating finesse, which usually is ultimately limited by the flatness-limited finesse. The apertures in Figure 4.161 should be circular and accurately coaxial with both lenses, or the aperture finesse will be further reduced. If the limiting aperture (either a lens or the Fabry–Perot device itself) is D, there is also a diffraction limit to the finesse, which on axis is:

$$F_{\mathrm{D}} = \frac{2D^2}{\lambda nl}. \tag{4.278}$$

At the pth fringe off axis:

$$F_{\mathrm{D}} = \frac{D^2}{2p\lambda nl} \tag{4.279}$$

where n is the refractive index of the material between the plates. The overall finesse of a Fabry–Perot system, F_l, is related to the individual contributions to the finesse, F_i, by

$$F_l^{-2} = \textstyle\sum_i F_i^{-2} \tag{4.280}$$

In the operating configuration of Figure 4.161, if the plate spacing is fixed, then with a broad-band source, all frequencies that satisfy Equation (4.280) will be transmitted. These frequencies become more closely spaced as the plate separation l is increased. There is a concomitant increase in resolution, but this may not prove useful if any of the spectral features under study are broader than the free spectral range. In this case, simultaneous transmission of two broadened spectral features always occurs. For example, for two lines of wavelength λ_1 and λ_2 and of FWHM $\Delta\lambda$, it is usually possible to find two integers m_1 and m_2 such that:

$$\begin{aligned} m_1\lambda_1' &= 2l, \quad |\lambda_1' - \lambda_1| \lesssim \Delta\lambda \\ m_2\lambda_2' &= 2l, \quad |\lambda_2' - \lambda_2| \lesssim \Delta\lambda \end{aligned} \tag{4.281}$$

Thus, for isolated, high-resolution studies of the spectral feature at λ_1, say, all potential interference features such as λ_2 must be filtered out. This is done with a color or interference filter, or a prism or grating monochromator, before the signal is sent to the interferometer. The choice of prefiltering element will depend on the relative wavelength spacing of λ_1 and λ_2 The optical throughput of filters can be very high, 50% or more, but will not allow prefiltering of lines closer than a few nanometers. When very high throughput coupled with high resolution is essential, one or more additional Fabry–Perot devices of appropriate free spectral range can be used. For example, an etalon of spacing 0.01 mm has a free spectral range of about 15 nm. If it has a finesse of 50, its useful transmission bandwidth is 0.3 mn. Such an etalon could be coupled with etalons of spacing 0.1 mm and 1 mm with similar finesse to isolate a band only 0.003 nm wide from an original relatively broad frequency band transmitted through a filter. The final transmitted wavelength of such a combination of etalons can be tuned by tilting.

The wavelength of maximum transmission of a single etalon varies as:

$$\lambda = \lambda_0 \cos\theta \tag{4.282}$$

where λ_0 is the wavelength for maximum transmission in normal incidence. In the interferometer arrangement shown in Figure 4.161(a), wavelength scanning can be accomplished in two ways: by pressure scanning, or by adjusting the axial position of one of the plates with a piezoelectric transducer.[145] To accomplish pressure scanning, the interferometer is mounted in a vacuum- or pressure-tight housing into which gas can be admitted at a slow steady rate. The resultant change of refractive index of the gas between the plates, which is approximately linear with pressure, causes a continuous, unidirectional scanning of the center transmitted frequency. The interferometer should be mounted freely within the housing so that the pressure differential between the interior and exterior of the housing causes no deformation of the interferometer. Pressure scanning is not convenient where rapid or bidirectional scanning is required. Because no geometrical dimensions of the interferometer change during the scan, no change in finesse should occur during scanning.

Piezoelectric scanning is very convenient, but the transducer material must be specially selected to give uniform translation of the moving plate without any tilting – which would cause finesse reduction during scanning. If separate piezoelectric transducers[145] are mounted on the kinematic-mounted alignment drives of the plate holders, it is possible to trim the finesse electronically after good mechanical alignment has been achieved by micrometer adjustment. The alignment of the plates during scanning can be maintained with a servo system.[146,147]

A Fabry–Perot etalon can be used in the configuration shown in Figure 4.163 to give a high-resolution display of a narrow-band spectral feature that cannot be displayed with a scanning interferometer because (for example) the optical signal is a short pulse. In the arrangement shown in Figure 4.163, all rays from a monochromatic source that are incident at angle θ_m on the plates will be transmitted and brought to a focus in a bright ring on a screen if:

$$\cos\theta_m = \frac{m\lambda}{2l} \tag{4.283}$$

In the paraxial approximation, θ_m is a small angle and the radius ρ_m of a ring on the screen is:

$$\rho_m = f\theta_m \tag{4.284}$$

which can be written as:

$$\rho_m = f\sqrt{2 - \frac{m\lambda}{l}} \tag{4.285}$$

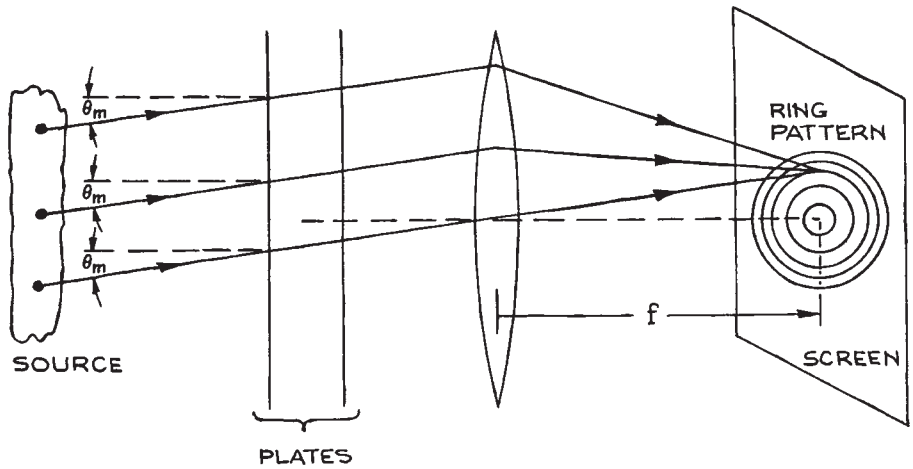

Figure 4.163 Arrangement for observing a ring interference pattern with a Fabry–Perot etalon.

The radius of the smallest ring corresponds to the largest integer m, for which $m\lambda/2l \leqslant 1$. Successive rings going out from the center of the pattern correspond to integers $m-1$, $m-2$, and so on.

If there is a bright spot at the center of the ring pattern, the radius of the pth ring from the center is:

$$\rho_p = f\sqrt{\frac{p\lambda}{l}}. \tag{4.286}$$

This ring will be diffuse because of the finite finesse of the etalon, even if the source is highly monochromatic. The FWHM at half maximum intensity of the pth ring in this case is:

$$\Delta\rho_p = \frac{\rho_p}{2pF} \tag{4.287}$$

which can be verified by expanding Equation (4.260) in the angle θ. This ring width is the same as would be produced by a source of FWHM $\Delta\lambda = \lambda^2/2lF$.

Equation (4.287) predicts that the total flux through each ring of the pattern will be identical, since the area of each ring is:

$$\Delta A = 2\pi\rho_p\Delta\rho_p = \pi f^2/2lF \tag{4.288}$$

The ratio of ring width to ring spacing for the pth ring in the pattern is:

$$\frac{\Delta\rho_p}{\rho_{p+1}-\rho_p} = \left[2Fp\left(1-\sqrt{1+\frac{1}{p}}\right)\right]^{-1} \tag{4.289}$$

which is close to $1/F$ except for the first few rings. Thus observation of the ring pattern from a quasimonochromatic source will yield its approximate bandwidth $\Delta\lambda$ as:

$$\Delta\lambda \simeq \frac{\lambda}{2l}\frac{\Delta\rho}{\rho_{p+1}-\rho_2} \tag{4.290}$$

A convenient way of making a qualitative visual observation of this kind is to use an etalon in conjunction with a small telescope, as shown in Figure 4.164.

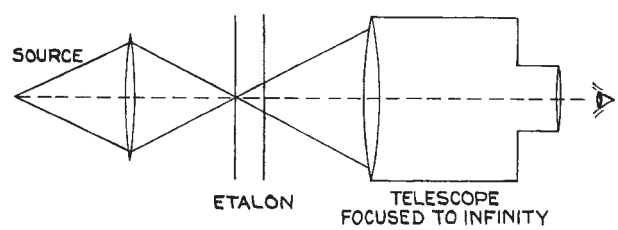

Figure 4.164 Arrangement for visual observation of Fabry–Perot fringes.

Luminosity, Throughput, Contrast Ratio, and Étendue. The luminosity of a Fabry–Perot system is, as already mentioned, much higher than that of any prism or grating monochromator. In the arrangement of Figure 4.161, the luminosity is:

$$\Phi = \left(\frac{T}{1-R}\right)^2 E_e(\lambda) S \frac{\pi W_2^2}{4f_2} \tag{4.291}$$

where $\pi W_2^2/4f_2$ is the solid angle subtended by the output circular aperture at the output focusing lens, and S is the illuminated area of the plates. If the system has an aperture-limited finesse, then, from Equation (4.277) the luminosity becomes:

$$\Phi = \left(\frac{T}{1-R}\right)^2 E_e(\lambda) \frac{\pi \lambda S}{\rho F_A} \tag{4.292}$$

which can be written in terms of the resolving power $\Re$ as:

$$\Phi = \left(\frac{T}{1-R}\right)^2 E_e(\lambda) \frac{2\pi S}{\Re} \tag{4.293}$$

The factor $[T/(1 - R)]^2$ is called the throughput of the system. To compare the luminosity predicted by Equation (4.293) with that of a grating, we shall assume that the throughput of the Fabry–Perot system is equal to the corresponding efficiency factor T of the grating in Equation (4.240). In this case, for identical resolving powers $\Re$, from Equations (4.293) and (4.240), we have:

$$\frac{\Phi(\text{F.P.})}{\Phi(\text{grating})} = \frac{\pi S}{(A \sin \beta)(l/f_2)} \tag{4.294}$$

where l/f_2 is the angular slit height at the output-focusing element of the grating monochromator. For a blaze angle of 30° and equal Fabry–Perot aperture and grating area:

$$\frac{\Phi(\text{F.P.})}{\Phi(\text{grating})} = \frac{\pi}{l/f_2} \tag{4.295}$$

For a 0.3 m focal length grating instrument and a slit height of 3 cm (which is a typical maximum value for a small instrument of this size), the luminosity ratio is 71.4. This probably represents an optimistic comparison as far as the grating instrument is concerned, since high-resolution grating monochromators typically have focal lengths in excess of 0.75 m.

The *contrast ratio* of a Fabry–Perot system is defined as:

$$C = \frac{(I_T/I_0)_{\max}}{(I_T/I_0)_{\min}} \tag{4.296}$$

which from Equation (4.258) clearly has the value:

$$C = \left(\frac{1+R}{1-R}\right)^2 = 1 + \frac{4F^2}{\pi^2} \tag{4.297}$$

The *étendue* U of a Fabry–Perot system is a measure of its light-gathering power for a given frequency bandwidth $\Delta\nu_{1/2}$. It is defined by:

$$U = \Omega S \tag{4.298}$$

where A is the area of the plates and Ω is the solid angle within which incident rays can travel and be transmitted with a specified frequency bandwidth. From Equation (4.276), since $\Omega = \pi\Delta\theta^2$:

$$\Delta\nu_{1/2} = \frac{\nu_0 \Omega}{2\pi} \tag{4.299}$$

Therefore:

$$U = \Omega S = \frac{2\pi \Delta\nu_{1/2}}{\nu_0} \frac{\pi D^2}{4} \tag{4.300}$$

which can be written in the form:

$$U = \Omega S = \frac{\pi^2 D^2 \lambda}{4 l F_1} \tag{4.301}$$

Spherical Mirror Fabry–Perot Interferometers. Fabry–Perot interferometers with spherical concave mirrors are generally used in a confocal arrangement, as shown in Figure 4.165. In this configuration the various characteristics of the interferometer can be summarized as follows:

$$\left(\frac{I_T}{I_0}\right)_{\max} = \frac{T^2}{2(1-R)^2} \tag{4.302}$$

$$\Delta\nu(\text{FSR}) = c/4l \tag{4.303}$$

$$\text{reflectivity-limited finesse} = \frac{\pi\sqrt{R}}{(1-R)} \tag{4.304}$$

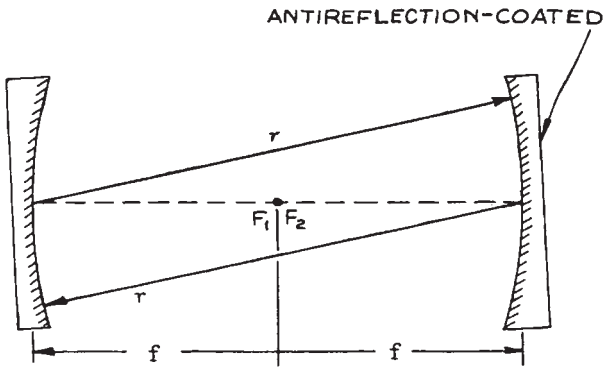

Figure 4.165 Confocal Fabry–Perot interferometer.

The approximate optimum radius of the apertures used in an arrangement similar to Figure 4.161 is 1.15 $(\lambda r_3/ff)^{1/4}$, where r is the radius of the spherical mirrors. Fabry–Perot interferometers with spherical mirrors can achieve very high finesse values.

The characteristics of all the possible combinations of two spherical mirrors that can be used to form a Fabry–Perot interferometer have been very extensively studied in connection with the use of such mirror arrangements to form the resonant cavities of laser oscillators.[14–16] In that application, these spherical-mirror resonators support Gaussian beam modes, and it is with such Gaussian beams that highest performance can be achieved with a spherical-mirror Fabry–Perot interferometer. Thus, a confocal Fabry–Perot interferometer is ideal for examining the spectral content of a Gaussian laser beam. The beam to be studied should be focused into the interferometer with a lens that matches the phase-front curvature and spot size of the laser beam to the radius of the Fabry–Perot mirror and the spot size of the resonant modes. (See Section 4.2.7.)

4.7.5 Design Considerations for Fabry–Perot Systems

Fabry–Perot interferometers and etalons are extremely sensitive to angular misalignment and fluctuations in plate spacing. Consequently, their design and construction are more demanding than for other laboratory optical instruments. The plates must be extremely flat, as already mentioned, and must be held without any distortion in high-precision alignment holders. The plate spacing must be held constant to about 1 nm in a typical high-finesse device for use in the visible, and the angular orientation must be maintained to better than 0.01 second of arc. Small-plate-spacing etalons are generally made commercially by optically contacting two plates to a precision spacer, or spacers, made of quartz. Such etalons are available from CVI Laser, II-VI Infrared, Michigan Aerospace, OFR, Research Electro-Optics, Rocky Mountain Instrument Co., TecOptics, Scientific Solutions, and SLS Optics, among others. Etalons of thickness in excess of 1 or 2 mm for use in the visible can be made from solid plane-parallel pieces of quartz or sapphire with dielectric coatings on their faces, or from materials, such as germanium or zinc selenide, for infrared use. Fabry–Perot interferometer plates are almost always slightly wedge-shaped and antireflection-coated on their outside faces to eliminate unwanted reflections, as shown in Figure 4.161(b). To prevent distortion of the plates they should be kinematically mounted in their holders. A good way to do this is to use three quartz or sapphire balls cemented to the circumferences of the plates and held in ball, slot, and plane locations with small retaining clips. For further details see Section 1.7.1 and Figures 1.52 and 1.53.

For the construction of Fabry–Perot interferometers, low-expansion materials should be used. The plate holders can be held at a fixed spacing by having them spring-loaded against three quartz or ceramic spacer rods or by the use of an Invar or Super-Invar spacer structure.

After a Fabry–Perot interferometer is aligned mechanically, it will creep slowly out of alignment, because of the easing of micrometer threads, for example. The alignment can be returned by having a piezoelectric element[145] incorporated in each plate-orientation adjustment screw.

Fabry–Perot interferometers are made commercially by Bernhard Halle Nachfl. GmbH, Bristol Instruments (who still provide service and parts for Burleigh interferometers), Hovemere, SSI, and Thorlabs.

The Fizeau interferometer is closely related to the Fabry–Perot, except that one of the mirrors is made totally reflecting and a beamsplitter is used to extract the interfering waves. They measure the phase difference between a reference surface and the object under test, as shown schematically in Figure 4.166. These interferometers are commonly used to test the flatness of optical surfaces.

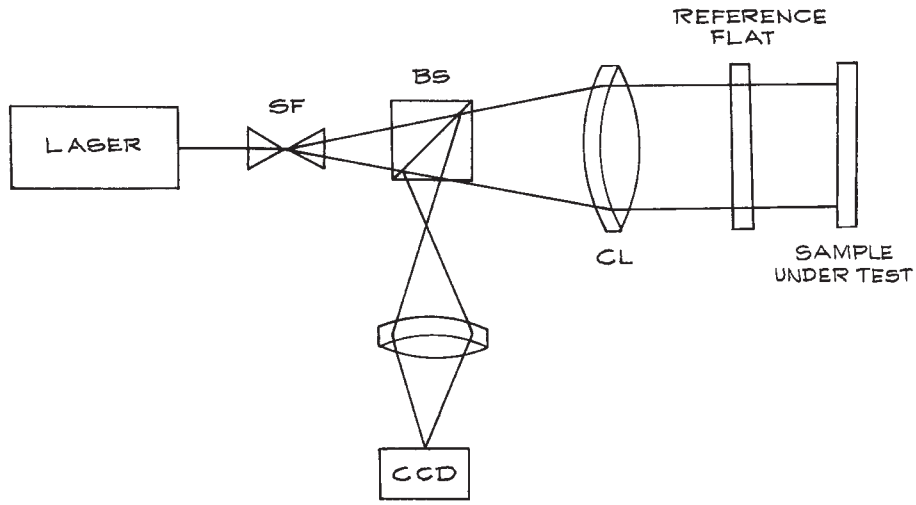

Figure 4.166 Fizeau interferometer. SF – spatial filter, BS – beamsplitter cube, CL – collimating lens.

They are available commercially from 4D Technology, Davidson Optronics, Logitech, Moeller-Wedel Optical GmbH, Sigma Koki Co, Silo, and Zygo.

4.7.6 Double-Beam Interferometers

In a double-beam interferometer, waves from a source are divided into two parts at a beamsplitter and then recombined after traveling along different optical paths. The most practically useful of these interferometers are the Michelson and the Mach–Zehnder.

The Michelson Interferometer. The operation of a Michelson interferometer can be illustrated with reference to Figure 4.167. Light from an extended source is divided at a beamsplitter and sent to two plane mirrors M_1 and M_2. If observations of a broad-band (temporally incoherent) source are being made, a compensating plate of the same material and thickness as the beamsplitter is included in arm 2 of the interferometer. This plate compensates for the two additional traverses of the beamsplitter substrate made by the beam in arm 1. Because of the dispersion of the beamsplitter material, it produces a phase difference that is wavelength-dependent, and without the compensating plate, interference fringes would not be observable with broad-band illumination (such as white light).

A maximum of illumination results at angle θ in Figure 4.167 if the phase difference between the two beams coming from M_1 and M_2 is an integral multiple of 2π. If M_2' represents the location of the reflection of M_2 in the beamsplitter, the condition for a maximum at angle θ is:

$$2l\cos\theta = m\lambda. \tag{4.305}$$

The positioning of M_1 at M_2 corresponds to $l = 0, m = 0$. If the output radiation is focused with a lens, a ring pattern is produced. A clear ring pattern is only visible if:

$$2l\cos\theta \lesssim l_c \tag{4.306}$$

where l_c, is the coherence length of the radiation from the source. The clearness of the rings is usually described in terms of their *visibility V*, defined by the relation:

$$V_{max} = \frac{I_{max} - I_{min}}{I_{max} + I_{min}} \tag{4.307}$$

To obtain a ring-shaped interference pattern, M_1 and M_2 must be very nearly parallel; otherwise a pattern of curved

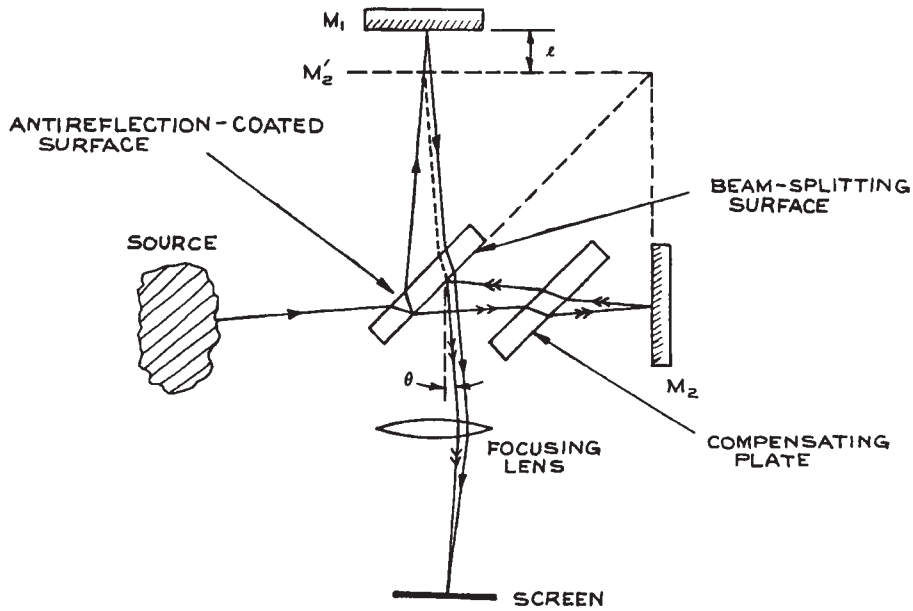

Figure 4.167 Michelson interferometer.

dark and light bands will result. To study the fringes, mirror M_1 must be scanned in a direction perpendicular to its surface. This can be done with a precision micrometer, or a piezoelectric transducer, if only small motion is desired. Because interference fringes are only observed with a broad-band source illuminating a Michelson (or other double-beam) interferometer when the two interferometer arms are of almost equal length, this mode of operation is extraordinarily sensitive. Such "white-light interferometry" forms the basis of a number of sensor systems for phenomena such as vibration, temperature, and pressure.[149,150]

In practice, Michelson interferometers are rarely used in the configuration shown in Figure 4.167, but are used instead with collimated illumination (a laser beam, or parallel light obtained by placing a point source at the focal point of a converging lens) as shown in Figure 4.168. In this case, the output illumination is (almost) perfectly uniform, being a maximum if:

$$2l = m\lambda \tag{4.308}$$

where $2l$ is the path difference between the two arms.

If monochromatic illumination of angular frequency ω is used, we can write the fields of the waves from arms 1 and 2 as:

$$\begin{aligned} V_1 &= V_0 e^{i(\omega t - \phi_1)} \\ V_2 &= V_0 e^{i(\omega t - \phi_2)} \end{aligned} \tag{4.309}$$

where it is assumed that the beamsplitter divides the incident beam into two equal parts. ϕ_1 and ϕ_2 are the optical phases of these two beams, which are dependent on the optical path lengths traveled in arms 1 and 2.

The output intensity is:

$$I \propto (V_1 + V_2) * (V_1 + V_2) \tag{4.310}$$

which gives

$$\begin{aligned} I &= I_0[1 + \cos(\phi_2 - \phi_1)] \\ &= I_0\left[1 + \cos\left(\frac{4\pi\nu l}{c}\right)\right] \end{aligned} \tag{4.311}$$

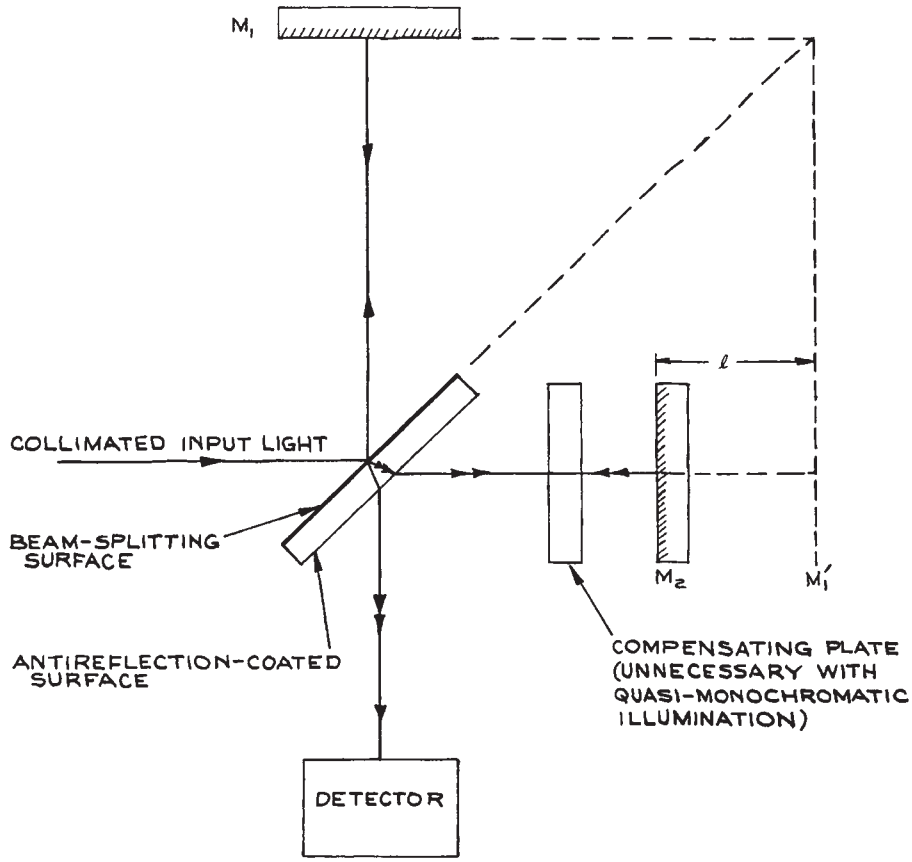

Figure 4.168 Simple Michelson interferometer for use with collimated input radiation.

in which I_0 is the intensity of the light from one arm alone. Suppose an optical component such as a prism or lens is placed in one arm of the interferometer, as shown in Figure 4.169, with the plane mirror replaced by an appropriate radius spherical mirror in the case of the lens, and quasi-monochromatic illumination is used. Then the output fringe pattern will reveal inhomogeneities and defects in the inserted component. A Michelson interferometer used in this way for testing optical components is called a *Twyman–Green interferometer*.[11]

Equation (4.302) illustrates why Michelson (and all other double-beam) interferometers are not directly suitable for spectroscopy. The distance the movable mirror must be adjusted to go from one maximum to the next is:

$$\Delta l = \lambda/2 \tag{4.312}$$

The distance required to go from a maximum- to a half-maximum-intensity point is:

$$\Delta l = \lambda/8 \tag{4.313}$$

Thus the effective finesse is only 4: sharp spectral peaks with monochromatic illumination are not obtained, as they are in multiple-beam interferometers.

Fourier Transform Spectroscopy. In an arrangement such as Figure 4.168, if the movable mirror is scanned at a steady velocity v, the resultant intensity as a function of position can be used to obtain considerable information about the spectrum of the source. If the

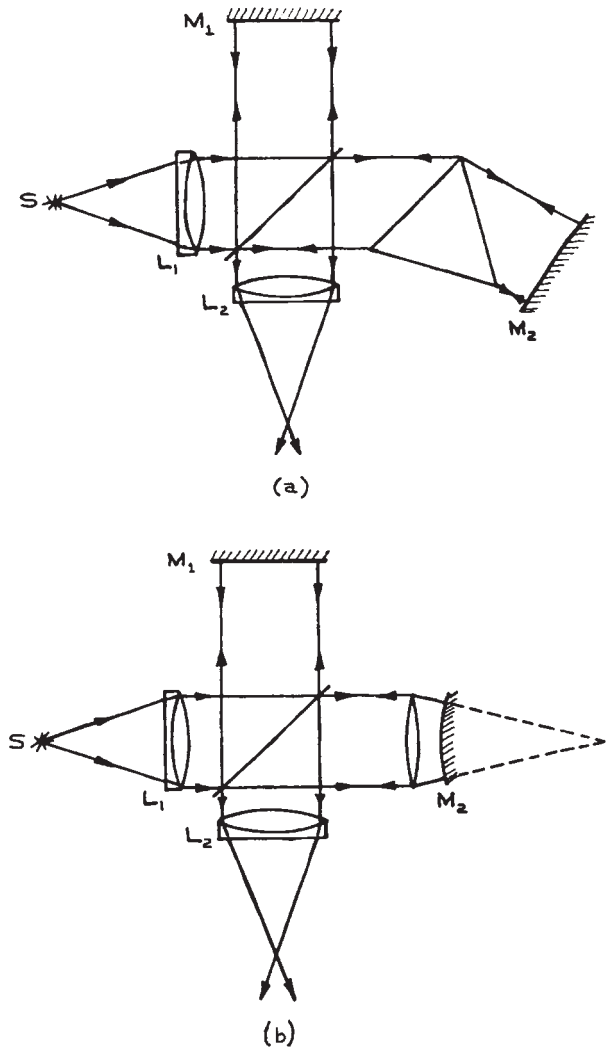

Figure 4.169 Twyman–Green interferometer: (a) arrangement for testing a prism; (b) arrangement for testing a lens. *S* is a monochromatic source, L_1 is a collimating lens, and L_2 is a focusing lens. (Adapted with permission from M. Born and E. Wolf, *Principles of Optics*, 3rd edn., Pergamon Press, Oxford, copyright © 1965.)

source has intensity $I(v)$ at v, the contribution to the intensity from the small band dv at v is:

$$I_v(l) = I(v)\left(1 + \cos\frac{4\pi vl}{c}\right)dv \tag{4.314}$$

where $l = vt$. The total observed output from the full spectrum of the source is:

$$\begin{aligned} I(l) &= \int_{v=0}^{\infty} I(v)\left(1 + \cos\frac{4\pi vl}{c}\right)dv \\ &= \frac{I_0}{2} + \int_{v=0}^{\infty} I(v)\cos\frac{4\pi vl}{c}dv \end{aligned} \tag{4.315}$$

The second term on the second line is essentially the cosine transform of $I(v)$. Thus $I(v)$ can be found as the cosine transform of $I(l) - (I_0/2)$:

$$I(v) = \frac{2}{c}\int_{l=0}^{\infty}\left(I(l) - \frac{I_0}{2}\right)\cos\frac{4\pi lv}{c}dl \tag{4.316}$$

This method for obtaining the spectrum of a source as the Fourier transform of an intensity recorded as a function of scanning mirror position is called *Fourier transform spectroscopy*. Such Fourier transform spectrometers have high luminosity and collect spectral information very efficiently: the whole emission spectrum is in reality sampled all at once, rather than one feature at a time, as in a conventional dispersive grating spectrometer. This is often called the Fellgett or Jacquinot advantage.

Commercial fourier transform spectrometers have become widely available and easy to use. Suppliers include ABB Bomen, Bruker Optics, Melles Griot, MIDAC, Newport/Oriel, Perkin-Elmer, ScienceTech, Shimadzu, Thermo-Fischer Scientific (formerly Nicolet), and Varian (previously Bio-Rad and Digilab). These instruments have replaced grating instruments in many analytical applications, especially for infrared absorption spectroscopy. They must be ''zeroed'' by running a spectrum of the source itself before any absorbing material is included in the sample path, and the absorption of the sample is obtained by ratioing with respect to the empty sample path. They can also be checked by measuring the absorption spectrum of a known sample, such as a thin polystyrene film. Commercial instruments often have interchangeable sources and detectors to cover different spectral regions.

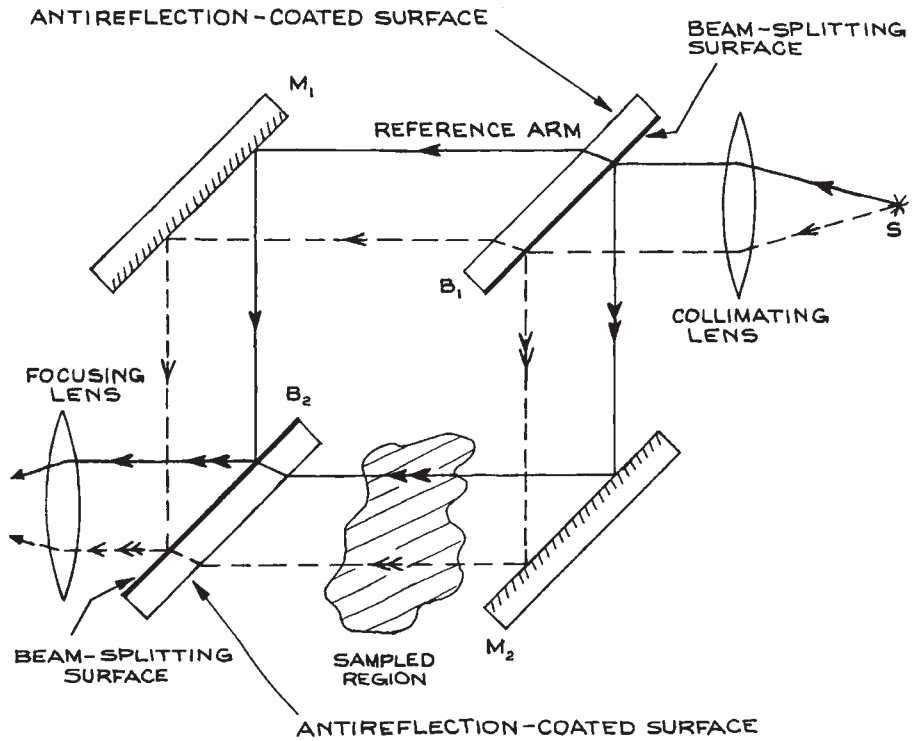

Figure 4.170 Mach-Zehnder interferometer. M_1, M_2 are totally reflecting mirrors; B_1, B_2 are beamsplitters (usually equally reflective and transmissive). The distribution of output illumination reflects the refractive-index distribution in the sampled region.

For example they might use a hot ceramic (globar type) source for infrared work, and germanium, InGaAs, HgCdTe, or triglycine sulfate (TGS) detectors, depending on the spectral region of interest.

The Mach–Zehnder Interferometer. The Mach–Zehnder interferometer, shown in Figure 4.170, is widely used for studying refractive-index distributions in gases, liquids, and solids. It is particularly widely used for studying the density variations in compressible gas flows,[151] the thermally induced density (and consequent refractive-index) changes behind shock fronts, and thermally induced density changes produced by laser beams propagating through transparent media.[152,153]

If the light entering the interferometer is perfectly collimated, uniform output illumination results, which is a maximum if the path difference between the two arms is an integral number of wavelengths. If the image of M_1 in beamsplitter B_2 is not parallel to M_2, the output fringe pattern is essentially the interference pattern observed from a wedge – a series of parallel bright and dark bands. If the medium in arm 2 is perturbed in some way, so that a spatial variation in refractive index results, the output fringe pattern changes. Analysis of the new fringe pattern reveals the spatial distribution of refractive-index variation along the beam path in arm 2. Various design variations on the Mach–Zehnder interferometer exist, notably the Jamin and the Sirks–Pringsheim.[11,154]

Design Considerations for Double-Beam Interferometers. Michelson and Mach–Zehnder interferometers are much easier to build in the laboratory than multiple-beam interferometers, such as the Fabry–Perot. Because the beams only reflect off the interferometer mirrors once, mirrors of flatness $\lambda/10$ or $\lambda/20$ are quite adequate for building a good instrument. The usual precautions should be taken in construction: stable rigid mounts for the mirrors and beamsplitters and, if long-term thermal stability is required, low-expansion materials. Piezoelectric control of mirror alignment is not generally necessary, as these instruments are less sensitive to small angular misalignments than Fabry–Perot interferometers. To achieve freedom from alignment disturbances along one or two orthogonal axes, the plane mirrors of a Michelson interferometer can be replaced with right-angle prisms or corner-cube retroreflectors, respectively. Some care should be taken to avoid source-polarization effects in these instruments; the beamsplitters are generally designed to reflect and transmit equal amounts only for a specific input polarization. If polarizing materials are placed in either arm of the interferometer, no fringes will be seen if, by any chance, the beams from the two arms emerge orthogonally polarized.

Endnotes

a 1 GHz (GigaHertz) $= 10^9$Hz, 1 THz (TeraHertz) $= 10^{12}$. The infrared range can also be somewhat arbitrily divided up into the submillimeter region ($\lambda = 0.1$–1 mm), far-infrared ($\lambda = 20$–100 μm), middle infrared ($\lambda = 3$–20 μm), and the near infrared ($\lambda = 0.7$–3 μm).

b At the boundary separating one or more anisotropic media, Snell's law must be used with some care as, in anisotropic media, the ray direction is not in general parallel to the wave vector (or wave normal), which is also used to characterize the direction of the ray.[15]

c Used by physicians for examining the retina of a patient's eye.[17]

d A pinhole camera is free of all aberrations in a geometrical optics description.

e A simple lens with just two spherical surfaces.

f Often called a TM wave.

g Often called a TE wave

h The old pressure unit of pounds per square inch (psi) = 6895 Pa

i The word rugate means corrugated, having alternating ridges and depressions

j The phosphorous is often omitted, and the precise stoichiometry of (In, Ga) and (As, P) determines the laser wavelength

k In practice, in any real system, transmission losses and aberrations will cause $B_2 < B_1$

Cited References

1. *Proceedings of the Symposium on Quasi-Optics*, New York, June 8–10, 1964, J. Fox (Ed.), Polytechnic Press of the Polytechnic Institute of Brooklyn, New York, 1964.
2. *Proceedings of the Symposium on Submillimeter Waves*, New York, March 31–April 2, 1970, J. Fox (Ed.), Polytechnic Press of the Polytechnic Institute of Brooklyn, New York, 1964.
3. A. Mortazawi, T. Itoh, and J. Harvey, *Active Antennas and Quasi-Optical Arrays*, Wiley-IEEE Press, New York, 1998.
4. J. Lesurf, *Millimeter-Wave Optics, Devices and Systems*, Lavoisier, Chachan, 1990.
5. K. M. Baird, D. S. Smith, and B. G. Whitford, Confirmation of the currently accepted value 299792458 metres per second for the speed of light, *Opt. Commun.*, **31**, 367–368, 1979.
6. E. R. Cohen and B. N. Taylor, *Committee on Data for Science and Technology, CODATA Bulletin*, No. **63**, 1986.
7. G. W. C. Kaye and T. H. Laby, *Tables of Physical and Chemical Constants*, 16th edn., Longman, London: 1995. Now available free online at http://www.kayelaby.npl.co.uk/
8. C. D. Coleman, W. R. Bozman, and W. F. Meggers, Table of Wavenumbers, *US Nat'l. Bur. Std. Monograph 3*, Vols. 1–2, 1960.
9. M. W. Urban, *Attenuated Total Reflectance Spectroscopy of Polymers: Theory and Practice*, American Chemical Society, Washington, DC, 1996.
10. R. Wiesendanger, *Scanning Probe Microsocopy and Spectroscopy*, Cambridge University Press, Cambridge, 1994.
11. M. Born and E. Wolf, *Principles of Optics*, 7th ed., Cambridge University Press, Cambridge, 1999.
12. E. E. Wahlstrom, *Optical Crystallography*, 5th edn., John Wiley & Sons, Inc., New York, 1979.
13. W. A. Shurcliff, *Polarized Light: Production and Use*, Harvard University Press, Cambridge, MA, 1962.
14. A. Yariv, *Optical Electronics in Modern Communications*, 5th edn., Oxford University Press, New York, 1997.

15. C. C. Davis, *Lasers and Electro-Optics*, Cambridge University Press, Cambridge, 1996.
16. H. Kogelnik and T. Li, *Proc. IEEE*, **54,** 1312–1329, 1966.
17. R. Kingslake, *Optical System Design*, Academic Press, Orlando, FL, 1983.
18. Code V. Available from Optical Research Associates.
19. Zemax. Available from Zemax Development Corporation.
20. Oslo developed by Sinclair Optics, Inc. Distributed by Lambda Research Corporation.
21. Solstis Odyssey. Available from Optis.
22. Optikwerk. Available from Optikwerk, Inc.
23. R. W. Ditchburn, *Light*, 3rd edn., Academic Press, New York, 1976.
24. L. Levi, *Applied Optics*, Vol.1 John Wiley & Sons, Inc., New York, 1968.
25. W. J. Smith, *Modern Optical Engineering*, 3rd edn., SPIE Press, Bellingham, WA, 2000.
26. W. J. Smith, *Modern Lens Design: A Resource Manual*, McGraw-Hill, New York, 1992.
27. R. R. Shannon, *The Art and Science of Optical Design*, Cambridge University Press, Cambridge, 1997.
28. M. Laikin, *Lens Design*, 3rd edn., Marcel Dekker, New York, 2001.
29. S. Ramo, J. R. Whinnery, and T. Van Duzer, *Fields and Waves in Communication Electronics*, 3rd edn., John Wiley & Sons, Inc., New York, 1994.
30. Diffraction-limited spherical lenses are available from Melles Griot, Optics for Research, Newport, Special Optics, and J. L. Wood Optical Systems, among others (see following reference).
31. *Laser Focus Buyers Guide,* published annually by Pennwell Publishing Co., 1421 South Sheridan, Tulsa, OK 74112 01460, lists a large number of suppliers of a wide range of optical components and systems as does the *The Photonics Buyers' Guide*, published annually by Photonics Spectra, Laurin Publishing Co., Berkshire Common, P.O. Box 4949, Pittsfield, MA 01202-4949. Additional valuable listings of this sort are: *Lasers and Optronics Buying Guide,* published annually by Cahners, 301 Gibraltar Drive, Box 650, Morris Plains, NJ 07950-0650; and Lightwave, 98 Spit Brook Road, Suite 100, Nashua, NH 03062–5737.
32. The "float" method for manufacturing plate glass (developed by Pilkington Glass) involves the drawing of the molten glass from a furnace, where the molten glass floats on the surface of liquid tin. The naturally flat surface of the liquid metal ensures the production of much larger sheets of better-flatness glass than was possible by earlier techniques.
33. Alexander Hornberg (Ed.), *Handbook of Machine Vision*, John Wiley & Sons, Inc., New York, 2006.
34. G. Rempe, R. J. Thompson, H. J. Kimble, and R. Lalezari, *Opt. Lett*., **17**, 363–365, 1992.
35. C. J. Hood, H. J. Kimble, and J. Ye, *Phys. Rev. A*, **64**, 033804, 2001.
36. H. R. Bilger, P. V. Wells, and G. E. Stedman, *Appl. Opt*., **33**, 7390–7396, 1994.
37. H.-J. Cho, M.-J. Shin, and J.-C. Lee, *Appl. Opt*. **45**, 1440–1446, 2006.
38. A. B. Meinel, in *Applied Optics and Optical Engineering*, Vol. 5, R. Kingslake (Ed.), Academic Press, New York, 1969.
39. W. Brouwer and A. Walther, Design of optical instruments, in *Advanced Optical Techniques*, A. C. S. Van Heel, (Ed.), North-Bouand, Amsterdam, 1967.
40. Celestron Telescopes are available from Celestron International, 2835 Columbia Street, P.O. Box 3578, Torrance, CA 90503; (310) 328–9560.
41. Meade Telescopes are available from Meade Instruments Corporation, 6001 Oak Canyon, Irvine, California 92618–5200, (949) 451–1450.
42. W. T. Wellford and R. Winston, *High Collection Nonimaging Optics*, Academic Press, San Diego, CA, 1989.
43. R. Winston, J. C. Miñano, and P. G. Benitez, *Nonimaging Optics*, Elsevier, Amsterdam, 2005.
44. A. Girard and P. Jacquinot, in *Advanced Optical Techniques*, A. C. S. Van Heel (Ed.), North-Bouand, Amsterdam, 1967.
45. J. D. Strong, *Procedures in Experimental Physics*, Prentice-Hall, Englewood Cliffs, NJ, 1938.
46. David R. Lide (Ed.), *Handbook of Chemistry and Physics*, 81st. edn., CRC Press, Boca Raton, FL, 2000.
47. D. R. Goff, *Fiber Optic Reference Guide*, 3rd edn., Focal Press (Elsevier), Amsterdam, 2002.
48. U. Hochuli and P. Haldemann, *Rev. Sci. Instr.,* **43**, 1088–1089, 1972.
49. Epoxy-removing solvents are available from Electron Microscopy Services, Oakite, or Hydroclean.
50. T. C. Poulter, *Phys. Rev.,* **35**, 297, 1930.
51. W. Paul, W. W. Meis, and J. M. Besson, *Rev. Sci. Instr*., **39**, 928–930, 1968.
52. I. L. Spain and J. Paawe (Eds.), *High Pressure Technology*, Dekker, New York, 1967.
53. *Compilation of ASTM Standard Definitions*, 3rd edn., American Society for Testing and Materials, Philadelphia, 1976.

54. Glass, quartz, and sapphire vacuum window assembles are available from Adolf Meller, Ceramaseal, Varian, and Vacuum Generators.
55. D. H. Martin (Ed.), *Spectroscopic Techniques for Far Infra-Red, Submillimetre and Millimetre Waves*, NorthHolland, Amsterdam, 1967.
56. K. D. Moller and W. G. Rothschild, *Far-Infrared Spectroscopy*, Wiley-Interscience, New York, 1971.
57. A. Hadni, *Essentials of Modern Physics Applied to the Study of the Infrared*, Pergamon Press, Oxford, 1967.
58. G. A. Fry, *Applied Optics and Optical Engineering*, Vol. 2, R. Kingslake (Ed.), Academic Press, 1965.
59. C. C. Davis and R. A. McFarlane, *J. Quant. Spect. Rad. Trans.*, **18**, 151–170, 1977.
60. P. W. Kruse, L. D. McGlauchlin, and R. B. McQuistan, *Elements of Infrared Technology: Generation, Transmission and Detection*, John Wiley & Sons, Inc., New York, 1962.
61. R. D. Hudson, Jr., *Infrared System Engineering*, Wiley-Interscience, New York, 1969.
62. J. A. R. Samson, *Techniques of Vacuum Ultraviolet Spectroscopy*, John Wiley & Sons, Inc., New York, 1967.
63. Available from EG&G Optoelectronics, ILC, Verre & Quartz, and Xenon Corporation.
64. Available from EG&G Optoelectroncs, Verre & Quartz, Resonance, and Xenon Corporation.
65. J. P. Markiewicz and J. L. Emmett, *IEEE J. Quant. Electron*., **QE-2**, 707–711, 1966.
66. J. G. Edwards, *Appl. Opt*., **6**, 837–843, 1967.
67. H. J. Baker and T. A. King, *J. Phys. E.: Sci. Instr.*, **8**, 219–223, 1975.
68. William T. Silfvast, *Laser Fundamentals*, 2nd edn., Cambridge University Press, Cambridge, 2004.
69. B. E. A. Saleh and M. C. Teich, *Fundamentals of Photonics*, John Wiley & Sons, Inc., New York, 1991.
70. A. E. Siegman, *Lasers*, University Science Books, Mill Valley, CA, 1986.
71. H. Rabin and C. L. Tang (Eds.), *Quantum Electronics*, Vols. 1A and 2A, *Nonlinear Optics*, Academic Press, New York, 1975.
72. *Nonlinear Optics,* Proceedings of the Sixteenth Scottish Universities Summer School in Physics, 1975, P. G. Harper and B. S. Wherrett (Eds.), Academic Press, London, 1977.
73. N. Bloembergen, *Nonlinear Optics*, Benjamin, New York, 1965.
74. F. Zernike and J. E. Midwinter, *Applied Nonlinear Optics,* John Wiley & Sons, Inc., New York, 1973.
75. R. W. Boyd, *Nonlinear Optics*, Academic Press, Boston, 1992.
76. D. Röss, *Lasers, Light Amplifiers and Oscillators*, Academic Press, New York, 1969.
77. W. Koechner, *Solid State Laser Engineering*, 5th revised and updated edn., Springer-Verlag, Berlin, 1999.
78. F. P. Schäfer (Ed.), *Topics in Applied Physics*, Vol. 1, *Dye Lasers*, 3rd revised and enlarged edn., Springer-Verlag, Berlin, 1990.
79. H. W. Furumoto and H. L. Ceccon, *Appl. Opt*., **8**, 1613–1623, 1969.
80. J. F. Holzrichter and A. L. Schawlow, *Ann. N.Y. Acad. Sci*., **168**, 703–714, 1970.
81. T. B. Lucatorto, T. J. McIlrath, S. Mayo, and H. W. Furumoto, *Appl. Opt*., **19**, 3178–3180, 1980.
82. C. C. Davis and T. A. King, *Advances in Quantum Electronics*, Vol. 3, D. W. Goodwin (Ed.), Academic Press, London, 1975, pp. 169–454.
83. W. B. Bridges, *Handbook of Laser Science and Technology*, Vol. 1: *Lasers in All Media*, M. J. Weber (Ed.), CRC Press, Boca Raton, FL, 1982.
84. C. C. Davis, *Handbook of Lasers Science and Technology*, Vol. 1, *Lasers in All Media*, M. J. Weber (Ed.), CRC Press, Boca Raton, FL, 1982.
85. D. C. Tyte, *Advances in Quantum Electronics*, Vol. 1, D. W. Goodwin (Ed.), Academic Press, London, 1970.
86. J. J. Degnan, *Appl. Phys.*, **11**, 1–33, 1976.
87. H. Seguin and J. Tulip, *Appl. Phys. Lett.*, **21**, 414–415, 1972.
88. J. D. Cobine, *Gaseous Conductors*, Dover, New York, 1958.
89. H. J. Seguin, K. Manes, and J. Tulip, *Rev. Sci. Instr.*, **43**, 1134–1139, 1972.
90. A. J. Beaulieu, *Appl. Phys. Lett.*, **16**, 504–505, 1970.
91. D. Basting, F. P. Schäfer, and B. Steyer, *Opto-electron*., **4**, 43–49, 1972.
92. P. Schenck and H. Metcalf, *Appl. Opt*., **12**, 183–186, 1973.
93. C. P. Wang, *Rev. Sci. Instr.*, **47**, 92–95, 1976.
94. A. J. Schwab and F. W. Bouinger, *IEEE J. Quant,. Electron*., **QE-12**, 183–188, 1976.
95. C. L. Sam, *Appl. Phys. Lett.*, **29**, 505–506, 1976.
96. M. Feldman, P. Lebow, F. Raab, and H. Metcalf, *Appl. Opt*., **17**, 774–777, 1978.
97. M. J. F. Digonnet (Ed.), *Rare Earth Doped Fiber Lasers And Amplifiers*, 2nd Revised edn., Taylor & Francis Ltd., Abingdon, 2001.
98. L. F. Mollenauer, *Opt. Lett.*, **1**, 164, 1977 (see also *Opt. Lett*. **3**, 48–50, 1978; **4**, 247–299, 1979; **5**, 188–190, 1980).
99. R. C. Greenhow and A. J. Schmidt, *Advances in Quantum Electronics*, Vol. 2, D. W. Goodwin (Ed.), Academic Press, London, 1973.

100. S. L. Shapiro (Ed.), *Ultrashort Light Pulses, Picosecond Techniques and Applications*, Topics in Applied Physics, Vol. 18, Springer, Berlin, 1977.
101. C. H. Lee (Ed.), *Picosecond Optoelectronic Devices*, Academic Press, Orlando, FL, 1984.
102. P. Bhattacharya, *Semiconductor Optoelectronic Devices*, 2nd edn., Prentice-Hall, Upper Saddle River, NJ, 1997.
103. J. Gowar, *Optical Communication Systems*, 2nd edn., Prentice-Hall, Englewood Cliffs, NJ, 1993.
104. D. Wood, *Optoelectronic Semiconductor Devices*, Prentice-Hall, New York, 1994.
105. G. P. Agrawal and N. K. Dutta, *Long-Wavelength Semiconductor Lasers*, Van Nostrand Reinhold, New York, 1986.
106. G. H. B. Thompson, *Physics of Semiconductor Laser Devices*, John Wiley & Sons, Ltd, Chichester, 1980.
107. S. L. Chuang, *Physics of Optoelectronic Devices*, John Wiley & Sons, Inc., New York, 1995.
108. J. Singh, *Semiconductor Optoelectronics*, McGraw-Hill, New York, 1995.
109. H. Kressel (Ed.), *Semiconductor Devices for Optical Communication*, Vol. 39, Topics in Applied Physics, 2nd updated edn., Springer-Verlag, Berlin, 1982.
110. E. Kapon (Ed.), *Semiconductor Lasers*, Vols. 1 and 2, Academic Press, San Diego, CA, 1999.
111. E. D. Hinkley, K. W. Nill, and F. A. Blum, *Topics in Applied Physics*, Vol. 2, H. Walther (Ed.), Springer, Berlin, 1976, pp. 125–196.
112. J. Faist, F. Capasso, D. L. Sivco, *et al., Science*, **264** (5158), 553–556, 1994.
113. T. J. Kane and R. L. Byer, *Optics Lett.*, **10**, 65–67, 1985.
114. T. W. Hänsch, *Appl. Opt*., **11**, 895–898, 1972.
115. R. Wallenstein and T. W. Hänsch, *Appl. Opt*., **13**, 1625–1628, 1974.
116. R. Wallenstein and T. W. Hänsch, *Opt. Commun*., **14**, 353–357, 1975.
117. G. L. Eesley and M. D. Levenson, *IEEE J. Quant. Electron.* **QE-12**, 440–442, 1976.
118. M. G. Littman and H. J. Metcalf, *Appl. Opt*., **17**, 2224–2227, 1978.
119. M. Littman and J. Montgomery, *Laser Focus/Electro-optics*, **24**, 70–86, 1988.
120. M. B. Radunsky, *Laser Focus World*, p. 107, October 1995.
121. B. J. Orr *et al.*, *Tunable Laser Applications*, F. J. Duarte (Ed.), Marcel Dekker, New York, 1995.
122. R. G. Batchko, D. R. Weise, T. Plettner, *et al*., *Opt. Lett.* **23**(3), 168, 1998.
123. M. E. Klein, D.-H. Lee, J.-P. Meyn, K.-J. Boller, and R. Wallenstein, *Opt. Lett.*, **24**, 1142–1144, 1999.
124. F. Müller, G. von Basum, A. Popp, *et al.*, *Appl. Phys.* **80**, 307–313, 2004.
125. I. P. Kaminow, *An Introduction to Electro-optic Devices*, Academic Press, New York, 1974.
126. A. Korpel, *Acousto-Optics*, Marcel Dekker, New York, 1988, see also Acousto-Optics – a review of fundamentals, *Proc. IEEE.*, **69**, 48–53, 1981.
127. I. C. Chang, *IEEE Trans. Sonics and Ultrasonics*, **SU-23**, 2–22, 1976.
128. American National Standard for Safe Use of Lasers, ANSI Z136-2-2000, Published by the Laser Institute of America, Suite 128, 13501 Ingenuity Drive, Orlando, FL 32826.
129. D. Sliney and M. Wolbarsht, *Safety with Lasers and Other Optical Sources: A Comprehensive Handbook*, Plenum, New York, 1980.
130. M. J. Weber (Ed.), *CRC Handbook of Laser Science and Technology*, Vol. 1, Lasers and Masers, CRC Press, Boca Raton, FL, 1982.
131. P. Jacquinot, *J. Opt. Soc. Am.*, **44**, 761–765, 1954.
132. R. Kingslake (Ed.), *Applied Optics and Optical Engineering*, Vol. 5: *Optical Instruments Part II*, Academic Press, New York, 1969.
133. J. F. James and R. S. Sternberg, *The Design of Optical Spectrometers*, Chapman and Hall, London, 1969.
134. *The Photonics Design and Applications Handbook*, published annually by Laurin Publishing Co. Inc., Pittsfield, MA.
135. W. G. Fastie, *J. Opt. Soc. Am.*, **42**, 641–647, 1952.
136. H. Ebert, *Annalen der Physik und Chemie*, **38**, 489–493, 1889.
137. M. Seya, *Sci. Light (Tokyo)*, **2**, 8–17, 1952.
138. T. Namioka, *Sci. Light (Tokyo),* **3**, 15–24, 1952.
139. P. Atherton, N. Reay, J. Ring, and T. Hicks, *Opt. Eng*., **20**, 806, 1981.
140. Available from numerous suppliers of vacuum equipment – for example, Ceram Tec (Ceramaseal Division), Edwards, Ferrofluidics Corp., Perkin Elmer, Vacuum Generators (VG), Varian, and Veeco.
141. Available from Carpenter Technology, P.O. Box 14662, Reading, PA 19612–4662; Tel: (800) 338–4592 and (610) 208–2000, FAX: (610) 208–2361.
142. Available from Burleigh.
143. Available from Heraeus-Amersil, Dynasil, Esco, and Quartz Scientific, among others.
144. Available from Corning Glass Works, Optical Products Department.

145. Piezoelectric transducers are available from American Piezo Ceramics, Burleigh, EDO, Polytec, Queensgate Instruments, and Xinetics, among others.
146. C. F. Bruce, *Appl. Opt*., **5**, 1447–1452, 1966.
147. Commercial Fabry–Perot Interferometers that can incorporate this feature are available from Burleigh.
148. P. Hariharan, *Optical Interferometry*, 2nd edn., Academic Press, 2003.
149. B. T. Meggitt and K. T. V. Grattan, *Optical Fiber Sensor Technology*, Springer, New York, 1999.
150. James C. Wyant, White light interferometry, paper presented at AeroSense, Orlando, Florida, 1–5 April 2002. (Available online at fttp://www.optics.arizona.edu/jcwyant/pdf/Meeting_papers/WhiteLightInterferometry.pdf)
151. R. Ladenburg and D. Bershader, *High Speed Aerodynamics and Jet Propulsion*, Vol. 9, *Physical Measurements in Gas Dynamics and Combustion*, R. Ladenburg (Ed.), Princeton University Press, Princeton, NJ, 1954.
152. P. R. Longaker and M. M. Litvak, *J. Appl. Phys.*, **40**, 4033–4041, 1969.
153. D. C. Smith, *IEEE J. Quant. Electron.,* **QE-5**, 600–607, 1969.
154. H. Kuhn, *Rep. Prog. Phys.*, **14**, 64–94, 1951.

General References

Comprehensive (General) Optics Texts

M. Born and E. Wolf, *Principles of Optics*, 7th edn., Cambridge University Press, Cambridge, 1999.
E. Hecht, *Optics*, 3rd edn., Addison-Wesley, Reading, MA, 1998.
R. W. Ditchburn, *Light*, 3rd edn., Academic Press, New York, 1976.
F. A. Jenkins and H. E. White, *Fundamentals of Optics*, 4th edn., McGraw-Hill, New York, 1976.
M. V. Klein and T. E. Furtak, *Optics*, 2nd edn., John Wiley & Sons, Inc., New York, 1986.
R. S. Longhurst, *Geometrical and Physical Optics*, 3rd edn., Longman, London, 1973.
F. G. Smith and J. H. Thomson, *Optics*, 2nd edn., John Wiley & Sons, Inc., Chichester, 1988.
J. Strong, *Concepts of Classical Optics*, Freeman, San Francisco, CA, 1958.

Applied Optics

W. J. Smith, *Modern Optical Engineering*, 3rd edn., SPIE Press, Bellingham, WA, 2000.
R. Kingslake (Ed.), *Applied Optics and Optical Engineering* Academic, New York, Vol. 1, 1965; Vol. 2, 1965; Vol. 3, 1965; Vol. 4, 1967; Vol. 5, 1969.
L. Levi, *Applied Optics*, John Wiley & Sons, Inc., New York, Vol. 1, 1968; Vol. 2, 1980.

Lens Design

W. J. Smith, *Modern Lens Design: A Resource Manual*, McGraw-Hill, New York, 1992.
R. R. Shannon, *The Art and Science of Optical Design*, Cambridge University Press, Cambridge, 1997.
M. Laikin, *Lens Design*, 3rd edn., Marcel Dekker, New York, 2001.

Electro-Optic Devices

M. A. Karim, *Electro-Optical Devices and Systems*, PWS-Kent Publishing, Boston, MA, 1990.
I. P. Kaminow, *An Introduction to Electro-Optics*, Academic Press, New York, 1974.
A. Yariv, *Optical Electronics in Modern Communications*, 5th edn., Oxford University Press, New York, 1997.

Far-Infrared Techniques

M. F. Kimmitt, *Far-Infrared Techniques*, Routledge, 1970.
A. Hadni, *Essentials of Modern Physics Applied to the Study of the Infrared*, Pergamon Press, Oxford, 1967.
K. D. Möller and W. G. Rothschild, *Far-Infrared Spectroscopy*, Wiley-Interscience, New York, 1971.
L. C. Robinson, *Physical Principles of Far-Infrared Radiation, Methods in Experimental Physics*, Vol. 10, L. Marton (Ed.), Academic Press, New York, 1973.

Fiber Optics

J. Hecht, *Understanding Fiber Optics*, 3rd edn., Prentice-Hall, Upper Saddle River, NJ, 1999.
A. Ghatak and K. Thyagarajan, *Introduction to Fiber Optics*, Cambridge University Press, Cambridge, 1998. A. Ghatak, A, Sharma, and R. Tewari, *Understanding Fiber Optics on a PC*, Viva Books Private Ltd., New Delhi, 1994. P.K. Cheo, *Fiber Optics and Optoelectronics*, 2nd edn., Prentice-Hall, Englewood Cliffs, NJ, 1990. L. Kazovsky, S. Benedetto, and A. Willner, *Optical Fiber Communication Systems*, Artech House, Boston, MA, 1996.

J. Gowar, *Optical Communication Systems*, 2nd edn. Prentice-Hall, Englewood Cliffs, NJ, 1993.
M. K. Barnoski, (Ed.,) *Introduction to Integrated Optics*, Plenum, New York, 1974.
D. Marcuse, *Principles of Optical Fiber Measurements*, Academic Press, San Diego, CA., 1981.
T. Okoshi, *Optical Fibers*, Academic Press, New York, 1982.
D. Gloge (Ed.), *Optical Fiber Technology*, IEEE, New York, 1976.
J. C. Palais, *Fiber Optic Communications*, 5th edn., Prentice-Hall, Upper Saddle River, NJ, 2004.
A. D. Snyder and J. D. Love, *Optical Waveguide Theory*, Chapman and Hall, London and New York, 1983.

Filters

D. R. Lide (Ed.), *Handbook of Chemistry and Physics*, 87th edn., Taylor and Francis, Boca Raton, Florida, 2000. Also available on line at http://www.hbcpnetbase.com/help/default.asp
R. J. Pressley (Ed.), *Handbook of Lasers*, CRC Press, Cleveland, OH, 1971.
L. Levi, *Applied Optics*, Vol. 2, John Wiley & Sons, Inc., New York, 1980.
H. A. Macleod, *Thin-Film Optical Filters*, American Elsevier, New York, 1969.
E. J. Bowen, *Chemical Aspects of Light*, 2nd revised edn., The Clarendon Press, Oxford, 1946.

Fourier Transform Spectroscopy

P. Griffiths and J. deHaseth, *Fourier Transform Infrared Spectroscopy*, John Wiley & Sons, Inc., New York, 1986.
B. C. Smith, *Fundamentals of Fourier Transform Infrared Spectroscopy*, CRC Press Inc., Boca Raton, IL, 1996.

Incoherent Light Sources

A. C. S. Van Heel (Ed.), *Advanced Optical Techniques*, North-Bouand, Amsterdam, 1967.
R. Kingslake (Ed.), *Applied Optics and Optical Engineering*, Vol. 1, Academic Press, New York, 1965.
R. J. Pressley (Ed.), *Handbook of Lasers*, CRC Press, West Palm Beach, FL, 1971.
L. Levi, *Applied Optics*, Vol. 1, John Wiley & Sons, Inc., New York, 1968.

Photometry

C. DeCusatis, *Handbook of Applied Photometry*, AIP Press, New York, (1997).
M. Rea (Ed.), *Lighting Handbook: Reference and Application*, 8th edn., Illuminating Engineering Society of North America, New York, 1993.

Infrared Technology

W. L. Wolfe and G. J. Zissis (Eds.), *The Infrared Handbook*, Office of Naval Research, Washington, DC, 1985.
A. R. Jha, *Infrared Technology*, John Wiley & Sons, Inc., New York, 2000.
A. Hadni, *Essentials of Modern Physics Applied to the Study of the Infrared*, Pergamon Press, Oxford, 1967.
R. D. Hudson, *Infrared System Engineering*, Wiley-Interscience, New York, 1969.
P. W. Kruse, L. D. McGlauchlin, and R. B. McQuistan, *Elements of Infrared Technology*, John Wiley & Sons, Inc., New York, 1962.

Interferometers and Interferometry

P. Hariharan, *Optical Interferometry*, Academic Press, Orlando, FL, 1985.
G. Hernandez, *Fabry–Perot Interferometers*, Cambridge University Press, Cambridge, 1986.
R. Jones and C. Wykes, *Holographic and Speckle Interferometry*, 2nd edn., Cambridge University Press, Cambridge, 1989.
J. C. Dainty (Ed.), *Laser Speckle and Related Phenomena*, *Topics in Applied Physics*, Vol. 9, Springer-Verlag, Berlin; New York, 1975.
M. Francon, *Laser Speckle and Applications in Optics*, Academic Press, New York, 1979.
M. Born and E. Wolf, *Principles of Optics*, 7th edn., Cambridge University Press, Cambridge, 1999.
M. Francon, *Optical Interferometry*, Academic Press, New York, 1966.
W. H. Steel, *Interferometry*, 2nd edn., Cambridge University Press, Cambridge, 1983.
S. Tolansky, *An Introduction to Interferometry*, Longman, London, 1955.
J. M. Vaughan, *The Fabry–Perot Interferometer: History, Theory, Practice and Applications*, Adam Hilger, Bristol, UK, 1989.

Fourier Optics and Holography

J. Goodman, *Introduction to Fourier Optics*, 2nd edn., McGraw-Hill, New York, 1996.
P. Hariharan, *Optical Holography*, Cambridge University Press, Cambridge, 1984.

Lasers

A. Yariv, *Optical Electronics in Modern Communications*, 5th edn., Oxford University Press, New York, 1997.
C. C. Davis, *Lasers and Electro-Optics*, Cambridge University Press, Cambridge, 1996.
C. R. Pollack, *Fundamentals of Optoelectronics*, Irwin, Chicago, 1995.
W. T. Silfvast, *Laser Fundamentals*, 2nd edn., Cambridge University Press, 2004.
B. E. A. Saleh and M. C. Teich, *Fundamentals of Photonics*, 2nd edn., John Wiley & Sons, Inc., New York, 2007.
M. Weber (Ed.), *Handbook of Laser Science and Technology,* Vol. 1, *Lasers and Masers;* Vol. II, *Gas Lasers*, CRC Press, Boca Raton, FL, 1982.
A. Maitland and M. H. Dunn, *Laser Physics*, North Holland, Amsterdam, 1969.
D. C. O'Shea, W. R. Callen, and W. T. Rhodes, *Introduction to Lasers and Their Applications*, Addison-Wesley, Reading, MA, 1977.
J. T. Verdeyen, *Laser Electronics*, 3rd edn., Prentice-Hall, Englewood Cliffs, NJ, 1995.
A. Yariv, *Quantum Electronics*, 3rd edn., John Wiley & Sons, Inc., New York, 1989.
A. E. Siegman, *Lasers*, University Science Books, Mill Valley, CA, 1986.

Nonlinear Optics

R. W. Boyd, *Nonlinear Optics*, Academic Press, Boston, MA, 1992.
N. Bloembergen, *Nonlinear Optics*, Benjamin, New York, 1965.
P. G. Harper and B. S. Wherrett (Eds.), *Nonlinear Optics*, Academic Press, New York, 1977.
C. L. Tang and H. Rabin, (Eds.), *Quantum Electronics,* Vols. 1A and 2A *Nonlinear Optics*, Academic Press, New York, 1975.
F. Zernike and J. E. Midwinter, *Applied Non-Linear Optics*, John Wiley & Sons, Inc., New York, 1973.
Y. R. Shen, *The Principles of Nonlinear Optics*, John Wiley & Sons, Inc., New York, 1984.

Optical Component and Instrument Design

A. C. S. Van Heel (Ed.), *Advanced Optical Techniques*, North Holland, Amsterdam, 1967.
R. Kingslake (Ed.), *Applied Optics and Optical Engineering*, Academic Press, New York, Vol. 3, 1965; Vol. 4, 1967; Vol. 5, 1969.

Optical Detectors

A. Rogalksi, *Infrared Detectors*, Gordon and Breadh, Amsterdam, 2000.
J. Gowar, *Optical Communication Systems*, 2nd edn., Prentice-Hall, Englewood Cliffs, NJ, 1993.
E. L. Dereniak and G. D. Boreman, *Infrared Detectors and Systems*, John Wiley & Sons, Inc., New York, 1996.
E. L. Dereniak and D. G. Crowe, *Optical Radiation Detectors*, John Wiley & Sons, Inc., New York, 1984.
J. Graeme, *Photodiode Amplifiers*, McGraw-Hill, New York, 1996.
J. B. Dance, *Photoelectronic Devices*, Iliffe, London, 1969.
P. W. Kruse, L. D. McGlauchlin, and R. B. McQuistan, *Elements of Infrared Technology*, John Wiley & Sons, Inc., New York, 1962.
L. Levi, *Applied Optics*, Vol. 2, John Wiley & Sons, Inc., New York, 1980.
R. S. Keyes (Ed.), *Optical and Infrared Detectors*, Topics in Applied Physics, Vol. 19, Springer, Berlin, 1977.

Optical Materials

R. Kingslake (Ed.), *Applied Optics and Optical Engineering*, Vol. 1, Academic Press, New York, 1965.
M. Weber (Ed.), *Handbook of Laser Science and Technology,* Vols. III–V, *Optical Materials*, CRC Press, Boca Raton, FL, 1986–87.
P. W. Kruse, L. D. McGlauchlin, and R. B. McQuistan, *Elements of Infrared Technology*, John Wiley & Sons, Inc., New York, 1962.
A. J. Moses, *Optical Material Properties*, IFI/Plenum, New York, 1971.

Optical Safety

M. J. Weber (Ed.), *Handbook of Laser Science and Technology,* Vol. 1, *Lasers and Masers*, CRC Press, Boca Raton, FL, 1982.

D. Sliney and M. Wolbarsht, *Safety with Lasers and Other Optical Sources: A Comprehensive Handbook*, Plenum, New York, 1980.

Polarized Light and Crystal Optics

R. M. A. Azzam and N. M. Bashara, *Ellipsometry and Polarized Light*, North-Bouand, Amsterdam, 1977.
D. Goldstein, *Polarized Light*, CRC Press, Boca Raton, FL, 2003.
W. A. Shurcliff, *Polarized Light*, Harvard University Press, Cambridge, MA, 1962.
E. Wahlstrom, *Optical Crystallography*, 5th edn., John Wiley & Sons, Inc., New York, 1979.
A. Yariv and P. Yeh, *Optical Waves in Crystals*, John Wiley & Sons, Inc., New York, 1983.

Spectrometers

N. B. Colthup, L. H. Daly, and S. E. Wiberley, *Introduction to Infrared and Raman Spectroscopy*, 2nd edn., Academic Press, New York, 1975.
Francis M. Mirabella Jr., (Ed.), *Internal Reflection Spectroscopy. Theory and Applications*, CRC Press, Boca Raton, 1993.
J. F. James and R. S. Sternberg, *The Design of Optical Spectrometers*, Chapman & Hall, London, 1969.
H. S. Strobel and W. R. Heineman, *Chemical Instrumentation*, 3rd edn., John Wiley & Sons, Inc., New York, 1989.

Spectroscopy

M. Pinta (Ed.), *Atomic Absorption Spectrometry*, John Wiley & Sons, Inc., New York, 1975.
J. R. Edisbury, *Practical Hints on Absorption Spectrometry*, Hilger and Watts, London, 1966.
R. J. Reynolds and K. Aldous, *Atomic Absorption Spectroscopy*, Barnes and Noble, New York, 1970.
A. Lee Smith, *Applied Infrared Spectroscopy: Fundamentals, Techniques and Analytical Problem-Solving*, Vol. 54 (Chemical Analysis, Vol. 21), John Wiley & Sons, Inc., New York, 1979.
R. A. Sawyer, *Experimental Spectroscopy*, Prentice-Hall, Englewood Cliffs, NJ, 1951.
D. Williams (Ed.), *Methods of Experimental Physics*, Vol. 13, Spectroscopy, Parts A and B, Academic Press, New York, 1968.
S. Walker and H. Straw, *Spectroscopy,* Vol. I, *Microwave and Radio Frequency Spectroscopy;* Vol. II, *Ultraviolet, Visible, Infrared and Raman Spectroscopy*, Macmillan, New York, 1962.

Submillimeter Wave Techniques

K. J. Button, *Infrared and Millimeter Waves: Submillimeter Techniques*, Academic Press, New York, 1980.
G. W. Chantry, *Submillimeter Spectroscopy*, Academic Press, New York, 1971.
E. Kollberg (Ed.), *Instrumentation for submillimeter spectroscopy*, SPIE Proceedings, Vol. 598, SPIE, Bellingham, WA, 1986.
D. H. Martin (Ed.), *Spectroscopic Techniques*, North-Holland, Amsterdam, 1967.

Tables of Physical and Chemical Constants

G. W. C. Kaye and T. H. Laby, *Tables of Physical and Chemical Constants*, 16th edn., Longman, London, 1995. Now available free online at http://www.kayelaby.npl.co.uk/

Tables of Spectral and Laser Lines

M. J. Weber, *Handbook of Lasers*, CRC Press, Boca Raton, FL, 2001.
M. J. Weber, *Handbook of Laser Wavelengths*, CRC Press, Boca Raton, FL, 1999.
G. R. Harrison, *MIT Wavelength Tables*, MIT Press, Cambridge, MA, 1969.
A. R. Striganov and N. S. Sventitskii, *Tables of Spectral Lines of Neutral and Ionized Atoms*, IFI/Plenum, New York, 1968.
A. N. Zaidel', V. K. Prokof'ev, S. M. Raiskii, V. A. Slavnyi, and E. Ya. Shreider, *Tables of Spectral Lines*, IFI/Plenum, New York, 1970.

Ultraviolet and Vacuum-Ultraviolet Technology

A. E. S. Green (Ed.), *The Middle Ultraviolet: Its Science and Technology*, John Wiley & Sons, Inc., New York, 1966.
J. A. R. Samson, *Techniques of Vacuum Ultraviolet Spectroscopy*, John Wiley & Sons, Inc., New York, 1967.

Suppliers of Optical Windows

Several of the suppliers listed will supply lenses, prisms, and other components fabricated from these materials:

AMTIR (GeAsSe Glass): Harrick Scientific, Janos, REFLEX Analytical

Arsenic trisulfide: Infrared Optical Products, REFLEX Analytical, Spectrum Thin Films Corp.

Arsenic triselenide: Infrared Optical Products, REFLEX Analytical, Spectrum Thin Films Corp.

Barium fluoride: Crystran, Del Mar Photonics, Harrick Scientific, Infrared Optical Products, ISP Optics, Janos, Koch Crystal Finishing, Molecular Technology.

Cadmium sulfide: Cleveland Crystals, Molecular Technology.

Cadmium selenide: Cleveland Crystals, Molecular Technology.

Cadmium telluride (Irtran 6): Cleveland Crystals, ISP Optics, Janos, Laser Research Optics, Molecular Technology.

Calcium carbonate (calcite): Crystran, Karl Lambrecht Corp (KLC), Photox, Thin Film Lab.

Calcium fluoride (Irtran 3): Argus International, Coherent, Inc., Crystran, Edmund Optics, EKSPLA, Gooch and Housego, Hellma International, Infrared Optical Products, ISP Optics, Janos, KLC, Koch Crystal Finishing, Lambda Research Optics, Meller Optics, Molecular Technology, Newport, Optimax, Opto-Sigma, Photox, REFLEX Analytical, Rocky Mountain Instruments, Spectrum Thin Films, Thorlabs.

Cesium bromide: Argus International, Crystran, Harrick Scientific, Janos.

Cesium iodide: Crystran, Koch Crystal Finishing, Molecular Technology, REFLEX Analytical.

Diamond: Argus International, Gist Optics, Coherent Photonics Group, II-VI Infrared, ISP Optics, Laser Power Optics, REFLEX Analytical, Optics for Research, Newport/Oriel.

Gallium arsenide: Argus International, Crystran, Infrared Optical Products, II-VI Infrared, ISP Optics, Lambda Research Optics, Laser Power Optics, Laser Research Optics, Meller Optics, REFLEX Analytical, Rocky Mountain Instruments, Sterling Precision Optics.

Germanium: Argus International, Coherent, Inc., Crystran, Edmund Optics, Gooch and Housego, II-VI Infrared, ISP Optics, Janos, Laser Power Optics, Laser Research Optics, Meller Optics, Photox, REFLEX Analytical, Rocky Mountain Instruments, Spectrogon, Spectrum Thin Films Corporation, Sterling Precision Optics, Unicore.

Glasses: Coherent, Ealing, Edmund Optics, Newport, Opto-Sigma, Rocky Mountain Instruments, Rolyn, Schott, Sterling Precision Optics, Thorlabs.

Lithium fluoride: Argus International, Crystran, Coherent, Inc., EKSPLA, Hellma International, Infrared Optical Products, ISP Optics, Lambda Research Optics, Macrooptica, Molecular Technology, OPCO, Photox, REFLEX Analytical, Rocky Mountain Instrument Co., Sterling Precision Optics.

Magnesium fluoride (Irtran 1): Argus International, Coherent, Inc., Crystran, Edmund Optics, EKSPLA, Gooch and Housego, Hellma International, Infrared Optical Products, ISP Optics, KLC, Lambda Research Optics, Macrooptica, Meller Optics, Molecular Technology, Newport, Optimax, Photox, REFLEX Analytical, Rocky Mountain Instruments, Sterling Precision Optics.

Magnesium oxide (Irtran 5): Crystran, Harrick Scientific.

Potassium bromide: Argus International, Crystran, EKSPLA, Hilger Crystals, Infrared Optical products, ISP Optics, Janos, Koch Crystal Finishing, Lambda Research Optics, Macrooptica, Molecular Technology, OPCO, Photox, REFLEX Analytical Corp., Spectrum Thin Films Corp., Thorlabs.

Potassium chloride: Crystran, ISP Optics, Janos, Koch Crystal Finishing, Macrooptica, Molecular Technology, Optovac, Photox.

Potassium iodide: Crystran.

Quartz (crystalline): Crystran, Esco, Infrared Optical Products, ISP Optics, Janos, Meller Optics, Molecular Technology, Newport, Opto-Sigma, Photox, REFLEX Analytical, Sterling Precision Optics, Continental Optical, Optics for Research, Newport/Oriel, Adolf Meller.

Sapphire: Crystran, Infrared Optical Products, ISP Optics, Laser Power Optics, Meller Optics, Newport, Opto-Sigma, REFLEX Analytical, Rocky Mountain Instruments, Rolyn, Sterling Precision Optics.

Silica (fused): Esco, ISP Optics, Janos, Macrooptica, Meller Optics, Newport, Opto-Sigma, Photox, REFLEX Analytical, Rolyn, Schott, Sterling Precision Optics, Thorlabs, Continental Optical, Optical Coating Lab (OCLI).

Silicon: Crystran, Infrared Optical Products, ISP Optics, Janos, Laser Power Optics, Macrooptica, Meller Optics, Molecular Technology, Photox, REFLEX Analytical, Rocky Mountain Instruments, Sterling Precision Optics.

Silver bromide: Crystran, Harrick Scientific, ISP Optics, REFLEX Analytical.

Silver chloride: Crystran, Harrick Scientific, ISP Optics, REFLEX Analytical.

Sodium chloride: Crystran, ISP Optics, Koch Crystal Finishing, Macrooptica, Molecular Technology, Photox.

Sodium fluoride: Crystran.

Strontium fluoride: Crystran, Harrick Scientific.

Strontium titanate: Commercial Crystal Labs, Harrick Scientific, Hibshman-Pacific Optical, Photox.
Tellurium: Molecular Technology.
Thallium bromide: Crystran, Korth Kristalle GmbH.
Thallium bromoiodide (KRS-5): Argus International, Crystran, Infrared Optical Products, ISP Optics, Janos, Koch Crystal Finishing, Macrooptica, Molecular Technology, Perkin-Elmer.
Thallium chlorobromide (KRS-6): Crystran, Macrooptica, Molecular Technology.
Titanium dioxide (rutile): Commercial Crystal Labs, Crystran, Harrick Scientific, ISP Optics, Molecular Technology, Thin Film Lab.
Zinc selenide (Irtran 4): Argus International, Coherent, Inc., Crystran, CVI Laser, Edmund Optics, EKSPLA, Gooch and Housego, Harrick Scientific, Hellma International, II-VI Infrared, Infrared Optical Products, ISP Optics, Janos, Laser Power Optics, Laser Research Optics, Meller Optics, Molecular Technology, REFLEX Analytical, Rocky Mountain Instruments, Sterling Precision Optics.
Zinc sulfide (Irtran 2): Crystran, Gooch and Housego, Infrared Optical Products, Laser Power Optics, Laser Research Optics, Meller, OPCO, Optimax, REFLEX Analytical, Rocky Mountain Instruments, Sterling Precision Optics,
Zirconium dioxide: Insaco.

INDEX

Note: Figures and Tables are indicated by *italic page numbers*

1/*f* noise 492, 549

Abbe diagram (glass chart) *169*
Abbe V number 168
aberrations, imaging system 169, 191, 161, 503, 561
  charged-particle optics 333–336
  and exact ray tracing 171
ABS thermoplastic *525*
a.c. line
  ground connection 501
  three-wire system 501, 525
a.c. line cord 526
  mounting at chassis end 526
a.c. line receptacles 18, 526
  circuit diagram symbol(s) *509*
accuracy of temperature measurement 600
achromat lens 169, 189
achromatic doublets (lenses) 169, 169, 191
acoustic absorber 229
acousto-optic modulators 238, 288
acrylic plastics 24
  jointing of 24
  in optical components 193, 241
  properties 20, 233, 234, 241, 525
  thermoforming of 24
  in vacuum systems 117
active electronic components 363, 402–421
  circuit diagram symbol(s) *509*
active filters 381, 431
adhesives 34
  in vacuum systems 117
admittance 366
Ahrens polarizer 208, 209
Airy function 301
alexandrite lasers *264*
aligned section (in drawing) 43
alkali-ion source *344*
alligator clips 529
alloy steels 18, 19, 20
alumina ceramics 24
  as electrical insulators 130, 356
  properties 20, 24, 356, 615
  in vacuum systems 116, 130
aluminum and alloys 22, 356
  properties 19, 141, 220, 615
  in vacuum systems 117, 139,140
aluminum coatings on mirrors 245
aluminum plate, vibration-isolated optical table 229
American Standard Pipe Thread 37
  specifications *73*
American Standard threaded fasteners 26
  specifications *71*
Amici prisms 199
amplifiers 421–435
  classifications 421, 422
  frequency ranges *422*
  impedances *422*
  stability 434
  types *421*
  see also instrumentation amplifiers; isolation amplifiers; operational amplifiers
analog input circuits 485
analog input signals, data acquisition 196, 472–474, 485
analog multiplexer 458, 474, 475
analog-to-digital converters (ADCs) 453, 456, 458
  applications 457, 472, 473, 103
anamorphic laser beam expanders 198, 278
annealing
  glass 88–89,166
  metals 14
antireflection coatings, dielectric coatings as 183–184
aperture lenses (electrostatic lenses) 331–332
aperture stop 163, 164
apertures in optical system 163
aplanatic imaging 162
apochromat lens 169
arc lamps 255–257
argon ion lasers 263, 270, 271
arithmetic units 448, 451
arsenic trisulfide glass 241
  properties 233, 234, 237, 242
ASA flange joints 119
ASCII computer code 469
aspheric lenses 191–193
aspheric surface 166
astigmatic mirrors 183
astigmatism 170, 171, 191

astronomical telescope 189
asymmetric electrostatic lens 330, 500
audio amplifiers 422, 423
auxiliary view 42
avalanche photodiodes (APDs) 574–577
  Geiger mode 577

backing pump (for vacuum system) 105
backstreaming in vacuum pumps 109, 110
baffles, vacuum system 127
Bakelite, properties 20, 615
baking, ultrahigh vacuum system 144–145
ball bearings 60–61
ball-mounting schemes for electrostatic lenses 358
ball-and-socket joints 79, 80
banana plugs 525, 528, 529
band-pass filters 380
  optical system 212, 213
band-reject filters 380
bandwidth, amplifier 422
Barber's rule 349, 354
barium fluoride 238
  properties 233, 234, 239
"barrel" distortion 172
barrier strips (connectors) 530, 531
baseline restorer circuit 439
BASIC programs, IEEE-488 system 484
batteries, circuit diagram symbol(s) *509*
baud rate 469
Bayard–Alpert ionization pressure gauge 102
Bayer pattern, in imaging arrays 580
bead blasting 142
beam angle 325, 326
beam expanders 190, 198, 355, 278
beam parameter, Gaussian beam 179
beam waist, Gaussian beam 180
beams
  bending of 50–52
  vibration of 54–55
beamsplitters 90, 182, 185, 186
  compared with pellicles 186
bearing mounts 59
bearings 59–61
  lubrication of 59, 61, 63,124
  in vacuum systems 124
Belleville spring washers 63,124
bending
  beams and shafts 50–52
  glass tubing 88, 89
  sheet metal 11, 10, 441
bending moment 50
  formulae *51*
beryllium copper (bronze) 19, 22
  springs 63
Bessel filter 381
"best form" lens 170, 188
biconcave lens 188
biconvex lens 187, 188
bimorph piezoelectric elements 221, 228
binary devices 447,585
binary number system 447
binding posts 528
bipolar junction transistors (BJTs) 406–410
  active loads 419
  applications 402
  case styles 406, 407
  circuit diagram symbol(s) *407*, *509*
  configurations 406
  current–voltage characteristics *408*
  current-source circuits 419
  junction capacitances 200, 409, 412
  operating conditions 410, 412
  properties 411, 413
  separate power supplies for biasing voltages 409, 410
  small-signal model 409, 412
bipolar operation of power supplies 443
bipolar pulse shaping 438, 440
birefringence 205
bits 467
black materials and coatings 296, 297, 356
blackbody pyrometry 611
blackbody sources 252–253
  practical designs 254
blaze angle (of diffraction gratings) 202
blind scew holes, pumpout holes for 142
block diagrams 436, 441, 455, 475, 479, 480, 489, 490, 494, 505, 506, 507, 508
  use when troubleshooting 534
blocking capacitors 425
"blooming" due to antireflection coatings 184
Bode plots 370
  inverting amplifier 422, 423
bolometers 548, 594–595
  characteristics 551, 592, 593
  as thermometers 611
bolted joints, designs 36
Boolean algebra 448
Boolean expressions
  logic units *449*, *364*
  vacuum system interlock circuits 460, 462, 522
bootstrapping technique, for photoconductive detectors 570
boring bar 2
borosilicate glasses 24, 76, 239
  properties 78, 79, 233, 235, 240
  tungsten-to-glass seal 90, 117, 132
  in vacuum systems 115, 116
  see also Pyrex glass
Bourdon gauge 100
boxcar integrator 494
brake bending of sheet metal 11, 10
brass 21
  properties *19*, *615*
  in vacuum systems 116
brass brazing alloy 32
brazed joints 36
  in tubing 39, 40
  in vacuum systems 132,141
brazing 30, 31–33
  thermocouples 604
breadboard circuit/model 508, 510
  prototype circuit boards 510
Brewster angle 177
Brewster-angle prisms 198
  in laser systems 269, 270
Brewster windows, lasers 268, 269, 272
bridges, electrical 445–446

brightness
in charged-particle optics 324–325
of light 162
brightness theorem 286
Brinell hardness scale 14
various materials (listed) 15, 19
British Standard Pipe Thread Tapered specifications 38, 73
broach 3, 4
broad-band antireflection (BBAR) coatings 185
bronzes 19, 22
Buna-N synthetic rubber 24, 118
butterfly valve 121
Butterworth filter 295, 381
bytes 467

cables and wires 524–528
see also coaxial cable
CAD (computer-aided design) programs 40
CAD/CAM software 40, 8, 517
cadmium telluride 245
Calbick lens 331
calcite ($CaCO_3$), properties 233, 235, 237
calcium fluoride 238
CAMAC sytem 476
bus *478*
connectors 533
camera lenses 189
Cameralink interface standard 581
cameras *see* digital cameras
capacitance, frequency response of detectors influenced by 553
capacitance manometers 100, 103
capacitance thermometers 611
capacitive effects, in electrical signal lines 503–504
capacitors
circuit diagram symbol(s) *509*
codes 387
equivalent circuits *386*
capillary (glass) tubing 79
carbide-tipped cutters and tools 6
carbon black coating 356
carbon-filament conductor cable 528
carbon steels 18, 19
card cage mounting for circuit boards 514
case hardening 15
cast iron 18, 19
casting 10–12
cathode-ray-tube guns 340
CCD imaging arrays 580–581
center drill 3, 6
centering optical mount 226
centroid 50
centroidal moment of inertia 50
centroidal polar moment of inertia 52
ceramic cements 34
ceramics 24–25
brazed joints 33
as electrical insulators 130
in vacuum systems 116, 130
cesium bromide 243
properties 233, 235, 237, 243
cesium chloride, properties 233, 235
cesium iodide 243
properties 233, 234, 237, 243
CF (ConFlat-compatible) sealing system 120
CGA (Compressed Gas Association) connections 38, 73
channel electron multipliers (CEMs) 556, 557, 587, 588
characters 467
charge-coupled device *see* CCD
charge-sensitive amplifiers 421, 422
charge-sensitive preamplifier
Bode plot *438*
combined with pulse detector 435, 438
test circuit 436, 438
charged-particle beam energy analyzers 345–353
charged-particle beam technology, applications 324
charged-particle detectors 358, 585–591
charged-particle lenses 327–338
compared with optical lenses 327
see also electrostatic lenses
charged-particle optical systems
construction of 355–360
magnetic-field control for 358–360
materials used in construction 356–357
vacuum requirements 355–356
see also electron-beam devices; ion-beam devices
charged-particle optics, basic concepts 324–327
charged-particle sources 338–345
chassis layout diagram (electronic circuit) 508
Chebyshev filter 381
chemically resistant glassware 77
chopping, amplifier 425
chopping wheels, optical modulation using 287
Christiansen filters 215, 216
chromatic aberrations 168, 191, 335
circle of least confusion 334
circuit analysis 365–369
computer-aided 381
Laplace-transform method 374–377, 376, 379
operational amplifier 428–432
circuit boards
extender boards used when troubleshooting 535
mounting of 514
perforated 510, 511
prototype 510
see also printed circuit boards
circuit breakers 501
circuit diagrams 508
symbols used *509*
circuit theory 362–365
circularly polarized light 147, 205
clamp, operational amplifier as 429, 432
closed-loop control systems 480, 479
closed-loop gain, operational amplifier 426
CMOS imaging arrays 580–581
CMOS logic devices 464, 465
conversion circuits *466*
power MOSFETs switched with 412
CNC (computer numerical control) machines 8, 9
CO lasers 263, 273
CO_2 lasers, *263*, *264*, 272–273, 290

coaxial cable 364, 389, 392
  applications 498
  procedure for stripping *504*
  properties 392, 393, 396
coaxial connectors 398–399
  assembly procedures 398
  circuit diagram symbol(s) *509*
  types 398
Code V analysis 166
  optical table for *167*
coherence properties of optical sources 248
coherent sources 247
  see also lasers
coil springs 63
coincidence measurements 436, 498–500
coincidence time spectrum 498, 499
cold-cathode ionization gauge 103
cold-junction compensation circuits 605
cold traps 126
cold working 14
cold-solder joint 521
collet chuck 5
collision frequency 94
color filters 212
color temperature of lamps 255
coma (aberration) 170, 191
comb filter
  electronic 380
  optical 212
combinatorial logic units 450
combined pulse detector and charge-sensitive preamplifier 435, 438
common-mode rejection ratio (CMRR)
  isolation amplifiers 433
  operational amplifiers 425, *426*, *433*, 507
  voltmeters 507
comparator circuits, operational amplifiers as 432
compensation, electronic circuit 380
compensator, in control system 489
complementary metal oxide semiconductor *see* CMOS
complex admittance 366
compound lenses 189
compound parabolic concentrators (CPCs) 195, 115, 196
compound turbomolecular/drag pumps 108
compression ratio, vacuum pumps 107, 108, 132, 137
computer-aided circuit analysis 381
computer simulations
  circuit analysis using 381
  electrostatic lenses 338
concave gratings 203
concave meniscus lens 188
concentration ratio, nonimaging light collector 196
condensers (lenses) 192
conductance of vacuum system 96, 97–98
  example calculations 139
confocal Fabry–Perot interferometer 308
conjugate points 162
connectors 528–534
  circuit diagram symbol(s) *509*
  see also coaxial connectors
constant-fraction discriminator 440
constantan 604, 610, 615
constrained motion 57–66
construction considerations
  charged-particle optical systems 355–360
  electronic equipment 508–533
  vacuum systems 131–145
continuous arc lamps 255–257
continuous wave (CW) CO_2 lasers 263, 272, 273
continuous wave (CW) dye lasers 280
  tuning range *265*
continuous wave (CW) gas lasers 270–273
  operating wavelengths *263*
continuous wave (CW) lasers, power outputs 266
continuous wave (CW) solid-state lasers 275
  operating wavelengths *264*
continuum sources 247, 252–261
contrast ratio, Fabry–Perot systems 307
control systems 479–481
  response parameters 480–481
converging thin lens, paraxial ray tracing for 160
convex meniscus lens 187, 188
cooling systems, lasers 268
copper 21
  oxygen-free high-conductivity 116, 356
  properties *19*, *615*
copper alloys 21
  brazing using 32
  properties *19*
copper mirrors 245
copper vapor lasers 264, 275
copper wire, insulated 524
corner-cube prisms 200–201
corner frequencies, in circuit analysis 369, 370
Coulomb blockade thermometers 611
counter digital-to-analog converter 456, 457
counterbore (tool) 3, 4
counters 453, 455
  and power-supply noise 467
crimped connectors, *531*, *532*, *533*
crimping tools 531
critical angle (optical reflection/refraction) 150, 151
critical backing pressure (vacuum pumps) 105, 107, 110
critical speed of shaft rotation 55
critically damped amplifiers 378
critically damped resonant circuit, response *378*
crowbar circuits 444
crown glasses 168, 239
cryogenic thermometry 610–611
cryopumps 114
  applications 132, 136
cryostats 620–621
cube beamsplitters 185, 186
current noise 549, 550
current sources, bipolar junction transistors 419
current-voltage relations 364
cutting fluids 4, 7
cuvettes 187

cyanoacrylate contact adhesives 34
cylindrical electrostatic analyzers 347
cylindrical lenses 195
  charged-particle system 329
cylindrical-mirror electrostatic analyzer 348, 532
cylindrical pressure vessels, design of 53
Czerny–Turner grating monochromator 296, 298
Czerny–Turner prism monochromator 295, 296

D-connectors 348, 532, 533
D (delay) flip-flop 453, 454
damping of vibrations 54
dark-noise level, optical detectors 553
data acquisition 467–491
data-acquisition interface *486*
data-acquisition systems 458
  noise elimination 485
  standardized 474–479
  see also CAMAC system; NIM system
data buffer 471
data format 469
data loggers 458, 474
data rates 467, 469
data selector 463, 464
data transmission 469
  cables 528
  system overhead 470–472
data units 448, 452
date code 535
datum 45
d.c. ground connection 501
d.c.-to-d.c. converters 443
decay time, sample-and-hold circuit 474
decelerating lens, in charged-particle system 336, 350
decibel (dB) scale 370
decimal number system 447
decoder (data unit) 117, 448, 452
degenerative feedback 434
delay-line applications 395, 498
delay-line shaping 439
Delrin 23, 117, 525
demosaicing 580
demountable glass joints 79–80
demountable pressure fittings 38
demountable vacuum system connections 118–120
demultiplexer (data unit) 448, 452
depletion-mode transistors 412, 414
  output current–voltage characteristics
derating 382
desoldering techniques 522
detectivity 550–551
  determination of 597
  optical detectors, 550, *567*, *568*, *570*, *571*, *573*, *575*
  thermal detectors *592*, *593*
  see also spectral detectivity
detector arrays 578–582
detectors
  calibration of 597
  charged-particle detectors 358, 585–591
  classification 548
  electronics used with 596
  equivalent circuits *435*, *583*, *590*
  figures of merit for 550–554
  ionizing-radiation detectors 591
  optical detectors 547
  particle detectors 435, 585
  photoconductive detectors 566–572
  photoemissive detectors 554–566
  photovoltaic detectors 572–578
  signal-to-noise ratio calculations 582–585
  thermal detectors 591–596
deuterium arc lamp 256
deuterium-filled thyratrons 421
diamond 239
  properties *234*, *240*
diaphragm pressure gauge/sensor 100, 103
  in vacuum system interlock circuit 461
diaphragm pumps 106–107
dichroic polarizers 208
dielectric coatings
  as antireflection coatings 183, 185
  as high-reflectance coatings 185
dielectric-coated mirrors 246
differential-equation method, circuit analysis using 369–372
differential-pressure flowmeters 104
differential pumping 130, 138–139
  applications 138, 257
differential-input amplifiers 425
differentiating circuits 369, 372
  charge-sensitive preamplifier 438
  operational amplifier 429, 431
  diffraction gratings 201–204
  see also grating spectrometers
diffractive optics 195
diffusion pumps 109–112
  applications 132, 132–135, 356
digital cameras, imaging arrays in 580
digital comparator (arithmetic unit) 448, 451
digital controllers, thermostat 616
digital electronics 447–467
digital multimeter (DMM) 491
digital-to-analog converters (DACs) 453, 456, 455
dimensions, on drawings 44–46
diode lasers 278
  operating wavelengths 279
diode-pumped solid-state (DPSS) lasers 279–280
  operating wavelengths *264*
diodes 402–406
  circuit diagram symbol(s) *509*
  configurations 402, 405
  current–voltage characteristics, *363*, 402, *403*, *405*
diopters (optical units) 155
direct-coupled amplifiers 425
disc of least confusion *334*
disc springs
dispersion
  diffraction gratings 203
  optical 150
  prisms 196
dispersive-type analyzers 346
displacement pumps 106
distortion, imaging system 172
distributed parameters, in high-frequency electrical connections 364

diverging thin lens, paraxial ray tracing for 161
doping, semiconductor materials 402
double-beam interferometers 309–314
  design considerations 314
  see also Mach–Zender interferometer; Michelson interferometer; Twyman–Green interferometer
double Gauss lens 166
  modulation transfer function 172, 174
  optical table for Code V analysis *167*
  spot diagrams for *170*
double-insulated cases 501
double refraction 151, 205
  polarizers using 204, 208, 209
doublets (lenses) 188
dove prisms 199, 200
drafting software 40
drag pumps 107
  applications 132, 137
drain wire 528
drawing tools 39
drawings *see* mechanical drawing(s)
drilled holes
  locational accuracy 3
  threaded 4
drilling 2–4
  glass sheet 91
drills
  sizes *68*
  tool speeds for *4*
dual-slope digital-to-analog converter 456, 457
duoplasmatron ion source 345
duty cycle, signal-enhancement systems 494, 496
dynamic mass spectrometers 355
dynamic resistance, diodes 405
dynamic systems (logic units) 450
dynamic transfer curve, diode 406
dynode chains (in photomultiplier tubes) 561–563
dynodes (in photomultiplier tubes) 555, 557
  materials used 556–561
Ebert–Fastie monochromator 297
echelle gratings 203
ECL devices 464, 465
  conversion circuits *466*, *477*
efficiency, diffraction gratings 203, 504
einzel (electrostatic) lens 331
elasticity modulus 13
  see also Young's modulus
elastomers 24
electrical connections, in vacuum systems 131
electrical discharge machining (EDM) 9
electrical grounds, safety aspects 500–503
electrical insulators, in vacuum systems 130
electrical signal pickup
  capacitive effects 503
  inductive effects 504
electrically erasable programmable ROMs (EEPROMs) 459
electromagnetic interference 505
electromagnetic radiation, fundamental parameters 147
electromagnetic relays 399
electromagnetic spectrum 147
electron-beam devices
  chromatic aberration in 335
  construction of 355–360
electron guns 338
  design example 340
electron-impact ionization ion source 343
  efficiency 345
electron multipliers 586
  coupling via transformer 587, 588
  see also channel electron multipliers (CEMs)
electronic compensation circuits (for thermocouples) 605
electronic components
  active 402–421
  circuit diagram symbol(s) *509*
  passive 382–402
  selecting 508
electronic devices, in vacuum systems 131
electronics
  amplifiers and pulse electronics 421–441
  basic concepts 362–382
  construction considerations 508–533
  digital electronics 447
  grounding 500–507
  laws and theorems 364
  power supplies 441–446
  troubleshooting 534–536
electro-optic modulators 287
electropolishing 142
electrostatic lenses 338
  compared with optical lenses 327
  computer simulations 338, 342
  design example 336
  electrodes 357
  mounting schemes 358
ellipsoidal mirrors 183
elliptically polarized light 147, 204, 485
embossing of sheet metal 11, 10
emissivity 252
enclosure thermostats 619, 620
encoder (data unit) 448, 452
energy analyzers, charged-particle beam 345–353
energy-add lens (in electrostatic energy analyzer) 350–352
energy-level diagram, lasers 267
enhancement-mode transistors 412, 414
  output current–voltage characteristics *415*
entrainment pumps 112–115
entrance pupil (in optical system) 162, 163
epoxy adhesives 34
epoxy resins, in vacuum systems 118
equivalent circuits 367, 368
  capacitors and resistors *386*
  detectors *435*, *583*, *590*
  field-effect transistor *590*
equivalent noise charge (ENC) 591
equivalent noise temperature (in amplifiers) 493
  detectors *583*, *590*

erasable programmable ROMs (EPROMs) 450, 459
erector lens 163
error band (of waveform) *379*
etalons 187, 299–302
  as filters 212, 284
  see also Fabry–Perot etalons
étendue
  Fabry–Perot system 307
  optical concentrator 195
eutectic temperature 613, 614
evanescent wave 150
exciplex (excimer) lasers 264, 273
expansion thermometers 601
exponential amplifiers 431
extended source(s), coupling to aperture 286
extension lines (on drawings) 46
extrinsic photoconductive detectors, properties *568*
extrinsic photoconductivity 566
eyepiece lens 163

F-center lasers 276
f/number
  lens 163
  monochromator/spectrometer 292
fabrication materials 12–25
fabrication processes 2–12, 25–39
Fabry–Perot etalons 212, 299
  properties 303, 304
Fabry–Perot fringes, observation of 305
Fabry–Perot interferometers 299–308
  alignment of 229
  characteristics *294*
  compared with other optical dispersing instruments 295
  practical operating configurations 303, 305
  spherical-mirror 307
Fabry–Perot semiconductor lasers 279
Fabry–Perot systems
  design considerations 308
  optical characteristics *303*
  performance limitations 303
fall time (of pulse) 364
Faraday cup (charged-particle detector) 358, 585
Faraday materials 211
FAST™ logic devices 456,467
ferrofluidic shaft seals 124
ferromagnetic table tops (optical tables) 229
fiber jumpers (for optical fibers) 219
fiber lasers 264, 275
fiber optic connectors 218
fiber optics 217–219
field curvature (aberration in imaging system) 172, 191
field lens, electron-optical analog 351
field programmable gate arrays (FPGAs) 460
field stop 163, 164
field of view (in camera lens) 189
field-effect transistors (FETs) 410–419
  applications 402
  small-signal equivalent circuit *590*
  see also junction field-effect transistor; metal oxide-semiconductor field-effect transistors
figures of merit
  amplifiers 422
  detectors 550–554
  sample-and-hold (S/H) circuits 474
filters
  electronic 380
  optical system 212–217
fine-scale movement in optical systems 220
finesse, in Fabry–Perot systems, 302, 303, 305
fire-polishing of cut glass tubing 83
first-angle projection 42
fits (between parts) 35, 48
fixed-point cells 605, 612, 613
fixed points (reference temperatures) 614
fixed resistors 383–384
  codes 386
  types *383*
fixed-voltage power supplies 444
fixed-voltage regulators 444
Fizeau interferometer 308
flash converter (digital-to-analog converter) 456, 457, 456
flashlamp-pumped dye lasers 270
flashlamps 257–261
  detector response determined using 597
flat mirrors 182
flexures 63–66, 224
flicker noise 492, 549
flint glasses 168, 239, 241
flip-flops 450, 454
float plate glass 315
  mirrors 182
floating power supplies 501
flowmeters, in vacuum systems 103
fluid baths (thermostats) 616, 617
  materials used *615*, *619*
fluorescence thermometry 622
fluorocarbon polymers 24, 117
  properties 20, 525, 615
  see also Teflon
focal lengths 152, 153
focal points 152, 153
foldback current limiting (in power supplies) 444
force fit(s) 35
forward bias, of diode 402
four-wire measurement techniques, resistance thermometry 608
Fourier transform spectroscopy 311
framegrabber card (in digital camera) 581
free spectral range, Fabry–Perot devices 302, 303
frequency response
  detectors 553
  operational amplifiers *426*
Fresnel criterion 159
Fresnel lenses 193, 194
Fresnel retardation rhombs 211
full adder (arithmetic unit) 448, 451
full-duplex transmission of data 469
fused silica 24, 77, 238
  properties *78*, *79*, *233*, *234*, *237*, *240*
  see also quartz
fuses 501
  circuit diagram symbol(s) *509*
fusion splicer (for optical fibers) 218

GaAlAs lasers 277, 280
gain, amplifier 421
gain margin, amplifier 423, 424
gain profile, laser 267, 268
gain-bandwidth product (GBWP) 422
  typical values *426*
Galilean telescope 189, 190
gallium arsenide
  in optical components 245, 273, 277
  properties 233, 235, 244
gas-filled photodetectors 547, 555
gas flow, parameters for specifying 95–96
gas jets, in vacuum systems 127–130
gas kinetic theory 93–95
gas thermometers 610
gaseous ion lasers 270–275
  operating wavelengths 263–264
gases
  bulk vs molecular behavior 95
  molecular velocity 94
  residual, in vacuum system 93
gate valves, in vacuum systems 122, 122
gated integrator 494, 495
Gauss lens *see* double Gauss lens
Gaussian beams 179–182, 278
Gaussian lineshape function 251
Gaussian optics 325
Gaussian waveform 438
Geiger mode avalanche photodetectors 577
generation–recombination (gr) noise 549, 550
geometrical aberrations 169, 333–335
Gerber file (for printed circuit board production) 518
germanium
  in optical components 244, 273
  properties 233, 234, 237, 244
germanium photodiodes 573, 574, 575
getter pumps 113–114
ghost reflections (from mirrors) 182
gimbal mounts 223, 226
Glan–Foucault polarizer 209
Glan–Taylor polarizer 208, 209
glass chart (Abbe diagram) 168, 169
glass fibers 78
glass joints 80
glass laboratory components 78–81
glass rod 78, 79
glass sheet
  drilling of 91
  sawing of 91–92
glass stopcocks 80–81
glass surfaces, cleaning of 143
glass tubing 78–79
  bending 82–83, 88, 89
  cutting 82–83, 89
  fire-polishing of cut end 83
  flaring end 87
  grinding end 91
  pulling points 83–84
  ring seal in 87–88, 89
  sealing off 84–85
  straight seal in 87, 88
  T-seal in 85–87
  test-tube end formed in 84–85
glass vacuum accessories 116
glass valves 80, 81
glass-to-metal seals 81, 89–90, 116, 132, 241
glassblower's tools 81–82
glassblowing skills 81–92
glasses
  Abbe diagram (glass chart) 168, 169
  chemical composition 76–77
  chemical properties 76–77
  mechanical properties 78, 233
  in optical components 239–241
  optical properties 78, 79, 234, 240
  thermal properties 77–78, 233, 234
  in vacuum systems 115–116
Golay cells 595
  characteristics 551, 592, 593
gold coatings on mirrors 247
graded index lenses 193
graded seals 81, 116, 231
granite table tops (optical tables) 229
graphical construction, of image size and position 159–161, 328
grating spectrometers
  characteristics 294, 295
  compared with prism spectrometers 293
graybody emitters 253
grinding 9–10
  glass tubing 91
ground loops 506–507
ground-fault interrupters (GFIs) 501
grounds and grounding 507
  circuit diagram symbol(s) *509*
Gullstrand opthalmoscope 163

Hagen–Poiseuille relation, tube conductance derived from 97, 104
half adder (arithmetic unit) 448, 451
half-duplex transmission of data 469
half-wave plates 206, 210
hand tools 2
hand-shaking (in data transmission) 470
Hänsch-type pulsed dye laser 282
hardness of materials 14
  various materials 19, 233
hardness scales 14
hardware, electron-equipment construction *516*
harmonic distortion, amplifiers 424
Hastelloy alloys 21
HC logic devices 467
HCT logic devices 467
heat-and-pull method of removing components from PCBs 522
heat treatments 14
heliarc welding 34, 117, 141
helical springs 63
helium–cadmium lasers 263, 270, 272
helium melting-curve thermometers 610
helium–neon lasers 263, 268, 272, 299
Helmholtz coils/pairs 359–360
Helmholtz–Lagrange law 325–326
  applications 334, 335, 342
hemispherical electrostatic analyzer *349*
hexadecimal number system 447

high-efficiency broad-band antireflection (HEBBAR) coatings 185
high-pass circuit *369*
analysis of 369–372
Bode plots *370*
idealized gain and phase responses 370, 371
Laplace-transform equivalent *377*
high-pass filters 380, 429, 431
high pressure, meaning of term 52
high-pressure arc lamps 255–256
high-pressure gas cylinders, CGA connections 38, 73
high-pressure pulsed discharge lamps 597
high-pressure systems, windows in 231
high-reflectance coatings, dielectric coatings as 185
high-temperature thermometry 611
high vacuum
  characteristics *94*
  pumps 109, 132
high-voltage cable 527–528
high-voltage connectors 533, 534
hole-making machines 2–4
holographic gratings 203, 295
holographic nondestructive testing (HNDT) 17
holographic notch filters 214
hookup wire 526
hoop strain 53
hoop stress 53
hot-carrier-effect photoconductive detectors 572
hot-cathode ionization pressure gauges 102, 103
hot-air rework station, removal of components from PCBs using 522
housekeeping signals (in data transmission) 470
human eye
  cones and rods (receptors) 249
  spectral response 249
hybrid pumps 108–109
hydrogen brazing 33
hydrostatic gauges 98–100
ice point (temperature reference) 605, 612–613
ice-point bath 605, 613
IEEE-488 system 482–483
  BASIC program for *484*
connectors 482
for measurement of temperature-dependent dielectric constant of liquid 482–484
image intensifiers 581
image plane 161, 162
imaging arrays 580–581
imaging spectrographs 299
imaging systems 161, 162–165
impedance
  amplifier *422*
  electric circuit 366–369
  optical medium 149, 148
  transformation through multilayer optical systems 177–178
impedances method, use in optics 174–179, 300
incoherent sources 247
Inconel alloys 19, 21
indium antimonide photodiodes 574
indium (gallium) arsenide photodiodes 573, 574, 575, 577
  in imaging arrays 580
  signal-to-noise ratio calculations 584
inductive effects, in electrical signal lines 504
inductors, circuit diagram symbol(s) *509*
infrared absorption spectrum, temperature measurement using 612
infrared lasers 273, 275, 277
  safety precautions 290
infrared polarizers 208
infrared thermometers 611
infrared-transmissive materials 241–245
  properties 233, 234–235
input plane (of optical system) 152
instrumentation amplifiers 432
  typical specifications *433*
insulated gate bipolar transistor (IGBT) 418
  compared with other transistors 418, 419
  inductive load switching circuit *418*
internal connections *418*
insulators, properties *615*
integral control, thermostat 616
integrated-circuit (IC) amplifiers 425
integrated-circuit packages
  abbreviations *503*
  code prefixes 151
  photodiode + op-amp 574
  temperature sensors 609–610, 612
integrated-circuit voltage references 445
integrated-circuits, packages *515*
integrating circuit 369
  operational amplifier 358, 429, 431
interference filters, characteristics *294*
interference fringes, observation of 305–306, 309
interferometers 299–314
  additional uses 291
  see also Fabry–Perot interferometer; Mach–Zender interferometer; Michelson interferometer; Twyman–Green interferometer
internal pressure 52–54
internal resistance, of voltage/current source 365
International Temperature Scale (ITS) 600, 612
  triple points used to define 612, 613
intrinsic photoconductive detectors, properties 567
intrinsic photoconductivity 554, 566
Invar alloy *19*, 21
inverting amplifier 422, *429*
ion-beam devices, construction of 355–360
ion pumps 115
  applications 132, 136, 356

with titanium sublimation pumps 115, 136
ion sources 343–345
ionization pressure gauges 101–103
vacuum system controllers based on 135
ionizing radiation, detection of 591
irradiance 249
ISO joints *119*, 120
ISO (metric) threads 25, *71*
isolation amplifiers 433–434
isolation transformers 503
isolation-mode rejection ratio (IMRR) 433
isolators, electronic 461
isothermal block 605

jig plate *229*
J/K flip-flop 450, *454*
Johnson noise 491
detectors 549, 583, 584, 590
joining of materials 25–39
joints
demountable glass 79–80
design of 34–37
piping and pressure vessels 37–39
types 35
junction field-effect transistor (JFET) 410
circuit diagram symbol(s) *509*
construction (N-channel JFET) *411*
current–voltage characteristics *413*

Kapton (polyimide) 117, 356, 525, 152–159, 528
Karnaugh maps 448, *450*, *462*
Kel-F polymer 24, 241
properties *20*, 234, 525
Kerr cells 288
KF (Klein flange) vacuum joints *119*
kinematic design 57–59
optical mounts 223
Kirchhoff's laws 365
application 380
Knoopness hardness scale 14, 236
various optical materials (listed) *236*
Kovar alloy 21, 81
Kovar-to-glass seals 81, 116, 243
KRS-5 (thallium bromoiodide) 243
properties 236, 237, 243
KRS-6 (thallium chlorobromide) 236, 237
krypton ion lasers *263*, 270, 271

laboratory glassblowing skills 81–92
Lambertian radiator 249
blackbody as diffuse radiator 252
radiant intensity characteristics *249*
Lambertian source 250
lamp-pumped solid-state laser 270, 271
lamps 254–261
Laplace-transform method
circuit analysis using 374–377, 379
control theory using 479
Laplace transforms *375*
control systems 481, 489
pulse electronics 435, 438, 439
large-scale integrated (LSI) circuits 458, 464
MOSFETs used in 412
laser beam
focusability parameter 181
focusing with lens 180–181
laser beam expanders 190, 198, 278
laser diodes 277
laser radiation 283–284
lasers 261–291
detector response time determined using 597
features of design 268–270
operating wavelengths 263–265
power output(s) 249, 266, 270–272
principles of operation 267–268
safety precautions 290–291
specific systems 270–283
types 266
latch 471
latching relay circuit, in vacuum system 135
lateral-effect photodetectors (LEPs) 578–580
lathe
component parts 5
cuts made by *5*
lathe cutting tools 6
speeds for *4*
lathe turning 4–7
lava (aluminium silicate) 25
layout diagram, electronic circuit 508
lead sulfide and lead selenide photoconductive detectors 570, 570
lead-free solders 31, 521
leak detection, in vacuum systems 143
"leak" valves 122
least significant bit (LSB) 447
left-hand circularly polarized light 205
lens aberrations 161, 168, 169, 191
lens aperture (camera lens) 189
lenses and lens systems 187–196
materials 236–245
Lexan (polycarbonate) plastic 20, 24, 525
light collectors, nonimaging 162, 195
light sources 147, 247–261
coupling light to aperture 284–286
safety precautions 289–291
light traps 216
line regulation of power supplies 442
line sources 247, 250–252
line-operated equipment, floating power supplies used 502
linear circuit theory 363
linear-motion bearings 61
linear polarizers 208
optical isolators using *210*
linearizing of response curve 363

linearly polarized light 147, 204
lineshape functions 251
liquid baths (thermostats), materials used 615, 617, 618, 619
liquid-in-glass thermometers 601–602, 612
liquid-nitrogen-cooled cryotrap (for diffusion pump) 111, 126
lithium fluoride 237
properties 10, 237, 238
Littrow monochromator 295
Littrow prisms 197
in laser systems 269,
Littrow-type dye laser 283
load-line analysis, diodes 405–406
load regulation of power supplies 442
lock-in amplifier 495
logarithmic amplifiers 429, 431
logic analyzers 535
logic functions, implementing 464–467
logic gates 447, 449
applications 460–464
sinking capabilities 469
sourcing capabilities 469
logic probe (in troubleshooting) 535
logic pulser (in troubleshooting) 535, 536
logical interlock system, vacuum system protection by 135
long items, representation on drawings 44
long-pulse flashlamps 257, 258–260
long-pulse solid-state lasers 266
long-wavelength-pass filters 214
Lorentzian lineshape function 251
low-pass circuit *369*
analysis of 369–372
Bode plots *370*
idealized gain and phase responses 69, 370
Laplace-transform equivalent *371*
low-pass filters 380, 429, 431
low-temperature thermometry 609–611
low-temperature thermostats 620
lubrication, of bearings 60
Lucite *see* acrylic plastics
luminance 250
luminosity, optical dispersing instruments 291, 307
luminous flux 250
lumped circuit components 383
Lyman ghosts 203

Mach–Zender interferometer 313
machinability of material 14
machine screws
materials 27–28
types 26–27
machine-tool operations
electrical discharge machining 9
grinding 9–10
lathe turning 4–7
milling 7–9
surface quality for 10, 12
tolerance for 7, 8, 10, 12
McLeod pressure gauge 99–100, 103
Macor ceramics 20, 25, 116, 356, 615
MacSimion simulation of charged-particle system 339, 343
Magnaflux stress-detection method 18
magnesia, thermal properties *615*
magnesium and alloys 22
magnesium fluoride 238
as coating on aluminum mirrors 245, 246, 247
properties 233, 234, 238
magnesium oxide, properties 234, 237, 242
magnet wire 528
magnetic energy analyzers 353
magnetic-field pickup 504,
magnetic sector mass analyzers 354
magnetic-shielding materials 359, 504
magnetic shields 359–360, 565
magnetic suspension systems 108,
magnetic thermometers 611
magnetoresistance 610
magnification
electrostatic lens 328
optical lens 161
maintenance, vacuum pumps 109, 109
manganin 112, 615
manufacturers' logos 536
manufacturing date code 535
marginal rays 164, 165
maria (in glass tubing) 87, 89, 245
mass analyzers 354–355
mass spectrometers 103
pressure measurement using 103, 144
mass spectrometry, silicon substrate 487–489, 509
materials 18–25
charged-particle optical system 356–357
joining of 25–39
magnetic-shielding 359
optical system 234–235, 236–247
properties 12–18, 19
vacuum system 115–118
matrix methods for optical analysis 152–159, 528
charged-particle optics 332–333
Maxwell–Boltzmann velocity distribution law 94
mean free path (between molecular collisions) 94, 355
mechanical design, physical principles 49–57
mechanical drawing(s) 39
abbreviations used 46, 47
basic principles 44
dimensions on 44–46
notes 44, 45, 46, 130
symbols used 6, 43, 44
tolerances expressed on 46–48, 49
mechanical pressure gauges 98–100
mechanical properties
brazed joints 32
metals 19
plastics *20*
soldered joints 30

mechanical pumps 105–109
mechanical relays 399
  contact-conditioning circuits 401, 402
medium-scale integration (MSI) 464
medium-scale movement in optical systems 220
melting point
  as fixed point temperature *614*
  various optical materials *233*
melting-point baths 613
memories 458–460
memory cell, one-bit 458–459
mercury arc lamp 255
mercury cadmium telluride (MCT) detectors 570, 574, 578
  properties 567, 571, 573, 575
mercury diffusion pumps 111
mercury lamp 251
  characteristic lines *252*
mercury manometer 98, 99, 103
mercury-in-glass thermometers 601–602
meridional rays, imaging of 170, 171
metal mirrors 245–246
metal oxide-semiconductor field-effect transistors (MOSFETs) 411–418
  circuit diagram symbol(s) *509*
  output current–voltage characteristics *414*
  structures *414*
  as switches 412, 474
metal resistance thermometers 605–607
metal-to-glass seals 81, 89, 116, 132, 241
metal vacuum chambers 139–141
metal vacuum gaskets 120
metal vacuum valves 121–123
metals 18
  machining of 4
metering valves 122
meters, circuit diagram symbol(s) *509*
metric threaded fasteners 25, 71
  specifications *25, 71*
mica sheets 357
Michelson interferometer 248, 309–311
microbolometers 595
microchannel plate (MCP) 556, 557, 588–589
  image intensifiers 581
microstrip line 389, 392
microwave lamps 257
Miller effect 367
Miller transform equivalent circuits 367, 368
milling 7–9
  cutting operations 7, 8
  dimensional accuracy 8, 59
milling cutters 7
  speeds for *4, 8*
milling machines, types 4, 8
mirror holders/mounts 222–225
mirrors 182–187
  materials for 245–247
  substrates for 246
"MISER" ring laser design *280*
mode-locked lasers 266, 284
modems 470
modulation transfer function 172
  double Gauss lens 173, 174
modulo-*N* counters 453
Mohs hardness scale 14
  various materials (listed) 15, 623
molecular beams, in vacuum systems 127
molecular-drag pumps 107
  applications 132, 137
molecular-nitrogen lasers 264, 275
molecular-sieve vacuum system traps 125–126
molecular thermometers 598
molybdenum 23, 599
Monel alloys 19, 21
monochromators 291
  design 295–299
  see also spectrometers
Mooney retardation rhomb *211*
most significant bit (MSB) 447
motherboard 514
mounts *see* optical mounts
multichannel analyzer (MCA) 441, 591
multiconductor cable 528
multilayer dielectric coatings on mirrors 246
multilayer dielectric interference filter, characteristics *294*
multilayer optical systems, transformation of impedance through 177–178
multimode lasers 274, 284
multiple-beam interferometers 299–309
  see also Fabry–Perot interferometers
multiple-contact connectors 458, 532
multiple-input data-acquisition systems 458, 474, 475, 532
multiple monochromators 298
multiplexer (data unit) 448, 452, 622
multiplying digital-to-analog converter 456
Mylar
  electrical properties *525*
  PCB drafting sheet 520

nanoscale movement in optical systems 220
nanoscale piezoelectric drives 220–221
near-infrared photodiodes, properties 573, 574
near-infrared-transmissive materials 239–241
  properties 233, 234
negative electron affinity (NEA) photocathode materials 558–559, 560
  properties 558, 560
negative feedback 434
  amplifiers with 378, 381
negative-logic system 447, 469
neodymium lasers 264, 265, 275, 290
netlist, printed circuit board production 517
neutral-density (ND) filters 216
Newton's formula 328, 332

Newton's law 328
nickel, properties 583, 615
nickel alloys 19, 20–21, 359
NIM system 474–476
  connectors 475, 476, 533
  ECL and TTL conversion circuits *477*
  logic level specifications *475*
  modules available *475*
nitrogen lasers 264, 275
NMR thermometers 611
noble-gas discharge 256
noise elimination
  in data acquisition 485–487
  in detectors 553
noise-equivalent power (NEP), of detectors 550, 584
noise figure (NF) 492
  detectors 553–554, 583
noise margin (in logic devices) 464, 465
  typical values *465*
noise sources 491, 493, 505–506
  optical detectors 548–550
noise temperature
  amplifiers 493
  detectors 588
noise thermometers 610
nonimaging light collectors 162, 195
nonlinear devices 363
nonlinearity, amplifier 441
Norton's theorem 365
notch hinge 65–66
nuclear instrumentation module *see* NIM system
nuclear-orientation thermometers 611
numerical aperture
  optical fiber 218
  optical system 162
nut-and-bolt assembly, locking methods 28
Nylon 20, 23, 117, 525, 615
Nyquist noise 549

O-ring joints 79, 80, 118–120
O-ring seals 231
object plane 22, 161
objective lens 163
octagonal prisms 199, 200
octal number system 447
off-null bridges 445
oil diffusion pumps 109–112, 356
oil manometers 98–99, 103
oil-sealed rotary vane pumps 105–106
oil-free vacuum systems 136–138, 356
on–off control, thermostat 234
open-loop control systems 479
open-loop d.c. gain
  operational amplifier 426
  typical values *426*
operational amplifier(s) 425
  circuit analysis 428–432
  comparison of 741 and OP7 components 426, 427
  design rules 427–428
  ideal characteristics 425
  parameters 425–427
  specialized *428*
  symbol *426*
optic axis 205
optical benches 227–228, 228
optical cells 187
optical components 182–219
  cleaning of 232–236
  mounting of 230–231
  positional and orientational adjustment of 219, 222–229
  precision mechanical movement systems for 219–222
optical concentrators 195–196
optical deflectors 289
optical design
  software 166
  wavelengths used 168
optical detectors 147, 547–548
  factors governing choice of 547–548
  noise in 548–550
  spectral detectivity 550–551, 551
  see also photoconductive . . .; photoemissive . . .; photovoltaic detectors
optical dispersing instruments 291–314
  see also interferometers; monochromators; spectrographs; spectrometers
optical fibers 217
  connectors 218–219
  types 218
optical filters 212–216
optical isolators 211–212
  see also optically isolated relay
optical lenses 187–196
  compared with charged-particle lenses 327
optical materials
  characteristics 233–235
  for diffraction gratings 201, 247
  factors governing choice 236
  for lenses, prisms and windows 236–245
  for mirrors 245–247
optical modulators 287–289
optical mounts
  characteristics required 220, 222, 230
  constructional details 223
optical multichannel analysers (OMAs) 299
optical parametric oscillators (OPOs) 266, 283
optical sources 147, 247–262
  coherence properties 248
optical system(s)
  alignment of 229
  characterization and analysis of 150–182
  design software 178
  schematic diagram(s) *152*
optical tables 229
  selection criteria 229
optical terminology 147–149
optical windows 187
  materials 236–245
  suppliers 322–323
  in vacuum systems 116, 231, 232
optical-frequency oscillator, laser as 267
optically isolated relay 461
orthographic projection 41–42
oscillators 434–435
outgassing 98

output plane (of optical system) 152
overdamped resonant circuit, response *379*
overshoot (of waveform)
overvoltage protection in power supplies *444*
oxygen-free high-conductivity (OFHC) copper 116, 356
P-polarized wave (TM wave) 176, 175

paraboloidal mirrors 183
parallel circuits, analysis of 366
parallel dimensions 45
parallel format 469
parallel-plate electrostatic analyzers 346–347
parallel resonant circuit 373
  current as function of frequency *373*
  phase relations between voltage and current *374*
parallel–series formats 469
paraxial optics 325
paraxial-ray analysis 151–162
paraxial ray tracing 159–161
parity bit (in data transmission) 470
parity generator/checker (arithmetic unit) 448, 451
particle-counting experiment 436, 441
particle detectors 435
  see also charged-particle detectors
parts identification 535
passband, energy analyzer 346
passivated implanted planar silicon (PIPS) solid-state detector, equivalent noise charge calculations 591
passive electronic components 363, 382–402
  circuit diagram symbol(s) *509*
  considerations in choice 382–383
peak reverse voltage (PRV), diodes 402, 403, 407
peak-to-peak voltage 364
pellicles 186–187
  compared with beamsplitters 186
Peltier devices 620
Peltier effect 602
pencil angle 326
penta prisms 199, 200
perforated circuit boards 510, 511
personal computer (PC) control of experiments 482–491
  dielectric-constant temperature experiment 482–484
  example of sensor and control electronics 487–489
  mass spectrometry of silicon substrate 487–491
Perspex *see* acrylic plastics
phase margin, amplifier 423, 424
phase-sensitive detection, signal-to-noise ratio improved by 287
phase-transition baths 613, 614
phase-transition temperatures 614, 612, 613, 619
phenol–formaldehyde thermosetting plastics 20, 23, 615
phone plugs 530
phosphor thermometry 612
photocathode materials 556–561
  properties 552, 559
photocathodes, types 558
photochemical detectors 548
  see also photographic film
photoconductive detectors 548, 566–572
  biasing circuit for operating 569, 569
  cooling of 568, 569
  op-amp circuit dor 569
  properties 567, 568
  spectral detectivity 551, 568, 570
photodiodes 548, 572–578
  equivalent circuit *583*
  signal-to-noise ratio calculations 583–584
photoelastic method of stress detection 16
photoemissive detectors 548, 554–566
photoemissive materials, properties 552, 559
photoemissive surfaces, quantum efficiency 551
photoexcitation at *p*–*n* junction 572, 573
photographic film 548
photometric quantities 250
  correspondence with radiometric quantities *250*
photometry 249–250
photomultiplier tubes (PMTs)
  anode signal coupling methods 562
  cooling of 564, 565
  dynode chains in 563
  dynodes in 555–556, 557
  focusing electrodes 562
  mounting of 563
  noise in 564–566
  practical operational considerations 561–566
  time-response characteristics 553, 555, 563
photomultipliers 555–556
  detectivity 555
  signal-to-noise ratio calculations 582
photon counting, signal-to-noise ratio calculations 585
photon detectors 548
  spectral sensitivity 548
  see also photochemical . . .; photoconductive . . .; photoemissive . . .; photovoltaic detectors
photon-drag detectors 548, 594
photon energy 149
photon-limited performance of detectors 553
photon noise 548
photons 147
Phototron lamp 144
photovoltaic detectors 548, 572–578
  spectral detectivity *551*
pickling of metal surfaces 143

piecewise linear model, diode *I–V* characteristic curve represented by 405
Pierce diode geometry (in electron guns) 340, 344
  pencil angle characteristic 340, 342
piezoelectric pressure transducer 100, 103
piezoelectric scanning (wavelength scanning) in interferometers 305
piezoelectric transducers (PZTs), positioning of optical components using 220–222, 228
piezotubes 221
"pincushion" distortion 172
pins 29
pipe threads 37, 118
  specifications
piping, joints in 37–39
Pirani pressure gauge/sensor 101, 103, 135
piston pumps 106
piston-type/poppet valves 121, 122
pitch, graded index lenses 193
pitch of threads 25
  pipe threads *73*
  screw threads *71*
plain bearings 59–60
plane mirrors, optical systems with 158
plano-concave lens 188
plano-convex lens 187, 188
plastic films, optical applications 244
plastics 23–24
  far-infrared optical applications 244
  in optical components 241
  properties 241
  in vacuum systems 117–118, 356
platinum, properties 615
platinum resistance thermometers (PRTs) 606, 612
Plexiglass *see* acrylic plastics
Pockel's cells (electro-optic modulators) 287
point source(s) 248
  coupling to aperture 284–286
  coupling to optical fiber 286
Poisson distribution 497
Poisson's ratio 14
polariscope, strain in glass observed by 89, 90
polarization-maintaining (PM) fiber 219
polarized light 204–206
polarizers 204–211
pole-zero compensation 380, 423, 438
polyamides 20, 23, 525
polycarbonate plastics 24, 117, 525
polyethylene 23, 525
polygon prisms 199, 200
polyimides
  insulated cables 528
  properties 20, 525
  in vacuum systems 117
polymethylmethacrylate (PMMA) *see* acrylic plastics
"pop" (blind) rivets 29, 28
population inversion, lasers 267
Porro prisms 198, 199
position-sensing potentiometers 367
position-sensitive electron detectors 588
positive feedback, in amplifiers 422, 434
positive-logic system 447, 469
potassium bromide, properties 233, 237
potassium chloride 242
  properties 145, 216, 242
potassium iodide, properties 233, 234, 237
potentiometers 384, 391
power, lens surface 155
power amplifiers 423
power bipoar junction transistors, compared with other transistors *419*
power bipolar junction transistors 406
power diodes 402
  configurations 404, 405
  properties *404*
power-failure safeguards, vacuum systems 134
power line *see* a.c. line
power line entry modules 526
power MOSFETs 412
  applications 416, 417
  compared with other transistors 418, 419, 37
  example circuits *417*
  operational characteristics 418
  output current–voltage characteristics *416*
  structure *416*
power supplies 441–446
  biasing voltages for transistors 409, 410, 425
  current–voltage characteristics *442*
  fixed-voltage 444
  floating 501–503
  regulator circuits 443–445
  specifications 442–443
power-line-coupled noise 505–506
power-supply noise, reduction of 467
Poynting vector 149, 205
preamplifiers 423
  pulse electronics 435
precision mechanical stages 219
precision rectifier, operational amplifier as 429, 431
precision of temperature measurement 600
preretardation, in charged-particle system 350
pressure, units 93
pressure gauges
  operating ranges *103*
  in vacuum systems 98–103
pressure scanning (wavelength scanning) in interferometers 305
pressure vessels
  design of 53
  joints in 37–39, 52
pressure-tight seals 231
principal planes 152, 153, 327
principal points 152, 153
principal rays 152, 153, 163, 164, 165, 328

printed circuit boards (PCBs) 516–523
circuit-board substrates *516*
construction considerations
fabrication from hand-drawn artwork 520
production of 516–518
schematic-capture and board-layout software 517, 538
soldering components to 518–520
prism beam-expanders 198
prism spectrometers 291
characteristics *294*
compared with grating spectrometers 293–295
prisms 201
materials 236–245
programmable logic arrays (PLAs) 459
programmable power supplies 443–444
programmable ROMs (PROMs) 450, 459
programmers for 459
truth tables implemented using 459, 460
proportional controllers, thermostat 616
proportional gain, thermostat 616
proportional, integral, and differential (PID) controllers 481, 616
proportional and integral (PI) control 616
protection diodes (for transistors) 416, 417, 535
prototype circuit boards 510
pulling points in glass tubing 82–83
pulse-counting applications 436, 441, 587
pulse detection and processing 435–441
pulse-height analysis 438
pulse-height analyzer (PHA) 441, 498
pulse timing systems 436, 439
pulsed amplifiers 378
pulsed dye lasers 281–283
pumping arrangements *281*
tuning range 265
pulsed gas lasers 270, 275
operating wavelengths *263*
pulsed lasers
detector response time determined using
energy outputs 266
pulsed solid-state lasers 276–277
mode configurations 266
operating wavelengths 264–265
pumpdown time (for vacuum system) 98
punch and die 11, 10
PVC, electrical properties 525
Pyrex glass 76, 239
properties, 78, 79, 233, 234, 240, 615
see also borosilicate glasses
pyroelectric detectors 548, 593–594
characteristics *551*, *592*, *593*
operating circuits for *594*
pyrometers 611

Q-switching in lasers 266, 276
QF (quick flange) vacuum joints 119
quadrant detectors 578, 579
quadrupole mass analyzer 355
quantum cascade lasers 277
quantum efficiency
photoemissive surfaces/materials 551, 558, 559
photon detectors 552, 554
quantum noise 548–549
quarter-wave plate 206, 208
optical isolator using *210*
quartz 24, 77
fiber torsion springs 24, 62
helium permeability 116
optical properties *237*, *240*
in vacuum systems 115–116
quartz crystal oscillators 434
quartz fibers 78
quartz windows in vacuum systems 116
quasi-optics 148
quenching, of metals 14
quick-connect joints 79, 80, 118, 119
quick-connect terminals 531

R/S (reset/set) flip-flop *454*
rack-mounted circuit board *515*
radial cylindrical electrostatic analyzer 347–348
fringing-field correction 352
radiant sensitivity, photoemissive materials 551, *62–63, 552*, *559*, *560*
radio-frequency interference 420, 443, 505
radiometric quantities 248
correspondence with photometric quantities *250*
radiometry, units and definitions 248–249
random-access memories (RAMs) 458
rare-earth glasses 168, 239
"rat nest," printed circuit board production 517
ray tracing 159
aberrations and 166–171
paraxial-ray analysis implemented using 159–161
ray transfer matrices 153
charged-particle optics analysis using 332–333
optical-system analysis using 153–159
Rayleigh criterion 302
razor-blade-stack light trap 217
reactances, capacitive or inductive 365
read-only memories (ROMs) 448, 452, 459
reamer 3, 4
recovery time of power supplies 442
rectifier, operational amplifier as 429, 431
reed relays 400
reference ground 507
reflectance 176
oblique-incident waves 177

reflection 150
  polarization changes due to 177, 206–208, 207
reflection coefficient of surface 176
refraction
  charged-particle beam
  of light 150
refractive index 149, 148
  glasses 77, 233
  various optical materials (listed) *233*
refractory metals 22, 356
  properties
regenerative feedback, in amplifiers 422, 434
regulator circuits (in power supplies) 443–445
relays 399–402
residual-gas analyzers (RGAs) 103
resistance temperature detectors (RTDs) 605
resistance thermometers 605
  compared with other thermometers 612
  dissipation factor(s) 608
  high-temperature use 611
  low-temperature use 610
  properties *606*
  stability requirements 610
resistance thermometry
  measurement systems for 608–609
  operating circuit(s) 614
resistor programming of power supplies 443
resistors
  circuit diagram symbol(s) 509
  codes 384, 386
  equivalent circuits 380
  fixed 383–384
  types *383*
  variable 384
resolution
  energy analyzers 346, 348, 350, 350
  mass analyzers 354
  optical stage 219
resolving power
  diffraction gratings 203
  Fabry–Perot devices 302, 303
  optical dispersing instruments 291
resonant circuits 372–374
  transient response 378
responsivity of detectors 551
  optical detectors *572*, *574*
  thermal detectors 593
Reststrahlen filters 215
retaining rings 29–30
retardation plates 208
retardation rhombs 211
retarding-potential analyzers 345
reticons 578
retroreflectors 198, 200–201
reverse bias, of diode 402
rheostats (variable resistors) 384
rhomb retards 211
rhomboid prisms 199, 200
ribbon-and-plane transmission line 384, 389
right-angle prisms 198
right-hand circularly polarized light 205
ring laser resonator 280
ring seal in glass tubing 87–88, 89
ringing (resonant circuits) 378
ripple binary counter 453, 455
rise time (of waveform) 363, 364, 371, 378
riveted joints, designs 36
rivets 28–29
RLC circuit(s) 377
  Laplace-transform equivalent *376*
  pole trajectory for *377*
Rochon polarizer 209
Rockwell hardness scale 14
  various materials (listed) *15*
rod mounts for electrostatic lenses 357
Rogowski TEA laser design 273
roll forming (sheet metal) 11, 10, 441
roller bearings 60
roller-slide assemblies 61
root-mean-square (rms) voltage 364
Roots blowers 106
rotary pumps 105–106
rotators for optical components 226
roughing pump (for vacuum system) 105
Rowland circle, for concave gratings 298
Rowland ghosts 203
RS 232 C serial interface 469, 471
  connector for 532–533
RTV (room temperature vulcanizing) silicone rubber 24, 34
ruby lasers 238, 276
rugate filters 214, 215

S-polarized wave (TE wave) 176, 175
safe operating area (SOA), semiconductors 383
safety precautions
  electrical 289, 500–503
  grinders 10
  light sources 289–291
  machine tools 8–9
sagittal rays, imaging of 170, 171
sample-and-hold (S/H) circuits 458, 473, 474, 485
sampling time, sample-and-hold circuit 474
sand casting 10–12
sapphire 25
  properties *233*, *234*, *237*, *239*
satellites, diffraction-grating defects 203
sawing, glass sheet 91–92
scattering, as diffraction-grating defect 203
schematic circuit diagrams 508
  symbols used *407*, *420*, *426*, *459*, *509*
  use when troubleshooting 534
Schmitt trigger 432, 432
Schottky devices 467
scintillation counters 591
screw thread
  standard specifications 25–26, *71*

terminology 25–26
section (in drawing) *43*, *44*
sector magnet energy analyzer 353
Seebeck effect 602
Seidel aberrations 170–172
semiconductor detectors
frequency dependence of noise in 549, 550
size/time-constant relationship 553
semiconductor lasers
properties 277–279
representative structures 278, 278
semiconductor materials
doping of 402
electronic applications 402
optical applications 244
properties 233–235, 237, 243, 244
semiconductor photocathodes 548
wavelength dependence of radiant sensitivity *552*
semiconductor resistance thermometers 607
properties *607*
semiconductor thermometers 609–610
low-temperature use 610
Senarmont polarizer *209*
sensitivity, control system 480–481
sensors, vacuum system 100–103, 135
serial format 469
series circuits, analysis of 366
series dimensions 45
series resonant circuit 373
current as function of frequency *373*
phase relations between voltage and current *374*
setscrews 27
settling time
analog-to-digital converter 472
digital-to-analog converter 453
waveform *379*
Seya–Namioka monochromator 298
shafts
bending of 50–52
twisting of 52
vibration of 54–55
whirl and vibration of 55–57
shear modulus 52, 79
various materials *19*
shears, sheet-metal 10
sheet-metal processes 10
for electronic-circuit chassis construction 515
shift registers 450, 455
and power-supply noise 467
shop processes
casting 10–12
drilling 2–4
electrical discharge machining 9
grinding 9–10
lathe turning 4–7
milling 7–9
sheet-metal processes 10
surface quality for 10, 12
tolerance for 7, 8, 10, 12
Shore hardness scale 14
short-circuit current 365
short-pulse high-power flashlamps 258, 260, 262
short-wavelength-pass filters 214
shot noise 492
detectors 548–549, 582, 583, 590
shoulder screws 29
shrink tubing (for connectors) 533
SI metric threads 25, 71
siemen (SI unit) 366, 421
signal averaging 494
signal diodes 403
properties *404*
signal injection, circuit fault diagnosis using 535
signal-enhancing techniques 494
signal-to-noise ratio (SNR) 491–492, 493
detectors 553–554, 582–585
optimizing 492–493
silicon 244
properties *233*, *234*, *237*, *244*
silicon-controlled rectifiers (SCRs) 419–420
applications 402, 421, 444
circuit diagram symbol *509*
current regulation by 420
silicon-controlled switch (SCS) 420
circuit diagram symbol
silicon photodiodes , 572, *573*, *63*, *575*
silicon substrate, mass spectrometry 487–491
silicone oils
in diffusion pumps 111
in thermostats 619, 617
silicone rubber
insulated cable 527–528
room temperature vulcanizing 24, 34
silver brazing alloys 32, 117
silver bromide, properties *233*, *234*, *243*
silver chloride, properties *233*, *234*, *237*, *243*
silver coatings on mirrors 246
simplex transmission of data 469
Simulation Program with Integrated-Circuit Emphasis (SPICE) 381
sine condition, imaging system 162, 163
single-mode lasers 284
singlet lenses 187–188
sinusoidally varying voltage
skimmers, vacuum system 130
skin effect (in electrical conductors) 364, 390
slew rate, operational amplifiers 426
sliding-gate valve 121
slow-blow fuse 501
slush baths 613
small-scale integration (SSI) 464
small-signal model
field-effect transistor *590*
transistors 409, 614
Snell's law 150, 151
applications 177, 196, 300
charged-particle analog 325
soda-lime glass 76
thermal properties *78*
sodium chloride 241–242
properties *233*, *234*, *237*

sodium fluoride, properties *233*, *234*, *237*
solder aspiration 522
solder wick/braid 522
soldered joints 31, 36
  in vacuum systems 141
soldering 30–31
  connectors 531
  printed circuit board components 518–522
  thermocouples 604
  third hand device used 532
  vacuum systems 141
soldering fluxes 30, 521
soldering guns 521
solid-state amplifiers, general operating principles 424–428
solid-state detectors (SSDs) 589–591
  equivalent circuit *590*
solid-state lasers 277
  operating wavelengths 264–265
solid-state relays 401–402, 462
sorption pumps 112–113
  applications 136, 356
space-charge effect 336
spatial coherence 248
spatial filtering 191
specific heat, various materials *615*
spectral detectivity (of detectors) 550–551
  various detectors *551*
spectral width of optical source 248
spectrofluorometers 291
spectrographs 291
  see also spectrometers and spectrographs
spectrometers and spectrographs 291
  calibration of 299
  design 295–299
spectrophotometers 291
spectroscopy experiment, data transfer rate 467, 470
spherical aberration 170, 191
spherical-aberration coefficient 334
spherical electrostatic analyzers 348–350
  fringing-field correction 352
spherical mirror Fabry–Perot interferometers 307
spherical mirrors 159, 183
  paraxial ray tracing for 160–161
"spike" filters, optical 214, 275
spinning of sheet metal 10, 11
spinning-rotor pressure gauges 101, 103
splice protector (for joined optical fibers) 219
spot diagrams (optical system) 168, 170
spot welding 34, 35
Sprague capacitors 273
spring rate 62
  helical springs
springs 62–63, 552
square-wave testing 371–372
stability, optical mount 220
stacked-plate polarizers 208
stainless steels 18, 21, 356
  properties 19, 220, 615
  in vacuum systems 116–117, 139–140
stall pressure (vacuum pumps) 105, 107, 110
stamp and die 10, 11
standard cubic centimeter 96, 104
standardized data-acquisition systems 474–479
static resistance, diodes 405
steady-state accuracy, control system 481
steatite *20*
steel(s) 18, 20
  properties 19, 141
steel bolts, SAE grades 27
steel vacuum fittings 117
Stefan–Boltzmann law 253
Steinhart–Hart equation 607
step-index optical fiber 218
stigmatic imaging 162
stirred-liquid thermostats 617–619
stopcocks 80–81, 121
straight seal in glass tubing 87, 88
strain 13, 53
stranded line cord 526
  tinning of wire 526
stray capacitances, in amplifiers 434
Strehl ratio 173
stress 13
  cylinder under internal pressure 53
stress concentration
  detection methods 16–18, 89, 90
  effect in materials 16–17
stress–strain curves 13
strip line *392*
strontium fluoride, properties *233*, *13*
strontium titanate ($SrTiO_3$), properties *233*, *234*, *237*
styrofoam, thermal properties *615*
subtractor circuit (operational amplifier) *429*
successive-approximation digital-to-analog converter 456, 457
summer circuit (operational amplifier) 428, 429
summing point (in operational amplifier) 428
super mirrors 182
superachromat lens 169
supersonic jets, in vacuum systems 128
surface collision frequency 95
surface-ionization ion source 344
surface-mount technology (SMT) components 384
  codes *390*
  soldering to PCBs 519
surface preparation, for vacuum systems 142–143, 356
swing valve 121
switches
  circuit diagram symbol(s) *614*
  electrically actuated 402, 409, 474
sync bit (in data transmission) 470

T-seal in glass tubing 85–87
T (toggle) flip-flop *454*
tantalum
  in capacitors 384, 385

properties *20*
taps and dies 3, 4
drill sizes for 68, 509
Teflon 24
in glass stopcocks and valves 80, 81, 121
insulated cable 528
properties *20*, *525*, *615*
Teflon thread tape 118
telecentric lenses 189
telescopes 189–190
tellurium 233, 235, 245
temperature
control of 600–621
measurement of 600
temperature-control system *487–489*, *490*
temperature ranges 536
tempering of metals 14
temporal coherence 248
tensile strength 13
glasses 78
various materials *19*
terminology
optical 147–149
screw thread 25–26
terrestrial telescope 189
Tesla coil (for vacuum leak detection) 144
test prod *536*
test-prod wire *527*
test-tube end, forming in glass tube 84–85
thallium bromide, properties *233*, *234*
thallium bromoiodide *see* KRS-5
thallium chlorobromide *see* KRS-6
thermal capacitance 614
see also specific heat
thermal circuit 614
thermal conductivity
aluminum compared with steel 220
glass 78
various materials *615*
thermal-conductivity pressure gauges 100–101
thermal conductors, properties *615*
thermal detectors 591–596
detectivity 550, 551
types 548, 592
see also bolometers; Golay cell; pyroelectric detectors; thermopiles
thermal e.m.f. 602
thermal energy 149
thermal expansion coefficient
various materials 19, 220
various optical materials 235
thermal insulators, properties *615*
thermal mass flowmeters 104
thermal noise 549, 550
thermal resistance 102
thermal time constant 614
thermionic electron guns 338
thermionic emission, noise due to 564
thermionic ionization pressure gauges 102, 103
thermistor-based thermometers 607, 612
thermistor bolometers 595
characteristics *551*, *592*
operating circuits for *595*
thermocouple pressure gauges 101, 103
vacuum system controllers based on 135
thermocouples 602–605
advantages and disadvantages as thermometers 605, 612
calibration of 605
construction details 604
high-temperature use 611
low-temperature use 610
principles governing 603
properties *604*
reference junction for 605
types 603–604
thermoelectric coolers (TECs) 620–621
thermoelectric effects 487
thermometers
calibration of 601–602, 605, 612–613
comparison of 607
expansion thermometers 601
resistance thermometers 605
semiconductor thermometers 609–610
very-low-temperature 610–611
thermopiles 548, 593, 603
characteristics *551*, *592*, *593*
thermoplastics, properties *20*, *525*
thermostat 378
thermostats 614–621
design considerations 170
materials used 615
thermowells 604
Thevenin's theorem 365
thick lens
charged-particle lens as 327
geometrical optics 327–328
ray diagrams *156*, *188*
ray transfer matrix analysis 155–157
thick-film circuits and components 520
"thimble" traps 126
thin lens
charged-particle analog 331
ray transfer matrix analysis 157
third-angle projection 41
threaded circular (military-style) connectors 533, 534
threaded fasteners 25–28
stress concentration in 16
see also machine screws; screw thread; steel bolts
three-cylinder electrostatic lens 330, 342
three-legged table, constrainted motion 57, 59
three-terminal circuit(s)
Miller transformations for 367, 368
Y–Δ transformation for 367, 368
three-terminal devices
fixed-voltage regulators 444
silicon-controlled rectifiers 419–420
transistors 406, 410
thrust bearings 59–60, 59, 60
thyratron 421
circuit diagram symbol
thyristor

circuit diagram symbol
See also silicon-controlled rectifier
tilt adjusters 223
time constant for detectors 553
determination of 597
optical detectors 567, 568, 573
thermal detectors *593*
time-correlation techniques 436, 439, 496–500
time-of-flight energy analyzers 345
time-of-flight mass spectrometer 355
time-to-amplitude converter (TAC) 441, 498
time-to-digital converter (TDC) 498
tin-based lead-free solders 31, 521
tin–lead solders 30, 142, 520
tip plugs 528
Ti:sapphire lasers , 264, 265, 275
titanium and alloys 23
titanium dioxide (TiO_2), properties *233*, *234*, *237*
titanium sublimation pump 113–114
applications 132, 136
with ion pump 115
tolerances
decimal system for specification 47, 48
on drawings 46–48, 49
machine-tool operations 7, 8, 10, 12
relation to production cost 46, 47
tools
electronic-circuit construction *515*
glassblowing 81–82
hand 2
sheet metal working 10
torch brazing 32–33
total internal reflection 150–151
transconductance amplifiers 422, 589
transfer functions 374
control systems 480, 482
high-pass circuit 376
low-pass circuit 376
pole-zero compensation network 380
pulse electronics 438, 439
transformer circuit *233*
Laplace-transform equivalent *476*
transformers 379
circuit diagram symbol(s)
transient response of power supplies 442
transistor-amplifiers, general operating principles 424–428
transistor isolators 461
transistor switches 409
transistor–transistor logic *see* TTL devices
transistors 406–419
circuit diagram symbol(s)
current–voltage characteristics 407
logic device interface circuits *466*
operating conditions 410, 412
properties *240*, *413*
protection diodes used, *416*, *417*, 535
separate power supplies for biasing voltages 409, 241, 425
see also bipolar junction transistors; field-effect transistors; unijunction transistors
transit time, photomultiplier tubes 556
transit-time spread, photomultiplier tubes 555
translation stages 225
with flexure mounts 226, 227
groove mounting arrangements for 226, 226
transmission coefficient, of optical media boundary
transmission curves, optical materials 79, 238–244
transmission lines 389, 389–396
configurations *392*
properties *392*. *see* coaxial cable
transmittance, optical media 175
transresistance amplifiers 422
transversely excited atmospheric-pressure (TEA) CO_2 lasers 273
traps, vacuum system 124–127, 132
triacs 420
applications 402
circuit diagram symbol *509*
triangular prisms 198
triboelectric induction 487
trihedral locating holes 223
trimmers (variable resistors) 384
triple-point measurements 612, 613
trochoidal analyzer 353
troubleshooting, electronics 534–536
truth tables
arithmetic units *451*
data units *452*
elementary logic gates *449*, *364*
flip-flops *454*
implementation by PROMs 459, 460
Karnaugh maps for 450, 462
vacuum system interlock circuits *461*, *462*, *463*, *522*
TTL devices 464, 465
conversion circuits *466*, *477*
edge-triggered 467, 468
level-triggered 467
logic probe and pulser *536*
open-collector output 467
power MOSFETs switched with 486
in signal-conditioning circuits 467, 468
three-state output 467
tunable diode lasers 277
tungsten 19, 23
tungsten-filament lamps 254–255
tungsten–halogen lamps 254–255
tungsten inert gas (TIG) welding 34, 117, 141
tungsten-to-Pyrex-glass seal 90, 132
tuning-fork chopper devices 287
turbomolecular pump 107–109
applications 137–138, 356, 460

combined with molecular drag pump 108–109, 137
TV tube electron guns 340
twist drills 3
twisted-pair cables 391, 392, 485, 504, 528
twisting, shaft 52
two-axis rotators (for optical components) 223–225
two-cylinder electrostatic lens 329–330
two-wire transmission line 389, 391
Twyman–Green interferometer 251, 311

ultrahigh pressure equipment 52
ultrahigh vacuum
characteristics *94*
pumps 113, 114, 132
sealing materials 120
valves 122
ultrahigh vacuum system(s)
baking of 144–145
oil-free 136–138
small inexpensive 135–136
ultrasonic cleaning
of metal surfaces 143
of optical components 235
ultraviolet detectors 566
ultraviolet lasers 266, 270, 272, 274
safety precautions 291
ultraviolet radiation, safety precautions 290
ultraviolet-transmissive materials 237–239
properties *233*, *234*
underdamped resonant circuit
output waveform 378
response *378*
unfolding technique, optical systems with plane mirrors analyzed using 158
uniaxial crystals 205
unijunction transistors (UJTs) 420–421
applications 420, 421
circuit diagram symbol *509*
current–voltage characteristics *421*
structure *420*
unipotential electrostatic lens 331
universal asynchronous receiver-transmitters (UARTs) 469

V-coating (antireflection coating) 184
vacuum photodiodes 554
vacuum pumps 104–115
costs 132
operating ranges 105, 106, 107, 109, 113, 114, 115
vacuum system(s)
analytical representation *96*
applications 93
conductance formulae 97–98
costs 124–127, 132
demountable connections in 118–120
design and construction 131–145
electronics and electrictricity in 130–131, 132–138
fail-safe mechanisms 120–123, 134
flow measurement in 95, 103–104
hardware 97, 115–131
interlock systems for 135, 139, 460–463
leak detection in 143
master equation for 96, 547
materials used 115–118
mechanical motion in 123–124, 555
molecular beam and gas jets introduced into 127
molecular-flow regime 95, 298, 97, 127
network equations 96
pressure measurement in 98–103
pumpdown time for 98
residual gases in 93
transition region 97–98
traps and baffles in 124–127, 132
typical systems 130–131, 132–138
valves in 120–123, 134
viscous-flow regime 95, 103–104, 97, 115–131, 139, 460–463
windows in 116, 231, 232
vacuum-tube photodetectors 96, 547, 123–124, 555
vacuum valves 120–123,134
vacuum-ultraviolet detectors 566
vacuum-ultraviolet monochromators 95, 298
valves
glassware 80, 81
vacuum system 120–123, 134
vapor-degreasing procedure, for optical components 236
vapor diffusion pumps 109–112
vapor-pressure thermometers 610
variable resistors 384
materials *444*
types 384, 390
see also potentiometers
variable-voltage regulators 444
velocity of light 148
Venturi pumps 136, 137
"Verdi" laser 280
very-high-temperature thermometry 611
very-large-scale integrated (VLSI) circuits 458, 464
MOSFETs used in 412
very-low-temperature thermometry 610–611
Vespel (polyimide) 20, 117, 525
VHDL programming language (for FPGAs) 459
vibration, beams and shafts 54–55
vibration isolation of optical system 229
Vickers hardness scale *15*
various materials (listed) *15*
vignetting 165
charged-particle beam 326
virtual ground 431
virtual images 160
virtual leaks (in vacuum systems) 132
viscous-drag pressure gauges 101
visible- and near-infrared-transmissive materials 239–241
properties *216*, *233*

visual checks (when troubleshooting) 534
Viton-A elastomer 24, 118, 122
voice coil actuators 228
Voigt lineshape profile 251
voltage-controlled resistor, transistor as 411
voltage dividers 366–367
  Thevenin equivalent 367
voltage programming of power supplies 443
voltage-to-frequency converters 472, 473
  applications 472
Vycor (96% silica) 77, 239
  properties *78*, *79*, *187*, *234*, *240*

water solubility, various optical materials 234–235
wave–particle duality 147
waveform recovery 495
wavelength scanning in interferometers 305
wavemeters 299
wedge prisms 199, 200
welded joints 36–37, 36
  in vacuum systems 142
welding 33–34
  thermocouples 604
Wheatstone bridge 445
white noise 491, 493, 549, 550
"white-light interferometry" 309
Wien filters 353, 354
Wien's displacement law 253
windows *see* optical windows
"Winston Cone" 195
wire nuts 526
wire-and-plane transmission line 389, 392
wire strippers 526, 527
wire terminals 530, 531
Wire Wrap™ boards 523–524
  advantages 523
  wrap list 523, 524
wires and cables 524–528
  stripping of 299, 526, 527
  see also coaxial cable
wiring, circuit diagram symbol(s) *302*
wiring diagrams *see* schematic wiring diagrams
Wollaston polarizer *209*
wood, properties *20*
Wood's horn (light trap) 216
words 467
work functions, photoemissive surfaces 554
working drawings, design translated to 48–49
working-standard thermometers 601–602, 612
working voltages, capacitors 383, 385

X-ray detectors 591
xenon arc lamp *256*
xenon flashlamps, 258, *260*, *261*

Y–Δ transformation 367, 368
yield strength 13
  various materials 19, 52
Young's modulus 13
  glasses 78
  various materials 78–81, 141

Zener diodes 402
zero crossing switching 420
zero potential 500
Zerodur glass ceramic 25
zinc selenide
  in optical components 243, 272
  properties *305*, *323*, *243*
zinc sulfide, properties *305*, *323*, *242*